

Alma Mater Studiorum – Università di Bologna

DOTTORATO DI RICERCA IN

Ingegneria chimica dell'ambiente e della sicurezza

Ciclo XXVII

Settore Concorsuale di afferenza: 09/D3 - Impianti e Processi Industriali Chimici

Settore Scientifico disciplinare: ING-IND/25 - Impianti Chimici

CASCADING EVENTS TRIGGERING INDUSTRIAL ACCIDENTS:
QUANTITATIVE ASSESSMENT OF NATECH AND DOMINO SCENARIOS

Presentata da: Amos Necci

Coordinatore Dottorato

Relatore

Prof.ssa Ing. Serena Bandini

Prof. Ing. Valerio Cozzani

Esame finale anno 2015

To my family...

“In three words I can sum up
everything I've learned about life:
it goes on.”

Robert Frost

Table of Contents

1. Preface: cascading events

2. State of the art on the research of Domino accidents

2.1. Introduction

2.2. Past accident analysis

2.3. Vulnerability models

2.3.1. Approach to the probabilistic modelling of Equipment Damage

2.3.2. Damage due to Blast Waves

2.3.3. Damage due to Fragment Impact

2.3.4. Damage due to Fire

2.3.4.1. *Equipment damage caused by fire*

2.3.4.2. *Time to failure of vessels under heat load*

2.3.4.3. *Vulnerability models for vessels under fire load*

2.4. Quantitative Risk Assessment and Safety Management

2.4.1. Key steps and level of detail of domino scenario assessment

2.4.2. Preliminary Hazard Analysis of Domino Scenarios

2.4.3. Quantitative risk assessment of Domino Scenarios

2.4.4. Safety management and accident prevention

2.5. Discussion

2.5.1. Vulnerability models and uncertainties affecting escalation probability

2.5.2. Risk Assessment

2.6. Conclusions

3. State of the art on the research of NaTech events

3.1. Introduction

3.2. Analysis of past accidents triggered by natural events

3.2.1. The analysis of Natech in the USA

3.2.2. The analysis of Natech in the EU

3.2.3. Discussion

3.3. Natech risk assessment and accident prevention

3.3.1. Natech and regulatory requirements in the EU

3.3.2. Preliminary Natech risk assessment

3.4. Quantitative risk assessment of Natech scenarios

3.4.1. General framework for the quantitative assessment of Natech

3.4.2. Identification of critical target equipment

3.4.3. Quantitative assessment of Natech due to earthquake

3.4.3.1. *Expected frequency and severity of the reference earthquakes*

3.4.3.2. *Reference scenario selection*

3.4.3.3. *Damage probability of critical equipment item*

3.4.3.4. *Consequence assessment*

3.4.4. Quantitative assessment of Natech due to flood events

3.4.4.1. *Expected frequency and severity of the reference floods*

3.4.4.2. *Identification of critical equipment items*

3.4.4.3. *Damage states and reference accidental scenarios*

3.4.4.4. *Damage probability of the critical equipment items, frequency and consequence assessment of the overall scenarios*

3.4.5. Discussion

3.5. Conclusions

4. Risk analysis of Natech accidents triggered by lightning strikes

4.1. Introduction

4.2. Past accident analysis of accident triggered by lightning event

4.2.1. **Data retrieval for past accident analysis**

4.2.2. **Results**

4.2.3. **Conclusions**

4.3. Quantitative risk assessment of accidents triggered by lightning

4.3.1. **Methodology overview**

4.3.2. **Identification of the vulnerable units**

4.4. Assessment of lightning impact frequency on target equipment

4.4.1. **Preliminary definition of geometrical features and lightning generation**

4.4.2. **Lightning attraction**

4.4.3. **Frequency assessment of attracted lightning strikes**

4.4.4. **Simplified assessment of attracted lightning strikes**

4.4.5. **Comparison of results obtained by the Monte Carlo and the simplified model**

4.4.6. **Results**

4.4.6.1. *Model application to stand-alone equipment items and to simple lay-outs*

4.4.6.2. *Results obtained in the analysis of an existing tank farm lay-out*

4.4.7. **Final consideration regarding lightning impact frequency assessment**

4.5. Identification of the damage modalities and of reference scenarios

4.5.1. **Characterization of the critical equipment**

4.5.2. **Determination of lightning damage modes**

4.5.3. **Schematization of fire safety barriers**

4.5.3.1. *Fire protection systems for Category "a" tanks*

4.5.3.2. *Fire protection systems for Category "b" tanks*

4.5.4. **Characterization of lightning-triggered accident scenarios**

4.6. Model for lightning damage

4.6.1. **Effect of lightning strikes on process equipment**

4.6.2. **Arc erosion modeling**

4.6.3. **Validation of the model for molten volume calculation**

- 4.6.4. Calculation of equipment damage probability due to lightning strike
- 4.6.5. Simplified method for damage probability assessment
- 4.6.6. Lightning damage probability calculation
- 4.6.7. The contribution of positive flashes
- 4.6.8. Damage probabilities for a reference set of equipment items
- 4.7. Assessment of accident frequency induced by lightning**
 - 4.7.1. Event tree analysis (ETA) and reference accident chains
 - 4.7.2. Validation of ETA results
 - 4.7.3. Quantification of event trees and frequency assessment
 - 4.7.3.1. *Lightning impact frequency assessment*
 - 4.7.3.2. *Probability of direct damage to the tank shell*
 - 4.7.3.3. *Assessment of safety barriers*
- 4.8. Consequence assessment of lightning-triggered scenarios**
 - 4.8.1. Conventional scenarios
 - 4.8.2. Lightning triggered scenario modelling
 - 4.8.3. Meteorological Data
- 4.9. Application of QRA procedure: results**
 - 4.9.1. “Conventional” risk assessment against risk contribution of “NaTech scenarios” for single equipment
 - 4.9.2. “Conventional” risk assessment against risk contribution of “NaTech scenarios”: case study
 - 4.9.3. Final considerations
- 4.10. Possible strategies for the lightning protection of storage tanks**
 - 4.10.1. Bonding
 - 4.10.2. External lightning protection system (ELPS)
 - 4.10.3. Lightning rods
 - 4.10.4. Lightning protection masts
 - 4.10.5. Overhead shield wire
- 4.11. Conclusions**

5. Development of fragility models for risk assessment of Natech due to flood

- 5.1. Introduction**
- 5.2. Modelling the equipment damage due to flood events**
 - 5.2.1. Representation of vessel geometry (step 1)
 - 5.2.2. Mechanical model set-up (step 2)
 - 5.2.3. Characterization of flood impact vector (step 3)
 - 5.2.4. Model validation (step 4)
 - 5.2.5. Dataset of failure conditions (step 5)

- 5.2.6. Simplified correlations for vessel damage (step 6)
- 5.3. Results and discussion
 - 5.3.1. Analysis of vessel failure conditions
 - 5.3.2. Sensitivity and uncertainty analysis
 - 5.3.3. Assessment of vessel damage probability
- 5.4. Application to a case-study
- 5.5. Conclusions

6. Probability assessment of multilevel domino scenarios

- 6.1. Introduction
- 6.2. Multilevel domino assessment using Markov analysis
 - 6.2.1. Methodology Overview
 - 6.2.2. Preliminary considerations regarding domino scenarios
 - 6.2.3. Secondary accident typology selection
 - 6.2.4. Identification of targets for the escalation process and domino system definition
 - 6.2.5. The accidental scenario set
 - 6.2.6. System and “states” description: the construction of the Directed Acyclic Graph (DAG)
 - 6.2.7. Probability of accident escalation: transition between states
 - 6.2.7.1. *Equipment vulnerability due to several secondary scenarios*
 - 6.2.7.2. *Transition probability calculation*
 - 6.2.8. Application of the Bayes theorem: Conditional transition probabilities calculation and domino frequency assessment
- 6.3. Results
 - 6.3.1. Application to simplified case study
 - 6.3.2. Comparison with previous models
- 6.4. Conclusions

7. Final conclusions

Appendix

Acknowledgements

Chapter 1:

Preface: cascading events

The increase of the industrial production of the past century generated a significant change in modern lifestyle, since industry provides most of the needs of people. The increase of energy demand and material supply are two of the requirements for the development of the modern mass productions. The relentless increase in population and their needs, which were fulfilled only thanks on innovation in technologies, determined an acceleration in the growth of chemical production.

Therefore, also the quantity of hazardous materials and their diffusion in industrial activities has had an increasing tendency in the recent years. New chemical plants are installed every years worldwide, often in the vicinity of urban areas, in order to provide the availability of plenty of personnel. In the same time, both process plants and residential areas has suffered a process of intensification. As a results, if in the one hand the happening of accidents related to the industrial activity has become a far more rare event than years before, on the other hand the few accidents that occurred and that may occur, have a greater potential to cause huge losses.

For this reason, the so called cascading events, which lead to high-impact low-frequency scenarios are rising concern worldwide. During those events, a chain of event result in a major industrial accident with dreadful (and often unpredicted) consequences.

A high level of concentration of industrial activities within chemical clusters generates the basis for accidents having a simultaneous impact on several plant units, eventually resulting in casualties, environmental contamination ad of course huge monetary losses. Cascading events can be the result of terrorist attack or of “domino effect”, an event in which the escalation of a primary accident is driven by the propagation of the primary event to nearby units, causing an overall increment of the accident severity. Also natural disasters, like intense flooding, hurricanes, earthquake and lightning are found capable to trigger industrial accidents as a result of an event cascade that result in loss of containment of hazardous materials and in major accidents. Has this event to happened the consequences of those technological accidents adds to the emergency situation left by the impact of natural disaster on urban areas. For this reason the scientific community usually refers to those accident as “NaTech”: natural events triggering industrial accidents.

The events related to the 2011 Tohoku Tsunami in Japan demonstrated the need for safety managers to an even more important necessity to explicitly prevent, model and manage the risks due to cascading events. There is growing evidence that loss of containment of hazardous material triggered by “external hazards” can pose significant risks to nearby population, which may be unprepared for such events. Also the response plan of the industries can be bound unprepared to face domino or NaTech events. Utilities used to fight the accidental situation (e.g. water, power, and communications ways) may not be available due to external damage. The chemical safety personnel supposed to fight the accident situation might be caught in the event

cascade or might be busy on finding a shelter. Finally, mitigation measures (e.g. containment dikes or foam systems) may not work properly due to the interference of the event cascade.

However, due to the fact that accidents scenarios due to cascading events are characterized by a very high complexity, in combination with the extremely low probabilities of such accidents, those events are often left out from the safety assessment of chemical activities. For this reason, one of the main topics of academic and industrial research in the field of industrial safety is the study of cascading events, aimed at the development of specific methodologies for risk assessment and safety management.

The activity of my PhD regarded cascading events, on the research of domino and NaTech events. In this thesis, a state of the art of available approaches to the modelling, assessment, prevention and management of domino and NaTech events is described. New methodologies, developed during my research activity, aimed at the quantitative assessment of domino and Natech accidents are also presented.

Chapter 2 reports the state of the art on the research regarding domino accidents. In this chapter three main topics are analyzed: the analysis of past accidents, the development of fragility models for process equipment and the development of risk analysis and safety management methods. Chapter 3 reports the state of the art on the study of NaTech events. In this chapter a review of past accidents is reported, observed both in the US and in the EU. Then, the efforts toward a common framework for the quantitative assessment of NaTech accidents are described.

Chapter 4 reports the efforts toward a novel methodology for the quantitative assessment of accidents due to lightning strikes. In this chapter contains: a detailed analysis of past accidents caused by lightning strikes, a statistical model for the assessment of lightning impact frequency on process units, the analysis and identification of possible accidents triggered by lightning strikes, a model for the assessment of process vessel vulnerability due to lightning strikes, the description of the protective barriers that protects storage tanks, event trees that helps the assessment of the probability of the final scenarios, a methodology for consequence assessment of accidents triggered by lightning strikes, a case study showing the result obtained by the use of the developed models to a real industrial installation.

Chapter 5 contains the development of fragility models for the assessment of the damage probability of storage and process vessels during intense floods events. In this chapter, a mechanical model for the damage to horizontal storage tank is presented. The extensive use of the mechanical model lead to the identification of a dataset of failure conditions, allowing the statistical interpretation for the assessment of a damage probability for a given tank involved in flood events.

Chapter 6 contains a novel methodology to describe and assess the possible scenarios that arise as a consequence of domino events. In this chapter the Markovian analysis is used in order to identify all the possible domino scenarios and their probability to occur.

Chapter 7 contains the final conclusions of the work.

This thesis presents the most up to date discussion, and uses the most advanced models, in order to provide the best methodologies to deal with cascading events, allowing their inclusion in safety management systems of the chemical and process industry. This study offers to be a milestone for the state-of-the-art for further research on the topic.

Chapter 2:

State of the art on the research of Domino accidents

2.1 Introduction

The growing public concern caused by high-impact low-probability (HILP) accident scenarios raised the attention in the scientific and technical literature on the analysis of the so called “domino effect” (Reniers and Cozzani, 2013). Domino effect was responsible of several catastrophic accidents that took place in the chemical and process industry (Abdolhamidzadeh et al., 2011; CCPS, 2000; Khan & Abbasi, 1999; Mannan, 2005). Although an increasing interest can be inferred from the available scientific publications, this subject has been afforded by a relatively limited number of authors. As a result, there is still a poor agreement on the main definitions of domino effect, and specific features of domino scenarios are still poorly known. Table 2.1 reports a summary of domino effects definitions (Reniers (2010); Abdolhamidzadeh et al. (2011), Reniers and Cozzani 2013b).

Table 2.1: Definitions Given for a “Domino Effect” or a “Domino Accident”

Author(s)	Domino effect definition
Third Report of the Advisory Committee on Major Hazards (HSE, 1984)	The effects of major accidents on other plants on the site or nearby sites.
Bagster and Pitblado (1991)	A loss of containment of a plant item which results from a major incident on a nearby plant unit.
Lees (1996)	An event at one unit that causes a further event at another unit.
Khan and Abbasi (1998b)	A chain of accidents or situations when a fire/explosion/missile/toxic load generated by an accident in one unit in an industry causes secondary and higher order accidents in other units
Delvosalle (1998)	A cascade of accidents (domino events) in which the consequences of a previous accident are increased by the following one(s), spatially as well as temporally, leading to a major accident.
Uijt de Haag and Ale (1999)	The effect that loss of containment of one installation leads to loss of containment of other installations.
AICHe-CCPS (2000)	An accident which starts in one item and may affect nearby items by thermal, blast or fragment impact.
Vallee et al. (2002)	An accidental phenomenon affecting one or more installations in an establishment which can cause an accidental phenomenon in an adjacent establishment, leading to a general increase in consequences.
Council Directive 2003/105/EC (2003)	A loss of containment in a Seveso installation which is the result (directly and indirectly) from a loss of containment at a nearby Seveso installation. The two events should happen simultaneously or in very fast subsequent order, and the domino hazards should be larger than those of the initial event.
Post et al. (2003)	A major accident in a so-called ‘exposed company’ as a result of a major accident in a so-called ‘causing company’. A domino effect is a subsequent event happening as a consequence of a domino accident.
Lees (2005)	A factor to take account of the hazard that can occur if leakage of a hazardous material can lead to the escalation of the incident, e.g. a small leak which catches fire and damages by flame impingement a larger pipe or vessel with subsequent spillage of a large inventory of hazardous material.
Cozzani et al. (2006)	Accidental sequences having at least three common features: (i) a primary accidental scenario, which initiates the domino accidental sequence; (ii) the propagation of the primary event, due to “an escalation vector” generated by the physical effects of the primary scenario, that results in the damage of at least one secondary equipment item; and (iii) one or more secondary events (i.e., fire, explosion and toxic dispersion), involving the damaged equipment items (the number of secondary events is usually the same of the damaged plant items).
Bozzolan and Messias de Oliveira Neto (2007)	An accident in which a primary event occurring in primary equipment propagates to nearby equipment, triggering one or more secondary events with severe consequences for industrial plants.
Gorrens et al. (2009)	A major accident in a so-called secondary installation which is caused by failure of a so-called external hazards source.
Antonioni et al. (2009)	The propagation of a primary accidental event to nearby units, causing their damage and further “secondary” accidental events resulting in an overall scenario more severe than the primary event that triggered the escalation.

Since there is not a widely accepted definition of domino effect, as a consequence most of the studies on domino effect are carried out independently and focus either on very particular aspects of accident escalation process, as vulnerability models, or on the definition of methodologies for hazard and/or risk assessment of domino scenario. This was evidenced in a recently published comprehensive review of the state of the art in domino effect assessment (Reniers and Cozzani, 2013a). Relevant research efforts are currently dedicated to domino effect assessment and to the development of safety management systems that allow coping with escalation and cascading events. Four main topics may be identified for the ongoing research activities on domino effect: past accident analysis; vulnerability models for equipment damage; quantitative risk assessment; and safety management of domino scenarios. Figure 2.1 shows the number of relevant publications on domino effect present published in scientific journals in the period 1985-2014 divided by topic. As shown in the figure, large part of the papers published were aimed at the study of equipment damage mechanism and at the development of vulnerability models. A quite high number of papers aimed at the inclusion of domino accidents in quantitative risk assessment, while a more limited number of studies were dedicated to innovative safety management tools for domino accidents and to the historical assessment of domino events through the analysis of past accident database. Further details on publications addressing domino effect are reported in Annex 1.

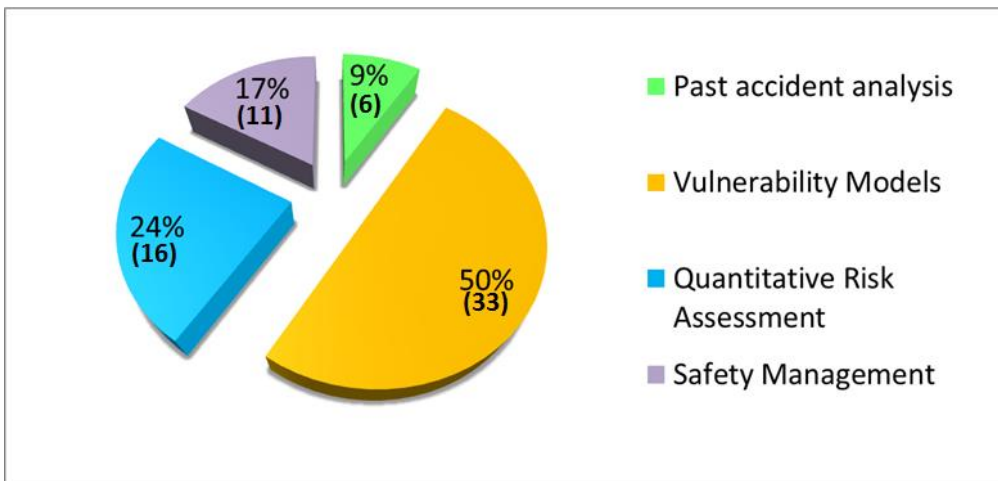


Figure 2.1: Scientific publications on domino effect in the period 1988 – 2014 divided by topic.

The present contribution is aimed at assessing the progress and providing a critical review of the most important studies on domino effect carried out in the last 25 years on three specific key points in domino effect assessment: i) past accident analysis; ii) vulnerability models for equipment damage; iii) quantitative risk assessment and safety management of domino scenarios. A summary of the contributions analysed, with particular focus on the progress provided by each reference to the overall knowledge concerning domino effect analysis can be found in Table 2.2. The final aim of the present analysis is to understand how the progress on such issues may affect the assessment of domino hazard, and to identify weak points of actual methodologies and possible directions of future studies, in order to fill the gaps that prevent an exhaustive scientific description of domino effect.

Table 2.2: The articles analysed in the present study divided by categories.

Document	Category	Methodology	Topic	Publication/Journal
<i>Kourniotis et al. (2000)</i>	Past accident Analysis	Past accident Analysis- Statistical analysis	Database research	Journal of Hazardous Materials
<i>Gómez-Mares et al. (2008)</i>	Past accident Analysis	Past accident Analysis- Event tree analysis	Database research	Fire Safety Journal
<i>Debara et al. (2010)</i>	Past accident Analysis	Past accident Analysis- Event tree analysis	Database research	Journal of Hazardous Materials
<i>Abdolhamidzadeh et al. (2011)</i>	Past accident Analysis	Past accident Analysis	Database research	Journal of Loss Prevention in the Process Industries
<i>Abdolhamidzadeh et al. (2012)</i>	Past accident Analysis	Investigation of a Case Study	Accident investigation	Process Safety and Environmental Protection
<i>Hemmatian et al. (2014)</i>	Past accident Analysis	Past accident Analysis- Event tree analysis	Database research	Journal of Loss Prevention in the Process Industries
<i>Eisenberg et al. (1975)</i>	Vulnerability models	Probit models	Overpressure	Report CG-D-136-75, Enviro Control Inc., Rockville, MD, 1975
<i>Cozzani and Salzano (2004 a)</i>	Vulnerability models	Threshold Values and Probit	Overpressure	Journal of Hazardous Materials
<i>Cozzani and Salzano (2004 b)</i>	Vulnerability models	Threshold Values and Probit	Overpressure	Journal of Hazardous Materials
<i>Mingguang and Juncheng (2008)</i>	Vulnerability models	Probit Models	Overpressure	Journal of Hazardous Materials
<i>Hauptmanns (2001 a)</i>	Vulnerability models	Monte Carlo	Fragments	Journal of Loss Prevention in the Process Industries
<i>Hauptmanns (2001 b)</i>	Vulnerability models	Monte Carlo	Fragments	Probabilistic Engineering Mechanics
<i>Gubinelli et al. (2004)</i>	Vulnerability models	Probabilistic	Fragments	Journal of Hazardous Materials
<i>Gubinelli and Cozzani (2009)</i>	Vulnerability models	Monte Carlo	Fragments	Journal of Hazardous Materials
<i>Nguyen et al. (2009)</i>	Vulnerability models	Monte Carlo	Fragments	Advances in Engineering Software
<i>Zang and Chen (2009)</i>	Vulnerability models	Monte Carlo	Fragments	Safety Science
<i>Tugnoli et al. (2014)</i>	Vulnerability models	Accident investigation	Fragments	Journal of Loss Prevention in the Process Industries
<i>Birk (1988)</i>	Vulnerability models	Modelling	BLEVE	Journal of Hazardous Materials
<i>Moodie (1988)</i>	Vulnerability models	Experimental	BLEVE	Journal of Hazardous Materials
<i>Droste e Schoen (1988)</i>	Vulnerability models	Experimental	BLEVE	Journal of Hazardous Materials
<i>Leslie and Birk (1991)</i>	Vulnerability models	Review	BLEVE	Journal of Hazardous Materials
<i>Prugh (1991)</i>	Vulnerability models	Past accident analysis	BLEVE	Hazard Reduction Engineering, Inc. Wilmington, DE (1991)
<i>Birk and Cunningham (1994)</i>	Vulnerability models	Experimental and modelling	BLEVE	Journal of Loss Prevention in the Process Industries
<i>Birk (1995)</i>	Vulnerability models	Experimental and modelling	BLEVE	Journal of Loss Prevention in the Process Industries
<i>Venart et al (1993)</i>	Vulnerability models	Experimental and modelling	BLEVE	Gas-Liquid Flows, vol. 165ASME, New York (1993)
<i>Venart (2000)</i>	Vulnerability models	Experimental and modelling	BLEVE	Proceedings of the IChemE Symposium Series No. 147
<i>Yu and Venart (1996)</i>	Vulnerability models	Experimental and modelling	BLEVE	Journal of Hazardous Materials
<i>Birk and Cunningham (1996)</i>	Vulnerability models	Experimental and modelling	BLEVE	Journal of Hazardous Materials
<i>Roberts et al. (1995a)</i>	Vulnerability models	Experimental only	BLEVE	HSL Report R04.029, IR/L/PH/95/11, Buxton, UK, July.
<i>Roberts et al. (1995b)</i>	Vulnerability models	Experimental only	BLEVE	HSL Report R04.029, IR/L/PH/95/11, Buxton, UK, July.
<i>Roberts et al. (1995c)</i>	Vulnerability models	Experimental only	BLEVE	HSL Report R04.029, IR/L/PH/95/11, Buxton, UK, July.
<i>Roberts et al. (1996a)</i>	Vulnerability models	Experimental only	BLEVE	HSL Report R04.029, IR/L/PH/95/11, Buxton, UK, July.
<i>Roberts et al.</i>	Vulnerability models	Experimental only	BLEVE	HSL Report R04.029, IR/L/PH/95/11,

(1996b)				Buxton, UK, July.
<i>Susan et al. (2005)</i>	Vulnerability models	Modelling wall temperature	BLEVE	HSL Report R04.029, IR/L/PH/95/11, Buxton, UK, July.
<i>Abbasi and Abbasi (2007)</i>	Vulnerability models	Past accident Analysis- Article review	BLEVE	Journal of Hazardous Materials
<i>Salzano et al. (2003)</i>	Vulnerability models	Equipment damage modelling	Thermal radiation	Industrial & Engineering Chemistry Research
<i>Raj (2005)</i>	Vulnerability models	Heat radiation-wall etmperature modelling	Thermal radiation	Journal of Hazardous Materials
<i>Landucci et al. (2009a)</i>	Vulnerability models	Experimental and modelling	Thermal radiation	Journal of Hazardous Materials
<i>Landucci et al. (2009b)</i>	Vulnerability models	Correlation for damage due to fire	Thermal radiation	Accident Analysis and Prevention
<i>Bagster and Pitbaldo (1991)</i>	Risk Assesement and Management	Methodology for domino assessment	QRA	Proc. Safety Environ. Protect
<i>Delvosalle (1996)</i>	Risk Assesement and Management	Methodology for domino assessment	QRA	uropean Seminar on Domino Effects, Federal Ministry of Employment, Brussels
<i>Gledhill and Lines (1998)</i>	Risk Assesement and Management	Methodology for domino assessment	QRA	CR Report 183, Health and Safety Executive
<i>Khan and Abbasi (1998a)</i>	Risk Assesement and Management	Methodology for domino assessment	QRA	Process Saf. Prog.
<i>Khan and Abbasi (1998b)</i>	Risk Assesement and Management	Software tool for domino assessment	QRA	Environ. Model. Softw.
<i>Khan and Abbasi (2000)</i>	Risk Assesement and Management	Methodology for domino assessment	QRA	Chem. Eng. Prog.
<i>Khan and Abbasi (2001a)</i>	Risk Assesement and Management	Application of QRA tool to case study	QRA	Cleaner Prod.
<i>Khan and Abbasi (2001b)</i>	Risk Assesement and Management	Application of QRA tool to case study	QRA	Journal of Loss Prevention in the Process Industries
<i>Cozzani et al. (2005)</i>	Risk Assesement and Management	Methodology for domino assessment	QRA	Journal of Hazardous Materials
<i>Cozzani et al. (2006)</i>	Risk Assesement and Management	Software tool for domino assessment	QRA	Journal of Loss Prevention in the Process Industries
<i>Antonioni et al (2009)</i>	Risk Assesement and Management	Software tool for domino assessment	QRA	Journal of Loss Prevention in the Process Industries
<i>Abdolhamidzadeh et al. (2010)</i>	Risk Assesement and Management	Software tool for domino assessment	QRA	Journal of Hazardous Materials
<i>Bernachea et al (2013)</i>	Risk Assesement and Management	Software tool for domino assessment	QRA	Process Safety and Environmental Protection
<i>Khakzad et al. (2013)</i>	Risk Assesement and Management	Software tool for domino assessment	QRA	Risk Analysis
<i>Rad et al. (2014)</i>	Risk Assesement and Management	Software tool for domino assessment	QRA	Process Safety and Environmental Protection
<i>Cozzani et al. (2014)</i>	Risk Assesement and Management	Methodology for domino assessment	QRA	Journal of Loss Prevention in the Process Industries
<i>Reniers et al. (2005a)</i>	Risk Assesement and Management	Risk Management and operation planning	Risk Management and AccidentPrevention	Journal of Loss Prevention in the Process Industries
<i>Reniers et al. (2005b)</i>	Risk Assesement and Management	Risk Management and operation planning	Risk Management and AccidentPrevention	Journal of Loss Prevention in the Process Industries
<i>Cozzani et al. (2006)</i>	Risk Assesement and Management	Thresholds and safety distances	Risk Management and AccidentPrevention	Journal of Hazardous Materials
<i>Cozzani et al. (2007)</i>	Risk Assesement and Management	Safety distances and Inherent safety	Risk Management and AccidentPrevention	Journal of Hazardous Materials
<i>Tugnoli et al. (2008a)</i>	Risk Assesement and Management	Inherent safety approach	Risk Management and AccidentPrevention	Journal of Hazardous Materials
<i>Tugnoli et al. (2008b)</i>	Risk Assesement and Management	Inherent safety approach	Risk Management and AccidentPrevention	Journal of Hazardous Materials
<i>Cozzani et al. (2009)</i>	Risk Assesement and Management	Key performance indicators	Risk Management and AccidentPrevention	Accident Analysis and Prevention
<i>Reniers et al. (2009)</i>	Risk Assesement and Management	Risk Management and operation planning	Risk Management and AccidentPrevention	Journal of Hazardous Materials
<i>Reniers et al. (2010)</i>	Risk Assesement and Management	Risk Management and operation planning	Risk Management and AccidentPrevention	Journal of Hazardous Materials
<i>Di Padova et al. (2011)</i>	Risk Assesement and Management	Identification of fireproofing zones	Risk Management and AccidentPrevention	Journal of Hazardous Materials
<i>Tugnoli et al. (2012)</i>	Risk Assesement and Management	Identification of fireproofing zones	Risk Management and AccidentPrevention	Reliability Engineering and System Safety

2.2 Past accident analysis

The analysis of past accidents is a powerful tool to understand and analyse domino scenarios. Past accidents are in fact the only source of “experimental data” available in this field. The analysis of domino accidents gives the possibility of investigating specific features of escalation scenarios: the events that more frequently trigger a domino sequence, the more frequent escalation sequences, the hazardous substances that are more prone to be involved in these accidents, etc. However, the survey of domino accidents has implicit difficulties, the most significant being the lack of information. Reports on accidents involving domino effect can be obtained from the scientific literature, from technical reports and in specific databases. Some cornerstone studies are present in the field.

The paper of *Kourniotis et al. (2000)* reports the analysis of a set of 207 major accidents retrieved from competent authorities reports and well established accident databases. The ratio of domino accidents on the total number of accidents analysed is of 0.386. Accidents have up to 600 recorded causalities. Data are analysed statistically in order to calculate the p-N distribution curves for the accident analysed.

Differences in the distribution shape and parameters have been observed between the entire set of accidents analysed and accidents where domino effect takes place, showing that the probability of numerous fatalities occurring is higher as a consequence of domino accidents than as a consequence of a general accident (see Figure 2.2). The conclusion is that domino scenarios show, in general, a higher severity to the respect of conventional scenarios.

The study of *Ronza et al. (2003)* is not focused at domino effect, however it performed a survey of 828 accidents in port areas recorded in the MHIDAS database (MHIDAS, 2001). A total of 108 out of 828 past accident records are domino accidents. Conditional probability event trees were built to identify the event sequences in the accident scenarios where a domino effect was observed. The most frequent event sequences were: fire→explosion, release→fire→explosion, and release→gas cloud→explosion.

The investigation of *Gómez-Mares et al. (2008)* is focused on the study of accidental scenarios involving jet fires. Events were retrieved from four different accident databases: MHIDAS, ARIA, MARS and FACTS. A total of 84 accidents involving jet fire were analysed. Event trees were created on the basis of available data in order to identify the probability of first and second level domino scenarios. In 27% of the cases, the sequence identified by the event tree analysis was loss of containment (LOC) to jet-fire to explosion. In 11% it was LOC to vapour cloud explosion to jet-fire, which in a few cases evolved in an explosion or in a Boiling Liquid Expanding Vapour Explosion (BLEVE). According to the data from the event tree, the probability of another accident occurring together with a jet fire is 0.49 (both causes and consequences), and the probability of occurrence of an explosion occurring is of 0.44.

In the paper from *Darbra et al. (2010)*, the main features of domino accidents in process/storage plants and in the transportation of hazardous materials were studied through the analysis of 225 accidents involving escalation. The more common causes of primary events triggering domino accidents resulted: external events, mechanical failure, human error. Most of the accidents took

place in storage installations, process installations and during transport. The statistics also point out high accident frequencies during loading and unloading operations. The severity of domino accidents is analysed with the use of p-N curves. The result of this analysis shows how in the last 20 years the number of accidents in Europe and in US decreased, while overall the number and also the severity of major accidents increased.

Figure 2.2 represents the p-N plots reported in the studies by Kourniotis et al. (2000), who studied accidents occurred in industrial installations, and by Darbra et al. (2010), who studied the accidents occurred during transport of hazardous materials. In the graph the abscissae represent the severity of the accident (the number of fatalities, N) and the values on the ordinate axis represent the conditional probability (p) of an accident (that occurred and resulted in fatal consequences) to result in N or more fatalities.

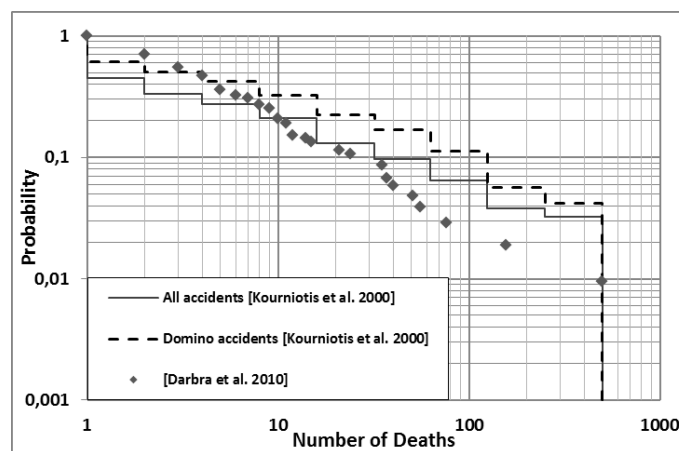


Figure 2.2 - The p-N graph that show the impact of domino accidents on population. The two black curves are those provided by Kourniotis et al. (2000), while the grey dots are those provided by Darbra et al. (2010)

The study of *Abdolhamidzadeh et al. (2011)* analysed a set of 224 domino accidents that occurred between 1910 and 2008 considering the type of activity, the substances involved, the level of domino effect and the impact on the affected population. The study focuses on a relatively small number of accidents, some of which occurred in the early 20th century. The study evidences that the most of the domino accidents considered involved flammable substances. Fires have been the accident trigger in 43 % of the recorded domino accidents. Among fires, pool fire was the specific scenario more frequently resulting in an escalation (80% of domino accidents initiated by fires). Explosions were the accident chain initiator in the 57% of cases, and vapour cloud explosions (VCEs) were the specific scenario more frequently resulting in an escalation (84%). The number of fatalities per accident was also examined and resulted increasing in time.

Thus, the analysis of domino accidents carried out in previous studies allows evidencing that the number of severe domino scenarios, although decreasing locally e.g. in Europe, is increasing worldwide, and the severity of domino scenarios is also increasing. Specific scenarios, in particular pool fires and VCEs, seem particularly prone to trigger domino scenarios. Thus, the assessment of the vulnerability of equipment items to fires and explosions emerges as a key issue to explore in escalation assessment and in the analysis of domino scenarios.

2.3 Vulnerability models

2.3.1 Approach to the probabilistic modelling of Equipment Damage

A primary accident scenario usually propagates due to the failure of other storage or process units. Direct damage causing the loss of the structural integrity of secondary (target) equipment is the more frequent cause of accident propagation. Seldom, indirect effects are responsible of accident propagation (e.g. loss of control of the installation due to control room damage or evacuation, e.g. in the case of explosions or toxic releases) (Khan and Abbasi, 1998b). Thus, in order to have a domino effect the presence of an “escalation vector” is required: a vector of physical effects generated by the primary accident scenario, which causes its propagation.

The study of domino scenarios therefore requires the analysis of the relation between the physical effects of the primary accident and the potential damage caused on nearby units and equipment items. These relations are usually referred to as vulnerability models (Cozzani et al., 2005; Cozzani et al, 2013a). Since both the behaviour of the accident scenarios and the resilience of the target units are stochastic, studies on vulnerability models are performed in a probabilistic framework. The goal of vulnerability models is to calculate a damage probability as a function of the intensity of the physical effect and of the constructive characteristics of the targets. Many studies in the past used Probit-like models (Lees, 1996; Van Den Bosh et al., 1989) to relate the damage probability of a given target to the intensity of the physical effects (Eisenberg et al. 1975; Cozzani and Salzano 2004a; *Mingguang and Juncheng 2008*). Nevertheless, some authors apply different types of damage probability models. In the following, a list of contributions aimed at the assessment of escalation probability is reviewed. The discussion is divided in three sections, according to the physical effect which may be responsible for the escalation:

- Blast Waves
- Heat Radiation
- Fragment projection

2.3.2 Damage due to Blast Waves

In industrial accidents, blast waves may be generated by several different accident scenarios: vessel bursts, vapor cloud explosions (VCEs.), Boiling Liquid Expanding Vapor Explosions (BLEVEs) and condensed phase explosions.

The consequences of the blast load effects on a structure or equipment will depend on both the characteristics of the blast load and on the target characteristics such as: shape, size, mass and dynamic resistance. Equipment may be sensitive to static overpressure, dynamic pressure or a combination of both (Di Benedetto et al., 2010).

The correct approach to assess equipment damage due to a blast wave would require the application of finite element models. However, such resource-demanding deterministic approach needs a very detailed characterization of both the explosion scenario and the mechanical features of the target equipment. These are difficult to obtain, in particular due to the inherent uncertainties associated to the definition of the explosion scenario.

Thus, the use of simplified models and approaches is presently the main option for escalation assessment. The simplest approach for the assessment of damage to equipment caused by shockwave is based on threshold values or vulnerability tables. For a overpressure value that overcome the threshold value a damage probability one is assumed, while damage probability zero is assumed for overpressure values below the selected limit. However, no agreement exists among different authors on the threshold values that range from 7 to 70 kPa, depending on the different damage typology considered (vessel rupture, vessel displacement, connection displacement, etc...) (Cozzani et al., 2006).

Threshold values were also used in empirical models to develop probabilistic correlations for equipment failure: e.g. the model of Bagster and Pitblado (1991) who proposed the following correlation for equipment damage due to blast waves:

$$F_d = \left(1 - \frac{r}{r_{th}}\right)^2 \quad (2.1)$$

Where F_d is the damage probability, r is the distance from the explosion and r_{th} is the distance at which the predicted overpressure equals the threshold value for equipment damage. The formula implies that the probability of damage is 1 where blasting occurs, which may lead to strongly unrealistic results.

Simplified deterministic approaches are also proposed in the literature. The DIN standard 4119 (*Deutsche Norme (DIN) 4119, 1979*) proposes the use of Equations (2.2) and (2.3) to calculate the maximum value of pressure that vertical atmospheric storage tank can withstand before a relevant deformation takes place (the “buckling” pressure):

$$\Delta P_F = 0.135B \left(\frac{D}{H}\right) \left(10^4 \frac{W^o}{H_L}\right)^{2.5} W_U > 1.5W^o \quad (2.2)$$

$$\Delta P_F = 0.135 \left(\frac{D}{H}\right) \left(10^4 \frac{W}{H_L}\right)^{2.5} W_U \leq 1.5W^o \quad (2.3)$$

where W is the mean wall thickness, W_U the shell thickness in the upper tank section, W^o is the shell thickness in the lower tank section, D is the tank diameter, H is the height of the empty section of the tank, H_L is the liquid level height and B is a coefficient having a value around 2.

More recently, Probit-like models (Lees, 1996; Van Den Bosh et al., 1989) were used to relate the peak overpressure to the expected damage probability (Eisenberg et al., 1975):

$$Y_{blast} = a + b \ln(\Delta P^0) \quad (2.4)$$

where Y_{blast} is the probit value for equipment damage, ΔP^0 is the peak static overpressure (in Pa), a and b are the probit coefficients. From the probit value, probability is easily calculated (Lees, 1996; Van Den Bosh et al., 1989). The probit approach was first applied in the pioneering work of Eisenberg and co-authors, which proposed a general correlation for any type of equipment (*Eisenberg et al. (1975)*).

More recently, specific probit models for different categories of equipment were proposed by Salzano and Cozzani (2004a; 2004b). The study, necessarily based on several simplifying assumptions (far field, no directionality effects, etc.) pointed out the importance of considering the different characteristics of equipment categories for the reliable assessment of blast wave damage. More recently, a different fitting of the damage data used by Salzano and Cozzani to develop the probit correlations was proposed by *Mingguang and Juncheng 2008*, resulting in higher damage probabilities at lower pressure and lower probabilities at higher pressure than

those provided in the original probit models. Table 2.3 reports the coefficients for the Probit equation, provided by above cited studies. Salzano and Cozzani (2005) also coupled the probit models to simplified models for peak overpressure as a function of distance from the explosion centre and of explosion strength, thus providing simplified correlations allowing a straightforward estimation of damage probability and of safety distances for escalation effects.

Table 2.3 - Probit equation coefficients for the calculation of the damage probability due to overpressure, provided by different authors

Equipment	a	b	Reference
Atmospheric Vessels	-23.8	2.92	Eisenberg et al. (1975)
Atmospheric Vessels	-18.96	2.44	Salzano and Cozzani (2004)
Pressurized Vessels	-42.44	4.33	Salzano and Cozzani (2004)
Elongated equipment	-28.07	3.16	Salzano and Cozzani (2004)
Small equipment	-17.79	2.18	Salzano and Cozzani (2004)
Atmospheric Vessels	-9.36	1.43	<i>Mingguang and Juncheng 2008</i>
Pressurized Vessels	-14.44	1.82	<i>Mingguang and Juncheng 2008</i>
Elongated equipment	-12.22	1.65	<i>Mingguang and Juncheng 2008</i>
Small equipment	-12.42	1.64	<i>Mingguang and Juncheng 2008</i>

2.3.3 Damage due to Fragment Impact

Beside blast waves, explosions in the process industry may result in the projection of fragments or debris. The impact of projected fragments was documented as a cause of domino effect (Gledhill and Lines, 1998; Khan and Abbasi, 1998). Fragment projection is usually caused by internal explosions (physical explosions, confined explosions, BLEVEs, runaway reactions) causing the catastrophic failure of vessels and the transfer of part of the explosion energy to the projected fragments. Fragment may be projected very far from the collapsed vessel (up to more than 1km), and the projected fragments have the potential to trigger secondary accidents causing the loss of integrity of the target vessel. When a fragment hits a target vessel, it may pierce the vessel shell (perforation), stop at some depth of penetration (embedment) or bounce back (ricochet). Thus the target can be damaged either by penetration or by plastic collapse.

Most of the studies concerning fragment projection were dedicated to the assessment of the probability of fragment impact. Less attention to date was dedicated to the conditional probability of damage given the impact, that was usually assumed equal to one (damage always follows the impact).

The early work on the topic was mainly based on direct statistical analysis of accident data (CCPS, 1994; Scilly and Crowter, 1992). More recently, models based on the analysis of fragment trajectory were proposed. Two papers by *Hauptmanns (2001a; 2001b)* describe a probabilistic method, based on Monte Carlo simulations, for the assessment of fragment impact probability. The fragments trajectories are described by the basic equation of motion, but the critical parameters are discussed and analysed in detail. The initial fragment velocity is calculated as a function of the explosion energy (CCPS, 1994; Baum, 1998). The operating conditions and the filling level result as the more important parameter for the calculation of the explosion energy.

Fragment mass and number are also relevant, not only to calculate the distance of projection, by also to assess the energy received by each fragment. Other important parameters are the projection angles, for which a uniform distribution is assumed. The probability of impact is assessed as a function of distance and average kinetic energy received by the fragments.

Gubinelli et al. 2004, starting from the work of Hauptmanns (2001a; 2001b), developed an improved model, specifically aimed at the assessment of fragment impact probability on a target vessel. The model calculates the instantaneous velocity of fragments as a function of the angle of departure. On the basis of target distance and geometry, the range of departure angles leading to fragment impact is then calculated. The probability of impact is then assessed as the integral of the probability distribution function assumed for the projection angles in polar coordinated. In analyses the relations among the vessel geometry, the characteristics of the accidental scenario causing the vessel shattering into pieces and the shape and number of fragments generated. In this study the critical parameters of fragment shape, velocity and energy are discussed in detail. Successive studies by Gubinelli and Cozzani (2009a; 2009b), Tugnoli et al., (2014) based on the analysis of a database of 143 accidents in which vessel fragmentation and fragment projection took place, provided statistical correlations on fragmentation patterns on the basis of accident scenario and vessel features (Gubinelli and Cozzani, 2009a), on the drag factor and expected number of fragments generated (Gubinelli and Cozzani, 2009b) and on the probability distribution functions for the initial projection angles (Tugnoli et al., 2014). The overall approach resulting by this set of publications was recently applied to the detailed analysis of a past accident occurred in 1993 in the Milazzo refinery, in Italy (Tugnoli et al., 2014). The accident features were found to be coherent with the results of the application of the modelling approach, and the accident consequences resulted among those having a higher probability according to the model.

The development of 3D simulators allowed Nguyen and coworkers (Nguyen et al., 2009) to use improved Monte Carlo simulations to assess the probability of fragment impingement in a 3D environment. Several improvements with respect of previous study are introduced in this model: a non-uniform probability for the fragment initial direction is assumed and a model for fragment penetration in metal enclosure as a function of the fragment speed and mass is applied. This simplified analytical model calculates the penetration probability of fragments in the metal wall, considered as a rigid object, and is adequate only for small fragments having a high velocity at the instant of the impact.

Finally, a study by Zang and Chen (2009) presents a procedure for the calculation of fragment impact probability based on the work on Hauptmanns (2001) and of Gubinelli et al. (2004). Monte Carlo simulations were used for impact probability assessment and a new methodology for the calculation of expansion energy and of the initial fragment velocity is presented. Furthermore, the model identifies automatically all the possible targets based on the maximum fragment projection distance.

Thus, it may be concluded that in the case of damage due to fragment impact, more complex and less consolidated approaches are present. The rather low number of escalation accidents caused by fragment impact and the very high number of parameters that may affect fragment impact and damage hindered the development and validation of vulnerability models. Only recently, the systematic studies based on a relevant number of accident by Gubinelli and Cozzani, and the use

of improved simulation tools by Nguyen and Mebarki, overcome the scarcity of data and the limitations due to computational results. Still, further work is needed to improve the available models for fragment impact and damage resulting in escalation.

2.3.4 Damage due to Fire

2.3.4.1 Equipment damage caused by fire

Fire acts as a severe heat load on structures, capable to cause damage and failure of process units, storage vessels, pipework and pipelines. A massive heat flow investing a vessel can produce many dangerous effects: a lower mechanical resistance of the shell wall, an increase of the internal pressure, local thermal stresses, the melting of seals and other non-metallic components and it may ignite flammable vapours (e.g. of flammable vapours around the rim seal of floating roof atmospheric storage tanks). There are many different types industrial fires, but in the framework of escalation assessment four categories of industrial fires are relevant: pool fires, jet fires, flash fires, and fireballs (Uijt de Haag and Ale, 1999).

2.3.4.2 Time to failure of vessels under heat load

The results of the analysis of past accidents evidences that long-lasting stationary fires, as pool fires and jet fires are responsible of the large majority of escalation events in industrial accidents (Gómez-Mares *et al.* 2008). In such scenarios, the heat load is a combination of the heat transferred from the fire by radiation and convection. While the target equipment receives the heat load, the shell of the target vessel heats up and heat is transferred into the liquid and vapour lading. Thus, the wall temperature increases and consequently the internal fluid temperature rises. For typical steel vessels the strength of the material drops rapidly at temperatures above 700K. The heating effect is time-dependent, since the higher the exposure time, the higher the consequences. For this reason the escalation is usually delayed with respect to the initiating event. The time lapse between the start of the fire accident and the failure of target equipment damaged by the fire takes the name of time to failure (tff).

In fire accident scenarios relevant for escalation, the resistance of the target equipment needs to be specifically evaluated, taking into account the characteristics of the fire scenario and the actual exposure to fire. Hence, reliable tools for the prediction of the tff are required in order to determine the likelihood of escalation. However, modelling the failure mechanisms of equipment effected by heat load due to fires is a very complex and multidisciplinary task. Semi-empirical correlations and simplified criteria for estimation of the vessel failure were proposed in earlier studies (Moodie, 1988), while more recently more complex two-dimensional and three-dimensional (3D) models were developed (Hadjisophocleous *et al.*, 1990; Venart, 1986).

Early work on the topic was mostly dedicated to the analysis of pressurized vessels failure leading to BLEVEs. The study by *Moodie 1988* is aimed at the effects of fire engulfment due to pool fire. The work of Birk and co-workers (*Birk, 1988; 1995; 1996; Leslie and Birk, 1991; Birk and Cunningham, 1994*) addressed the experimental analysis of the catastrophic failure of liquefied gas stored in pressurized vessels engulfed by fire. Different heat loads are considered: pool fire engulfment, partial pool fire engulfment, jet fire impingement and distant heat radiation. The studies of Birk and Cunningham (1994) and Birk (1996) evidence the role of liquid temperature

stratification in conditions leading to pressure safety valve opening and in determining vessel time to failure. Temperature stratification consist in the formation of different temperature liquid layers. This phenomenon is due to a density gradient that creates as the liquid inside the vessel is heated and temperature rises non uniformly. Venart and coworkers 1993-2000 (Venart et al., 1993; You and Venart, 1996; Venart, 1999; 2000) also report important data and models for the determination of time to failure leading to BLEVE of pressurized vessels containing liquefied gas under pressure.

Based on these early studies, several lumped parameters models are now available in the literature for the assessment of the thermal response of both the vessel and its content when invested by a heat load (Landucci et al., 2009a; Birk, 2006; Persaud et al., 2001; Hadjisophocleous et al., 1990; Moodie, 1988; Graves, 1973; Forrest, 1985; Beynon et al., 1988; Birk, 1988; Ramskill, 1988; Birk and Leslie, 1991; Johnson, 1998; Shebeko et al., 2000; Salzano et al., 2003; Gong et al., 2004). These models are in general dedicated to the assessment of the resistance of horizontal cylindrical vessels storing liquefied petroleum gas (LPG) to engulfing fire, predicting the wall temperature rise and the vessel internal pressure.

More recently, the study of Raj (2005) aimed at modelling the effect of external non-engulfing pool fire on liquefied gas storage tanks. The main focus of this paper is to identify the heat transferred to the storage vessel shell by heat radiation in order to evaluate the vessel wall temperature rise with time. The study of Landucci et al. (2009b) also presents a model for the assessment of the failure conditions of LPG tanks exposed to external fire. The model describes the vessel wall using finite elements, for the description of the transient temperature and mechanical stress distribution on the entire vessel surface. Specific key performance indicators (KPIs) were introduced to identify safe operating zones and for the selection of the different coating design solutions.

2.3.4.3 Vulnerability models for vessels under fire load

The assessment of escalation possibility and/or probability in the framework of the risk assessment of complex industrial areas may require the assessment of hundreds of different fire scenarios. Thus, the use of distributed parameter models and even of lumped models may become critical in this context, requiring the collection of a huge amount of data and unaffordable computational resources.

Thus, simplified approaches might be preferred in escalation assessment carried out in the framework of quantitative risk assessment (QRA) studies. Rules of thumb were adopted to directly predict vessel failure conditions: e.g. in several studies escalation is considered as taking place if radiation intensity caused by the fire on the target vessel exceeds a threshold value (Cozzani et al., 2006; Health and Safety Executive, 1978; British Standards Institution (BSI), 1990; Mecklenburgh, 1985) or if the vessel wall temperature increases over critical values (Khan and Abbasi, 1998). More recently, simplified correlations, based on the results of models and empirical work, were developed for the calculation of the failure probability (Cozzani et al., 2006a; Landucci et al., 2009a; Landucci and Cozzani, 2009). A summary of threshold criteria is reported elsewhere (Cozzani et al 2013b).

More recently, a study by *Landucci et al. (2009a)* aimed at the development of Probit like correlation for the assessment of damage probability to storage tanks both atmospheric and pressurized. The model is based on a simplified correlation for the assessment of the time to failure of the target equipment (ttf):

$$\ln(ttf) = c \log_{10}(I) + d(V) \quad (2.5)$$

Where I is the thermal radiation c is a constant and d is an analytic function of the vessel volume, V . Several fire conditions and tank sizes were tested to derive the correlation, that was validated using both experimental results and results of finite element models. The probability of failure is then calculated comparing the ttf with the time of response of the fire-fighting system (tte). A Probit model is obtained applying a lognormal probability density function to the tte (*Landucci et al. (2009a)*):

$$Y = 9.25 - 1.85 \ln(ttf) \quad (2.6)$$

The Probit value Y is then easily converted to the value of the vessel failure probability. Recent developments allow including specific features of the site emergency procedures and of fire protection barriers may be integrated in the approach.

2.4 Quantitative Risk Assessment and Safety Management

2.4.1 Key steps and level of detail of domino scenario assessment

Risk assessment and safety management are mandatory requirements for the installations dealing with hazardous materials. In recent years, several methodologies were proposed for the assessment of risk due to domino scenarios. Domino events are the result of a complex propagation and escalation process of a primary event. For this reason, specific methodologies are required for the analysis of the hazard, potential damage and risk to human being that may derive from this category of accidents.

The procedure for the identification and evaluation of domino scenarios demands for a detailed analysis of the consequences of the primary scenario and of the potential structural damage caused to secondary targets. Equipment vulnerability models are the tool more used to allow the assessment of probability and intensity of secondary scenarios.

The specific analysis required by domino scenarios may be divided in two main stages: the assessment of the escalation vector generated by the primary scenario and the assessment of possible escalation effects. In this framework, two key elements in domino scenario assessment are the evaluation of escalation probabilities and consequences following the failure of the identified secondary targets.

A detailed analysis of all the possible domino scenarios may be very complicated and time consuming. Thus, domino assessment may be carried out at different levels of detail, depending on the context and aims of the analysis. In the following, the state of the art of procedures for preliminary hazard analysis and quantitative risk assessment is briefly summarized.

2.4.2 Preliminary Hazard Analysis of Domino Scenarios

A preliminary hazard analysis (PHA) may be useful to identify the presence of hazards related to domino scenarios and to screen the critical escalation sources and targets. A qualitative assessment of escalation hazards is required in this framework. The possibility of accident escalation may be carried out on the basis of a simplified assessment of primary scenarios. The possibility of escalation may be assessed comparing the escalation vector (namely, the intensity of the physical effects generated by the primary scenario at the position of a potential target vessel) to an escalation threshold. Escalation thresholds are tabulated values of physical effects (e.g. a maximum peak overpressure for blast waves or a radiation intensity for a fire) below which no damage to the target item is expected. However, caution is needed when using this simplified assessment, since escalation thresholds represent an oversimplification of the escalation process. In the study of Cozzani et al. 2006, equipment failure conditions using threshold values are examined in detail. Accident scenarios that can trigger the escalation process are presented, and both explosion and fires are analysed. If fire is the primary scenario, the time evolution of the fire scenario needs to be taken into account, comparing the duration of the primary scenario with the characteristic “time to failure” (ttf) of the target equipment involved in the fire. In the case the fire duration exceeds the ttf, escalation is possible. When explosion is the primary scenario, the target equipment shape and size are found to be determinant for the assessment of possible damage. An example of escalation thresholds derived from this analysis is provided in Table 2.3.

Table 2.3: Probit equation coefficients for the calculation of the damage probability due to overpressure, provided by different authors

Equipment	a	b	Reference
Atmospheric Vessels	-23.8	2.92	Eisenberg et al. (1975)
Atmospheric Vessels	-18.96	2.44	Salzano and Cozzani (2004)
Pressurized Vessels	-42.44	4.33	Salzano and Cozzani (2004)
Elongated equipment	-28.07	3.16	Salzano and Cozzani (2004)
Small equipment	-17.79	2.18	Salzano and Cozzani (2004)
Atmospheric Vessels	-9.36	1.43	<i>Mingguang and Juncheng 2008</i>
Pressurized Vessels	-14.44	1.82	<i>Mingguang and Juncheng 2008</i>
Elongated equipment	-12.22	1.65	<i>Mingguang and Juncheng 2008</i>
Small equipment	-12.42	1.64	<i>Mingguang and Juncheng 2008</i>

Cozzani et al. 2007 discuss the role of inherent safety criteria to prevent accident escalation, based on a detailed consequence analysis of each possible scenarios that may trigger the escalation. Safety distances are calculated based on the fireball radii, jet-fire flame length, pool fire radii, overpressure effect, based on the operative condition and generic characteristic of the substance. Using the safety distance criterion, safe and unsafe regions can be identified in lay-outs, and accident mitigation and domino prevention can be addressed by inherent safety criteria, increasing the distance among the different unit or limiting vessel hold-up.

2.4.3 Quantitative Risk Assessment of Domino Scenarios

When a relevant hazard due to domino scenarios is detected, a more detailed risk assessment is needed. Quantitative Risk Assessment (QRA) is nowadays used as a standard tool to analyze and compare the risk due to industrial installations (Lees, 1996; CCPS, 2000). Despite the fact that QRA is a mature and consolidated tool, only few applications to domino effect have been performed. Domino effects are usually excluded from QRAs in common professional practice, due to the fact that quantitative assessment of domino scenarios requires high computational resources that were not available or not easy to accessible until recent years. Actually, the quantitative risk assessment of domino scenarios is a complex industrial installation or in an industrial cluster, a huge number of possible scenarios need to be considered. It was demonstrated that for each primary scenario which is able to target n equipment items, up to 2^n different domino scenarios are possible (Cozzani et al., 2005).

The inclusion of domino scenarios in framework of quantitative risk assessment was addressed in several studies (Delvosalle, 1998; Khan and Abbasi, 1998; Abdolhamidzadeh et al., 2010; Reniers et al., 2005; Cozzani et al., 2005). Specific methods (Abdolhamidzadeh et al., 2010; Reniers and Dullaert, 2007; Cozzani et al., 2005) were proposed for the calculation of individual and societal risk (Lees, 1996; CCPS, 2000) caused by domino scenarios. In recent years, methods and models become available to allow the quantitative assessment of domino accidents in a QRA framework, supported by specific software tools based on geographic information systems (Cozzani et al., 2006). Further progress in the field allows the frequency assessment of multilevel escalation scenarios, e.g. by the use of statistical tools such as Bayesian analysis (Khakzad et al., 2013) and Monte Carlo simulations (Abdolhamidzadeh et al., 2010). More recently, a procedure based on acyclic graphs was also proposed and would be further discussed in chapter 6. The discussion of

such approaches is needed to understand the state of the art of domino risk assessment. For this reason, details regarding the proposed approaches to the QRA of domino scenarios will be presented in the following, starting from the tools dedicated to allow the inclusion of domino scenarios in conventional QRA procedures.

Efforts to develop quantitative methodologies for the assessment of domino accidents are documented since the early 1990s. Bagster and Pitblado (1991) described an approach for the inclusion of domino events in risk assessment. The procedure is based on the evaluation of the domino scenario as an external event, which increases the frequencies of corresponding incidents, evaluated according to conventional methodologies (fault trees analysis). Several other authors addressed the specific topic of the inclusion of the domino effect in QRA during the '90s developing risk assessment methodologies (Delvosalle, 1996; Contini et al., 1996; Gledhill and Lines, 1998), focusing the specific issue of the escalation frequency assessment (Pettitt et al., 1993) and analysing the escalation triggered by fires (Latha et al., 1992; Morris et al., 1994). At the time, oversimplified vulnerability models were used (Bagster and Pitbaldo, Khan and Abbasi) for the assessment of domino escalation probability (P_d). The domino event frequency was then calculated as follows:

$$f_{de} = P_d f_p \quad (2.7)$$

where f_{de} is the domino event frequency and f_p is the frequency of the primary accident that triggers the accident chain. The domino frequency is used to update the accident frequencies of conventional accident scenarios:

$$f_{se} = f_{de} + f_{pe} \quad (2.8)$$

where f_{se} is the overall event frequency that include escalation as a cause of the scenario, and f_{pe} is the frequency of the primary event only. There is general agreement that such methodologies are insufficient to describe all possible domino accident scenarios and that more research was needed at the time in order to fulfil the scientific and technical gap that prevent an exhaustive analysis of such complex phenomenon.

The work by Khan and Abbasi (1998a) had the aim to track a procedure for Domino Effect Assessment (DEA) within quantitative assessment of risk in the chemical and process industry. The proposed methodology was introduced in the software tool "DOMIEFFECT" (Khan and Abbasi, 1998a), a tool of the "MAXCRED" software for risk analysis (Khan and Abbasi, 1997). DOMIEFFECT enabled its users to understand the likelihood of domino effect in an industrial lay-out, the identification of the most probable accident scenarios, and the expected consequences of the different domino scenarios (Khan and Abbasi, 1998). The tool was aimed at supporting the decision making toward strategies aimed at the prevention of domino effect. Thus, one of the major issues was the assessment of escalation probabilities for simple and/or complex accidental scenarios, in particular for the possible secondary accidents with the worse consequences on humans, as toxic releases. A list of possible escalation vectors and of the critical parameters identified is presented in Table 2.4.

Table 2.4: Escalation vectors and critical parameters identified in the study by Khan and Abbasi (1998b).

Damage typology	Possible Mechanisms	Important parameters
Thermal damage	Heat radiation Convection	View factor: flame slope, distances, position, orientation Air Transmissivity*** Transient flame temperature, velocity and emissivity <i>Vessel shape</i> <i>Hot spots</i>
Overpressure	<i>Shock Overpressure Pulse</i> <i>Drag force</i>	<i>Overpressure absolute</i> <i>Overpressure difference between the object front and back</i>
Missile	<i>Impact</i>	<i>Fragment velocity</i> <i>Shape</i> <i>Kinetic energy</i> <i>Penetrative capability</i> <i>Direction</i>

The proposed approach has the following main features: i) estimation of all possible hazards from toxic release to explosion; ii) handling of interaction among different accidental events (generation of domino or cascading accident scenarios); iii) estimation of domino effect probability; and iv) estimation of domino effect consequences. The DOMIEFFECT model and approach allows the identification the most critical scenario, in order to select and design effective safety measures. Several illustrative applications of DOMIEFFECT were carried out, considering refineries, petrochemicals plants (Khan and Abbasi, 2001a) and chemical or fertilizer production units (Khan and Abbasi, 2001b).

The growing concern on domino effect was highlighted in Europe by the Seveso Directives (Directive 82/501/EEC and 96/82/EC). Several research projects were promoted aiming at the improvement of tools for the assessment of domino effect. Among the more important results, Delvosalle et al. (2002) proposed a methodology to assess the probability of domino effect inside an industrial site (internal domino effect) or between different establishments (external domino effect). The methodology was compiled in a software package called Domino XL 2.0, which aimed at the assessment of possible domino effects in the Seveso industries and which can also be used as a safety tool in these industries (Delvosalle et al., 2002).

In 2005, Cozzani et al. (2005) presented a methodology that allows the calculation of individual and societal risk caused by domino accidents contribution in the risk profile of an industrial plant, providing for the first time a procedure for the quantitative assessment of domino effect within QRA studies. Domino effect calculation is based on several sequential steps. The detailed assessment of primary events is required (frequency and consequence assessment), as well as the position of the primary accident source on the layout, and the assessment of the possible secondary scenario consequences. Once the primary events are characterized, it is possible to associate a single escalation vector and a single vulnerability vector to each scenario. Domino accident frequencies are calculated as follows:

$$f_{de} = f_{pe}P_d = f_{pe}P(E|PE) \quad (2.9)$$

where f_{de} the domino event frequency, f_{pe} is the primary event frequency, P_d the secondary target vulnerability and $P(E|PE)$ is the conditional probability of escalation (E) given the primary event (PE). The probability of accident escalation is calculated by the use of dedicated vulnerability models (Cozzani and Salzano 2004a; 2004b; Landucci et al. 2009; Gubinelli and Cozzani, 2009a; 2009b). In a complex layout, usually a single primary event may be able to trigger several

secondary events simultaneously. In this case, the probabilities of accident escalation are mutually conditioned and all the possible combinations of the credible and relevant secondary events should be considered in the analysis. Each accident combination represent one possible domino scenario. Therefore the probability of all accident combination must be calculated in order to assess the risk related to escalation scenarios for a given primary event. If first level escalation is considered (Reniers and Cozzani, 2013b), the event combinations may be reasonably considered as independent from a probabilistic point of view. Therefore, if N secondary events are possible, the probability of a secondary scenario given by a generic combination m of k secondary events ($k \leq N$) is the following:

$$P_d^{(k,m)} = \prod_{i=1}^N [1 - P_{d,i} + \delta(i, J_m^k)(2 \cdot P_{d,i} - 1)] \quad (2.10)$$

here $P_{d,i}$ is the probability of escalation for the i -th secondary event defined by Eq.(9), J_m^k is a vector whose elements are the indexes of the m -th combination of k secondary events, and the function $\delta(i, J_m^k)$ is defined as follows:

$$\delta(i, J_m^k) = \begin{cases} 1 & i \in J_m^k \\ 0 & i \notin J_m^k \end{cases} \quad (2.11)$$

If k is the number of contemporary secondary accidents, the total number of domino scenarios in which the primary event triggers k contemporary secondary events is:

$$v_k = \frac{N!}{(N-k)!k!} \quad (2.12)$$

Therefore, the total number of different domino scenarios that may be generated by the primary event is:

$$v = \sum_{k=1}^N v_k = 2^N - 1 \quad (2.13)$$

where v is the total number of domino scenarios that need to be assessed in the quantitative analysis of domino effects. Cut off criteria based on frequency values may be applied to limit the secondary scenarios (Antonioni et al 2009; Cozzani et al 2006).

In the original framework proposed by Cozzani et al. (2005; 2006), only domino scenarios deriving directly from the primary events are considered. Thus, only first level escalation is considered and scenarios deriving from the further escalation of secondary events (the so called multilevel-escalation (Cozzani et al., 2013 DB)) is not considered. However, it was recently demonstrated that the approach presented above may be extended to assess higher level domino events (Cozzani et al., 2014; Antonioni et al., 2009).

The assessment of the consequences of complex domino scenarios with multiple secondary events was also afforded by Cozzani and coworkers (Cozzani et al., 2005; Cozzani et al., 2004 ESREL). Models created for the assessment of consequences used in the framework of risk analysis are not conceived to assess the effects of multiple simultaneous events (e.g. several pool and/or jet fires, etc.). Thus, the proposed methodology evaluates the consequences of complex scenarios superimposing the physical effects of each separate event (radiation, overpressure, toxic gas concentration) that compose the specific combination of a given domino scenario. This procedure, which neglects the assessment of possible synergetic effects, is obviously an oversimplification of the problem. Nevertheless, this approach seems acceptable if compared to other approximation present in a QRA framework. For each primary and secondary accident in the complex scenario, a "vulnerability map" is provided (Leonelli et al., 1999). In each position on a map, the vulnerability

of an exposed individual with respect to a domino scenario (V_d) may be calculated as a combination of the vulnerabilities caused by the physical effect of the single events that compose the domino scenario. Vulnerability may thus be calculated according to the following equation:

$$V_d^{(k,m)} = \min\left[V_p + \sum_{i=1}^n \delta(i, J_m^k) V_{d,i}, 1\right] \quad (2.14)$$

In other words, the combined vulnerability is a sum of the death probabilities due to all the scenarios that compose the domino sequence, limited to 1. In order to actually calculate the vulnerability values and obtain vulnerability maps for domino scenarios, the domino methodology was introduced in a GIS software tool for QRA (Cozzani et al 2006): the ARIPAR-GIS software (Egidi et al., 1995). The results obtained allowed the calculation of individual (Cozzani et al., 2005) and societal risk (Cozzani et al., 2006), and highlighted the great influence that domino scenarios and escalation may have on the risk profile of an industrial activity. A more recent application to an industrial park evidences that the methodology can be applied also to assess domino threat between different industrial installations or within an industrial cluster (Antonioni et al., 2009).

The requirements in terms of computational resources required by the extension to the proposed methodology to the quantitative assessment of higher level domino scenarios (Cozzani et al., 2014) supported the investigation of alternative approaches to the assessment of domino scenario frequencies. The study by Abdolhamidzadeh et al. (2010) presents a methodology based on Monte Carlo simulations aimed at the assessment of domino scenarios frequencies in industrial facilities. The edge of Monte Carlo simulations is the possibility to avoid the complexity of calculating conditional probabilities necessary to account for domino accident scenarios and allow the use of independent probability relations. For this reason, the procedure was proposed also to assess accident frequencies of multilevel domino scenarios. The study of *Bernachea et al. (2013)* is aimed at the description of a methodology to assess the risk of domino accidents using an advanced event tree method. Each equipment item is analysed considering all the possible releases and per every release all the possible scenarios are considered. Depending on the consequences of the primary accident scenario on the target, rules are set to identify the probability of damage and the expected reference releases. The reference release causes different scenarios, and each can trigger other accidents in adjacent units. The procedure iteratively continues until all equipment are considered. In this approach simultaneous events are not considered, and each scenario is considered singularly.

As an alternative to conventional frequency assessment and Monte Carlo procedures, Bayesian networks may be applied. A Bayesian network can be represented as a directed acyclic graph, a graphical tool for reasoning under uncertainty in which the nodes represent variables and are connected by means of oriented arcs. The arcs denote dependencies or causal relationships between the linked nodes, while the conditional probability tables assigned to the nodes determine the type and strength of such dependencies. In the study of *Khakzad et al. (2013)* a methodology based on Bayesian Networks for the assessment of the probability of escalation from one unit in which a primary accident occurs to other units in the plant is presented. It is intended as a supplement for QRA, since it allows the calculation of domino accident frequencies. The propagation pattern of the first level domino scenarios is identified evaluating the equipment vulnerabilities using Probit functions (Cozzani and Salzano 2004a). The escalation probability is

then obtained by Bayesian Networks. Using the chain rule and the d-separation criterion, a Bayesian network expands the joint probability distribution of a set of linked nodes. One crucial step for the simplification of the propagation pattern construction, which may become more and more complicated as the number of equipment increases, is the identification of the “more likely” direction for the propagation pattern between the primary accident to the second, from the second to the third, and so on. By the use of this hierarchical approach, the interdependencies between the accident are described and the “conditioned” direction of the propagation pattern is drawn. An example of Bayesian network is provided in Figure 2.3; the joint probability distribution of the events contributing to the combination $U = \{X_1, \dots, X_6\}$ is given by Eq. (2.15):

$$P(U) = P(X_1)P(X_3|X_1)P(X_2|X_1, X_3)P(X_4|X_1, X_3)P(X_5|X_2, X_3)P(X_6|X_3, X_4) \quad (2.15)$$

The great flexibility of Bayesian Network application can lead to a further improvement of the model, by the identification and evaluation of contemporary and sequential events.

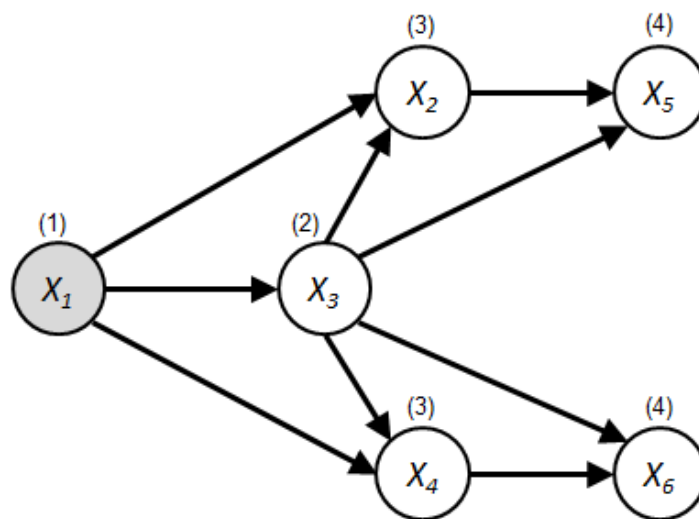


Figure 2.3: A likelihood propagation pattern of escalation in a process plant composed by six units (a unit where the primary scenario happens, X_1 , and five possible target units, X_2 to X_6). The possible sequential order is represented by the numbers in parenthesis (1 to 4). (Khakzad et al., 2013).

In the study of Antonioni et al. (2009) the proposed methodology for domino accidents was modified to allow the quantitative assessment of NaTech events triggered by earthquakes and floods. A combinatorial evaluation, similar to the procedure used for domino effect, was proposed to assess the probability and consequence of contemporary accidents (Campedel et al., 2008, Antonioni et al., 2007). A recent contribution (Cozzani et al. 2014) highlights the analogy between the assessment of domino scenarios and technological effects of natural disasters (Natech scenarios). In perspective this may lead to a comprehensive assessment of cascading events in technological systems.

2.4.4 Safety management and accident prevention

Two basic elements are required for a domino escalation to take place: a primary scenario with enough energy to damage one or more than one “domino target units” and the presence of at least one “domino target unit” within the reach of the primary scenario. Acting on the plant and lay-out design is a possible route to affect both the elements. The severities of the primary and

secondary scenarios depend, among the other, on the inventory of hazardous substances, on the operating conditions, and on the unit size and design features. All these are key elements which can be managed in order to reduce the effect of accident scenarios and therefore the likelihood of escalation. The presence and position of target units, which also influences the escalation process, depend on the plant siting and layout design. Since the very beginning of process industry, distances among the units composing an industrial facility were applied in the layout design, in order to avoid the spread of industrial accidents (*Mecklenburgh, 1985; Mannan, 2005*). Therefore, adequate measures implemented in the design phase may result in safer plants from the point of view of escalation. Design optimization tools mainly focus on economic aspects, even if safety issues have been considered in some recent works (*Díaz-Ovalle et al., 2010; Jung et al., 2010; Jung et al., 2011; Nolan and Bradley, 1987; Penteado and Ciric, 1996; Patsiatzis et al., 2004*). Several tools can be applied in order to anticipate safety issues related to the prevention of escalation in layout design. One example is the application of safety indicators, aimed at the identification of escalation hazard and of the optimal layout configuration (*Tugnoli et al., 2007; 2008a; 2008b; 2012*). Increasing the safety of process plant with respect to domino accidents is a multidisciplinary subject which includes elements of security management (*Reniers et al., 2008*), loss of containment prevention (*Reniers and Dullaert, 2007*), emergency planning (*Reniers et al. 2005a*), fireproofing design (*Di Padova et al. 2011; Tugnoli et al., 2012*) and personnel training. The role of the research in the understanding of escalation phenomenon allowed the development of methodologies for the prevention of domino accidents. In this section, recent studies concerning different aspects of safety management and safety design of industrial facilities related to escalation and domino risk management are presented.

As discussed above, the specific features of the accident scenario and of the target may play an important role in the escalation potential and deserve a throughout discussion. The minimum segregation distance between units required to avoid an escalation event is called “safety distance”. If threshold values for escalation are available (*Cozzani et al. 2006*), the safety distances may be easily calculated by the application of standard literature models for consequence assessment (*CCPS, 1994; Uijt de Haag and Ale, 1999; Van Den Boshet al, 1989*).

An application of such concepts was carried out by Di Padova and coworkers (*Di Padova et al., 2011*), that aimed at the development of a risk-based methodology for the identification of fireproofing zones applied to protect assets. The methodology was extended to specifically address domino effect prevention, also introducing key performance indicators for inherent safety assessment (*Tugnoli et al 2012*])

The potential role of inherent safety in the prevention of escalation leading to domino scenarios was first evidenced by Bollinger and coworkers (*Bollinger et al., 1996*), that state that it is possible to reduce (or even to eliminate) the domino propagation by inherently safer design, to limit its effects by engineered barriers (passive or active systems) and/or to manage accident escalation by appropriate procedural safeguards. The application of an inherent safety philosophy leads to several advantages, highlighted by Kletz (*Kletz, 1978; 1991; 1998; Kletz and Amyotte, 2010*) and other studies (*Bollinger et al., 1996; Hendershot, 1997; Hurme and Rahman, 2005; Khan and Amyotte, 2003*). The optimum application of inherent approach to domino prevention is at the early stage of plant design. The study by *Cozzani et al. (2007)* discusses the role of inherent safety criteria to prevent accident escalation, based on a detailed consequence analysis of each possible scenarios that may trigger the escalation. Safety distances were calculated based on the fireball radii, jet-fire flame length, pool fire radii, overpressure effect, based on the operative condition and generic characteristic of the substance. Using the “safety distance” criterion, the safe and unsafe regions in a plant footprint can be identified. Then, different solutions for accident mitigation and domino prevention can be compared, using the inherent safety criteria. For

instance where possible increasing the distance among the different unit could be economically convenient or in other cases the hold-up reduction could be a suitable solution, instead.

Cozzani and coworkers (Cozzani et al., 2007, 2009; Tugnoli et al., 2008a) also analyzed the application of a set of classical inherent safety guide words (intensification, moderation, substitution, simplification and limitation of the effects) to the layout definition activities. Tugnoli and coworkers (Tugnoli et al. 2008a; 2008b) provide a methodology for the application of inherent safety criteria for the improvement of the safety of an industrial facility dealing with hazardous materials by lay-out optimization. The Integrated Inherent Safety Index (I2SI), developed by Khan and Amyotte (2004; 2005), was used to implement inherently safer solutions, also accounting for domino scenarios.

Inherent safety criteria have been quantified by the use of dedicated indicators (Cozzani et al., 2009). The indexes provide useful information on the potential hazard of escalation events: critical sources as well as critical targets of escalation events could be identified. The application of indexes allows a fast assessment of the effect of different solution and can be used for streamlined decision-making, providing a useful support for risk based methodologies for design and cost benefit analysis.

Domino scenarios due to events originating outside the area of the facility may be indicated as external domino effects. The risk management of this particular type of hazard needs the involvement of personnel from different plants and a detailed exchange of information. As a consequence, specific tools are required for the identification and management of thiOs type of domino scenarios, due to implicit difficulties in information exchange, coordination and communication between different companies. Reniers et al. (2005a) remark the importance of cross-company cooperation for domino risk reduction. Hazwim, an economically viable External Domino Accident Prevention (EDAP) framework used for structuring cooperation between neighbouring enterprises was developed to this purpose (Reniers et al. 2005b). After the preliminary assessment of domino hazard by the use of conventional risk assessment methods, inter-company risk assessment procedures are carried out using simple methods: HazOp, What if and Risk Matrices. This methodology allows companies to be aware of the risk due to neighbouring industrial facilities and to properly manage risk due to external domino events.

Reniers and Dullaert (2007) have elaborated a 10-step methodology to prioritize domino effects in an industrial area. Based on the Oil&Gas producer model for human factors, three dimensions are identified: People, Procedures and Technology. Measures can be taken in these three dimension to avoid and to prevent industrial accidents, and to mitigate their consequences.

Reniers and coworkers (Reniers et al. 2009; Reniers 2010) also propose the use of game theory as a tool to analyse external domino hazard from a management point of view. The theory is based on the assumption that the risk of an industrial plant is not only function of the decision taken inside the plant, but also of the decisions taken by the other plants in the industrial cluster. Furthermore, decision taken outside the plant may affect, not only the overall safety, but also the decision taken inside the plant. The study analyses this situation as a so called "game", in particular the possible conditions that lead every company (player) to invest on safety (win) are searched (Nash equilibrium). The push for every company to invest in domino prevention is described in terms of prevented economic loss. The study demonstrates that the conventional methods for cost benefit analysis may be insufficient to evaluate the convenience of one investment on domino prevention, because the effect of one investment reflects on the other's company choices and therefore may result in a higher (or lower) benefit than predicted, depending on the mutual relation between the companies.

2.5 Discussion

2.5.1 Vulnerability models and uncertainties affecting escalation probability

All the available vulnerability models are important tools to assess equipment vulnerability, but by concept are simplified models, thus suffering of large uncertainties. It is worth to remark that the failure of a vessel is a deterministic event, in the sense that for a given accident scenario and a given target, equipment damage and accident escalation takes place or not. The idea of an “escalation vector” and of an “equipment vulnerability” are intended to take into account by a probabilistic approach the inherent knowledge gap regarding actual primary scenario that will take place and the uncertainties in the escalation process. The so called “damage probability” is therefore obtained from the simultaneous application of deterministic damage models and of probabilistic approaches to primary scenario selection, and introduce also the related uncertainties in the analysis.

Some of the vulnerability models available in the literature focus on the maximum intensity of the escalation vector at the position of the target equipment, but this is only one of the variables to account in the damage of an equipment item. In fact, also the direction, the transient behaviour, the environment and the safety measures play a determinant role on the chances to damage other units. Moreover, the target may undergo many different operating conditions during its operative life, thus different responses to the same accidental scenario may occur, due to process variables (pressure, temperature, liquid fraction, etc...) and due the ageing/corrosion of construction material that cause a reduction of resistance with the time (Susan et al., 2005).

A qualitative collection of the uncertainties that rule the damage and the vulnerability of process equipment is reported in Figure 2.4. Figure 2.4 shows the more important parameters that affect equipment damage and divides them in three areas: parameters of the accident, parameters of the target, and parameters of the safety barriers. The description of such parameters according to their role on the escalation potential could be of large interest: dividing the parameters into independent categories may allow the specific study of domino effect separating the different contributions deriving from each category. without influencing aspects of the other category. Figure 2.4-b shows a tentative definition of three main categories that represents the three main contributors to vulnerability calculation and that may include all the parameters defined in figure 2.4-a:

- **Escalation potential** of an accident represents its severity and its capability of cause damage to nearby equipment. It depends on accident variables only. In particular, it is a function of the accident severity (the intensity of the physical effect against the distance) and of the accident duration. The escalation potential concept can be expressed as a map of the area of impact of the physical effect generated by the primary scenario. The analysis of accident consequences is required to retrieve this information. Even though there are large uncertainties on physical effects calculations, due to simplified model assumptions and to uncertainties in the source term that should be considered, it is a common practice to assume these variables as deterministic, although a probability or expected frequency may be associated to the actual generation of the escalation vector. It is important to

remark that the escalation potential of secondary accident scenarios to involve undamaged equipment items is strongly dependent on the damage mechanism (Birk et al., 2007; Venart 1993) and on the LOC type (Bernachea et al., 2013).

- **Target exposure** represents the portion of the accident potential that actually affects the target. Distance from the source, target shape and orientation have a dominant role on vulnerability assessment. Safety barriers and emergency response time also effect the exposure of the target to the hazardous effect, as well as the presence of other structure, equipment, walls and bunds. All these effects may reduce significantly the chances of equipment damage. Also the installed fire fighting system and the time to response of the plant to the play a critical role on the vessel damage probability (Landucci et al., 2009). Even though target shape and orientation are deterministic data, the physical effect intensity (that may be influenced by wind speed and direction (Raj; 2005)), the response time and the fire fighting system reliability are probabilistic variables. Lay-out data are necessary to obtain these information, and a detailed knowledge of safety management system is required. Most studies on accident escalation introduce conservative assumptions to reduce the parameters actually used for the calculation of equipment vulnerability.
- **Target resistance** depends on target structure and represents the capability to withstand a given physical effect. It depends on the equipment size, on the mechanical properties of the construction material (Susan et al., 2005), on the operating conditions and on the presence of protections as passive fireproofing materials used for fire protection (Di Padova et al. 2011; Tugnoli et al. 2012). The resistance of target equipment items may be obtained experimentally or simulating the effect of fire, explosion or missile impact on the target equipment by simplified or finite element models (Landucci et al., 2009a; 2009b). On one hand, target volume, mechanical properties and protections are mainly deterministic data, even though uncertainties may be present due to material corrosion and ageing. On the other hand, operating conditions, as the filling level of a tank, may be considered stochastic variables.

The type of damage experienced by target equipment in an escalation scenario depends on both the target features (e.g. the equipment size, shape, construction material) and the operating conditions and the accident characteristics (e.g. engulfing fire, peak overpressure, distances). Depending on the damage mechanism, the relation between the uncertainties changes, thus the probability of damage and the consequences of secondary accidents change as well (Birk et al 2007; Roberts 2000). In particular, in the case of pressurized vessels the fragmentation pattern could be totally different, changing the damage mode (Leslie and Birk, 1991; Susan et al., 2005). The future work on vulnerability models will benefit if different damage mechanisms will be accounted, with different models addressing the different types of failure.

Even though the complexity of the domino accident requires complex models for dealing with multiple uncertainties, the main application for vulnerability models is the QRA, which demands

for simple and fast calculation methods due to the large number of possible accidental scenarios that must be processed. Although the further progress of vulnerability models is on its way, existing vulnerability models provide a sufficiently detailed conservative assessment of damage probability, suitable for the calculation of risk due to domino scenarios in a QRA study.

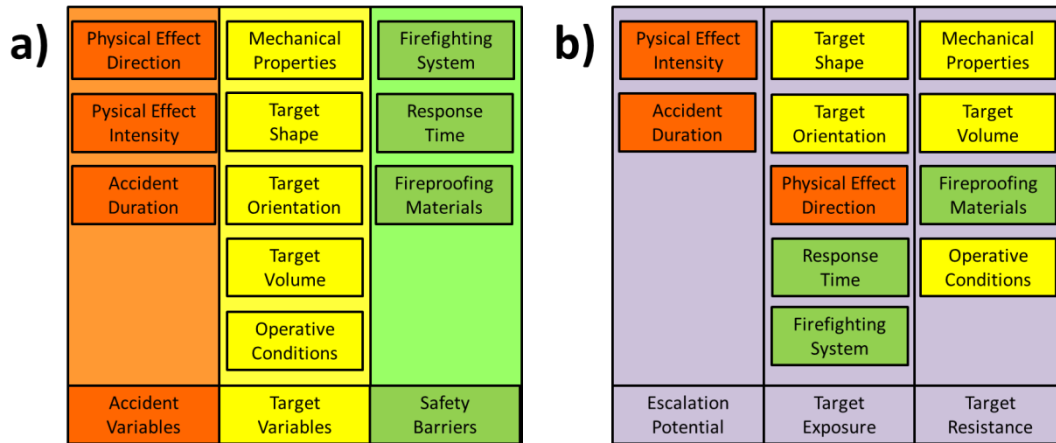


Figure 2.4 Lists of variables which effects the equipment vulnerability; a) grouped according to their source; b) grouped according to their actual contribution to the equipment vulnerability

2.5.2 Risk Assessment

In the past several methodologies were proposed for the assessment of risk caused by domino scenarios. The different studies focused on four main tasks: the identification of domino scenarios, the assessment of escalation frequencies, the calculation of human lethality due to complex domino scenarios and the assessment of equipment vulnerability.

The very first studies on the quantitative assessment of domino scenarios (Khan and Abbasi, 1998a; Delvosalle, 1996; Bagster and Pitbaldo, 1991) considered the secondary accidents as independent scenarios, therefore only their frequency and their consequences were considered for the assessment of risk. Simple “domino chains” were considered (a primary event causing a single secondary event, that may further escalate causing a tertiary event, and so on). Such methodologies, used since the beginning in the assessment of domino effect, are still used to date. Their main limitation is that the consequences of secondary scenarios are not considered simultaneously. As an example, DOMIFFECT (Khan and Abbasi 1998b) is not capable of dealing with potential synergic effect of secondary accidents. Actually, simultaneous events affecting more than one unit need a specific approach to consequence and damage assessment, and existing software cannot be directly used to such purpose. Domino XL 2.0 (Delvosalle et al., 2002) is specifically focused on the identification of critical equipment and on the assessment of the effectiveness of safety systems with respect to domino effects by the use of relative factors, but does not address multiple scenarios. A few methodologies are aimed at the calculation of the frequencies of combined simultaneous secondary accidents. In particular, the methodology proposed by Cozzani and coworkers (Cozzani et al., 2005; 2006, Antonioni et al., 2009) allows the identification and assessment of all the possible first level domino scenarios involving the simultaneous failure of secondary units. The combinatorial procedure itself is conceptually simple,

and it has been automatized by the use of a dedicated GIS software (Egidi et al. 1995), allowing model application to industrial clusters and industrial parks (Antonioni et al., 2009).

An extension of the methodology to consider higher domino level was demonstrated (Cozzani et al., 2014). Unfortunately, the application of combinatorial analysis is demanding for second or higher level domino scenarios, due to the huge number of event combinations that should be considered and to the calculation resources needed. Therefore, combinatorial analysis has been applied only for the calculation of first level domino scenarios (Cozzani et al. 2005; 2006). The extension of domino assessment to higher level scenarios may benefit in perspective of dedicated mathematic formulations for domino frequency estimation.

A proposal for the calculation of domino accident frequencies is the application of Bayesian networks for the calculation of accident escalation probabilities (Kharzad et al., 2013). This methodology is capable to assess frequencies of complex accidental scenario and is used for the assessment of second and higher level domino based on the identification of the most probable secondary target and accident scenario. However, one of the largest model limits is that the most likely escalation pattern is not always immediate to identify. Some equipment may have similar escalation probabilities and in this case the only way to apply the methodology the description of the escalation pattern direction is an operator choice, depending on the accident features and wind direction. Furthermore, in the present state the methodology is not automatized and requires an active participation of the user, which excludes its extensive application to large industrial installations or to industrial clusters.

When coming to shortcuts of current methodologies, three issues emerge. In the assessment of domino scenarios, almost all quantitative risk assessment methods consider one and only one secondary scenario per each target considered (Cozzani et al., 2005; Khan and Abbasi, 1998a; Abdolhamidzadeh, 2010; Kahkzad et al., 2013). The study of Bernachea et al. (2013) remarks the limitations introduced by this assumption, since many different possible release categories and accident scenarios may follow the damage on a secondary unit. Moreover, in several approaches, a single scenario causing escalation is also considered for primary units triggering domino events.

A second issue is the issue of the time gap between accident scenarios. This may play a critical role on the assessment of human vulnerability, since survivors may have the chance to move in a safe position during the time of the accident escalation process due to the application of the emergency plan. However, this effect is still not included in dedicated risk assessment methodologies for domino scenarios. Similarly, this limit is also evident in the assessment of equipment damage probabilities in case of second (or higher) level domino: for instance it is easier for an explosion to damage an equipment that was previously weakened by fire.

Third issue is the appropriate calculation of the impact of domino scenarios. Although it was demonstrated that sufficiently conservative results may be obtained superimposing vulnerability maps (Cozzani et al., 2005; 2006), the lack of well-defined methodologies for the assessment of human lethality due to composed scenarios hinders the correct assessment of the impact of domino scenarios on the nearby population (Cozzani et al., 2006; Antonioni et al., 2009): e.g. the assessment of human vulnerability of both an explosion and a toxic release, since possible synergic effects are still unknown. A further example is a toxic dispersion moving over a pool fire, that

could have mitigated effects since the fire may either increase the air entrainment in the cloud and therefore dilute the toxic concentration, or burn and decompose the toxic substance.

2.6 Conclusions

The analysis of scientific publications concerning domino effect in the process industry resulted in a database of more than 60 documents, addressing four main issues: past accident analysis, vulnerability models, risk assessment and safety management of domino scenarios. This huge research effort allows a quantitative assessment of domino scenarios in risk analysis and safety management of industrial sites. Nevertheless, a number of open point still remain, where existing tools may be improved and uncertainty may be reduced. In particular, escalation assessment may benefit from more detailed vulnerability models and dynamic tools for consequence assessment may consistently improve the results obtained when the impact of domino scenarios is of concern. Finally, a second generation of risk assessment tools addressing escalation effects and multi-level scenarios should pave the way to a holistic assessment of cascading events involving industrial sites and critical industrial infrastructures.

References

- T Abbasi, S.A. Abbasi. The boiling liquid expanding vapour explosion (BLEVE): Mechanism, consequence assessment, management. *Journal of Hazardous Materials*, Volume 141, Issue 3, 22 March 2007, Pages 489-519
- Abdolhamidzadeh B, Abbasi T, Rashtchian D, Abbasi SA. A new method for assessing domino effect in chemical process industry. *Journal of Hazardous Materials*, 2010; 182:416–426.
- B Abdolhamidzadeh, T Abbasi, D. Rashtchian, S.A. Abbasi, Domino effect in process-industry accidents – An inventory of past events and identification of some patterns. *Journal of Loss Prevention in the Process Industries*, 24, 5, 2011, 575-593
- B Abdolhamidzadeh, Che Rosmani Che Hassan, M D Hamid, S FarrokhMehr, N Badri, D Rashtchian, Anatomy of a domino accident: Roots, triggers and lessons learnt. *Process Safety and Environmental Protection*, Volume 90, Issue 5, September 2012, Pages 424-429
- American Petroleum Institute (API). Fireproofing practices in petroleum and petrochemical processing plants. 2nd ed. Washington DC: API publication 2218; 1999.
- Antonioni, G., Cozzani, V., Gubinelli, G., Spadoni, G., & Zanelli, S. (2004). The estimation of vulnerability in domino accidental events. In *Proceedings of the European conference on safety and reliability* (pp. 3653-3658). London: Springer
- G. Antonioni, G. Spadoni, V. Cozzani, A methodology for the quantitative risk assessment of major accidents triggered by seismic events, *J. Hazard. Mater.* 147 (2007) 48–59.
- Antonioni, G., Spadoni, G., & Cozzani, V. (2009). Application of domino effect quantitative risk assessment to an extended industrial area. *Journal of Loss Prevention in the Process Industries*, 22(5), 614-624.
- Argenti F., Landucci G. Experimental and numerical methodology for the analysis of fireproofing materials. *Journal of Loss Prevention in the Process Industries* 28, 11 (2014) 60-71
- D.F. Bagster, R.M. Pitblado, *Proc. Safety Environ. Protect.* 69 (1991) 196.
- M.R. Baum The velocity of large missiles from axial rupture of gas pressurized cylindrical vessels *J. Loss Prev. Process Ind.*, 14 (2001), pp. 199–203
- A.M. Birk, M.H. Cunningham The boiling liquid expanding vapor explosion *J. Loss Prev. Process Ind.*, 7 (1994), pp. 474–480
- A.M. Birk, Scale effects with fire exposure of pressure-liquefied gas tanks *J. Loss Prev. Process Ind.*, 8 (1995), pp. 275–290
- A.M. Birk Hazards from propane BLEVEs: an update and proposals for emergency responders *J. Loss Prev. Process Ind.*, 9 (1996), pp. 173–181
- Bollinger, R.E., Clark, D.G., Dowell III, A.M., Ewbank, R.M., Hendershot, D.C., Lutz, W.K., Meszaros, S.I., Park, D.E., Wixom, E.D., 1996. *Inherently Safer Chemical Processes: A Life Cycle Approach*. American Institute of Chemical Engineers. CCPS, New York, NY.
- M Campedel, V Cozzani, A Garcia-Agreda, E. Salzano Extending the quantitative assessment of industrial risks to earthquake effects, *Risk Analysis*, 28 (2008), 1231–1246
- CCPS, *Guidelines for Evaluating the Characteristics of Vapor Cloud Explosions, Flash Fires and BLEVEs*, AIChE, New York, 1994
- CCPS *Guidelines for Consequence Analysis of Chemical Releases*, Center for Chemical Process Safety American Institute of Chemical Engineers, New York (1999)
- V. Cozzani, E. Salzano, The quantitative assessment of domino effects caused by overpressure. Part I: probit models, *J. Hazard. Mater.* A107 (2004a) 67–80.
- V. Cozzani, E. Salzano, The quantitative assessment of domino effects caused by overpressure Part II: case studies, *J. Hazard. Mater.* A107 (2004b) 81–94.

- Cozzani, V., Gubinelli, G., Antonioni, G., Spadoni, G., & Zanelli, S. (2005). The assessment of risk caused by domino effect in quantitative area risk analysis. *Journal of Hazardous Materials*, 127(1e3), 14-30.
- Cozzani, V., Gubinelli, G., & Salzano, E. (2006a). Escalation thresholds in the assessment of domino accidental events. *Journal of Hazardous Material*, 129(1-3), 1e21.
- Cozzani, V., Antonioni, G., & Spadoni, G. (2006b). Quantitative assessment of domino scenarios by a GIS-based software tool. *Journal of Loss Prevention in the Process Industries*, 19(5), 463-477.
- Cozzani, V., Tugnoli, A., & Salzano, E. (2007). Prevention of domino effect: from active and passive strategies to inherently safer design. *Journal of Hazardous Materials*, 139(2), 209-219.
- Cozzani, V., Tugnoli, A., & Salzano, E. (2009). The development of an inherent safety approach to the prevention of domino accidents. *Accident Analysis & Prevention*, 41(6), 1216-1227.
- Cozzani V., Antonioni G., Khakzad N., Khan F., Taveau J., Reniers G., *Quantitative Assessment of Risk Caused by Domino Accidents, Domino Effects in the Process Industries, Modeling, Prevention and Managing*, Elsevier, Amsterdam, The Netherlands, (2013a)
- Cozzani V., Tugnoli A., Bonvicini S., Salzano E., *Threshold-Based Approach, Domino Effects in the Process industries, Modeling, Prevention and Managing*, Elsevier, Amsterdam, The Netherlands, (2013b)
- Cozzani V, Antonioni G, Landucci G, Tugnoli A, Bonvicini S, Spadoni G, *Quantitative assessment of domino and NaTech scenarios in complex industrial areas .Journal of Loss Prevention in the Process Industries* 28 (2014) 10-22
- R.M. Darbra, A Palacios, J Casal, *Domino effect in chemical accidents: Main features and accident sequences. Journal of Hazardous Materials, Volume 183, Issues 1–3, 15 November 2010, Pages 565-573*
- Delvosalle C., *Domino effects phenomena: definition, overview and classification*, in: *Direction Chemical Risks (Ed.)*, European Seminar on Domino Effects, Federal Ministry of Employment, Brussels, 1996, pp. 5–15.
- Delvosalle, C., Fievez, C., Brohez, S., 2002. A methodology and a software (Domino XL) for studying domino effects. In: *Chisa 2002 15th International Congress of Chemical and Process Engineering*.
- Deutsche Norme (DIN) 4119, 1979, *Oberirdische zylindrische Flachboden-Tankbauwerke aus metallischen Werkstoffen*, 1979.
- Díaz-Ovalle, C., Va'zquez-Roma'n, R., Mannan, S., 2010. An approach to solve the facility layout problem based on the worst-case scenario. *Journal of Loss Prevention in the Process Industries* 23 (3), 385–392.
- Di Padova A, Tugnoli A, Cozzani V, Barbaresi T, Tallone F. Identification of fireproofing zones in oil & gas facilities by a risk-based procedure. *Journal of Hazardous Materials* 2011; 191:83–93.
- A. Di Benedetto, E. Salzano, G. Russo, *Predicting pressure piling by semi-empirical correlations, Fire Safety Journal*, 40, 3 (2005), 282-298
- A. Di Benedetto, E. Salzano. *CFD simulation of pressure piling, Journal of Loss Prevention in the Process Industries* 23, 4, (2010) 498-506
- Egidi, D., Foraboschi, F. P., Spadoni, G., & Amendola, A. (1995). The ARIPAR project: analysis of the major accident risks connected with industrial and transportation activities in the Ravenna area. *Reliability Engineering & System Safety*, 49(1), 75-89.
- Eisenberg NA, Lynch CJ, Breeding RJ. 1975, *Vulnerability model: a simulation system for assessing damage resulting from marine spills. . In: Rep. CG-D-136-75. Rockville, MD: Enviro Control Inc.;*
- Gledhill, J, Lines, I., 1998, *Development of methods to assess the significance of domino effects from major hazard sites, CR Report 183, Health and Safety Executive.*

- M. Gómez-Mares, L. Zárate, J. Casal, Jet fires and the domino effect, *Fire Safety J.* 43 (2008) 583–588.
- Gubinelli, G., Zanelli, S., & Cozzani, V. (2004). A simplified model for the assessment of the impact probability of fragments. *Journal of Hazardous Materials*, 116, 175e187.
- Gubinelli, G., & Cozzani, V. (2009a). Assessment of missile hazard: reference fragmentation patterns of process equipment. *Journal of Hazardous Materials*, 163, 1008-1018.
- Gubinelli, G., & Cozzani, V. (2009b). The assessment of missile hazard: evaluation of fragment number and drag factors. *Journal of Hazardous Materials*, 161, 439-449.
- Hadjisophocleous, G.V., Sousa, A.C.M., Venart, J.E.S., 1990. A study of the effect of the tank diameter on the thermal stratification in LPG tanks subjected to fire engulfment. *Journal of Hazardous Materials* 25 (1–2), 19–31.
- U. Hauptmanns A Monte Carlo-based procedure for treating the flight of missiles from tank explosions *Probab. Eng. Mech.*, 16 (2001), pp. 307–312
- U. Hauptmanns A procedure for analyzing the flight of missiles from explosions of cylindrical vessels *J. Loss Prev. Process Ind.*, 14 (2001), pp. 395–402
- Health and Safety Executive, 1978. Canvey: An Investigation of Potential Hazards from Operations in the Canvey Island/Thurrock Area. Health and Safety Executive, London.
- Health and Safety Executive, 1996. Jet-Fire Resistance Test of Passive Fire Protection Materials (Report Oti 95 634). Health and Safety Executive, Merseyside, UK.
- B. Hemmatian, B. Abdolhamidzadeh, R.M. Darbra, J. Casal, The significance of domino effect in chemical accidents. *Journal of Loss Prevention in the Process Industries*, Volume 29, May 2014, Pages 30-38
- Hendershot, D.C., 1997. Inherently safer chemical process design. *Journal of Loss Prevention in the Process Industries* 10, 151–157.
- Hurme, M., Rahman, M., (2005). Implementing inherent safety throughout process lifecycle. *Journal of Loss Prevention in the Process Industries* 18 (4–6), 238–244.
- Jung, S., Ng, D., Lee, J.-H., Vazquez-Roman, R., Mannan, M.S., 2010. An approach for risk reduction (methodology) based on optimizing the facility layout and siting in toxic gas release scenarios. *Journal of Loss Prevention in the Process Industries* 23 (1), 139–148.
- Jung, S., Ng, D., Díaz -Ovalle, C., Vazquez-Roman, R., Mannan, M.S., 2011. New approach to optimizing the facility siting and layout for fire and explosion scenarios. *Industrial and Engineering Chemistry Research* 50 (7), 3928–3937
- Khakzad N, Faisal Khan F.I., Amyotte P, Valerio Cozzani V *Risk Analysis* Volume 33, Issue 2, pages 292–306, 2013
- Khan, F.I., Abbasi, S.A., 1997. Risk analysis of epichlorohydrin manufacturing industry using new computer automated tool MAXCRED. *J Loss Prevention In Process Industries* 10 (2), 91.
- F.I. Khan, S.A. Abbasi Models for domino effect analysis in the chemical process industries *Process Saf. Prog.*, 17 (1998a), pp. 107–123
- F.I. Khan, S.A. Abbasi DOMIFFECT: a new user friendly software for domino effect analysis *Environ. Model. Softw.*, 13 (1998b), 163–177
- F.I. Khan, S.A. Abbasi, Studies on the probabilities and likely impacts of chains of accident (domino effect) in a fertiliser industry, *Process Saf. Prog.*, 19 (2000a), 40–56
- F.I. Khan, B. Natarajan, S.A. Abbasi, Avoid the domino effect via proper risk assessment, *Chem. Eng. Prog.*, 96 (2000b), 63–76
- F.I. Khan, S.A. Abbasi. Estimation of probabilities and likely consequences of a chain of accidents (domino effect) in Manali Industrial Complex. *J. Cleaner Prod.*, 9 (2001a), 493–508

- F.I. Khan, S.A. Abbasi. An assessment of the likelihood of occurrence, and the damage potential of domino effect (chain of accidents) in a typical cluster of industries. *J. Loss Prev. Process Ind.*, 14 (2001b), 283–306
- Khan, F.I., Amyotte, P.R., 2003. How to make inherent safety practice a reality. *Canadian Journal of Chemical Engineering* 81, 2–16.
- Khan, F. I., & Amyotte, P. R. (2004). Integrated inherent safety index (I2SI): a tool for inherent safety evaluation. *Process Safety Progress*, 23(2), 136-148.
- Khan, F. I., & Amyotte, P. R. (2005). I2SI: a comprehensive quantitative tool for inherent safety and cost evaluation. *Journal of Loss Prevention in the Process Industries*, 18(4-6), 310-326.
- Kletz, T.A., 1978. What you don't have, can't leak. *Chemistry and Industry* 6, 287–292.
- Kletz, T.A., 1984. *Cheaper, Safer Plants, or Wealth and Safety at Work*. Institution of Chemical Engineers, Rugby, UK.
- Kletz, T.A., 1991. *Plant Design for Safety, a User-Friendly Approach*. Hemisphere – Taylor & Francis, New York, NY.
- Kletz, T.A., 1998. *Process Plants: A Handbook for Inherent Safer Design*. Taylor & Francis, Bristol, PA.
- Kletz, T.A., Amyotte, P., 2010. *Process Plants: A Handbook for Inherent Safer Design*, second ed. Taylor & Francis, Boca Raton, FL.S.P.
- Kourniotis, C.T. Kiranoudis, N.C. Markatos, Statistical analysis of domino chemical accidents, *J. Hazard. Mater.* 71 (2000) 239–252.
- G. Landucci, G. Gubinelli, G. Antonioni, V. Cozzani, The assessment of the damage probability of storage tanks in domino events triggered by fire, *Accident Anal. Prev.* 41 (6) (2009a) 1206–1215.
- G. Landucci, M. Molag, V. Cozzani, Modeling the performance of coated LPG tanks engulfed in fires, *J. Hazard. Mater.* 172 (1) (2009b) 447–456.
- Latha, P., Gautam, G., Raghavan, K.V., (1992). Strategies for the quantification of thermally initiated cascade effects. *Journal of Loss Prevention in the Process Industries* 5, 18.
- F.P. Lees, *Loss Prevention in the Process Industries-Hazard Identification, Assessment, and Control*, vols. 1–3 Butterworth-Heinemann, Oxford (1996)
- Leonelli, P., Bonvicini, S., Spadoni, G., 1999. New detailed numerical procedures for calculating risk measures in hazardous materials transportation. *Journal of Loss Prevention in the Process Industries* 12 (6), 507–515.
- I.R.M. Leslie, A.M. Birk, State of the art review of pressure liquefied gas container failure modes and associated projectile hazards, *J. Hazard. Mater.*, 28 (1991), 329–365
- Mannan, S., 2005. *Lees' Loss Prevention in the Process Industries*, third ed. Elsevier, Oxford, UK.
- Mecklenburgh, J.C., 1985. *Process Plant Layout*. George Goodwin, London, UK.
- Major Accident Hazards Bureau. (2005). *Guidance on the preparation of a safety report to meet the requirements of directive 96/82/EC as amended by directive 2003/105/EC (Seveso II)*. European Commission Joint Research Centre – Institute for the Protection and Security of the Citizen. Report EUR 22113 EN.
- Major Hazard Incident Data Service (MHIDAS), Health and Safety Executive, United Kingdom, 2001.
- Z Mingguang, J Juncheng. An improved probit method for assessment of domino effect to chemical process equipment caused by overpressure. *Journal of Hazardous Materials* 158 (2008) 280–286
- Moodie, K., 1988. Experiments and modelling: an overview with particular reference to fire engulfment. *Journal of Hazardous Materials* 20, 149–175.
- Morris, M., Miles, A., Copper, J., (1994). Quantification of escalation effects in offshore quantitative risk assessment. *Journal of Loss Prevention in the Process Industries* 7, 337.

- Q.B. Nguyen, A. Mebarki, R. Ami Saada, F. Mercier, M. Reimeringer. Integrated probabilistic framework for domino effect and risk analysis. *Advances in Engineering Software* 40 (2009) 892–901
- Nolan, P.F., Bradley, C.W.J., 1987. Simple technique for the optimization of lay-out and location for chemical plant safety. *Plant/Operations Progress* 6, 57–61.
- Patsiatzis, D.I., Knight, G., Papageorgiou, L.G., 2004. An MILP approach to safe process plant layout. *Chemical Engineering Research and Design* 82, 579–586.
- Penteado, F.D., Ciric, A.R., 1996. An MILP approach for safe process plant layout. *Industrial and Engineering Chemistry Research* 4, 1354–1361.
- Pettitt, G.N., Schumacher, R.R., Seeley, L.A., (1993). Evaluating the probability of major hazardous incidents as a result of escalation events. *Journal of Loss Prevention in the Process Industries* 6, 37.
- E. Planas-Cuchi, J.M. Salla, J. Casal Calculating overpressure from BLEVE explosions *J. Loss Prev. Process Ind.*, 17 (2004), pp. 431–436
- R. W. Prugh, Quantitative Evaluation of "Bleve" Hazards, Hazard Reduction Engineering, Inc. Wilmington, DE (1991)
- A. Rad, B. Abdolhamidzadeh, T. Abbasi, D. Rashtchian. FREEDOM II: An improved methodology to assess domino effect frequency using simulation techniques. *Process Safety and Environmental Protection*, In Press, Corrected Proof, December 2013
- P.K. Raj Exposure of a liquefied gas container to an external fire *J. Hazard. Mater. A*, 122 (2005), 37–49
- Reid, R.C., 1979. Possible mechanism for pressurized-liquid tank explosions or BLEVE's. *Science* 203, 1263–1265.
- Reniers, G., Dullaert, W., Ale, B., Soudan, K., Developing an external domino accident prevention framework: *Hazwim Journal of Loss Prevention in the Process Industries* 18 (2005a), 127–138
- Reniers, G., Dullaert, W., Soudan, K., & Ale, B. The use of current risk analysis tools evaluated towards preventing external domino accidents. *Journal of Loss Prevention in the Process Industries*, Volume 18, 3, (2005b), 119–126
- G.L.L. Reniers, W. Dullaert, A. Audenaert, B.J.M. Ale, K. Soudan. Managing domino effect-related security of industrial areas. *Journal of Loss Prevention in the Process Industries*, 21, 3, (2008) 336–343
- G. Reniers, W. Dullaert, K. Soudan, Domino effects within a chemical cluster: a game-theoretical modeling approach by using Nash-equilibrium, *J. Hazard. Mater.* 167 (1/3) (2009) 289–293.
- G. Reniers An external domino effects investment approach to improve cross-plant safety within chemical clusters, *Journal of Hazardous Materials* 177 (2010) 167–174
- G. Reniers, V. Cozzani, *Domino Effects in the Process Industries, Modeling, Prevention and Managing*, Elsevier, Amsterdam, The Netherlands, (2013a)
- G. Reniers, V. Cozzani, *Features of Escalation Scenarios, Domino Effects in the Process Industries, Modeling, Prevention and Managing*, Elsevier, Amsterdam, The Netherlands, (2013b)
- A.F. Roberts Thermal radiation hazards from releases of LPG from pressurized storage *Fire Saf. J.*, 4 (1982), pp. 197–212
- Roberts, T., H. Beckett, G. Cooke, and D. Brown. 1995a. Jet Fire Impingement Trial on a 41% Full Unprotected, 2 Tonne Propane Tank, HSL Report R04.029, IR/L/PH/95/11, Buxton, UK, July.
- Roberts, T., H. Beckett, G. Cooke, and D. Brown. 1996a. Jet Fire Impingement Trial on a 60% Full, Unprotected, 2 Tonne Propane Tank, HSL Report R04.029, IR/L/PH/95/12, Buxton, UK, August.
- Roberts, T., H. Beckett, G. Cooke, and D. Brown. 1995b. Jet Fire Impingement Trial on a 20% Full, Unprotected, 2 Tonne Propane Tank, HSL Report R04.029, IR/L/PH/95/13, Buxton, UK, October.

- Roberts, T., H. Beckett, G. Cooke, and D. Brown. 1995c. Jet Fire Impingement Trial on a 85% Full, Unprotected, 2 Tonne Propane Tank, HSL Report R04.029, IR/L/PH/95/14, Buxton, UK, October.
- Roberts, T., and H. Beckett. 1996b. Hazard Consequences of Jet-Fire Interactions with Vessels Containing Pressurised Liquids: Project Final Report, HSL Report R04.029, PS/96/ 03, Buxton, UK, February.
- T. Roberts, A. Gosse, S. Hawksworth, Thermal radiation from fireballs on failure of liquefied petroleum gas storage vessels, *Trans IChemE*, Vol 78, Part B, May 2000
- A. Ronza, S. Félez, R.M. Darbra, S. Carol, J.A. Vílchez, J. Casal, Predicting the frequency of accidents in ports areas by developing event trees from historical analysis, *J. Loss Prevent. Proc.* 16 (2003) 551–560.
- N.F. Scilly, J.H. Crowter, Methodology for Predicting Domino effects from Pressure Vessel, International Conference on Hazard Identification and Risk Analysis, Human Factors and Human reliability in Process Safety, 1992, p.1
- E Salzano, B Picozzi, S Vaccaro, P Ciambelli. Hazard of Pressurized Tanks Involved in Fires . *Ind. Eng. Chem. Res.* 2003, 42, 1804-1812
- E. Salzano, V. Cozzani. The analysis of domino accidents triggered by vapor cloud explosions *Reliability Engineering & System Safety* 90, 2–3 (2005) 271-284
- Tugnoli A, Cozzani V, Di Padova A, Barbaresi T, Tallone F, Mitigation of fire damage and escalation by fireproofing: A risk-based strategy, *Reliability Engineering and System Safety* 105 (2012)25–35
- Tugnoli A., Gubinelli G., Landucci G., Cozzani V. Assessment of fragment projection hazard: Probability distributions for the initial direction of fragments, *Journal of Hazardous Materials* 279 (2014) 418-427
- Uijt de Haag, P. A. M., & Ale, B. J. M. (1999). Guidelines for quantitative risk assessment (Purple book). The Hague (NL): Committee for the Prevention of Disasters.
- Van Den Bosh, C. J. H., Merx, W. P. M., Jansen, C. M. A., De Weger, D., Reuzel, P. G. J., Leeuwen, D. V., (1989). Methods for the calculation of possible damage (Green Book). The Hague, NL: Committee for the Prevention of Disasters.
- J.D.J. VanderSteen, A.M. Birk, Fire tests on defective tank-car thermal protection systems *J. Loss Prev. Process Ind.*, 16 (2003), pp. 417–425
- Venart, J.E.S., 1986. Tank Car Thermal Response Analysis – Phase II. Tank Car Safety Research and Test Project, Chicago.
- J.E.S. Venart, K.F. Sollows, K. Sumathipala, G.A. Rutledge, X. Jian, Boiling Liquid Compressed Bubble Explosions: Experiments/Models, Gas–Liquid Flows, vol. 165ASME, New York (1993) pp. 55–60
- Venart, J.E.S., 1999. Boiling Liquid Expanding Vapor Explosions (BLEVE): Possible Failure Mechanisms, vol. 1336. ASTM Special Technical Publication. pp. 112–134.
- J.E.S. Venart, Boiling liquid expanding vapor explosions (BLEVE); possible failure mechanisms and their consequences *Proceedings of the IChemE Symposium Series No. 147* (2000), pp. 121–137
- C.M. Yu, J.E.S. Venart, The boiling liquid collapsed bubble explosion (BLCBE): a preliminary model *J. Hazard. Mater.*, 46 (1996), pp. 197–213

Chapter 3:

State of the art on the research of NaTech events

3.1 Introduction

The impact of the natural events on industrial sites often resulted in large losses, and in some cases on the releases of huge quantities of hazardous materials. In these events at the side of the initial natural disaster, a severe technological accidents starts, eventually causing extended damage to the industrial area or to the nearby population (Natural-Technological or NaTech events). Industrial operators were often found unprepared or off-guard for unannounced events, but also when they had received early warnings. Due to these occurrences, public awareness has raised and the issue of NaTech is now considered as an emerging risk (Salzano et al., 2013). Due to the climate change and increase in the frequency of some categories of natural disasters, the likelihood of NaTech scenarios is growing, thus NaTech may be also considered as a new risk in some areas of the world.

In the present chapter a short review of some important studies regarding NaTech events produced in the recent years has been carried out. Three main research fields have been identified: the past accident database analysis for the identification of the domino accident real impact on industrial safety, the development of vulnerability models for the assessment of the probability of accident escalation, and the methodologies to account of domino accident in risk assessment and safety management.

3.2 Analysis of past accidents triggered by natural events

In order to prevent industrial disasters involving hazardous material the knowledge of the causes and modality by which accident occurs, is a crucial step to achieve. The systematic study of the interaction between natural and technological disasters is an area that has attracted growing attention in the last decade. Awareness of NaTechs as an “emerging systemic risk” has grown in Europe. NaTech incidents among Seveso II industrial facilities have been rare, thus difficult to analyze. Data from the Major Accidents Reporting Systems (MARS, 2008) database of the Major Accident Hazards Bureau (MAHB) at the JRC reveals on average at least one NaTech incident per year since 1985. Although NaTechs have been relatively rare events, there is growing evidence that NaTechs are on the rise. In the United States an increase in NaTechs has been reported over the last 20 years (Lindell and Perry, 1996a; 1996b; Showalter and Myers, 1994).

Rasmussen (1995) indicates that between 1% and 5% of accidents in fixed installations reported in the accident databases have natural events as a causative factor, possibly near the upper limit, or above. Most of the accidents identified have happened in Western Europe and North America. In this study the most often reported natural cause of NaTech is ‘ Atmospheric Phenomena ’, which accounts for 80% of the initiating factors; the remaining portion is mainly due to geologic activity

18%. Among atmospheric phenomena one of the major contributors is lightning strikes, which account for the 33% of the total accidents triggered by natural events.

3.2.1 The analysis of NaTech in the USA

Lyndel and Perry (1998) recounts actual releases that were documented in the Northridge earthquake of 1994. Smith (1997) analyzed NaTech caused by lightning strike, which caused a fire and explosion that ultimately resulted in the collapse of a 55000-barrel tank of crude oil. The accident caused the death of two fire fighters when the tank experienced a catastrophic rupture. Young (2002) analyzed the National Response Center (NRC, 2008) database and the Federal Emergency Management Agency (FEMA, 2004) records searching for natural disasters and related NaTech events in the period 1990-1999. A total of 480 natural, non-fire disasters and 1152 NaTech events were found. Furthermore, more than an half of the natural disasters were associated with at least one NaTech, being wind storms and floods the main causes of NaTech events.

Young et al. (2004) performed a systematic review which summarizes several research works of the 90s about direct and indirect disaster-associated releases, as well as environmental contamination and adverse human health effects that have resulted from natural disaster-related hazmat incidents. The goal is to use disaster-related hazmat releases to identify future threats and to improve mitigation and prevention efforts.

Steinberg et al. 2008 provides an overview of the state of the art in NaTech risk assessment and management in the United States. This work tries to assess the extent of NaTechs analyzing accident databases; the data show a fairly constant number around 650 of NaTechs per year over the time period studied, with a low of 530 in 1997 and a high of 820 in 1994. Moreover the authors discuss the possible safeguards against NaTechs and indicate: design criteria, safety measures, land use planning, community disaster mitigation and response, adoption of sustainable industrial processes, as the key tasks that need particular attentions to reduce possible NaTech risk.

Ruckart et al. (2008) analyzed a set of 166 hurricane-related events occurred in industrial settings in Louisiana and Texas in 2005, with an eye on those events triggered by hurricane Katrina and Rita. Most (72.3%) releases were due to emergency shut downs in preparation for the hurricanes and start-ups after the hurricanes. For this reason all the possible contributing causal factors have been highlighted, as well as the hazardous substances released, and event scenarios.

Reible et al. (2006) discussed a set of NaTech events that happened in New Orleans during hurricane Katrina, with particular emphasis on water contamination, which caused long term damages to the population, in particular chronic diseases, and environmental pollution. The most abundant contaminants were arsenic and organic liquids, with toxic and/or carcinogen properties.

Sengul et al.,(2012) analyses the hazardous materials involved in the NaTech accidents and in particular the quantity released. Storage tank releases make up 11% of all NaTech releases and result most often from rain, hurricanes, and floods (Fig. 3.1a). However, since the volume released often is highly dependent on a few large releases, the very majority of hazardous materials released was from storage facilities (Figure 3.1b). Petroleum (in particular crude oil) was released during 60% of NaTech events, whereas various chemical releases made up another 30%, aqueous materials comprised 5% of releases, and natural gas 3%. Nitrogen oxides (NO_x) and benzene, the

two most common chemical compounds, resulted by flare stack combustion following NaTechs. The total volume of petroleum released during NaTechs (approximately 29 million litres between 1990 and 2008) comprises 3% of the volume of all petroleum releases reported to the NRC.

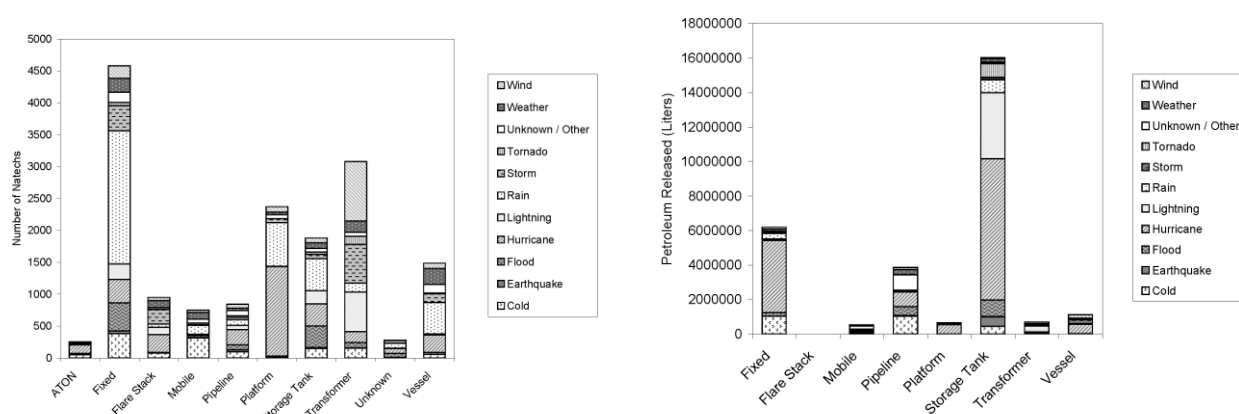


Figure 3.1: NaTech causes and targets to the respect of a) the number of NaTech; b) quantity of petroleum released (Sengul et al., 2012)

3.2.2 The analysis of NaTech in the EU

Steinberg and Cruz (2004) discussed the enormous Tupras oil refinery fire and naphtha, ammonia, and toxic acrylonitrile releases which occurred as a result of the 1999 Kocaeli earthquake in Turkey. Fendler (2008) discusses the recommendations for those industrial establishments containing large quantities of hazardous materials to the respect of the threat of floods. Recent studies have indicated that legislation and standards for chemical-accident prevention do not explicitly address NaTech risk (Krausmann and Baranzini, 2009; Krausmann, 2010).

Krausmann et al. (2011a; 2011b) discusses the efforts toward the development of dedicated tools for NaTech risk management for earthquakes, floods and lightning. According to Steinberg and Cruz (2004) more than 21 incidents of NaTech (natural hazards triggering technological disasters) events followed the August 17, 1999 earthquake in Turkey; among those events eight resulted in off-site consequences and in the damage of surrounding population. In another major incident resulting from the recent floods in the Czech Republic in August 2002, 400 kilograms of chlorine were released from the Spolana Chemical Works company, situated at the river Labe in Neratovice, north of Prague.

Cozzani et al. (2010) performed a study of past accidents caused by flood events; data on 272 NaTech events triggered by floods were retrieved from some of the major industrial accident databases (MARS, 2008; MHIDAS, 2001; TAD, 2004; NRC, 2008). Several specific elements that characterize NaTech events have been investigated. In particular, the damage modes of equipment and the specific final scenarios that may take place in NaTech accidents are key elements for the hazard and risk assessment (Figure 3.2). The figure indicates that item displacement and subsequent failure of flanges and connections due to water drag and/or to floating are among the principal causes for loss of containment.

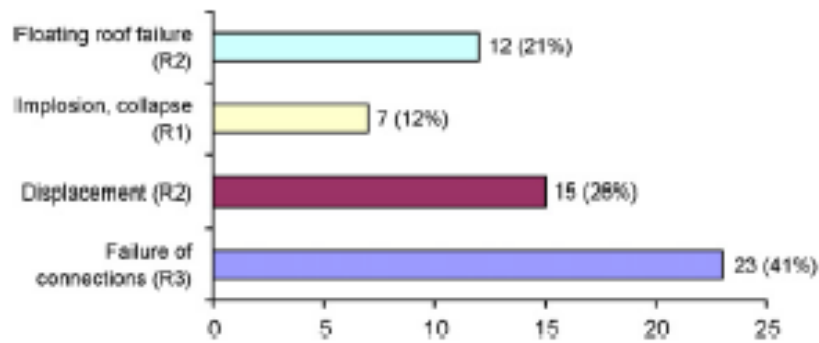


Figure 3.2: Available data for different structural damage typologies experienced by process equipment items during flood events and associated release category (Cozzani et al., 2010).

A more detailed analysis of the accident files collected allowed the identification of the equipment categories that are most frequently damaged as a consequence of floods. As shown in Fig. 3.3, storage tanks (and pipework) are the equipment items that were most frequently damaged during flood events while cylindrical vessels, compressors and pumps resulted less affected.

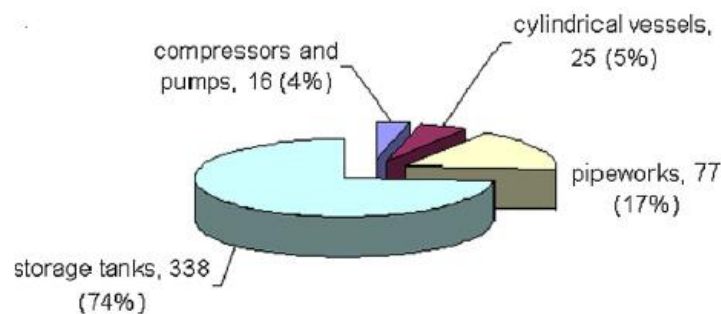


Figure 3.3: Categories of equipment items mainly involved in the accidents triggered by flood events (Cozzani et al., 2010)

It is interesting to analyze the data available on the final scenarios (Figure 3.4): in NaTech accidents triggered by floods the two scenarios typical of the process industry, fire and toxic dispersion, can have specific non-conventional causes due to the presence of wide amounts of water in flood events. The systematic analysis of data presented in Cozzani et al. (2010) allowed the development of post-release event trees.

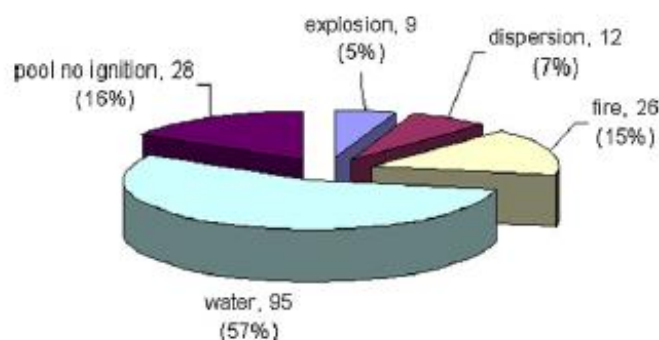


Figure 3.4 Accident scenarios initiated by flood events (Cozzani et al., 2010)

From the detailed historical analysis of industrial accidents triggered by natural disaster over several decades, Salzano et al. (2013) discusses the process that promoted the public awareness to the respect of these events. The tools and methodologies for the assessment of NaTech risk are described and their provision to the general NaTech knowledge and response capability.

3.2.3 Discussion

The past accident analysis showed that the most important causes of NaTech events are atmospheric phenomena: hurricanes, heavy rain, winds, etc... However, the happening of a few tremendous earthquakes that caused numerous contemporary NaTech events highlighted the hazard behind seismic events as well. For this reason most of studies regarded those two main topics.

Several aspects of NaTech events are important in understanding the significance of NaTechs versus other types of industrial accidents. First, natural disasters influences large areas, therefore those events are capable of induce many accidents simultaneously, even in different industrial facilities. Thus, the number of releases may easily overwhelm the available emergency response capacity. Mitigation measures may not work properly because they may be damaged by the natural event as well. Therefore, the possibility of cascading disasters (domino effects) particularly high. Response personnel and equipment may not be available. In addition to the possible need to respond to a large number of simultaneous releases, response personnel and their equipment may be called to respond to the natural disaster-caused catastrophe, or even blocked by the natural disaster itself. The physical environment created by the natural disaster may slow response to the chemical release by reducing people moving capability and blocking communication lines. The recovery and rebuilding processes of the damaged equipment, the clean-up of the contaminated environment, and the overall ability of the industrial facility to resume operation may be significantly slowed by impacts from the natural disaster. NaTechs also offer different response and mitigation characteristics than other types of chemical accidents.

On the contrary of seismic or lightning hazard the risk of flood is very site specific, thus the industrial installation have the chance to avoid to be exposed to such a threat simply being built at a safe distance from rivers or at some height over the water level. However, most of industrial facilities have been established along the banks of large rivers to facilitate transport of raw materials and finished product, and also to provide water supply for industrial processes and waste disposal. Industry has been prone to accept the risk of inundation from flood waters in in exchange for evident advantages, but has also exposed population centers to industrial accidents and in particular to NaTechs (Steinberg et al, 2008).

Policies on the prevention of riverine floods exist for a lot of river systems. The prevention of flash floods requires changes in the use of land, the reduction of draining and appropriate agriculture. A policy to support this may be in place in a few cases only. Authorities, the public and operators have to be aware of the possibility of natural impact. Therefore, communication between authorities, industry and the public plays a determinant role on disaster prevention.

3.3 NaTech risk assessment and accident prevention

At the European Community level there are several legal acts that directly or indirectly address NaTech risk through rules governing industrial establishments housing hazardous materials, landfill sites and waste treatment plants. Regulations that govern lifeline systems operations such as electrical power plants, gas and oil pipelines, and water resources and trans-boundary issues may also indirectly address NaTech risk reduction. However, any guideline that encompasses the entire NaTech disaster risk assessment and management at the EU level are only partial and contain only vague recommendations. Most important for NaTech risk reduction is the knowledge that NaTech risk exists. If NaTech risks have not been identified, communities and industrial facilities cannot take action to reduce potential NaTech related losses. The higher rank attributed in public awareness to NaTech scenarios required the development of a specific approach to assess and manage NaTech risk (Salzano et al., 2013). While developing a specific approach for NaTech risk assessment and management, one must comply with the standard risk management procedure, which involves the following consolidated process:

- (1) planning the risk management process, which involves the definition of the level of detail and of the tools to be used in the analysis, so that it will fit the available resources and the defined goal;
- (2) identification of the hazards, which involves all the activities required to identify all the hazards related to the system under examination;
- (3) qualitative risk analysis, which involves screening activities (for instance through some key performance indicators – KPIs (Tugnoli et al. 2008) aimed to identify if and where more detailed analyses are required;
- (4) quantitative risk analysis, which involves quantifying both occurrence probability and expected magnitude of the consequences of each previously identified hazard, in order to estimate overall risk indexes
- (5) planning of mitigation measures, which requires implementing all the prevention and protection measures required to reduce the risk level below to some predetermined threshold; and
- (6) risk monitoring and control, which involves the activities required to avoid that changes in the situation examined would increase the risk level above the acceptable threshold.

In this general framework, both the steps of qualitative and quantitative risk assessments involve peculiar aspects when investigating NaTech events. In particular, the characterization of the initiating event and of the final scenarios needs a dedicated approach.

3.3.1 NaTech and regulatory requirements in the EU

Requirements for the management of chemical accident prevention in the European Community first appear in the Seveso II Directive (98/82/EC). The aim of the Seveso Directive is to: “Prevent major accidents which involve dangerous substances, and to limit their consequences for man and the environment with a view to ensuring high levels of protection throughout the Community in a consistent and effective manner.”

The Seveso Directive demands for the institution of major-accident prevention policy, for the publication of a safety report, and for the establishment of emergency plans in the case of an accidental chemical release for those industrial facilities that store, use or handle large quantities of dangerous substances. Several issues must be completed in order to assess all the possible hazard: process safety analysis; process safety information; evaluation of mitigation measures; external events analysis; and consequence analysis.

Although no specific requirement have been introduced by the Seveso II Directive for NaTech risk management, it is addressed indirectly, since the Directive requires the analysis of external events, which may lead to a chemical accident. The potential threat of natural hazards in the hazard analysis is exactly what the directive intends for external events. All the suitable preventive measures able to reduce the likelihood of an accident must be carried out together with the development of specific procedures in case such an accident occurs. Nevertheless, methodologies or actions that can be taken to achieve these requirements are not specified in the directive, therefore the levels of preparedness vary among countries (Cruz et al., 2004). Finally, competent authorities can assure the safety for the population living in the vicinity of plant by keeping appropriate distances between industrial activities and residential areas, through the definition of proper land use policies for those areas affected by particular "natural sensitivity".

Furthermore, the Directive calls for the analysis of potential domino effects. Therefore, the competent authority must study the likelihood of domino effects in the specific industrial setup analyzed. The study of domino events needs advanced models for risk analysis, which motivated many researchers to address this specific topic. Moreover, a sort of synergy can be evidenced between NaTech and domino effect (Cozzani et al., 2014). Several researchers have noted that the probability of domino effect increases during natural disasters (Cruz and Steinberg 2005, Cruz et al. 2001, Lindell and Perry 1997). The most relevant publications regarding domino effect are fully addressed in chapter 2.

3.3.2 Preliminary NaTech risk assessment

The implementation of the risk assessment procedure requires qualitative screening to identify when a detailed (and much more resource-demanding) analysis is required (Busini et al., 2011). Such procedure should be easy to apply, requiring a limited amount of information and of resources. The procedure should provide, also through suitable indicators, which is the NaTech risk level associated to a given situation (that is, a process plant located in a given position) and eventually a ranking among different situations.

A first level in the assessment of NaTech hazard is the identification of the sites where such hazard is relevant. The problem is usually of concern at district, regional or national level, thus requiring the analysis of extended areas. Therefore, the most suitable tools for the assessment of NaTech hazard, for a preliminary evaluation of the possible vulnerable sites, are simplified screening methods. Cruz and Okada (2008b) proposed a detailed screening methodology mostly useful at a district level and the paper by Sabatini et al. (2008) extends the evaluation to regional level. A ranking of the equipment vulnerability to natural events could be useful for designing and planning prevention and mitigation measures and systems.

A similar approach was adopted for the vulnerability ranking of typical industrial equipment found in process plants or storage sites. As a first step, critical equipment categories and their associated four-level hazard index under natural event loading were determined, based on the extent of damage of an equipment item, its operating conditions and the hazard posed by the released substance. This was based on an extensive analysis of NaTech accidents, as well as on a review of the technical literature (Campedel et al., 2008; Fabbrocino et al., 2005; Salzano et al., 2003; Talaslidis et al., 2004). Furthermore Cruz and Okada (2008a) show possible strategies to design process equipment in order to obtain protection from natural events.

Using the above natural-hazard and technological-hazard classifications, vulnerability analyses for industrial equipment under natural-event loading can be performed and the risk from possible damage can be estimated. In order to define credible accidental scenarios a number of discrete states for structural damage to equipment (damage state, DS) were defined, in order to assess the extent of the LOC. Damage states typologies ranged from the total absence of damage (DS1) to total collapse of the structure (DS3) (Antonioni et al., 2007).

In order to obtain a measure of the quantity and rate of hazardous substance releases from damaged equipment due to a specific natural-hazard impact, three risk states (RS) were defined, which are a function of an equipment's damage state and the type of equipment affected (e.g. pressurised or at atmospheric pressure)(Antonioni et al., 2007). The possibility of equipment damage is addressed using dedicated fragility models (Salzano et al., 2003; Fabbrocino et al., 2005; Iervolino et al., 2004, Landucci et al., 2012). Each risk state can then be associated with a specific accident scenario (toxic dispersion, fire, explosion).

More recently, Rota and coworkers proposed the application of the Analytical Hierarchy Process and through suitable Key Hazard Indicators (KHIs) (Busini et al., 2011) to screening procedures for the ranking of NaTech hazard. The application of all these methods to case-studies proved to yield effective results in the identification of "hot-spots" and critical sites where the application of more detailed assessment techniques is recommended.

Software package tools have been recently provided in order to assist companies in the preliminary evaluation of NaTech accidents (Girgin and Krausmann, 2013).

3.4 Quantitative risk assessment of NaTech scenarios

The issue of extending the bow-tie approach to NaTech hazards, schematized in figure 2, was proposed since the development of the MIMAH technique within the ARAMIS project (Delvosalle et al., 2006). Bow-ties including natural events as failure causes were developed in the approach. In parallel, Hazard Identification (HazId) Analysis technique spread out as a structured review technique able to account also threats caused by natural hazards to industrial facilities and assets. More recently, the bow-tie approach was extended to allow a comprehensive quantitative assessment of the contribution of NaTech scenarios to industrial risk. A detailed procedure and specific fragility models were developed for the calculation of individual and societal risk due to NaTech scenarios triggered by earthquakes and by floods (Antonioni et al., 2007; Campedel et al., 2008; Antonioni et al., 2009). More recently the proposed approach was further extend to other natural events, as lightning (Renni et al., 2009). The results obtained evidenced the important contribution of NaTech scenarios to industrial risk, due to the high expected frequencies that intense natural events may have in prone areas and to the absence of a risk-based design of industrial facilities where relevant quantities of hazardous substances are present.

Due to the complexity of NaTech events, there is still debate about the possibility to assess the risk related to such accidents. The main argue on the application of quantitative methodologies for the calculation risk related to NaTech events is that such scenarios are often unpredictable, since that the common sense often refers to them as “acts of God”. Furthermore, the consequences of those events are hard to describe. Nevertheless, increasing efforts in research are dedicated to the prediction of natural disaster and to the risk assessment of natural disasters and NaTechs, as well.

3.4.1 General framework for the quantitative assessment of NaTech

The study by Antonioni et al. (2009) is focused on the development of procedures aimed at the quantitative assessment of the risk due to accidents triggered by natural disasters impacting on the industrial installation. Two types of natural events are considered: earthquakes and floods. The study also aimed at the development of a more general framework allowing a unified approach to the quantitative assessment of the risk related to Na-Tech events. As shown in the flowchart (Figure 3.5), the starting point of the methodology is the identification of the credible external disastrous events (step 1) and of critical equipment items, that are likely to cause major accidents as a consequence of damage caused by natural events (step 2).

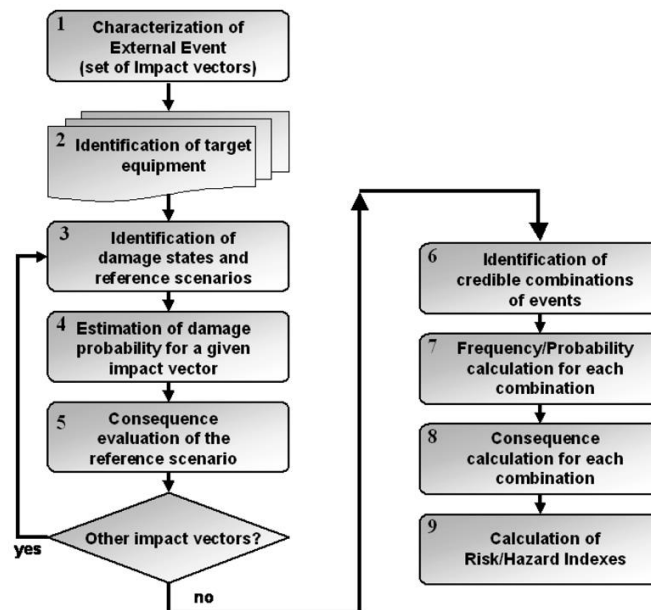


Figure 3.5: Flow chart of the procedure for the quantitative risk assessment of NaTech risk (Campedel et al., 2008)

A set of impact vectors are defined, the elements of the vectors being the intensity of the natural events classified by one or more intensity parameters selected to characterize the natural event. Critical equipment items are those that have the potentiality to cause a severe scenario due to an escalation triggered by the natural event. In this section the proposed methodologies for risk assessment of accidents triggered by seismic events (Antonioni et al., 2007) and by floods (Antonioni et al., 2009; Campedel et al., 2008) are discussed and showed in detail. Reference scenarios should be associated to each critical equipment item (step 3). On the basis of the reference scenarios identified for each equipment item, a specific procedure should be applied for the identification of the overall expected scenarios, in order to take into account that more than one reference scenario may take place simultaneously due to the damage of more than one unit (steps 4–7). Thus, also the consequence assessment of the resulting scenarios should be carried out combining the consequences of each of the reference accidental events identified (step 8). Finally, the conventional risk recomposition procedure may be applied for the calculation of the additional contribution to individual and societal risk of the accidental scenarios induced by seismic events and identified by the above procedure.

3.4.2 Identification of critical target equipment

Large atmospheric vessels, mainly used for the storage of liquid hydrocarbons, are the category of equipment more frequently involved in these accidents. Several events are reported in which the damage of this category of tanks following an earthquake resulted in tank or pool fires. Contamination of surface water as a result of the LOC was also reported. Pressurized storage vessels and long pipelines were also involved in severe LOC events following. Atmospheric and pressurized vessels having a large inventory of flammable or toxic substances, as well as large diameter pipelines, should be considered as the more critical equipment items in the assessment of risk due to external events in process plants (Antonioni et al., 2007). Table 3.1 reports the

preliminary criteria, based on operating conditions, volume, hold-up and physical state of hazardous substances, which may be used together with vessel inventory for a preliminary ranking of the critical equipment items (Antonioni et al., 2009).

<i>Class of critical equipment items</i>	<i>Gas liquefied</i>	<i>Liquid (cryogenic, evaporating, stable)</i>	<i>Gas</i>
Vessels	4	4	3
Piping	4	3	2
Columns	4	2	1
Reactors/heat exchangers	3	2	1

Table 3.1: Matrix for the identifying the more critical equipment item for different storage conditions (Antonioni et al., 2009).

3.4.3 Quantitative assessment of NaTech due to earthquake

Antonioni et al. (2007) developed a procedure for the quantitative risk assessment of accidents triggered by seismic events in industrial facilities. The procedure was derived from conventional risk assessment and previous studies regarding fragility of equipment items exposed to violent earthquakes (Salzano et al., 2003; Fabbrocino et al., 2005; Iervolino et al., 2004).

3.4.3.1 Expected frequency and severity of the reference earthquakes

The first step in the assessment of the expected frequencies of the reference scenarios is the evaluation of the expected frequencies of the seismic events. The return time of an earthquake is often obtained on the basis of historical data. Furthermore, the evaluation of the expected damage due to a seismic event requires the estimation of the severity of the event. This “magnitude” may be expressed by qualitative approaches (e.g. by the well known Mercalli–Cancani–Sieberg, or MCS scale) or using quantitative indexes (e.g. the Richter scale). A quantitative scale based on clear physical assumptions must be used when the purpose is to assess the seismic risk. In order to be suitable for QRA framework the severity of the seismic event was described using a single parameter, the peak ground acceleration (PGA), which may be sufficient when the behavior of steel equipment is under investigation.

In order to define correlation between magnitude and frequency of the seismic event, a PGA vector having an arbitrary number of elements, n , may be defined in order to represent the discretization of all the possible earthquake severities, expressed in terms of peak ground acceleration. In this approach, the frequency of exceedance of a given PGA value is expressed by Eq. (3.1), developed from data of available seismic studies:

$$f_i = f(PGA_i) \quad (3.1)$$

where PGA_i is the i^{th} element of the PGA vector, representing a PGA value. Usually, the above function is derived from conventional exceedance probability curves, which report the expected probability of an earthquake with a PGA higher than a given value over a time interval T :

$$P = P(PGA > a, T) \quad (3.2)$$

The conventional exceedance probability curves are easily available from governmental agencies as well as from scientific institutions.

3.4.3.2 Reference scenario selection

Two main factors influence the accidental scenarios that may follow the damage of industrial equipment caused by an earthquake: the characteristics of the substance released and the LOC entity. Quite obviously, the hazardous properties of the substance released influence the scenarios that may follow the release, and thus they can be described using event tree approach. On the other hand, the LOC intensity directly related to: the extent of the structural damage, the operating conditions of the damaged vessel (in particular, operating pressure and temperature at the release) and the physical state of the released substance. Thus, a schematic identification of the reference scenario for the equipment item of concern may be based on three main factors: (i) the extension of the damage reported by the vessel, (ii) the operating conditions, and (iii) the hazard posed by the released substance (Antonioni et al., 2007).

Moreover, the framework of risk assessment demands for the use of simplified methodologies for the description of the damage intensity that may follow an earthquake. The damage of a structure or of an equipment item may be roughly evaluated defining a limited number of damage states (DS). In the approach presented by Antonioni et al. (2007), two damage states were defined to classify the damage experienced by equipment items in a seismic event:

- Damage state 1 (DS1): Limited structural damage, as the rupture of connections or the buckling of equipment, resulting in a low intensity of the loss of containment, causing a partial loss of vessel inventory or the entire loss in a time interval higher than 10 min.
- Damage state 2 (DS2): Extended structural damage, causing the rapid loss of containment of the entire inventory

For the sake of simplicity, only two categories of equipment items were considered: atmospheric and pressurized equipment. As a working hypothesis, a limited volatility was assumed for atmospheric releases, a high volatility was assumed in the case of pressurized releases. The framework of the proposed approach suggests to consider the worst credible scenario among those listed in the table for each damage state and substance hazard. Moreover, the possible unavailability of the safety systems for the mitigation of accidental scenarios that may be triggered by seismic events must be taken into account, given that the safety barrier can suffer damage as well from the earthquake. On the basis of this approach, the suggested reference scenarios are summarized in Table 3.2.

Table 3.2: Expected scenarios of LOC events following the damage of atmospheric and pressurized vessels in seismic events (Antonioni et al., 2007)

Damage state	Substance hazard	Atmospheric vessels	Pressurized vessels
DS1	Flammable Toxic	Pool Fire Toxic dispersion from evaporating pool	Jet Fire Toxic dispersion from jet release
DS2	Flammable Toxic	Pool Fire Toxic dispersion from evaporating pool	Jet Fire Toxic dispersion from jet release

3.4.3.3 Damage probability of critical equipment item

As discussed above, in the framework of the QRA of industrial plants undergoing an earthquake, “vulnerability models” are required to estimate the expected probability of a given damage state following an earthquake of given magnitude. A simplified correlation linking the conditional probability of the *i*th damage state, $P(DS_i)$, to the PGA of the earthquake is required for each equipment item (Salzano et al., 2003; Fabbrocino et al., 2005). In the conventional approach to the probabilistic analysis of damage caused by seismic events, fragility curves are used to assess the resistance of a structure to a given PGA. Fragility curves are based on the assumption of a log-normal distribution of damage probability data with respect to PGA values. In this approach, the mean, μ , and the standard deviation, σ , of the data are usually provided:

$$P_s = \frac{1}{\sqrt{2\pi}\sigma} \int_{-\infty}^x \exp\left(-\frac{(z-\mu)^2}{2\sigma^2}\right) dz \quad (3.3)$$

where P_s is the probability of the damage state to which the parameters of the fragility curve are referred. Fragility curves based on the analysis of historical data were proposed for anchored and unanchored atmospheric tanks (Fabbrocino et al., 2005; Chopra, 1995) and for pressurized equipment (Di Carluccio et al., 2006). However, in conventional QRA, the so called “probit” functions are more widely used than fragility curves to correlate data that are expected to follow a log-normal distribution.

$$P_s = \frac{1}{\sqrt{2\pi}\sigma} \int_{-\infty}^{\text{Pr}(x)-5} \exp\left(-\frac{(z-\mu)^2}{2\sigma^2}\right) dz \quad (3.4)$$

A linear correlation is thus assumed between the “probit” variable and the independent variable, x , which is the PGA value.

$$\text{Pr} = a + b \cdot \ln(\text{PGA}) \quad (3.5)$$

Approaches based on fragility curves (Eq. (3.2)) and on “probit” functions (Eqs. (3.4) and (3.5)) are equivalent and the constants of the “probit” function are given by:

$$a - \mu = 5 \quad b \cdot \sigma = 1 \quad (3.6)$$

Table 3.3 reports the “probit” coefficients used for the different categories of industrial equipment considered in the case-studies.

Table 3.3: “Probit” function coefficients for equipment seismic fragility (Antonioni et al., 2007)

Target	a	b
Atmospheric vessel unanchored	-8.833	1,25
Atmospheric vessel anchored	-2,43	1,54
Pressurized vessel	5,146	0,884

Once the frequency of a seismic event having a given PGA and the relation between the magnitude of the seismic event and the damage probability of the given equipment are known, the expected frequency of a reference scenario involving a single equipment item may be calculated as follows:

$$f(R)_i^k = f_i \cdot P(DS_j)_i^k \quad (3.7)$$

where $f(R)_i^k$ is the expected frequency of the reference scenario involving the k^{th} equipment item following a seismic event having a PGA value equal to PGA_i ; f_i is the expected frequency of the *i*th

PGA value; and $P(DS_j)_i^k$ is the expected probability of the j th damage state of unit k following a seismic event having a PGA equal to PGA_i . Since different earthquakes may be considered as mutually exclusive, the overall expected frequency of the reference scenario R involving equipment k may be calculated as follows:

$$f(R)_k = \sum_{i=1}^n f_i \cdot P(DS_j)_i^k \quad (3.8)$$

where n is the total number of elements of the PGA vector defined above. However, contemporary damage of more than one unit may follow the seismic event. Therefore, the accidental scenario that follows the seismic event may either be caused by a single LOC (if a single equipment item is damaged) or by a combination of reference LOCs (due to the damage of multiple units at the same time). Thus, the actual overall scenarios that may follow a seismic event in a process plant are all the possible combinations of the reference scenarios associated to each of the critical equipment items identified in step 2 of the procedure.

If m critical items were identified and an index r is arbitrarily associated to each different reference scenario considered in the procedure, each overall scenario that may follow the seismic event may be identified by a vector S having s elements ($1 \leq s \leq m$):

$$S_{s,t} = [r_{1,t}, \dots, r_{s,t}] \quad (3.9)$$

where the elements of the vector are the indexes of the reference scenarios that take place in the t -th combination of s scenarios considered, $S_{s,t}$. The probability of the scenario $S_{s,t}$ may thus be calculated from the probabilities of each of the reference scenarios considered in the combination:

$$P_{s,t}^i = \prod_{j=1}^m [1 - P_j^i + \delta(j, S_{s,t})(2 \cdot P_j^i - 1)] \quad (3.10)$$

where P_j^i is the probability of each reference scenario considered, obtained from the above discussed probabilistic damage models, and the function $\delta(j, S_{s,t})$ equals 1 if the j th event belongs to the t -th combination, 0 if not. The overall expected frequency of the $S_{s,t}$ combination may thus be obtained:

$$f_{s,t} = \sum_{i=1}^n f_i \cdot P_{s,t}^i \quad (3.11)$$

On the other hand, if m is higher than 1, the total number of different scenarios that may be generated by a seismic event with a given PGA is:

$$v_i = 2^m - 1 \quad (3.12)$$

The total number of scenarios that need to be assessed in the quantitative analysis of the risk caused by seismic events, v , is given by the sum of all the scenarios considered for each element of the PGA vector:

$$v = \sum_{i=1}^n v_i = n(2^m - 1) \quad (3.13)$$

This means that a huge number of possible scenarios may be present. Therefore, a cut off criteria based on the calculated frequency and/or the conditional probability of the scenario must be applied before the consequence assessment.

3.4.3.4 Consequence assessment

If more than one reference scenario is expected to take place (due to the damage of more than one equipment item) there are several issues that should be addressed in this step: accidental

events may take place simultaneously or subsequently, and their effects may be synergetic, simply additive or mutually exclusive, depending on the type of scenarios and on the distance of the damaged units. Moreover, the physical effects of the different events that may take place may be different (e.g. thermal radiation from a fire and a toxic release). A complete analysis of the effects of interacting scenarios is still an open problem in consequence analysis, even considering the use of approaches based on advanced tools as computational fluid dynamic codes. In the framework of risk analysis, due to the uncertainties present in the assessment of the single scenarios that are likely to take place, a simplified approach to the problem is acceptable to obtain at least a rough estimate of the magnitude of the expected consequences.

In “Chapter 2”, which was mainly addressed to the analysis of domino effect, the consequence assessment of complex scenarios has been already discussed (Cozzani et al., 2005;2006) and the same procedure was used for the assessment of complex scenarios due to NaTech. Since a huge number of possible scenarios may arise, the development of a software tool that makes risk calculations automatic was a necessary step in order to apply the methodology discussed above. A specific software package was added to the Aripar-GIS software (Egidi et al., 1995).

3.4.4 Quantitative assessment of NaTech due to flood events

In the study by Campedel et al. (2009) a general framework is proposed in order to assess the risk associated to industrial accidents triggered by floods. The starting point of the methodology was the assessment of reference flood scenarios. The selection and characterization of the flood scenarios was made in terms of maximum water speed and maximum water height. Simplified fragility models were used for the assessment of the LOC scenarios that may be triggered by the reference floods. Everything just said for the assessment of NaTech risk due to seismic event is valid also in case of flood with the following exceptions.

3.4.4.1. Expected frequency and severity of the reference floods

Three specific characteristics of the flood: the return time, the maximum water depth expected at the site and the maximum expected water speed are the three parameters that have been taken into account for the selection and characterization of reference flood events. These data can be obtained by the public authorities or by specific analyses carried out on the site. Once more, it is worth of mention that by no means these parameters may be sufficient to fully characterize the flood hazard of a site, but they are suitable to characterize the severity of the reference events in the discussed approach (Antonioni et al., 2009).

3.4.4.2. Identification of critical equipment items

In the case of floods, besides substances having “conventional” Hazards considered in off-site consequence assessment of industrial accidents (flammability or toxicity), the analysis should be extended to substances reacting with water and/or developing flammable/toxic gases in contact with water. Thus, besides conventional release scenarios (fires, explosions and toxic cloud dispersion), floods may add other important threats: significant environmental contamination and release of toxic gases and flammable vapors generated by reactions of chemicals with water.

3.4.4.3. Damage states and reference accidental scenarios

Reference damage states were defined to characterize equipment damage in case of flood. Damage states were defined on the basis of equipment typology according to structural characteristics. The equipment categories defined are (i) cylindrical vertical vessels having diameter to height (D/H) ratio higher than 1 (atmospheric); (ii) cylindrical vertical vessels having D/H lower than 1 (atmospheric and pressurized); (iii) cylindrical horizontal vessels (atmospheric and pressurized).

The flood characteristic may change drastically the response of the exposed equipment. In particular three possible flood wave typologies have been identified and associated to specific structural damage: slow submersion (water velocity negligible), low-speed wave (water velocity below 1 m/s), and high-speed wave (water velocity higher than 1 m/s). Three release classes were considered for storage and process equipment, as well as for piping: R1 for the instantaneous release of the whole inventory following severe structural damage; R2 for the continuous release of the complete inventory in more than 10 min; R3 for the continuous release from a hole having an equivalent diameter of 10 mm. Table 3.4 shows the release categories and the associated modalities of flood action. The accidental scenarios that are expected to follow the releases were identified by the event tree technique, taking into account the possible scenarios deriving from substances reacting with water.

Table 3.4: Damage modality and release category considered (Antonioni et al., 2009)

Modality of water impact	Type of structural damage	Release category
Slow submersion	Failure of flanges/connections	R3
Moderate speed wave	Failure of flanges/connections	R3
High speed wave	Shell fracture	R2
	Impact with/of adjacent vessels	R1
	Failure of flanges/connections	R3

3.4.4.4. Damage probability of the critical equipment items, frequency and consequence assessment of the overall scenarios

In the case of floods a few equipment damage models are available in the literature (Landucci et al., 2012). Very limited data are available in the open literature to analyze in detail the damage caused by floods to industrial equipment. Thus, starting from the analysis of the limited data available, a simplified damage model was used, relating maximum ranges of water speed and maximum water height to different equipment damage probabilities. Fig. 3.6 shows an example of simple models that can be used for the damage probability assessment. Different damage probability values are associated to different combinations of water height and wave speed. Further details on vulnerability models for vessel involved in flood events will be discussed in the following.

Once equipment damage probabilities have been obtained (Fig. 3.6) and release modes have been assessed, the approach to consequence evaluation and frequency calculation for overall scenarios triggered by floods is the same described in the case of earthquakes. This analysis includes the calculation of all the expected frequency for all the combination of scenarios.

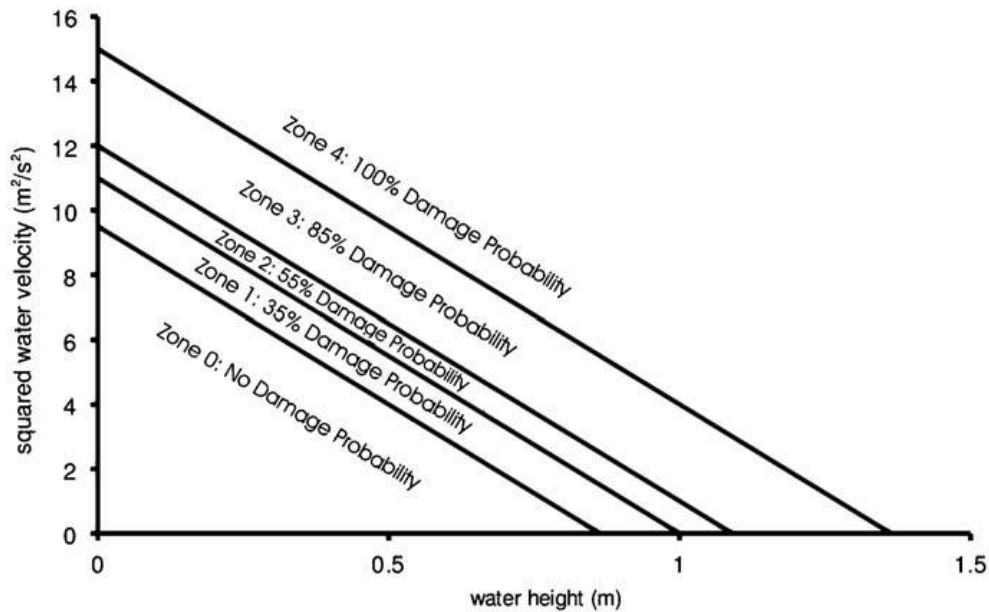


Figure 3.6: Estimation of equipment damage probability with respect to maximum water height and of the square of maximum water velocity (Antonioni et al., 2009).

3.4.5 Discussion

Specific equipment damage models and procedures were developed to build up a general framework allowing the extension of quantitative risk assessment to the analysis of industrial accidents caused by natural events. The tools developed allowed the assessment of accidents triggered by earthquakes and floods.

However, more detailed studies are needed at the national and local levels that assess risk management and emergency response practices by government agencies, industrial facilities, and communities to natural disaster-induced technological disasters and other systemic risks. These studies would also serve to identify innovative NaTech risk reduction strategies and to assist knowledge transfer to other regions in Europe by the adoption of a common EC policy for NaTech accident prevention, which has been only partially introduced in the current directives for accident prevention (Seveso Directive).

It is not clear what a NaTech disaster, as compared to a natural disaster, means in terms of economic, human, and environmental costs. The collection of data on social-economic losses due to NaTechs is crucial, both to clearly identify the magnitude of the problem, and to permit cost-benefit studies to determine if prevention and mitigation of NaTechs really pays.

Natural disasters have the potential to trigger simultaneous technological failures from single or multiple sources. Designing preparedness plans for multiple and simultaneous accidents would prove valuable not only for addressing NaTechs, but other type of disasters involving multiple accidents such as domino accident scenarios and accidents caused by acts of terrorism.

3.5 Conclusions

In this chapter a short review of the past works regarding NaTech accidents has been carried out. Attention was focused on several research addressing NaTech data collection from past accident studies, as well as the improvements of risk analysis methodologies to the respect of NaTech accident has been discussed.

However, the availability of partial or fragmented data regarding this kind of accidents, while systematic data on NaTech incidents are instead needed, increases the difficulty of this research. Since most countries already record data on chemical accidents, the collection of information on NaTechs would require only a limited further effort.

Land use planning has been found to be an important factor for the control of natural disasters consequences and economic losses from disasters in those regions subject to natural hazards. Analysis of economic development policies and industrialization to determine how they affect vulnerability to NaTech disasters and other systemic risks would help guide future development programs in the developing world. In addition, case studies could be developed to promote sustainable risk reduction practices and coping mechanisms in regions of high NaTech risk.

Another possible strategy to improve safety of the industrial installation is by providing useful design indications, which account for a safer layout disposal and recommendation on equipment construction in NaTech prone zones. Furthermore, by the tool of preliminary hazard analysis it is possible identify with relatively limited efforts the critical equipment units that require an improved design attention.

Finally, the current research shows that preparedness for NaTech disasters is low, though it is difficult to establish actual levels of preparedness for NaTechs or any other type of disaster. The development of comparative indicators of preparedness for NaTechs and other hazards would help decision- makers design appropriate policy options to protect those regions that need it the most.

However, a huge work is still needed to increase the understanding of this particular risk, in order to prevent and to mitigate the impact of such scenarios. It is worth of mentioning that other than seismic events and floods, many other natural events, and in particular lightning strikes, have the potential to trigger tremendous accidents and to cause huge losses to process industries. Therefore, there is the need of dedicated procedures for the risk assessment of such events. The aim of the current research work is to investigate more in detail the NaTech hazard, providing tools to assist operators in the assessment of NaTech risk. In particular the inclusion of NaTech due lightning strikes in the framework of quantitative risk assessment of NaTech events and the development of more detailed fragility models for equipment involved in flood events are important steps to achieve an overall improved assessment of NaTech hazard. Therefore the work produced during my PhD study regarding those two topics will be further discussed in the following chapters.

Reference

- Analyse, Recherche, et Information sur les Accidents (ARIA), French Ministry of Ecology and Sustainable Development, <http://www.aria.developpementdurable.gouv.fr/> (accessed 2006).
- G. Antonioni, G. Spadoni, V. Cozzani, A methodology for the quantitative risk assessment of major accidents triggered by seismic events, *J. Hazard. Mater.* 147 (2007) 48–59.
- G. Antonioni, S. Bonvicini, G. Spadoni, V. Cozzani, Development of a framework for the risk assessment of Na-Tech accidental events, *Reliability Engineering and System Safety* 94 (2009) 1442–1450
- Booyesen H.J., Viljoen M.F. and de Villiers G.T., Methodology for the calculation of industrial flood damage and its application to industry in Vereeniging, *Water SA*, Vol. 25, No.1, 1999.
- Busini, V., E. Marzo, A. Callioni, and R. Rota. 2011. Definition of a short-cut methodology for assessing earthquake-related NaTech risk. *Journal of Hazardous Materials* 192: 329–39.
- Campedel, M., V. Cozzani, A. Garcia-Agreda, and E. Salzano. 2008. Extending the quantitative assessment of industrial risks to earthquake effects. *Risk Analysis* 28: 1231–46.
- Campedel M., Antonioni G, Cozzani V. and Di Baldassarre G., A framework for the assessment of the industrial risk caused by floods, *Safety Reliability and Risk Analysis: Theory, Methods and Applications*, Martorell et al. (eds), Taylor and Francis Group, 2749-2755, 2009.
- Chopra, A.K., *Dynamics of Structures*, Prentice Hall, (1995) New York
- V. Cozzani, G. Gubinelli, G. Antonioni, G. Spadoni, S. Zanelli, The assessment of risk caused by domino effect in quantitative area risk analysis, *J. Hazard. Mater.* 127 (2005) 14–30.
- V. Cozzani, G. Antonioni, G. Spadoni, Quantitative assessment of domino scenarios by a GIS-based software tool, *J. Loss Prev. Proc. Ind.* 19 (2006) 463–477.
- Cozzani, V., M. Campedel, E. Renni, and E. Krausmann. 2010. Industrial accidents triggered by flood events: analysis of past accidents. *Journal of Hazardous Materials* 175: 501–9.
- Cozzani V, Antonioni G, Landucci G, Tugnoli A, Bonvicini S, Spadoni G, Quantitative assessment of domino and NaTech scenarios in complex industrial areas. *Journal of Loss Prevention in the Process Industries* 28 (2014) 10-22
- Cruz, A. M., Steinberg, L. J., Vetere-Arellano, A. L., Nordvik, J. P., and Pisano, F.. State of the Art in Natech (Natural Hazard Triggering Technological Disasters) Risk Assessment in Europe. Report EUR 21292 EN, DG Joint Research Centre, European Commission and United Nations International Strategy for Disaster Reduction, Ispra, Italy, 2004
- Cruz, Ana M., Laura J. Steinberg, and Ronaldo Luna. Identifying Hurricane-Induced Hazardous Material Release Scenarios in a Petroleum Refinery. *Natural Hazards Review*, 2001, 2 (4): 203-210.
- Cruz, A. M. and L. J. Steinberg. Industry Preparedness for Earthquakes and Earthquake-Triggered Hazmat Accidents During the Kocaeli Earthquake in 1999: A Survey; *Earthquake Spectra*, 2005, 21(2): 285-303.
- Cruz AM, Okada N. Consideration of natural hazards in the design and risk management of industrial facilities. *Nat. Hazards* 2008a; 44:213–27.
- Cruz AM, Okada N. Methodology for preliminary assessment of NaTech risk in urban areas. *Nat. Hazards* 2008b; 46:199–220
- Delvosalle C, Fievez C, Pipart A, Debray B. ARAMIS project: a comprehensive methodology for the identification of reference accident scenarios in process industries. *J. Hazard. Mater.* 2006; 130:200–219.
- A. Di Carluccio, I. Iervolino, G. Manfredi, G. Fabbrocino, E. Salzano, Quantitative probabilistic seismic risk analysis of storage facilities *Chem. Eng. Trans.*, 9 (2006), 215

- Directive 96/82/EC, Council Directive 96/82/EC of 9 December 1996 on the Control of Major-Accident Hazards Involving Dangerous Substances. Official Journal of the European Communities, L 10/13, Brussels, 14.1.97.
- Directive 2012/18/EU, European Parliament and Council Directive 2012/18/EU of 4 July 2012 on Control of Major-Accident Hazards Involving Dangerous Substances, Amending and Subsequently Repealing Council Directive 96/82/EC. Official Journal of the European Communities, L 197/1, Brussels, 24.7.2012
- Egidi, D., Foraboschi, F. P., Spadoni, G., & Amendola, A. (1995). The ARIPAR project: analysis of the major accident risks connected with industrial and transportation activities in the Ravenna area. *Reliability Engineering & System Safety*, 49(1), 75-89.
- G. Fabbrocino, I. Iervolino, F. Orlando, E. Salzano, Quantitative risk analysis of oil storage facilities in seismic areas, *J. Hazard. Mater.* 123 (2005) 61–69.
- Fendler, R., Floods and safety of establishments and installations containing hazardous substances, *Natural Hazards*, 46 (2), (2008), 257-263
- Girgin S. and Krausmann E., RAPID-N: Rapid NaTech risk assessment and mapping framework, *J. Loss Prev. Proc. Ind.* 26 (2013) 949-960. <http://rapidn.jrc.ec.europa.eu>
- I. Iervolino, G. Fabbrocino, G. Manfredi, Fragility of standard industrial structures by a response surface based method, *J. Earth. Eng.* 8 (2004) 1.
- E. Krausmann, F. Mushtaq, A qualitative NaTech damage scale for the impact of floods on selected industrial facilities, *Nat. Hazard.* 46 (2008) 179–197.
- Krausmann, E., A.M. Cruz, and B. Affeltranger. 2010. The impact of the 12 May 2008 Wenchuan earthquake on industrial facilities. *Journal of Loss Prevention Process Industries* 23: 242–8.
- Krausmann, E., E. Renni, M. Campedel, and V. Cozzani. 2011a. Industrial accidents triggered by earthquakes, floods and lightning: Lessons learned from a database analysis. *Natural Hazards* 59: 285–300.
- Krausmann, E., V. Cozzani, E. Salzano, and E. Renni. 2011b. Industrial accidents triggered by natural hazards: An emerging risk issue. *Natural Hazards and Earth System Sciences* 11: 921–9.
- Krausmann E. and Baranzini D., NaTech risk reduction in the European Union, *Journal of Risk Research*, Vol.15, No. 8, 1027-1047, 2012.
- Landucci, G., G. Antonioni, A. Tugnoli, and V. Cozzani. 2012. Release of hazardous substances in flood events: Damage model for atmospheric storage tanks. *Reliability Engineering & System Safety* 106: 200–16.
- Lindell, M.K. and R.W. Perry (1996a) 'Addressing gaps in environmental emergency planning: hazardous materials releases during earthquakes'. *Journal of Environmental Planning and Management*. 39(4). pp. 529–543.
- Lindell, M.K. and R.W. Perry (1996b) 'Identifying and managing conjoint threats: earthquake-induced hazardous materials releases in the US'. *Journal of Hazardous Materials Releases*. 50(1). pp. 31–46.
- Lindell MK, Perry RW (1997) Hazardous materials releases in the Northridge earthquake: implications for seismic risk assessment. *Risk Anal* 17(2):147–156
- Lindell, M.K. and R.W. Perry (1998) 'Earthquake impacts and hazard adjustments of acutely hazardous materials facilities following the Northridge earthquake'. *Earthquake Spectra*. 14(2). pp. 285–299.
- Major Hazard Incident Data Service (MHIDAS), Health and Safety Executive, United Kingdom, 2001.
- Major Accident Reporting System (MARS), European Commission, Joint Research Centre, Institute for the Protection and Security of the Citizen, Italy, <http://emars.jrc.ec.europa.eu/>, 2008.
- Mc Bean E., Fortin M. and Gorrie J., A critical analysis of residential flood damage estimation curves, *Can.J.Civ.Eng.*,13, 86-94, 1986.

- Middelmann-Fernades M.H., Flood damage estimation beyond stage-damage functions: an Australian example, *Journal of Flood Risk Management*, 3,88-96, 2010.
- NIBS, National Institute of Building Science, Flood loss estimation methodology, HAZUS technical manual, Federal Emergency Management Agency (FEMA), Washington, 2004.
- Rasmussen, K. (1995) 'Natural events and accidents with hazardous materials'. *Journal of Hazardous Materials*. 40(1). pp. 43–54.
- Reible, D.D., C.N. Haas, J.H. Pardue and W.J. Walsh (2006) 'Toxic and contaminant concerns generated by Hurricane Katrina'. *The Bridge*. 36(1). pp. 5–13.
- Reitherman, R.K. (1982) 'Earthquake-caused hazardous materials releases'. *Hazardous Materials Spills Conference Proceedings*. Milwaukee, WI, 19–22 April. pp. 51–58.
- J.E.A. Reinders, J.M. Ham, *Casualties Resulting from Flooding of Industrial Sites*. DC1-233-10, Delft Cluster publication, Delft (NL), 2003.
- E. Renni, E. Krausmann, G. Antonioni, S. Bonvicini, G. Spadoni, V. Cozzani, Risk assessment of major accidents triggered by lightning events, *AIDIC Conference Series vol. 9*, pp. 233-242, 2009
- Rota R., Caragliano S., Manca D. And Brambilla S., A short cut methodology for flood-technological risk assessment, *Third International Conference on Safety and Environment in Process Industry*, May 11-14, Rome, Italy, 2008.
- Ruckart, P.Z. M.F. Orra, K. Lanier and A. Koehler (2008) 'Hazardous substances releases associated with Hurricanes Katrina and Rita in industrial settings, Louisiana and Texas'. *Journal of Hazardous Materials*. 59(1). pp. 53–57
- Sabatini, M., Ganapini, S., Bonvicini, S., Cozzani, V., Zanelli, S., Spadoni, G., 2008, *Proc. Eur. Safety and Reliability Conf.*, Taylor & Francis: London; p.1199-205
- Salzano, E., Iervolino, I., Fabbrocino, G., Seismic risk of atmospheric storage tanks in the framework of quantitative risk analysis, *Journal of Loss Prevention in the Process Industries* 16 (5), 2003, 403-409
- Salzano, E., Garcia Agreda, A., Di Carluccio, A., Fabbrocino, G., Risk assessment and early warning systems for industrial facilities in seismic zones, *Reliability Engineering and System Safety* 94 (10), 2009, 1577-1584
- Salzano, E., Basco, A., Busini, V., Cozzani, V., Marzo, E., Rota, R., Spadoni, G., Public awareness promoting new or emerging risks: Industrial accidents triggered by natural hazards (NaTech), *Journal of Risk Research* 16 (3-4), 2013, 469-485
- Santella N., Steinberg L.J., Aguirra G.A., Empirical estimation of the conditional probability of NaTech events within the United States, *Risk Analysis*, Vol. 31, No. 6, 951-968, 2011.
- Sengul, N. Santella, L. J. Steinberg and A. M. Cruz, Analysis of hazardous material releases due to natural hazards in the United States, *Disasters* 36 (2012), 4, 723–743
- Showalter, P.S. and M.F. Myers (1992) *Natural Disasters as the Cause of Technological Emergencies: A Review of the Decade 1980–1989*. Working Paper. 78. Natural Hazards Research Center, Boulder, CO.
- Showalter, P.S. and M.F. Myers (1994) 'Natural disasters in the United States as release agents of oil, chemicals, or radiological materials between 1980–1989: analysis and recommendations'. *Risk Analysis*. 14 (2). pp. 169–182.
- Smith, D.P. (1997) 'ATTCO pipeline tank fire: responding to the volcanic inferno'. 1997 International Oil Spill Conference. pp. 926–927 http://www.iosc.org/papers_posters/00121.pdf (accessed on 2 December 2011).
- Smith, K. (2001) *Environmental Hazards: Assessing Risk and Reducing Disasters*. Third Edition. Routledge, New York, NY
- Steinberg, L.J. and A.M. Cruz (2004) 'When natural and technological disasters collide: lessons from the Turkey earthquake of August 17, 1999'. *Natural Hazards Review*. 5(3). pp. 121–130.

- Steinberg, L.J., H. Sengul and A.M. Cruz (2008) 'NaTech risk and management: an assessment of the state of the art'. *Natural Hazards*. 46(2). pp. 143–152.
- D.G. Talaslidis, G.D. Manolis, E. Paraskevopoulos, C. Panagiotopoulos, N. Pelekasis, J.A. Tsamopoulos, Risk analysis of industrial structures under extreme transient loads, *Soil Dynamic Earthquake Engineering*, 24 (2004), 435
- The Accident Database (TAD), version 4.1, Institution of Chemical Engineers (ICChemE), United Kingdom, 2004.
- Tugnoli, A., F. Khan, P. Amyotte, and V. Cozzani. 2008. Safety assessment in plant layout design using indexing approach: Implementing inherent safety perspective, part 1 - Guideword applicability
- P.A.M. Uijt de Haag, B.J.M. Ale, Guidelines for Quantitative Risk Assessment (Purple Book), Committee for the Prevention of Disasters, The Hague, The Netherlands, 1999.
- United States National Response Center (NRC) Database, United States Coast Guard, <http://www.nrc.uscg.mil/nrchp.html> (accessed 2008).
- US Army Corps of Engineers, Beyond the factor of safety: developing fragility curves to characterize system reliability, Report ERDC-SR-10-1, Washington DC, 2010.
- Young, S. (2002) 'Natural-technologic events: the frequency and severity of toxic releases during and after natural disasters with emphasis on wind and seismic events'. Paper presented at the UJNR (US–Japan Cooperative Program in Natural Resources) 34th joint meeting panel on wind and seismic effects, Gaithersburg, MD, 13–18 May.
- Young, S., L. Balluz and J. Malilay (2004), 'Natural and technologic hazardous material releases during and after natural disasters: a review'. *Science of the Total Environment*. 322(1–3). pp. 3–20.

Chapter 4:

Risk analysis of Natech accidents triggered by lightning strikes

4.1 Introduction

NaTech events often lead to catastrophic consequences, as shown by the analysis of major accident databases (Krausmann et al. 2011a,b), as well as from specific studies on the single causes (Cruz and Okada 2008a; 2008b; Renni et al. 2010; Salzano et al. 2003; 2009; 2013). In particular lightning has identified as the most frequent NaTech accident initiator, since the 33 % of the analyzed NaTech past accidents has lightning strikes as initiative event (Rasmussen, 1995); this value rises to 61 % for process installations (Renni et al., 2010).

Atmospheric storage tanks are the equipment which is more frequently damaged by lightning strikes, usually leading to severe fires (Renni et al., 2010). Nevertheless, lightning strikes are one of the major causes of tank fires and explosions (Argyropulos et al., 2012; Chang and Lin, 2006). Furthermore, tank fire statistics shows that 35% of all floating roof tank fires are caused by lightning related issues (LASTFIRE, 1997) and that lightning strikes are the absolute main cause of fires at the rim-seal for external floating roof tanks (95%) (Persson and Lönnermark, 2004), LASTFIRE, 1997).

For this reason codes and standards for the construction of atmospheric storage tanks must be constantly up to date. The API RP 545 (2009) and OISD 180 (1999) are the most advanced standard for lightning protection of above ground atmospheric storage tanks and provide all the available technical knowledge for an accurate bonding of the structure. However, they warn that total ignition protection is an utopic target and therefore the installation of protective devices should be accompanied by a proper risk assessment. Unfortunately, standards for risk analysis in the framework of lightning protection (e.g. CEI (2013), NFPA (2004)) lack of the knowledge necessary do deal with industrial installation in which huge amounts of hazardous materials are present. Furthermore, while performing risk analysis one must take into account that fires caused by lightning have the potential to trigger cascading effects on nearby equipment, leading to severe accident escalation or domino effects (Cozzani et al., 2014).

The extension of Quantitative Risk Analysis (QRA) to the assessment of Natech scenarios has been recently recognized as an important issue to obtain comprehensive data when assessing industrial risk related to major accident hazards (Antonioni et al., 2007; 2009; Campedel et al., 2008). However, in spite of the relevant frequency of Natech events triggered by lightning, specific methodologies for the detailed assessment of Natech scenarios initiated by lightning impact still needed to be developed.

Depending on the plant location, the contribution of NaTech events, and in particular of lightning, may be relevant or even crucial on the overall risk profile of an industrial installation. Therefore, the implementation of NaTech scenarios in the framework of Quantitative Risk Assessment (QRA) is a critical research task that was addressed in the past by different authors (Campedel et al.

2008, Antonioni et al. 2009). More recent contributions to NaTech accident research are the work of (Landucci et al., 2012) who developed a straightforward methodology for the evaluation of Risk due to flood events and the work by (Cozzani et al., 2014) who applied a methodology for QRA to NaTech events and domino accidents.

According to Antonioni et al. (2007; 2009), who first developed and applied a methodology for the inclusion of NaTech accident in the framework of Quantitative Risk Assessment, the first step for the calculation Risk due to NaTech is the assessment of the expected frequency of natural events on the process installation. The study authored by Necci et al. (2014a) is aimed at the evaluation of lightning impact probability on atmospheric storage tanks in a complex industrial layout.

Another key issue for the QRA implementation of such particular events is the evaluation of frequencies for NeTech accidental scenarios, in particular fragility models for the estimation of equipment damage probability on the basis of the severity of the natural event are demanded. Furthermore, QRA study requires the assessment of a high number of scenarios, for this reason there is the need to use of simplified models for the estimation of equipment vulnerability, which at the same time are capable to yield conservative results (Landucci et al. 2009).

Recent works have provided a systemic analysis of lightning triggered damage mechanism (Necci et al., 2013a) and on the role of safety barriers for lightning triggered accident prevention (Necci et al., 2014b).

Considering NaTech scenarios triggered by lightning, recent works allowed determining specific fragility models for storage and process equipment, in particular for above ground atmospheric and pressurized storage tanks, considering different types of geometries (Landucci et al., 2012; Landucci et al., 2014).

This chapter discusses the application of the models developed during the PhD studies, to the assessment of lightning-triggered accident frequency (Necci et al., 2013; 2014-a; 2014-b) for implementation in a Quantitative Risk Assessment study. The aim of this work is to provide a methodology which is able to assess the risk contribution of lightning triggered accidents: the features of lightning accidents are discussed, the accident modelling is addressed with particular interest on lightning singularities and the influence of NaTech caused by lightning on the overall risk profile of a facility is showed by the use of a case study.

4.2 Past accident analysis of accident triggered by lightning event

In order to identify and analyse lightning threat to industrial activities evidences of this hazards must be collected. While many different types of natural events have triggered Natech accidents, lightning strikes were the most common cause. Rasmussen (1995) analysed accident case histories in the industrial accident databases MHIDAS and FACTS and concluded that 61% of the accidents initiated by natural events at storage and processing activities were triggered by lightning strikes. Lightning was also found to be the most frequent cause of failure in the set of storage tank accidents analysed in the study of Chang and Lin (2006) and appears with very high frequency in the study performed by Persson and Lönnermark (2004).

4.2.1 Data retrieval for past accident analysis

The paper by Renni et al. (2010) is dedicated at the data retrieval and analysis of those industrial accidents that have been triggered by the impact of lightning. The data sources used for the analysis were the European industrial accident databases ARIA (2006), MHIDAS (2001), MARS (2008) and IChemE's (2004) The Accident Database (TAD). In addition, the US National Response Centre (NRC, 2008) database was interrogated. The accident coverage in the databases is global with the exception of the NRC database where hazardous-materials-release and oil-spill reports are restricted to the United States and its territories.

The analysed databases contain accident data from the open technical literature, government authorities, or in-company sources. Commonly, accident information from the chemical industry undergoes an abstraction process for confidentiality reasons.

The ARIA and NRC databases are publicly available; access to MHIDAS, FACTS and TAD requires a license. The MARS database contains confidential information on major accidents submitted to the European Commission by the Competent Authorities.

For the data extraction, selection criteria were defined in agreement with those used in a previous study on flood-triggered Natech accidents (Cozzani et al., 2010). Therefore, the following criteria were used:

1. The loss of containment of a hazardous substance occurred or could have occurred.
2. An industrial activity having a relevant inventory of hazardous substances was involved.
3. The event generated or had the potential to generate an accident scenario with off-site consequences (major accident).

For the purposes of this study "hazardous substances" are chemicals that are classified in the European Dangerous Substances Directive (Council Directive 67/548/EEC, 1967) and its later amendments, including those that extended the Directive to mixtures of chemical substances (Directive 1999/45/EC, 1999). The above selection criteria led to the inclusion in the analysis of industrial activities mainly falling under the provisions of the European Seveso II Directive on the control of major accident hazards (Council Directive 96/82/EC, 1996) and similar legislation. However, accidents in industrial sites not covered by these types of legal frameworks were also included in the present study if they were considered useful for lessons learning.

The following categories of process equipment were selected for the data analysis on the basis of the results of previous studies (Antonioni et al., 2007; 2009):

- Storage: atmospheric or pressurized storage tanks, warehouses.
- Process: reactors, heat exchangers, columns, separators, others.
- Auxiliary: pipework, pumps and compressors.

Electric and electronic systems, as well as flare stacks were also considered as specific targets of lightning-induced accidents. Although their failure may not directly result in loss of containment of hazardous substances, secondary effects due to collapse or loss of utilities have the potential to trigger a major accident.

The quality of the reported information was often poor and in many cases the accident description was not very detailed or incomplete and in most of the cases analysed the entire chain of events leading to the loss of containment was not described. Therefore, the analysis has been limited to subsets of the retrieved 721 accidents with a sufficient level of detail.

4.2.2 Results

Fig. 4.1 gives an overview of the industrial sectors for which accidents were recorded in the analysed databases. According to the data (a subset of 190 accident records that provided the required information) 95% of lightning-triggered Natech events occurred in oil and gas facilities (mainly oil refineries) and the petrochemical sector, including storage sites and tank farms. Obviously, the large number of industrial sites in operation within these sectors increases the frequency of lightning accidents in these sectors, as well as their susceptibility to lightning. However, accidents in chemical and petroleum industries account almost for the total of NaTech triggered by lightning strikes, therefore the high vulnerability of equipment categories present in such facilities is evident.

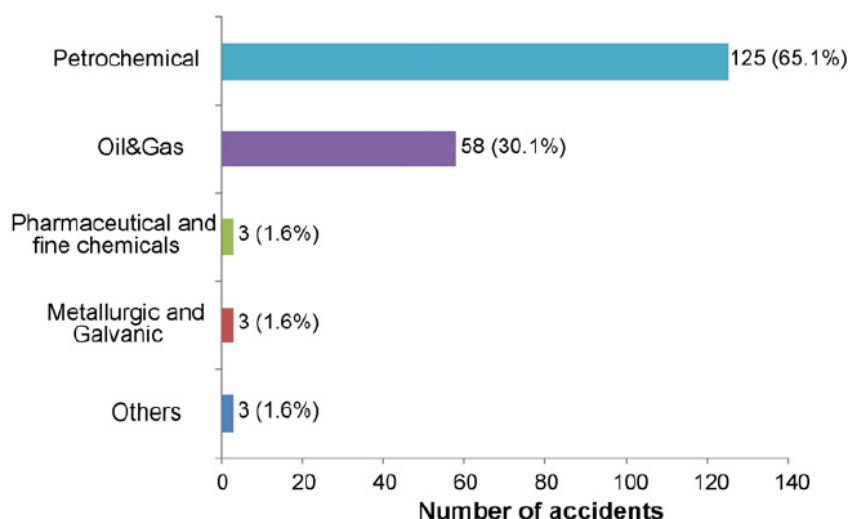


Fig 4.1: Industrial activities involved in lightning-triggered accidents, with release of hazardous materials (Renni et al., 2010).

Fig. 4.2 shows a summary of the different equipment typologies damaged by lightning strikes, based on the analysis of 485 accident records. The Storage tanks is the equipment category which shows the highest number of accidents due to lightning impact. Within this category, atmospheric tanks, and in particular floating-roof tanks which are commonly used for the storage of liquid hydrocarbons, are the most vulnerable equipment. Only 3 out of 289 accidents affecting storage tanks involved pressurised tanks, evidencing low vulnerability of this equipment typology. Other categories of process equipment were less susceptible to the impact of lightning: compressors and pumps and distillation columns, while flare stacks, pipes and electrical devices showed a high vulnerability lightning.

Lightning impact also resulted in the disruption of control systems and electrical circuitry which led to corrupted data, false signals, and damage to sensitive electronic devices. Several loss of containment events were reported as a consequence of this type of lighting-induced damage.

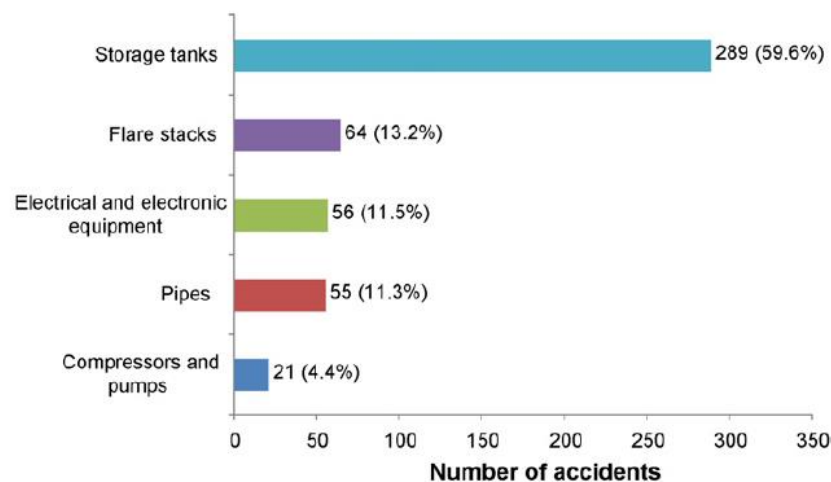


Figure 4.2: Equipment categories involved in Natech accidents due to lightning (Renni et al., 2010)

Regarding the structural damage to equipment due to the impact of lightning, only limited information is available. In the reports failure modes that equipment may be subject to during a lightning strike are described only in very general, while more information regarding the firefighting efforts are reported in the analysed accident databases. From the limited information reported, two different failure modes were identified, which are direct and indirect structural damage.

In addition to loss of containment caused by structural damage, damage to electric and electronic systems and immediate ignition of flammable substances were found. In several cases the electric field generated by the lightning caused the failure of control devices, with consequent loss of containment from vent and blow-down systems. Immediate ignition of flammable substances at the rim seal of storage tanks was also reported to have caused several fires and explosions.

Due to the fact that storage tanks in chemical and oil industries, which are the most vulnerable equipment category, usually contain large amounts of flammable substances, severe off site effects might be expected due to lightning triggered accidents. Not surprisingly, the hazardous substances mainly involved in this type of Natech accident were found to be oil, diesel and

gasoline which constitute the typical inventory for atmospheric storage tanks. Table 4.1 gives an overview of the released substances and the number of accident records associated with each. The accident scenarios initiated by a lightning strike are therefore influenced by the type of equipment damaged, the substance inventory and the operating conditions.

Table 4.1: Hazardous substances released during 713 lightning-triggered Natech accidents. (Renni et al., 2010).

Substance category	Hazard	N° Accidents
Oil, diesel and gasoline	Extremely flammable	389
Oxides	Explosive	122
Natural gas	Extremely flammable, Explosive	105
Aromatics	Extremely flammable, Dangerous for the environment	34
Chlorine	Toxic, Dangerous for the environment	32
Ammonia	Toxic, Dangerous for the environment	19
Acid products	Toxic, Dangerous for the environment	10
Cyanides	Toxic, Dangerous for the environment	1
Explosives	Oxidising	1

According to the analysis of the whole accident case histories performed by Renni et al. (2010), the majority of lightning-triggered events resulted in the release of hazardous substances (58%), while lower number of accidents resulted in fires (35%) and explosions (7%). Obviously, limiting the analysis to those accidents regarding storage tanks, fires and explosions constitute the large majority of the scenarios reported. However, limiting the analysis to release scenarios only, an ignition probability of 0.82 was estimated from the data analysis of 252 lightning-triggered releases of flammable substances from storage tanks.

In 10 accident records the tank roof is specifically indicated as the position where the fire takes place, while most records refers to general fires. It is highly likely that ignition in atmospheric floating-roof tanks occurs at the rim seal of the floating roof where flammable vapours may be present (Renni et al., 2010). According to a dedicated study regarding fires in storage areas (LASTFIRE, 1997), 95% of rim-seal fires are caused by lightning strikes. This result is so explicative that it is worth to analyse what is peculiar about the rim-seal region of a FRT that makes it susceptible to lightning. By design to ensure ease of movement of the floating roof within the tank shell, there exist a gap between the tank shell and the edge of the floating roof. This eliminates friction, guarantees ease of movement but creates issues in the following areas when lightning strikes.

Limited information on the on-site and off-site consequences of lightning-triggered accidents was provided in the analysed databases. In 6 out of 721 records fatalities were reported. The two most severe accidents analysed by Renni et al. (2010) resulted in over 400 and 16 fatalities, respectively. In 11 accident case histories information injured people were reported. In 34 accident records workers and/or residents were evacuated. Reported direct and indirect costs due to accidents triggered by lightning show significant economic losses due to the loss of expensive equipment,

other than huge inventories of products. The most costly reported Natech accident triggered by lightning resulted in damage of the order of 140 million US\$ (in 1994 Dollars).

4.2.3 Conclusions

The results, obtained by the mean of lightning triggered accident data analysis, provided useful information on the equipment categories most vulnerable to lightning impact as well as on damage to and release modes of equipment impacted by lightning. A very high ignition probability for released flammable substances was estimated from the analysed data, highlighting once more the threat of lightning ignition of flammable materials. Thus, the development of specific tools for the quantitative risk analysis of Natech accidents triggered by lightning has started with a robust data analysis of real accidents.

4.3 Quantitative risk assessment of accidents triggered by lightning

4.3.1 Methodology Overview

The methodology for the NaTech scenarios implementation in Quantitative Risk Assessment study was described in the previous chapter. Even if there are evidences of rare accidental scenarios in the past in which multiple units are damaged at the same time by a single lightning strike, in the present methodology it is assumed that a single stroke can affect a only one equipment. Data regarding multiple accidents triggered by lightning are poor in the accident databases and it is hard to tell whether the multiple damage was produced by the lightning strike itself or by accident propagation due to domino effect. This assumption makes lightning strikes different from the other NaTech accidents, such as floods and earthquake, in which multiple units are hit at the same time and complex accidental scenarios must be analyzed (Antonioni et al., 2009). A simpler methodology than this presented by Antonioni et al. (2009), is therefore required. A summary of the proposed methodology is presented in Figure 4.3.

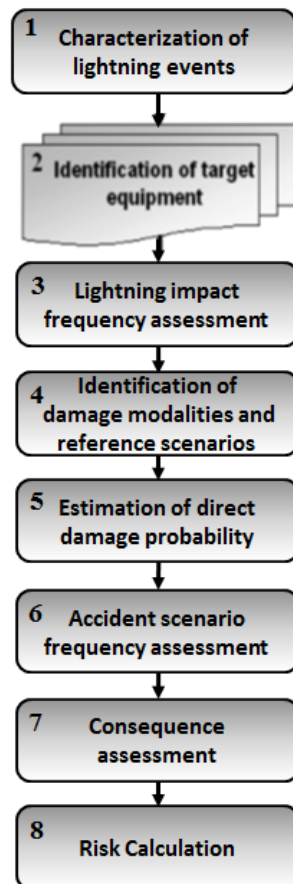


Figure 4.3: Flow chart of the procedure for the quantitative risk assessment of Natech accidents due to lightning

The first step of the methodology is the characterization of the frequency and of the severity of the natural event by a sufficiently simple approach, suitable for the use in a risk assessment framework. It must be remarked that this step by no way is intended to supply a characterization

of the natural hazard at the site, nor to provide data for a detailed analysis of the damage to structures, but only to obtain the input data necessary for simplified equipment damage models. Data on the flash frequency at ground are available from several sources: scientific publications, lightning protection standards (e.g. see (CEI, 2013; Cooray and Becerra 2010)), or directly consulting the databases obtained by the constant monitoring of lightning strikes carried out by competent authorities (SIRF, 2013). Then, the identification of vulnerable equipment is carried out for the entire industrial facility. The analysis of past accidents due to lightning evidences storage areas as the most vulnerable plant zones, which will be further discussed in section 4.3.3.

Both the constructive specifications for the target equipment units and their relative position on the tank footprint are then used to apply a dedicated model for the assessment of the expected frequency of a generic lightning strike on every target unit. The damage modalities and the possible accidental scenarios must be assessed in the following step. Since one of the mayor lightning threat is the ignition of flammable material, dedicated event trees has to be applied to evaluate the possibility of all the possible lightning-triggered accidental scenario, also considering the inability to face the fire emergency. In order to assess the frequency of every possible accidental scenarios the application of vulnerability models is needed to assess the equipment damage probability. These models are discussed in the following sections.

Consequence assessment of the single scenarios triggered by the natural event (step 7) may be carried out by conventional models, although a limited number of NaTech-specific final outcomes may arise (Cozzani et al., 2010; Renni et al., 2010; Necci et al. 2014b; Persson and Lönnemark, 2004). The final steps of the procedure are aimed at individual and societal risk calculation by the use of a dedicated GIS software (Egidi et al., 1995).

4.3.3 Identification of the vulnerable units

The first step of the quantitative risk assessment procedure is the identification of target equipment. As a result of the historical analysis of past accidents due to lightning strikes (see section 4.2), above ground atmospheric storage tanks shows the highest rate of lightning-triggered NaTech events. Large storage vessels containing hazardous liquids and gases are the critical equipment identified by the historical analysis. Thus, even if the present methodology is applicable to every critical unit in a hazardous site, it is developed in the detail for storage tanks only. In particular for above ground atmospheric storage tanks.

In fact, the review of records on industrial accidents triggered by lightning on atmospheric storage tanks allowed to identify:

- the more recurrent damage modalities, which are: direct damage to the metal enclosure with consequent release of hazardous materials, ignition of flammable vapors, damage to instrumentation and loss of power supply
- the associated recurrent scenarios: fire and explosion (both at the tank roof or in the bund area), toxic dispersion and soil/water contamination
- a possible correlation between the severity parameter of the natural event and the vulnerability: high vulnerability for external floating roof atmospheric tanks, and in particular at the rim-seal area, has been highlighted

4.4 Assessment of lightning impact frequency on target equipment

The approach used to develop the model for estimating lightning capture frequency is summarized in Figure 4.4. The model is aimed at assessing the expected equipment capture frequency in a specific lay-out. The preliminary step (Step 1 in Figure 4.4) is the definition of the main geometrical features of the area of interest, of the lay-out and of the specific characteristics of the considered equipment items. A Monte Carlo model is then used to generate a wide number of events each representing a lightning strike (Step 2 in Figure 4.4). Events are randomly generated with different perspective striking points (i.e., the strike location at ground without the presence of any structure), polarities and peak values of the lightning current waveform at the channel base. Probability distribution functions available in the literature (Anderson and Erikson, 1980; CEI, 2013) or derived from lightning location systems (e.g. SIRF (2013)) are used to define polarity and current parameters, while a uniform distribution is assumed for the initial striking position. The final striking point of the lightning is then determined on the basis of the perspective striking point and of the lightning current amplitude (Step 3 in Figure 4.4). The results of the Monte Carlo simulations are then used to assess the expected capture frequency of each equipment item (Step 4 in Figure 4.4). A simplified model, based on the calculation of an average attraction distance, was derived from the complete model developed (Steps 5 to 7 in Figure 4.4), in order to provide a tool more suitable for use in a quantitative risk assessment (QRA) framework. The features of the model and the approach needed for its application are described in detail in the following.

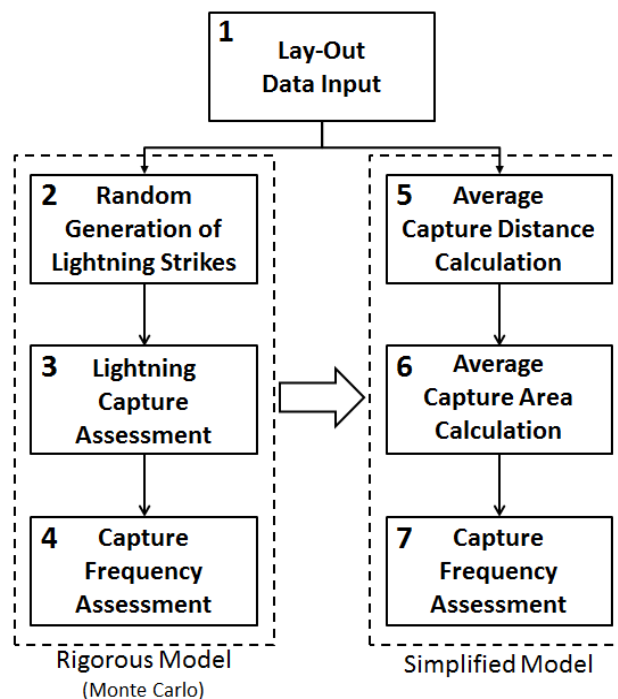


Figure 4.4: Modelling approach: Monte carlo simulations and simplified model

4.4.1 Preliminary definition of geometrical features and lightning generation

Before model application it is necessary to define the features and the limits of the area of interest, \mathbf{A} . The position, shape and height of each item present in the area of interest need to be defined. In the case of equipment items for which structural damage may be of interest, also data on type and thickness of the shell need to be collected. It should be remarked that the area of interest should be extended to include any element having a relevant height above ground with respect to that of the equipment items considered (e.g. buildings, stacks, flares and trees).

In the application of the Monte Carlo method, the number of simulations needed to obtain stable results is usually in the range between 10^5 and 10^8 , and depends on the complexity of the system analyzed. Random generation of flash polarities and of peak values of the lightning current is carried out taking into account the statistical data for lightning distribution. In particular, the log-normal distributions having mean value, μ_{ln} , and standard deviation, σ_{ln} , proposed by Anderson and Eriksson (1980) are assumed for the lightning peak current intensity I_p of both positive and negative first strokes of the flashes. The ground impact position in the absence of attraction due to structures is then randomly defined assigning uniformly random generated values to the x and y coordinates of the strike location within the area \mathbf{A} of concern. For each generated event, the triplet of values (x, y, I_p) attributed by the Monte Carlo procedure is then checked with respect to a capture condition described in the following.

4.4.2 Lightning attraction

In order to evaluate whether a lightning flash is attracted by one of the relevant items defined in the area of interest or hit a non-hazardous zone, a specific capture model is applied, derived from the Electro-Geometrical Model (EGM) (Cooray and Becerra, 2010). The model calculates a maximum attraction distance for the item of concern as a function of the lightning peak current intensity and of the height of the structure. When the distance between the lightning strike original impact position and the nearest point of equipment perimeter is lower than the attraction distance, the lightning strike is assumed to be captured by the item. The theoretical background of the EGM and its limitations are discussed in the literature (Cooray and Becerra, 2010; Borchetti et al., 2010; CEI, 2013; Love, 1973). The overall attraction distance, r_s , may be calculated as follows:

$$r_s = 10 \cdot I_p^{0.65} \quad (4.1)$$

where I_p is the peak return stroke current associated to the lightning strike by the Monte-Carlo method (expressed in kA), and r_s is the attraction distance from the structure, or lightning final jump, (expressed in m). The attraction distance from the ground, r_g , may then be calculated as a fraction of r_s (Cooray and Becerra, 2010; CEI, 2013):

$$r_g = 0.9 \cdot r_s \quad (4.2)$$

The projection on the ground of the attraction distance, r , is obtained as follows (see Figure 4.5) (Cooray and Becerra, 2010; CEI, 2013):

$$\begin{cases} r = \sqrt{r_s^2 - (r_g - H)^2} & H < r_g \\ r = r_s & H \geq r_g \end{cases} \quad (4.3)$$

where H is the height of the structure. The lightning is captured by the equipment if the distance between the original strike location (x, y) and the nearest point of the equipment perimeter (d_{sl}) in

Figure 4.6-(a)) is lower than the projection on the ground of the capture distance, r , calculated from Eqs.(4.1-4.3).

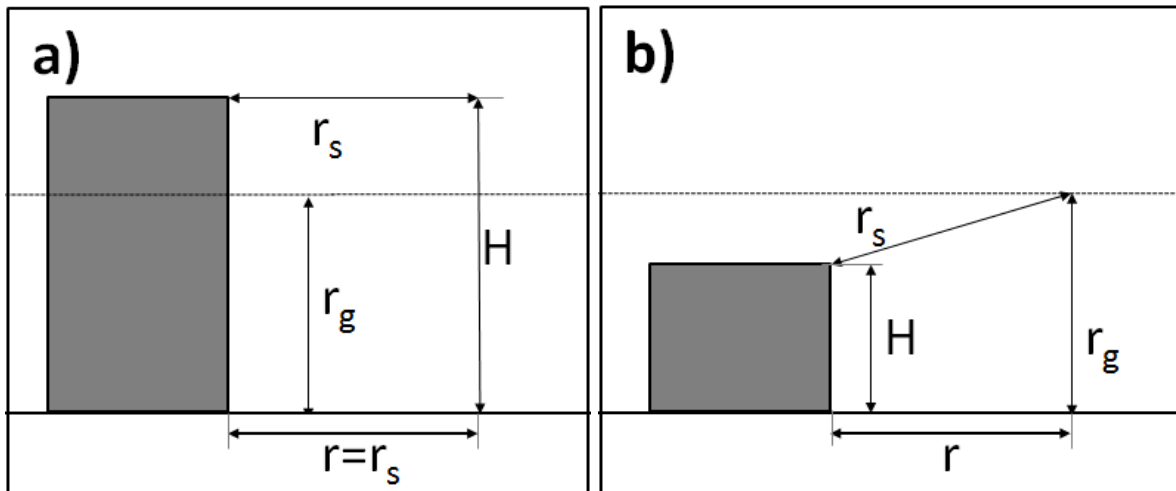


Figure 4.5: Procedure for the calculation of the ground projection of the capture distance: (a) equipment height H higher than attraction distance from the ground r_g ; (b) equipment height H lower than attraction distance from the ground r_g . (Necci et al., 2014a)

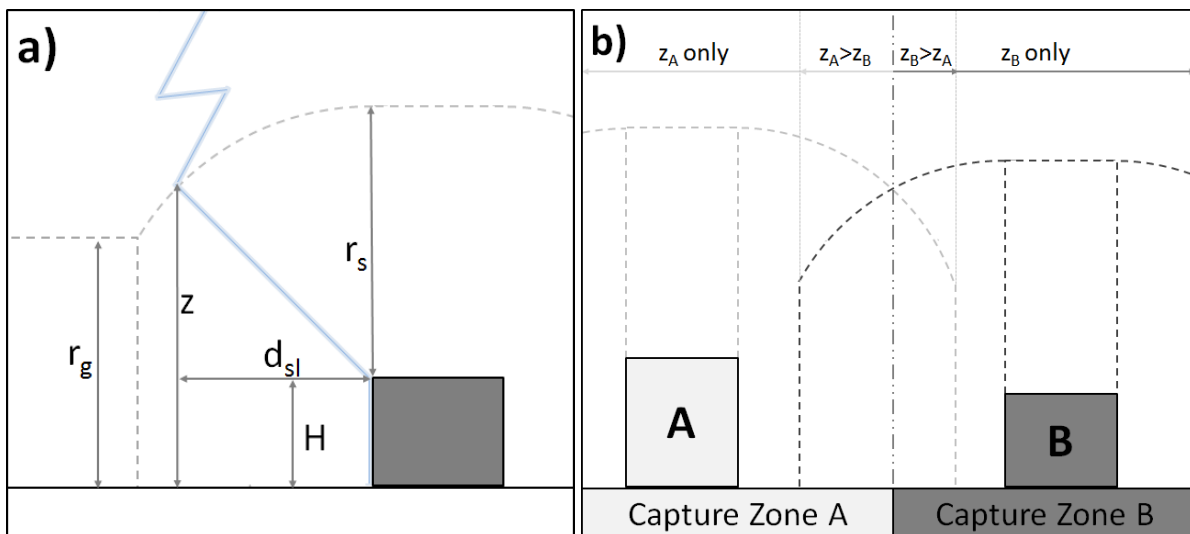


Figure 4.6: Calculation of the attraction height for the assignment of a lightning strike among different structures: (a) geometrical parameters for the calculation of capture height; (b) allocation zones based on the capture height criterion. (Necci et al., 2014a)

However, the above model is only suitable to calculate the capture frequency in the absence of interference from any other structure or relevant item in the surroundings. In most applications, it may well be that capture condition is satisfied by more than one item. Buildings, tanks, trees, columns, flares, etc. can all attract lightning strikes. When the capture condition is satisfied for more than one item, each lightning strike must be properly allocated. The EGM model can be applied to assign a lightning event to each structure.

Considering that the capture condition of a lightning with original position (\mathbf{x}, \mathbf{y}) is satisfied for a number k of items of concern, a “capture height” can be calculated for each of the k targets by the following equation (see Figure 4.6-(a) (Necci et al., 2014a)):

$$z_j = \sqrt{r_s^2 - d_{sl,j}^2} + H_j \quad (4.4)$$

where z_j is the capture height of the j -th item, $d_{sl,j}$ is the distance between the j -th item and the original strike location (\mathbf{x}, \mathbf{y}) calculated from the nearest point of the structure, and H_j is the height of the j -th structure. The values calculated for z_j are then compared for the k items of concern, and the lightning is assigned to the item having the highest value of the capture height. Figure 4.6-(b) exemplifies the procedure for two storage tanks.

4.4.3 Frequency assessment of attracted lightning strikes

The application of the Monte Carlo method allows the assessment of the expected frequency of lightning impact on each of the items considered in the area of interest. The capture frequency may be thus assessed as follows (Necci et al., 2014a):

$$f_{c,j} = f_l \cdot P_{c,j} = \left(n_g \cdot A \right) \frac{n_{c,j}}{n_{tot}} \quad (4.5)$$

where $f_{c,j}$ is the frequency of capture of the j -th item, f_l is the expected frequency of a lightning at the ground in area A expressed as number of lightning flashes per year, $P_{c,j}$ is the conditional probability of lightning impact on the j -th item given the lightning, n_g is the annual flash density (that is the number of expected lightning strikes per year per square km), A is the extension of the area of interest expressed in square km, n_{tot} is the total number of lightning events of the Monte Carlo simulations, and $n_{c,j}$ is the number of flashes captured by the j -th equipment. The capture frequency varies widely with the geographical region of interest, since n_g is comprised between 10^{-2} and 10^2 flashes \cdot km $^{-2}$ \cdot year $^{-1}$ depending on the geographical area of interest. Typical values of n_g range between 0.1 and 10 flashes \cdot km $^{-2}$ \cdot year $^{-1}$ (Cigré, 2013). Data on the flash frequency at ground are available from lightning location systems available in many countries (e.g. SIRF (2013)).

It is important to remark that the role of layout and of nearby items that are able to attract lightning strikes is relevant in determining the capture frequency. Thus, when considering the actual capture frequency for an equipment item of interest, a lay-out index may be defined to underpin this aspect. The lay-out index may be defined as the ratio between the lightning capture frequency of the unit of concern in its specific layout and the capture frequency that the same unit would have in an open flat field:

$$LI_j = \frac{f_{c,j}}{f_{cs,j}} \quad (4.6)$$

where LI_j is the layout index and f_{cs} is the capture frequency of equipment j in an open flat field where no other structure is present. The lay-out index is thus always comprised between 0 and 1, and is equal to 1 when no other nearby structure is present that may be able to attract and capture a lightning strike.

4.4.4 Simplified assessment of attracted lightning strikes

The model developed above provides a sound assessment of lightning capture frequency based on the EGM model and lay-out characteristics. However, in order to apply it, the user is required to carry out a high number of Monte Carlo simulations that increases with the complexity of the lay-out of interest. Thus, a simplified approach was developed, aimed to provide a model more suitable for the use in a QRA framework and validated by the comparison of the results with those obtained by the Monte Carlo method. As shown in Figure 4.4, the first step of the simplified model is based on the calculation of an average capture distance.

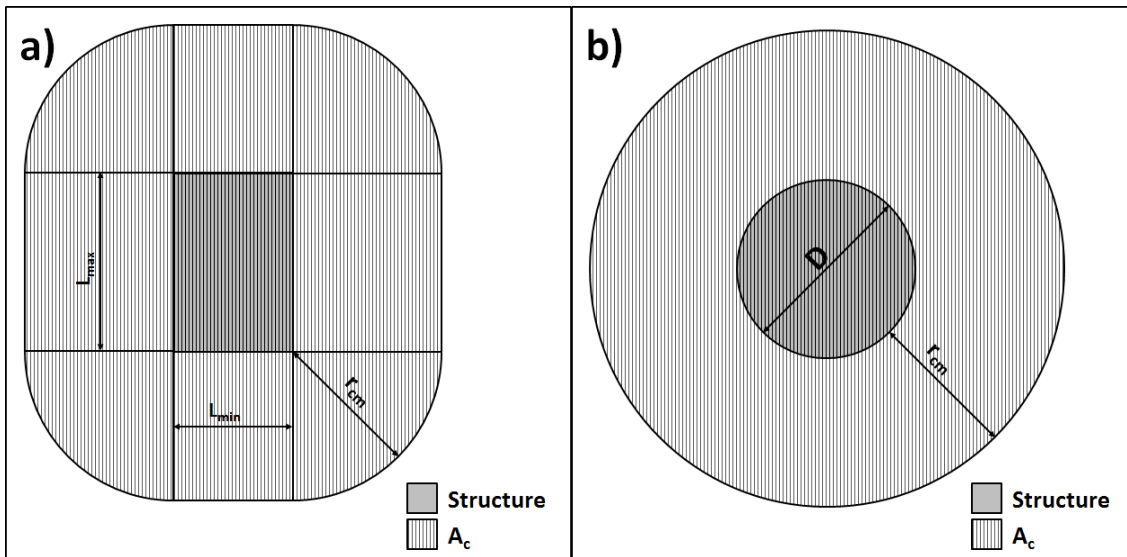


Figure 4.7: Average capture area of a vertical cylindrical structure: (a) generic structure; (b) vertical cylindrical structure (e.g. atmospheric storage tank). D : tank diameter; L_{min} and L_{max} : the two main horizontal dimensions of the structure; r_{cm} : average ground projection of the capture distance. (Necci et al., 2014a).

A mean peak current intensity, $I_{p,m}$, can be obtained from the distribution of peak current intensity values, I_p (Andersen and Eriksson, 1980; CEI, 2013). On the basis of the mean peak current intensity of the lightning, a mean attraction distance from the structure, r_{sm} , may be calculated from Eq. (4.1). The value of r_{sm} can be used to calculate a mean attraction distance from the ground, r_{gm} , using Eq. (4.2). The values calculated for these parameters using the distribution data for lightning current intensity provided by Andersen and Eriksson (1980), considering both positive and negative flashes are reported in Table 4.2.

Table 4.2: Average capture parameters obtained from the Andersen and Eriksson (1980) probability distribution data of peak lightning current intensity.

Mean Peak Current Intensity, $I_{p,m}$ (kA)	42.4
Mean Attraction distance, r_{sm} (m)	114.3
Mean Attraction Distance from the Ground, r_{gm} (m)	102.8

Since in an ordinary lay-out no element reasonably exceeds the height of 100m, it was assumed that the mean capture height is always higher than any structure considered. Thus, using Eq.(4.3) an average value may be obtained for the ground projection of the capture distance considering the height of the structure(Necci et al., 2014a):

$$r_{cm} = \sqrt{r_{sm}^2 - (r_{gm} - H)^2} \quad (4.7)$$

where r_{cm} is the average ground projection of the capture distance and H is the structure height expressed in meters. If the average values in table 1 are used for r_{sm} and r_{gm} , Eq.(4.7) can be approximated as follows (Necci et al., 2014a):

$$r_{cm} = 50.07 + 1.89 \cdot H - 2.33 \cdot 10^{-2} \cdot H^2 \quad (4.8)$$

As shown in Figure 4.7, the correlation given by Eq.(4.8) allows the calculation of an average capture area for any item of interest, A_c . In the case of a vertical cylindrical structure, such as an atmospheric storage tank, the capture area can be calculated as follows (Necci et al., 2014a):

$$A_c = \pi \left(r_{cm} + \frac{D}{2} \right)^2 \quad (4.9)$$

where D is the tank diameter.

If two or more structures are present in the area considered, it may happen that part of the capture areas of different units will overlap. In this case, the overlapping parts of the capture areas must be allocated among the structures. In order carry out such task, the adoption of a “cell method” is proposed. The area of interest is divided into square cells of uniform size. The ground projection of the capture distance is then calculated for each of the k equipment items present in area A of concern using Eqs. (4.7) or (4.8). A capture area, $A_{c,j}$, is then calculated for each equipment item. The capture area is obtained attributing to the equipment capture area, $A_{c,j}$, the area of each cell that verifies the following condition (see Figure 4.8-(a)):

$$d_{cc,i,j} \leq r_{cm,j} \quad (4.10)$$

where $d_{cc,i,j}$ is the distance between the center of cell i and the nearest point of the j -th equipment item.

If the same cell verifies the condition given by Eq.(4.10) for two or more equipment items or structures present in the area, the capture height of the j -th equipment in the center of the i -th cell, $z_{i,j}$, is calculated applying Eq.(4.4) to the average value of the attraction distance (Necci et al., 2014a):

$$z_{i,j} = \sqrt{r_{sm}^2 - d_{cc,i,j}^2} + H_j \quad (4.11)$$

where H_j is height of the j -th structure. The cell is then allocated to the capture area of the structure with the highest value of $z_{i,j}$ (see Figure 4.6). The overall value of the capture area of each equipment item or structure considered is thus calculated as follows (Necci et al., 2014a):

$$A_{c,j} = \sum_{i=1}^{N_c} \delta_{i,j} \cdot A_i \quad (4.12)$$

where A_i is the area of cell i , N_c is the total number of cells considered, and $\delta_{i,j}$ is equal to 1 if the i -th cell is attributed to the capture area of equipment j by the conditions discussed above. Otherwise $\delta_{i,j}$ is equal to 0.

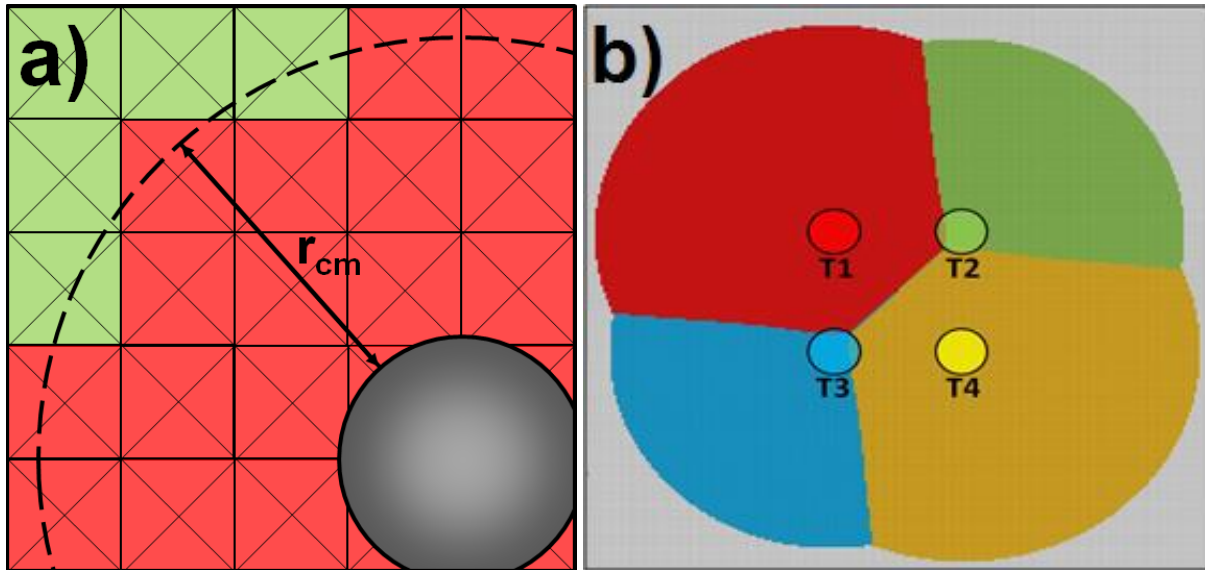


Figure 4.8: Procedure to assess the capture area of equipment items or structures by the cell method: (a) assignment of cells to the equipment capture area (grey: equipment item; red: cells attributed to equipment item capture area; green: cells not belonging to capture area); (b) capture areas calculated by the cell method for four equipment items using the criterion given by Eq.(11). Tank geometries are reported in Table 4.3. (Necci et al., 2014a)

The accuracy of this simplified method, as well as the computational effort required for its application, increase with the number of cells in which the area of interest, A , is divided. Usually a sufficient accuracy is obtained if square cells of equal area are defined with size lower than the lower value of ground projection radius r_{cm} calculated for the equipment items or structures considered in the area of concern using Eqs. (4.7) and (4.8).

The capture frequency for the j -th equipment item considered, $f_{c,j}$, may be then calculated on the basis of the capture area obtained from Eq.(4.12) and of the annual flash density, n_g (Necci et al., 2014a):

$$f_{c,j} = n_g \cdot A_{c,j} \quad (4.13)$$

As an example, the above-described procedure is applied to the simplified lay-out reported in Figure 4.8-(b). Square cells of 1m^2 are defined, having a size much lower than the capture radius. Area A is represented by 50,000 square cells. Among these, the procedure attributes 38,460 cells to the capture area of the tanks in the lay-out. Figure 4.8-(b) shows the shape of the capture areas calculated for the four tanks. The tank geometries are described in Table 4.3. The table also reports the calculated extent of the capture areas and the capture frequencies calculated by using both the Monte Carlo and the simplified model. The lay-out index was also estimated and is reported in the table. As shown by the table, the two models provide quite similar results for this case-study.

Table 4.3: Geometrical features and capture frequencies calculated for the four tanks in the lay-out shown in Figure 4.8-(b); $f_{c,MC}$: results obtained from the Monte-Carlo model; $f_{c,S}$: results obtained from the simplified model; RE%: relative error of the capture frequency obtained from the simplified model with respect to the corresponding capture frequency obtained from the Monte-Carlo model, calculated using Eq.(14). (Necci et al., 2014a)

Tank id.	D (m)	H (m)	A_c (m ²)	$f_{c,S}$ (y ⁻¹)	$f_{c,MC}$ (y ⁻¹)	RE%	LI (MC)	LI (Simplified)
T1	20	15	12900	3.87×10^{-2}	3.79×10^{-2}	2.11	0.581	0.594
T2	20	10	6330	1.90×10^{-2}	1.91×10^{-2}	-0.64	0.340	0.343
T3	20	10	6330	1.90×10^{-2}	1.88×10^{-2}	1.06	0.340	0.343
T4	20	15	12900	3.87×10^{-2}	3.80×10^{-2}	1.84	0.582	0.593

4.4.5 Comparison of results obtained by the Monte Carlo and the simplified model

The simplified model described above leads to a more simple calculation of the capture frequency for stand-alone equipment items as well as for complex lay-outs. However, since the model introduces some approximations, it is important to understand the expected differences in the results obtained with respect to those obtained from the complete Monte Carlo model. A vessel database, developed in a previous study (Landucci et al., 2012) was used to obtain an exhaustive and representative range of possible vessel geometries and was used for model validation. The database was obtained considering available data on tanks present at several industrial tank farms, data from widely-used design standards (e.g. API Standard 650 (2003)) and available design standards from engineering companies. Table 4.4 reports a summary of the ranges of tank volumes and geometrical data considered in the database, which includes 116 different vessel geometries. Further details on the vessel database used are reported in (Landucci et al., 2012). Standalone capture frequencies and a total of 96 lay-outs were defined to assess the effect on model results of simple lay-out geometries composed of a variable number of storage tanks, including 2 to 20 items. A square area A with the tanks at its center was considered in the calculations, having an extension of 1 km². A value of 3 flashes·km⁻²·year⁻¹ was assumed for the flash density at the ground (n_g). The relative error of the simplified model was calculated as (Necci et al., 2014a):

$$RE\% = \frac{(f_{c,S} - f_{c,MC})}{f_{c,MC}} \cdot 100 \quad (4.14)$$

where $f_{c,S}$ is the capture frequency obtained from the simplified model and $f_{c,MC}$ is the capture frequency obtained from the Monte Carlo model.

Table 4.4: Ranges of main geometrical data assumed for the atmospheric storage tanks considered in simplified model assessment; D: tank diameter; H: tank height (Necci et al., 2014a).

Tank Type	Capacity (m ³)	D (m)	H (m)
Atmospheric	38-16300	3-66	5.4-18

Figure 4.9 shows the parity plot obtained for the values of the capture frequencies calculated by the two models. As evident from the figure, the results expressed in terms of capture frequency show only limited differences. The relative error is always below 10%. The recorded maximum positive relative error is 8.5%, while the maximum negative relative error is -6.6%. On the one hand, the simplified model shows to be slightly conservative for tanks in lay-outs where several structures capable of attracting lightning flashes are present. On the other hand, somewhat higher capture frequencies are obtained by using the Monte Carlo model for standalone tanks.

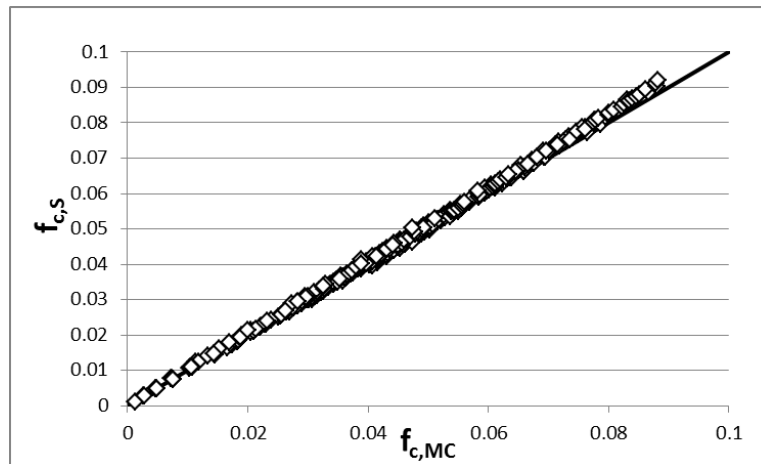


Figure 4.9: Parity plot showing the capture frequencies (events/year) calculated with the simplified model, $f_{c,S}$, versus the capture frequencies obtained with the Monte Carlo model, $f_{c,MC}$ for all the simulations carried out for both stand-alone vessels and more complex lay-outs (Necci et al., 2014a).

4.4.6 Results

4.4.6.1 Model application to stand-alone equipment items and to simple lay-outs

In order to verify the applicability of the model in a realistic framework, the lightning capture frequency was calculated for a reference set of equipment items in industrial lay-outs, identifying tank geometries widely used in industrial sites and considering actual lay-outs for unprotected structures.

As a first step, the capture frequency was calculated for all the tanks assumed to be stand-alone, i.e., neglecting the influence of nearby structures. Since previous studies showed that atmospheric storage tanks are the structures most affected by lightning strikes (Renni et al., 2010; Necci et al., 2013a), vertical cylindrical atmospheric storage tanks of different geometries were considered. The tanks were assumed to be on an open flat ground without any other structure in the vicinity. A square area A of 1 km^2 with the tank at its center was considered. A value of $3 \text{ flashes} \cdot \text{km}^{-2} \cdot \text{year}^{-1}$ was assumed for the flash density n_g . Table 4.5 reports some sample results obtained for the capture frequency using both the complete Monte Carlo model and the simplified model. As shown in the table, the attraction frequency for unprotected stand-alone structures is rather high (of the order of 10^{-2} events/year) for flash densities typical of European regions.

Table 4.5: Capture frequencies calculated for a reference set of stand-alone vertical cylindrical tanks assuming a flash density of 3 flashes·km⁻²·year⁻¹ using the Monte Carlo ($f_{cs,MC}$) and the simplified models ($f_{cs,S}$). D : tank diameter; H : tank height; $RE\%$: relative error (%) calculated from Eq.4.13 (Necci et al., 2014a).

Tank ID	Volume (m ³)	D (m)	H (m)	w (mm)	$f_{cs,MC}$ events/year	$f_{cs,S}$ events/year	$RE\%$
1	38	3	5.4	5	3.71×10^{-2}	3.53×10^{-2}	-4.85%
2	100	4.4	7	5	4.04×10^{-2}	3.91×10^{-2}	-3.14%
3	250	7.7	7.5	5	4.36×10^{-2}	4.21×10^{-2}	-3.40%
4	500	7.8	11	6	4.94×10^{-2}	4.87×10^{-2}	-1.36%
5	750	10.5	9	7	4.77×10^{-2}	4.68×10^{-2}	-1.89%
6	1000	15	6	9	4.57×10^{-2}	4.38×10^{-2}	-4.16%
7	2500	20	5.4	11	4.77×10^{-2}	4.58×10^{-2}	-4.01%
8	5200	25	11	11	6.15×10^{-2}	6.11×10^{-2}	-0.68%
9	7634	30	10.8	12	6.49×10^{-2}	6.45×10^{-2}	-0.60%
10	9975	42	7.2	12	6.67×10^{-2}	6.58×10^{-2}	-1.38%
11	12367	54	5.4	13	7.15×10^{-2}	7.08×10^{-2}	-0.92%
12	16303	66	5.4	15	8.09×10^{-2}	8.10×10^{-2}	0.11%

These values are actually conservative since they neglect lay-out effects from nearby structures that in real-life situations would lead to lower values of capture frequency. Lay-out effects may derive from other equipment items in the area, but also from buildings, electric lines, trees, and other tall structures. Lay-out effects depend on the distance and on the geometrical features of the other structures (the height being the most important parameter). Thus, it is important to understand which are the reference distances below which lay-out effects become significant and need to be considered in the assessment of the capture frequency.

As a starting point to understand lay-out effects due to nearby equipment items, a simplified lay-out is analyzed, composed of two tanks having the same diameter and height, and positioned at different distances (Figure 4.10).

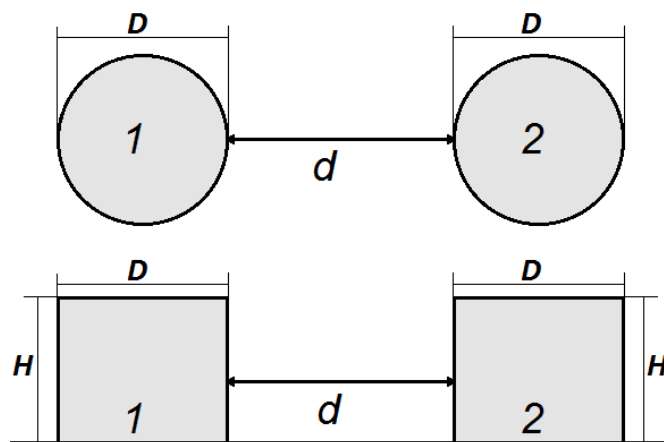


Figure 4.10: Simplified lay-out considered to assess lay-out effects: footprint and side view (H : tank height; D : tank diameter; d : distance among tank shells). (Necci et al., 2014a)

Table 4.6: Geometrical features assumed for tanks in Figure 4.10 (D: diameter; H: height; H_r : ratio of height on tank 2 over height of tank 1;; f_{cs} : capture frequency). (Necci et al., 2014a)

ID	Tank 1, D (m)	Tank 1, H (m)	Tank 2, D (m)	Tank 2, H (m)	H_r	Tank 1, f_{cs} (events/year)
A	10	12.6	10	9; 12.6; 16.2; 18	0.71-1.43	5.42×10^{-2}
B	20	12.6	20	9; 12.6; 16.2; 18	0.71-1.43	6.09×10^{-2}
C	30	12.6	30	9; 12.6; 16.2; 18	0.71-1.43	6.87×10^{-2}
D	60	12.6	60	9; 12.6; 16.2; 18	0.71-1.43	9.33×10^{-2}
E	5-100	9	20	9	1	4.33×10^{-2} - 1.25×10^{-1}
F	10-100	9	20	9	1	4.65×10^{-2} - 1.25×10^{-1}

Figure 4.11 shows the values of the lay-out indices calculated with the Monte Carlo model and the simplified model for the lay-out of Figure 4.10 (case b reported in Table 4.6 for a height of 12.6m for Tank 2). As shown in Figure 4.11, the lay-out index ranges from 0.6 to 1, depending on the distance between the tanks. Although the results shown in Figure 4.11 refer to a specific tank geometry, similar trends were obtained for all the tank geometries reported in the database, thus allowing us to draw some general conclusions. The values of the lay-out index obtained with the two models are very similar, with differences lower than 5%. It should be noted that differences between the two models in general are negligible (lower than 1%) up to distances of 50m that are those of interest in industrial lay-outs. Moreover, the results obtained with the simplified method are always conservative with respect to those obtained with the Monte-Carlo model.

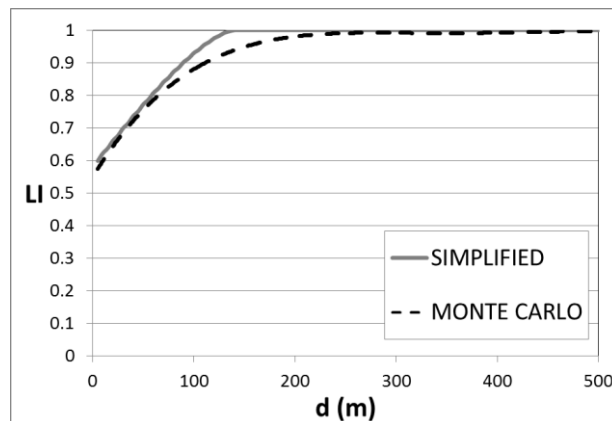


Figure 4.11: Values calculated for the lay-out index as a function of distance between vessel shells for two identical storage tanks having a diameter equal to 20 m and height equal to 12.6m. (Necci et al., 2014a)

In order to assess the influence of tank diameter and height on the lay-out index, Figures 4.12-(a) to 4.12-(d) show the values of the lay-out indices calculated with the Monte Carlo model for simplified lay-outs in which two tanks having the same diameter and different heights are considered. As shown in the figure, the lay-out index ranges from 0.2 to 0.8, depending on the relative height and on the diameter of the tanks. As shown in the figure, the lay-out index shows a limited dependency on the tank height ratio when the tanks have very large diameters (e.g. see Figure 4.12-(d), where diameters of 60m were assumed). In contrast, the lay-out index is highly

influenced by the height ratio of the structures for small tank sizes and short distances, as shown in Figure 9-(a) and 4.12-(b). Figures 4.12-(e) and 4.12-(f) show some results obtained for tanks with different diameters and the same height. The LI lies between 0.4 and 0.9 and increases with the difference between the diameters. Moreover, when diameters have the same order of magnitude or are larger than the mean capture radius (60m), the variation of the LI as a function of the distance among the tanks is very limited or almost negligible.

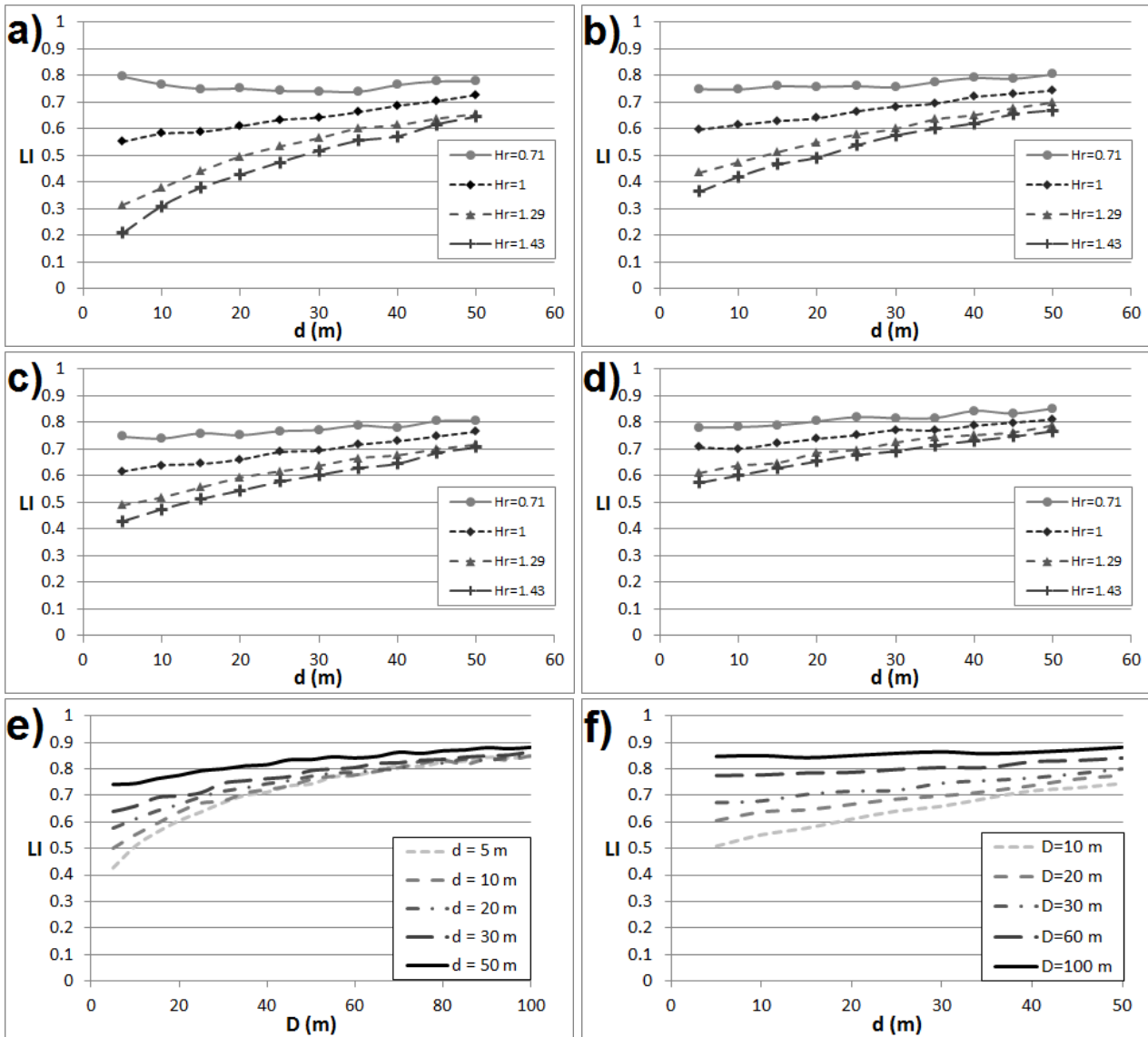


Figure 4.12: Lay-out index (LI) calculated for Tank 1 in the simplified lay-out shown in Figure 4.10. (a) LI vs. distance for Tank 1 and Tank 2 diameters equal to 10 m and different H_r values; (b) LI vs. distance for Tank 1 and for Tank 2 diameters equal to 20 m and different H_r values; (c) LI vs. distance for Tank 1 and Tank 2 diameters equal to 40 m and different H_r values; (d) LI vs. distance for Tank 1 and Tank 2 diameters equal to 60 m and different H_r values; (e) LI vs. Tank 1 diameter and different distances among tanks (Tank 1 and Tank 2 heights equal to 9 m; Tank 2 diameter equal to 20 m); (f) LI vs. distance considering for Tank 2 $D=20$ m and different values of Tank 1 diameter. Other geometrical parameters of the tanks are reported in Table 4.6; H_r is the ratio of the height of Tank 2 with respect to the height of Tank 1. (Necci et al., 2014a)

When more complex and more realistic lay-outs are considered, edge effects become evident. Figure 4.13 shows a simplified regular lay-out consisting of 12 tanks all having the same distance one to another and disposed along square cells. Such simplified geometries are typical for tank farms in oil refineries.

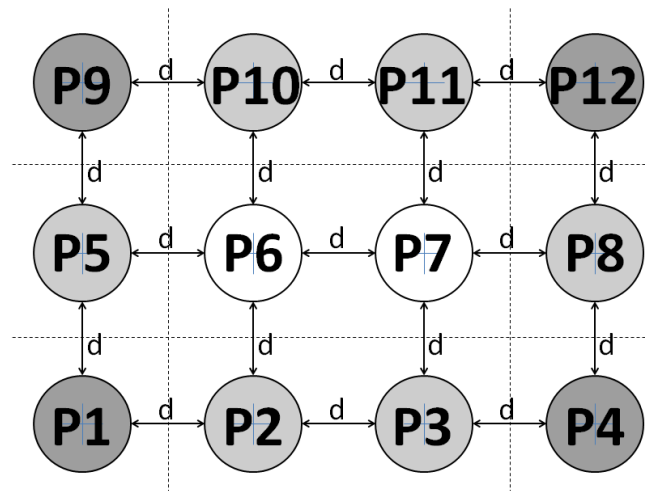


Figure 4.13: Lay out of 12 identical tanks having the same geometrical features. Tank centers are positioned at the same distance to each other. P1, P4, P9, P12 : tanks in angle position; P2, P3, P5, P8, P10, P11: tanks in edge position; P6,P7: tanks in central position. (Necci et al., 2014a)

Table 4.7 shows the results obtained for the lay-out indices calculated by the Monte Carlo model using 10^7 simulations. For the sake of simplicity, a single tank geometry was considered for all the tanks in the lay-out (Tank 9 in Table 4.5).

Table 4.7: Values of LI calculated for the lay-out in Figure 4.13 assuming for all the tanks the geometrical features of tank 9 in table 4.5 and considering different distances, d , between tank shells. (Necci et al., 2014a)

Position	Type	Distance, d			
		10 m	20 m	30 m	50 m
P1	Angle	0.41	0.46	0.50	0.60
P2	Edge	0.18	0.24	0.30	0.42
P3	Edge	0.18	0.24	0.30	0.42
P4	Angle	0.41	0.46	0.50	0.60
P5	Edge	0.18	0.24	0.30	0.42
P6	Centre	0.073	0.12	0.17	0.29
P7	Centre	0.073	0.12	0.17	0.29
P8	Edge	0.18	0.24	0.30	0.42
P9	Angle	0.41	0.46	0.50	0.60
P10	Edge	0.18	0.24	0.30	0.42
P11	Edge	0.18	0.24	0.30	0.42
P12	Angle	0.41	0.46	0.50	0.60

As shown in the table, the lay-out index is influenced both by the distance and the position of the tanks in the lay-out. In particular, tanks having a similar position in the lay-out (angle, edge,

center) have very similar values of the lay-out indices (see Tables A1, A2, A3 in the Appendix). As a matter of fact, differences in the value of lay-out indices are almost negligible for tanks in the same type of position (angle, edge, center) in the lay-out.

4.4.6.2 Results obtained in the analysis of an existing tank farm lay-out

In order to understand the values of capture frequencies in real-life application, the lay-out of an existing tank farm in an oil refinery was considered. Figure 4.14 shows the lay-out of the considered tank farm. Several atmospheric tanks with different geometries are present: external floating roof tanks, internal floating roof tanks and fixed cone roof tanks. Table 4.8 summarizes the features of the tanks present in the lay-out. Two different assessments were carried out: i) taking into account only atmospheric tanks; ii) taking into account all tall structures (e.g. also power lines, flares, columns, etc.). No specific lightning protection was assumed to be present. Both the Monte Carlo and the simplified model were applied to calculate the capture frequency values. The capture frequencies calculated from the simulations carried out using both the Monte Carlo and the simplified models, and considering a flash density n_g typical of an Italian site and equal to $2.5 \text{ flashes} \cdot \text{km}^{-2} \cdot \text{year}^{-1}$ (SIRF, 2013), are reported in Table 4.8. The table shows the stand-alone capture frequency calculated for each tank and the actual capture frequency calculated neglecting and considering the effect of structures different from storage tanks. The table shows that when surrounding structures are not considered the capture frequencies of the tanks in the lay-out are between $2 \cdot 10^{-2}$ and $10^{-1} \text{ events} \cdot \text{year}^{-1}$. Lay-out indices are between 0.25 and 0.75, depending on the size and position of the tank (angle, edge, or centre), with the exception of Tanks 1 and 2 that have a more isolated position and thus a higher lay-out factor than the others (between 0.75 and 1). When the effect of surrounding tall structures, such as flares, is considered, capture frequencies slightly decrease, falling into the range of 10^{-2} to $7 \cdot 10^{-2} \text{ events} \cdot \text{year}^{-1}$. Lay-out indices also decrease, being between 0.25 and 0.5 for most of the tanks. Table 4.8 also confirms that the results of the simplified method are in good agreement with those obtained by Monte Carlo simulations, with an error in the assessment of capture frequencies that is below the inherent uncertainties of QRA calculations.

Figure 4.15 reports a ranking of the lay-out indices calculated either excluding or including in the analysis the surrounding structures. The figure allows a better understanding of how the position on the lay-out of the equipment items influences the lay-out index calculated from the method.

Comparison of Figures 4.15-(a) and 13-(b) clearly shows the indirect protection effect of surrounding tall structures. In particular, this effect is evident for Tanks 6, 9 and 18, that receive a considerable indirect protection from the presence of adjacent tall structures. As expected, the LI calculated for the largest tanks, with $D > 50 \text{ m}$, are generally less influenced by the presence of nearby tanks (Case 1). However their capture frequency and LI can still be effected by the vicinity of very tall structures (Case 2). This result is coherent with the historical data on accidents triggered by lightning strikes, which reports that most of fires and explosions involved very large tanks (Persson and Lönnermark, 2004).

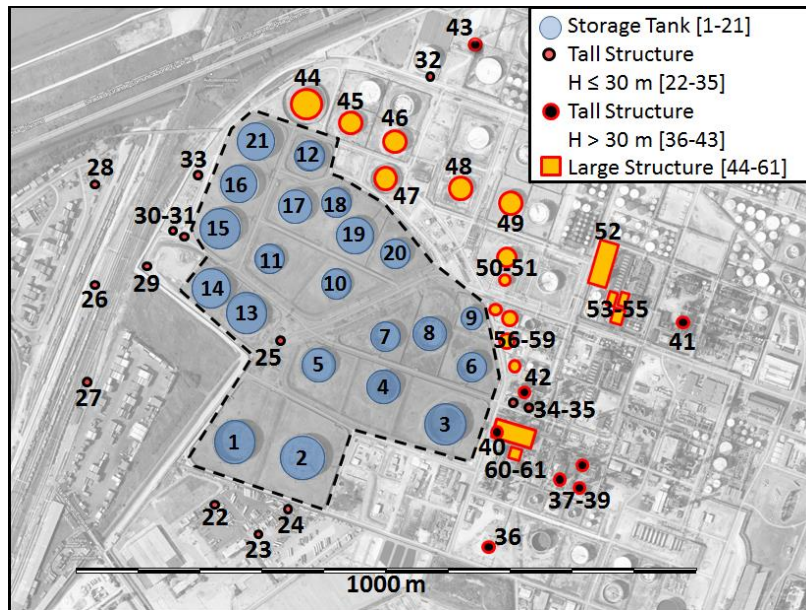


Figure 4.14: Lay-out considered for the extended case study: the zone of interest is highlighted in grey and delineated by a dashed line; the storage tanks under analysis are blue; other relevant structures considered in the analysis are displayed with different symbols and colours. (Necci et al., 2014a)

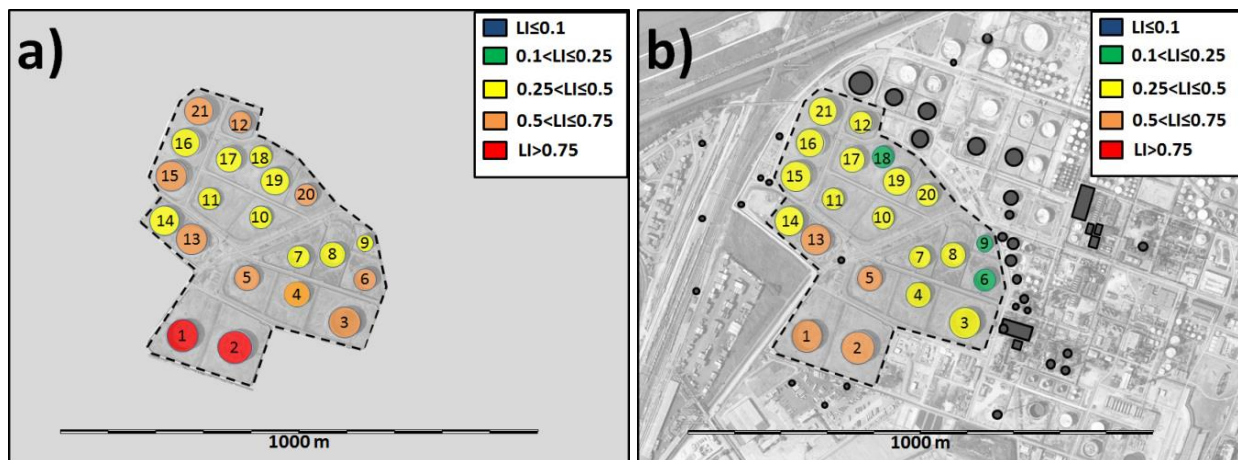


Figure 4.15: Lay-out indices calculated for the structures considered in the lay-out reported in Figure 4.14. a) lay-out indices calculated considering only storage tanks; b) lay-out indices calculated considering all structures in the vicinity of the storage tanks. (Necci et al., 2014a)

Table 4.8: Results of the analysis of lay-out in Figure 4.13. Case 1: only storage tanks considered; Case 2: all structures considered (*D*: diameter or equivalent diameter of the structure; *H*: height of the structure; *f_c*: capture frequency; *LI*: lay-out index; *ID*: structure number in Figure 4.14). (Necci et al., 2014a)

TANK FEATURES			MONTE CARLO METHOD					SIMPLIFIED METHOD				
			Stand alone	Case 1		Case 2		Stand alone	Case 1		Case 2	
ID	<i>D</i> (m)	<i>H</i> (m)	<i>f_{cs,MC}</i> (y ⁻¹)	<i>f_{c,MC}</i> (y ⁻¹)	<i>LI_{MC}</i>	<i>f_{c,MC}</i> (y ⁻¹)	<i>LI_{MC}</i>	<i>f_{cs,S}</i> (y ⁻¹)	<i>f_{c,S}</i> (y ⁻¹)	<i>LI_S</i>	<i>f_{c,S}</i> (y ⁻¹)	<i>LI_S</i>
1	72	10.8	8.21x10 ⁻²	6.93 x10 ⁻²	0.84	5.35 x10 ⁻²	0.65	8.00 x10 ⁻²	7.01 x10 ⁻²	0.88	5.86 x10 ⁻²	0.73
2	72	10.8	8.21 x10 ⁻²	6.72 x10 ⁻²	0.82	4.84 x10 ⁻²	0.59	8.00 x10 ⁻²	6.95 x10 ⁻²	0.87	5.28 x10 ⁻²	0.66
3	60	9.0	7.09 x10 ⁻²	5.14 x10 ⁻²	0.72	2.20 x10 ⁻²	0.31	6.76 x10 ⁻²	5.19 x10 ⁻²	0.77	2.37 x10 ⁻²	0.35
4	48	10.8	6.69 x10 ⁻²	3.37 x10 ⁻²	0.50	3.26 x10 ⁻²	0.49	6.21 x10 ⁻²	3.63 x10 ⁻²	0.58	3.63 x10 ⁻²	0.58
5	48	10.8	6.69 x10 ⁻²	4.00 x10 ⁻²	0.60	3.90 x10 ⁻²	0.58	6.21 x10 ⁻²	4.50 x10 ⁻²	0.72	4.31 x10 ⁻²	0.69
6	48	12.6	6.71 x10 ⁻²	3.91 x10 ⁻²	0.58	1.61 x10 ⁻²	0.24	6.51 x10 ⁻²	3.92 x10 ⁻²	0.60	1.64 x10 ⁻²	0.25
7	48	12.6	6.71 x10 ⁻²	2.73 x10 ⁻²	0.41	2.69 x10 ⁻²	0.40	6.51 x10 ⁻²	2.82 x10 ⁻²	0.43	2.82 x10 ⁻²	0.43
8	48	12.6	6.71 x10 ⁻²	2.75 x10 ⁻²	0.41	2.69 x10 ⁻²	0.40	6.51 x10 ⁻²	2.84 x10 ⁻²	0.44	2.84 x10 ⁻²	0.44
9	30	12.6	6.71 x10 ⁻²	3.29 x10 ⁻²	0.49	1.68 x10 ⁻²	0.25	5.29 x10 ⁻²	3.30 x10 ⁻²	0.62	1.85 x10 ⁻²	0.35
10	48	10.8	6.69 x10 ⁻²	3.17 x10 ⁻²	0.47	3.13 x10 ⁻²	0.47	6.21 x10 ⁻²	3.43 x10 ⁻²	0.55	3.43 x10 ⁻²	0.55
11	36	9.0	5.51 x10 ⁻²	1.90 x10 ⁻²	0.34	1.98 x10 ⁻²	0.36	5.13 x10 ⁻²	2.04 x10 ⁻²	0.40	2.04 x10 ⁻²	0.40
12	48	18.0	7.93 x10 ⁻²	4.31 x10 ⁻²	0.54	2.53 x10 ⁻²	0.32	7.38 x10 ⁻²	4.28 x10 ⁻²	0.58	2.59 x10 ⁻²	0.35
13	66	12.6	8.18 x10 ⁻²	4.92 x10 ⁻²	0.60	4.65 x10 ⁻²	0.57	7.86 x10 ⁻²	5.29 x10 ⁻²	0.67	4.90 x10 ⁻²	0.62
14	66	10.8	7.92 x10 ⁻²	3.62 x10 ⁻²	0.46	2.73 x10 ⁻²	0.34	7.54 x10 ⁻²	3.63 x10 ⁻²	0.48	2.90 x10 ⁻²	0.38
15	66	12.6	8.18 x10 ⁻²	4.16 x10 ⁻²	0.51	2.93 x10 ⁻²	0.36	7.86 x10 ⁻²	4.13 x10 ⁻²	0.52	2.99 x10 ⁻²	0.38
16	66	12.6	8.18 x10 ⁻²	3.11 x10 ⁻²	0.38	2.16 x10 ⁻²	0.26	7.86 x10 ⁻²	3.17 x10 ⁻²	0.40	2.13 x10 ⁻²	0.27
17	54	14.4	7.64 x10 ⁻²	2.42 x10 ⁻²	0.32	2.50 x10 ⁻²	0.33	7.25 x10 ⁻²	2.50 x10 ⁻²	0.34	2.50 x10 ⁻²	0.34
18	48	14.4	7.20 x10 ⁻²	1.94 x10 ⁻²	0.27	1.53 x10 ⁻²	0.21	6.81 x10 ⁻²	1.98 x10 ⁻²	0.29	1.62 x10 ⁻²	0.24
19	54	14.4	7.64 x10 ⁻²	2.80 x10 ⁻²	0.37	2.04 x10 ⁻²	0.27	7.25 x10 ⁻²	2.90 x10 ⁻²	0.40	2.03 x10 ⁻²	0.28
20	48	14.4	7.20 x10 ⁻²	4.54 x10 ⁻²	0.63	3.55 x10 ⁻²	0.49	6.81 x10 ⁻²	4.70 x10 ⁻²	0.69	3.94 x10 ⁻²	0.58
21	66	14.4	8.55 x10 ⁻²	5.14 x10 ⁻²	0.60	3.88 x10 ⁻²	0.45	8.19 x10 ⁻²	5.10 x10 ⁻²	0.62	3.94 x10 ⁻²	0.48

4.4.7 Final consideration regarding lightning impact frequency assessment

The calculation of the lightning impact frequency provides the essential information to approach the assessment of the quantitative contribution of lightning-triggered accidents to industrial risk. A specific model based on a Monte Carlo procedure was developed to assess the capture frequency of lightning by equipment items in complex lay-outs. A simplified method, devoted to QRA application, was also proposed and validated on the basis of the results of the Monte Carlo model. Both modelling approaches allow the calculation of capture frequencies either for stand-alone tanks or considering the lay-out and the effect of nearby structures. Because of the crucial contribution of the layout on lightning attraction, a lay-out index was defined as the ratio of the actual capture frequency with respect to that calculated for a stand-alone situation (corresponding to a lay-out in which no other structure is present), in order to evaluate the effect of the surrounding buildings and items on lightning impact frequency. The lay-out index was shown to

depend on the separation distances between the structures, on the relative height, as well as on the relative position of equipment items and structures. In particular, when tank farms are considered, non-uniform capture frequencies are present and tanks positioned on angles or edges show higher capture frequencies than tanks in the centre of the tank farm. The layout index calculated for reference realistic case studies ranged between 0.1 to 0.8, for the critical equipment units: the biggest atmospheric tanks of a storage tank park. This is a useful information, because it assesses the error present on lightning impact frequency assessment in the case simplified correlations, such as those presented in section 4.4.4 are used and the layout effect is neglected (i.e. Eq. 7 to 9). Even with this extremely simplified approach, the assessed lightning impact frequency by the use of simplified correlations does not exceed of more than one order magnitude the lightning impact frequency values, assessed by methodologies, such as Monte Carlo simulations or the “cell method”, which requires a higher computational effort.

4.5 Identification of the damage modalities and of reference scenarios

4.5.1 Characterization of the critical equipment

Above ground atmospheric tanks for the storage of large amounts of liquids are typically vertical cylinders made of low carbon steel, with a flat bottom resting on a uniform specifically prepared ground layer. The storage capacity of these tanks depends on the tank diameter and height. Due to their size, these tanks are usually built directly on site and obtained assembling steel plate courses having different thicknesses. The more common course heights (h) used in industrial practice are 1800mm or 2400mm (API Std 650, 2003). As shown in the sketch reported in Fig. 4.16, the bottom courses are usually thicker than the higher ones, since they need to resist to a higher hydrostatic pressure. However, courses having a constant thickness may be used in low volume tanks. The tank construction features that are relevant with respect to the vulnerability to lightning are (with reference to Fig. 4.16: tank diameter, D ; tank height, H ; type of construction material; height, h_j , and thickness, t_j , of the j -th level of courses. Exhaustive details about of welded storage tank design are reported in API Standard 650 (2003).

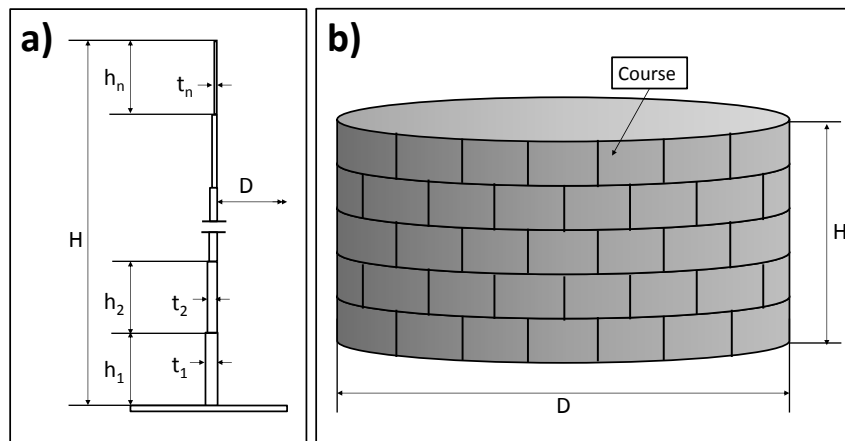


Figure 4.16: Typical sketch of a welded above ground atmospheric tank. a) typical arrangement of shell thicknesses with respect to tank height (t_j : course thickness; h_j : course height; n : total number of courses); b) overall geometrical parameters of a tank (D : diameter; H : height). (Necci et al., 2014b)

Depending on the roof shape, three main categories of atmospheric storage tank may be identified in storage tank farms (see Fig. 4.17) (Necci et al., 2014b):

- Cone roof (CR) tanks, having a flat bottom, a vertical cylindrical shell and a fixed cone-shaped roof welded to the top of the tank. In these tanks, an inert blanketing system is generally used to avoid the formation of flammable mixtures in the confined volume above the liquid level.
- External floating roof (EFR) tanks, having a flat bottom, a vertical cylindrical shell and a pontoon type roof floating directly on the surface of the stored liquid. The floating roof has a mechanical shoe or tube seal on its perimeter. This “rim-seal” covers the space between the floating roof and the tank shell.

- Internal Floating Roof (IFR) tanks, having a cone roof but with the addition of an internal floating roof or pan that floats directly on the liquid surface. Depending on the seal used to limit evaporation through the gap between the floating roof and the shell, and on the properties of the stored substance, the installation of an inert blanketing system may be required.

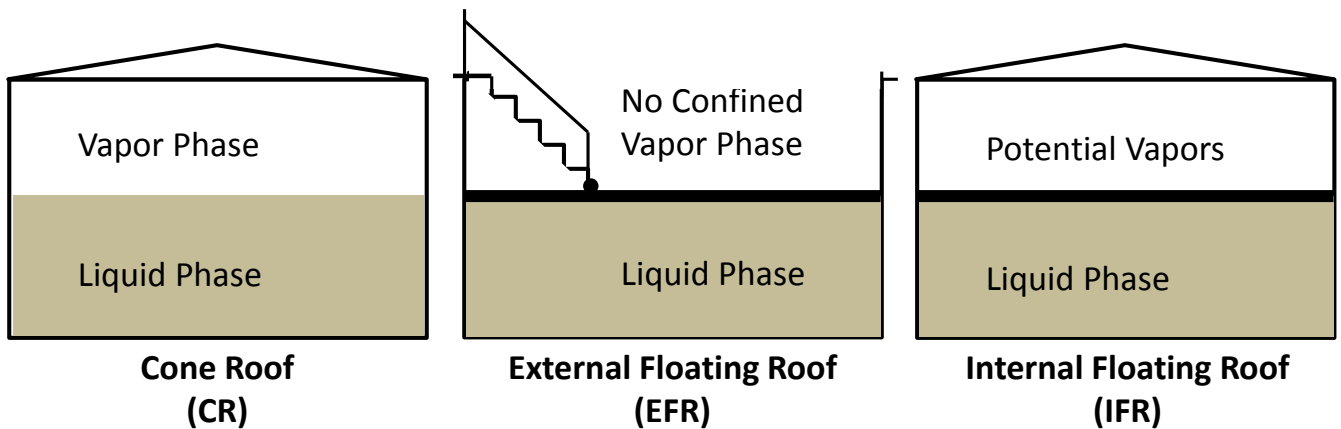


Figure 4.17: Sketch of the more frequently applied above ground design solutions for large volume atmospheric storage tanks. (Necci et al., 2014b)

4.5.2 Lightning damage modes

The impact of lightning strike can trigger different accidental scenarios, depending on the features of the target tank and on the properties of the stored substance. The direct action of lightning impact on tank shells may result in the damage of vessel shell (puncturing) and in the consequent release of liquid. If puncturing does not occur (e.g. since the lightning energy is not sufficient to perforate the vessel shell), the only consequence of lightning impact may be the ignition of flammable vapor mixtures in the vicinity of the impact point (Renni et al., 2010). Thus, in the case of tanks storing non-flammable materials, the only possible hazard is the perforation of the tank due to direct lightning impact, with the consequent release of liquid and its evaporation from the bund surface. The conditional probability of this scenario derives from the assessment of lightning damage probability and may be estimated by the model proposed by Necci et al. (2013a).

When flammable substances are stored, more complex scenarios are possible. In particular, the possible ignition of flammable vapors due to the lightning may cause fires and/or confined explosions, depending on the type of tank, even in the absence of direct damage to tank shell. Ignition hazard, both outside and inside the tank may derive from electric arcs that can be generated at junctions between non-welded components (e.g. manholes, etc.). Also for this reason, welded storage tanks are always protected from arc formation by providing electrical contacts among all metal components (e.g. the vessel wall and the floating roof) (API RP 2003, 2008). However, even if these systems provide a sufficient protection from indirect lightning strikes, there is evidence that such ordinary systems are not able to protect a process item from the effects of a direct lightning strike (API RP 545, 2009; OISD GDN 180, 1999). Two main categories of tanks may thus be identified, where different scenarios are possible in the case of lightning impact:

- *Category “a”*: External floating roof (EFR) tanks containing flammables, characterized by the possibility of formation of flammable mixtures in the open space, mainly at the rim-seal position. In these tanks, beside direct damage, a rim-seal fire may start following vapour ignition caused by the lightning, with possible escalation to a full surface fire (Sengupta et al., 2011).
- *Category “b”*: Fixed roof (FR) tanks, both cone roof (CR) and internal floating roof (IFR) tanks, containing flammables, characterized by the possibility of formation of flammable mixtures in the confined top space inside the tank above liquid level. In these tanks, beside direct damage, confined explosions and escalation to full surface fire are possible if a flammable mixture is present in the vapor space when lightning strike takes place. When low flammable vapor emissions are expected in IFR tanks (e.g. if the stored flammable liquid has low volatility, or if the seal has a tight vapor containment) inert gas blanketing may not be installed, since the chances of flammable mixture formation are very low. Nevertheless, in case of lightning direct hit a rim-seal fire may start inside the tank, following the vapour ignition caused by the lightning, with possible escalation to a full surface fire.

Therefore, safety barriers that prevent or mitigate fire scenarios play a determinant role on the impact of lightning strikes; therefore they deserve to be discussed in detail in order to assess possible scenarios triggered by lightning and to assess their likelihood.

4.5.3 Schematization of fire safety barriers

In order to prevent fires in storage installations, several protection barriers are applied. These aim either to minimize the probability of presence of flammable mixtures in the tank or to mitigate the effect of accidental fires. The presence of such barriers needs to be accounted in the development of quantified reference event trees following lightning impact.

Table 4.9: Petroleum products classification (OISD, 2007).

Petroleum Class	Flash point range
A	< 23 °C
B	23-65 °C
C	65-93 °C
Excluded Petroleum	> 93 °C

Storage tanks for petroleum products were considered as a reference in the present study, since they account for wide part of large scale tank farms worldwide. Moreover, protections barriers associated to such tanks are somehow representative of the safety barriers adopted on most atmospheric tanks storing flammable substances.

Therefore, safety barriers considered in the present study were defined accordingly to standards for tanks storing petroleum products, taking into account the tank geometry (see Section 2.2) and the flammability hazard class of the stored substance. Table 4.9 summarizes the classification of petroleum products based on the flash point used to select tank protection methods according to OISD standards (OISD, 2007). Table 4.10 reports a summary of the required fire protection systems

for each tank geometry and flammability hazard allowed by OISD standard (OISD, 2007). In the following, the technical features of the safety systems summarized in Table 4.10 are briefly outlined, in order to provide the necessary data needed to assess their expected performance in the case of lightning impact. Fig. 4.18 reports the functional scheme of each safety system considered in the Fault Tree Analysis (FTA) discussed in Section 3.3.3.

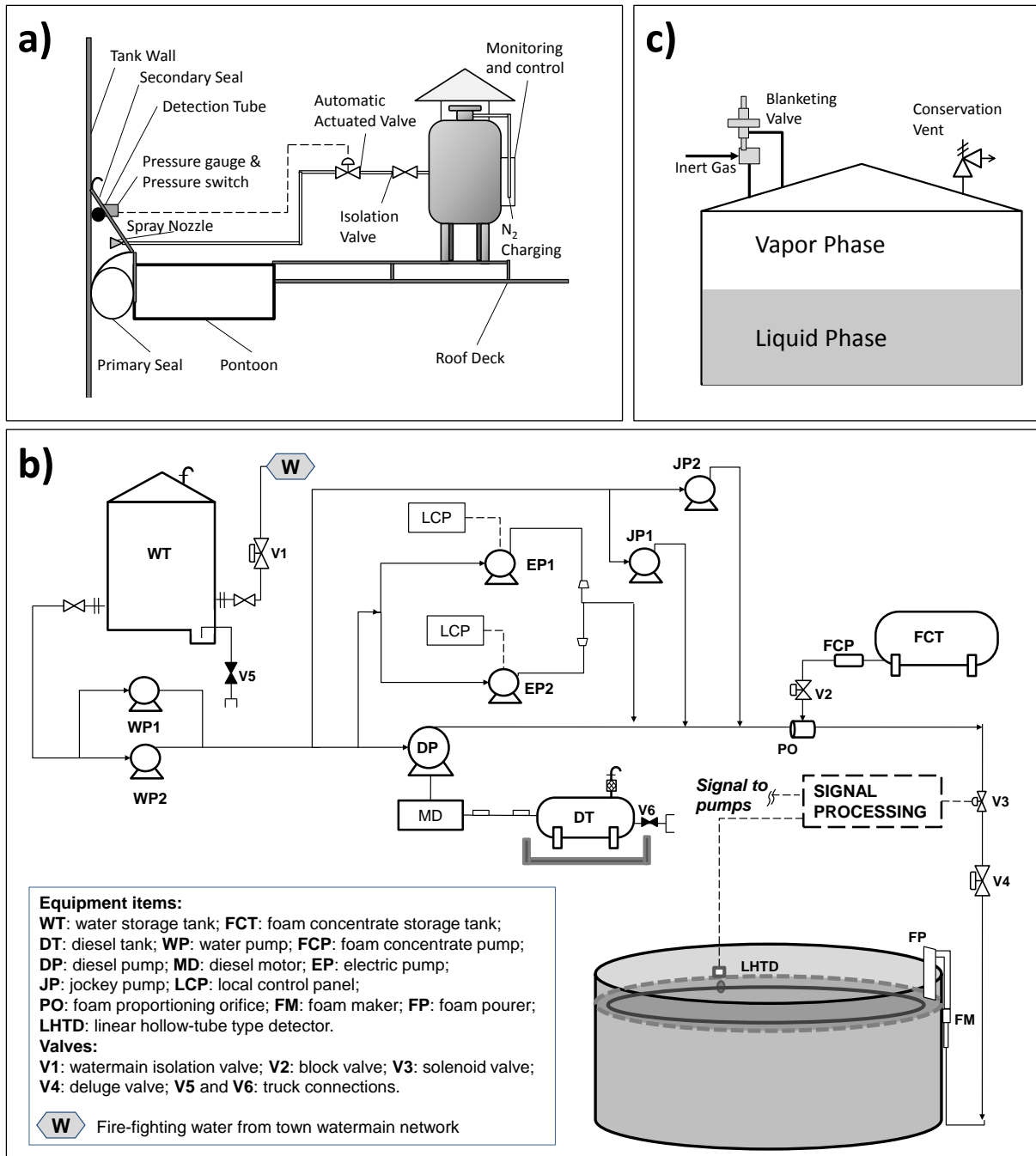


Figure 4.18: Scheme of the fire protections considered: a) automatic actuated rim-seal fire suppression system; b) fixed foam system and foam pouter; c) inert gas blanketing system and pressure vacuum vents. (Necci et al., 2014b)

Table 4.10: Summary of fire protection systems for atmospheric tanks storing flammable products based on OISD standards (2007). Tank category, according to definitions given in section 2.3, is also reported. (Necci et al., 2014b)

Substance Hazard Category	Type of tank	Tank Category (Sect. 2.3)	Size	Type of protection systems
A	Floating Roof	a	All sizes	Fixed water spray system + Fixed or semi-fixed Foam system + Automatically Actuated Rim-seal Protection System (Foam flooding mechanism)
A	Cone Roof	b	All sizes	Fixed water spray system + Fixed or semi-fixed Foam system
B	Floating Roof	a	Diameter > 30 m	Fixed water spray system + Fixed or semi-fixed Foam system + Automatically Actuated Rim-seal Protection System (Foam flooding mechanism)
B	Floating Roof	a	Diameter < 30 m	Fixed or semi-fixed Foam system + Automatically Actuated Rim-seal Protection System (Foam flooding mechanism)
B	Cone roof	b	Diameter > 20 m	Fixed water spray system + Fixed or semi-fixed Foam system
B	Cone roof	b	Diameter < 20 m	Fixed or semi-fixed Foam system
C	Cone roof	b	Diameter > 40 m	Fixed or semi-fixed Foam system

4.5.3.1 Fire protection systems for Category “a” tanks

In this category of tanks the ignition of flammable vapours leaking from the floating roof seal may result in a rim-seal fire, which may evolve to a full-surface tank fire scenario in the case of ineffective mitigation. Thus, specific active protection systems are installed on floating-roof storage tanks for rim-seal fire extinction, based on foam flooding.

A widely used solution for storage tank fire protection are fixed foam systems. In fixed systems, foam is transferred from a central foam station to the protected area. The fixed system consists of pumps and fixed piping for water supply at adequate pressure, a foam concentrate tank, suitable proportioning equipment for the production of foam solution from foam concentrate, a fixed piping system for onward conveying to the foam maker, and a foam pourer or other discharge devices designed to distribute foam effectively over the hazard area (see Fig. 4.18b). A suitable detection system, typically a Linear Heat Detector of the hollow metallic tube type, may be provided to activate the foam system.

Foam is poured from the foam makers at the foam dam to blanket the rim-seal of the roof. Fixed foam discharge outlets can be mounted above the top of the tank shell or on the periphery of the floating roof. The foam dam is designed to retain foam at the seal area, at a sufficient depth to cover the seal area while causing the foam to flow laterally to the point of seal rupture. The dam is welded or securely fastened to the floating roof. Foam application from fixed discharge outlets can be achieved from above the mechanical shoe seal, the metal weather shield, or the secondary seal or either below a mechanical shoe seal directly onto the flammable liquid, behind a metal weather shield directly onto the tube seal envelope, or beneath a secondary seal onto the primary seal.

Automatically actuated rim-seal protection systems represent a further protection for EFR tanks. These systems consist on an adequate number of equally spaced modular foam units positioned on the tank roof, near to, but outside, the containment area of the foam dam, in order to protect the entire rim-seal area. For large storage tanks, more than one modular unit is required for foam application over the entire rim-seal area. Each modular unit typically consists of a storage vessel containing pre-mix foam connected to a distribution pipe laid along the tank perimeter over the rim-seal area. Spray nozzles for foam application are positioned at suitable intervals along the rim-seal area (OISD, 2007). A schematic representation of a modular unit is presented in Fig. 4.18-a.

4.5.3.2 Fire protection systems for Category “b” tanks

Category “b” tanks designed in accordance with API standards (2003) have a weak seal at the joint where the roof and lateral vessel shell meet. In the event of an internal explosion, the roof ejection typically occurs, in order to protect the tank cylindrical shell. This system allows the tank to retain its contents and any resulting fire will involve the full surface of the exposed flammable liquid (i.e. a tank fire).

Both in CR and IFR tanks, risk reduction measures may also include inertization/void-compensation system and provision of pressure vacuum vents which afford some degree of flashback protection (Fig. 4.18-c). It has to be remarked that inert gas blanketing represents a mandatory requirement for the protection of fixed roof storage tank from fire and explosion hazards (NFPA, 2008). API Std 2000 (1998), API RP 2003 (2008) and API RP 2210 (2000) require the installation of pressure vacuum valves or back flash protection in all vents, as pressure vacuum

vents on tank openings prevent propagation of flame into a tank if escaping vapour ignites. A pressure/vacuum (PV) valve, also called “breather valve” or “conservation vent” consists of two vent valves: a pressure valve which opens to let vapour out and a vacuum valve which opens to let air in (see scheme in Fig. 4.18-c). Hence, a PV valve is effective in reducing volatile vapour loss (API, 1998; Lees, 1996). A fixed or semi-fixed fire suppression system may be also installed in order to mitigate and control fires on the tank or in the bund area. However, the extinction of a full surface tank fire may not be guaranteed only by the application of these systems, for this reason those system will not be considered in this study.

The same type of protection systems was assumed for IFR tanks, based on indications reported in (OISD, 1999; API, 1998; 2000). IFR tanks typically require the installation of fixed foam systems for the rim-seal fire extinguishment similar to those applied on category “a” tanks, especially for those IFR tanks that do not include the inert gas the blanketing system. This system will be considered, where installed.

4.5.4 Characterization of lightning-triggered accident scenarios

In the case perforation of the tank body occurs, the material contained is released through the hole in the vessel. According to the specific studies on lightning thermal damage (Necci et al. 2013a) a credible reference size for this leak release is 10 mm.

In the case an atmospheric storage tank is struck and damaged a liquid release is obtained. In the case the vessel has a uniform thickness of the tank shell, then the conservative assumption of a release at a height of 1 m from the ground is considered. In the case the atmospheric tank body is made with courses of different thickness with the tank height (the bottom courses are usually thicker than the higher ones), thus the higher courses have higher chance to be damaged by the lightning strike. The lower height of the courses with the lower thickness is the height where the release is assumed.

If a pressurized vessel is struck and damaged both horizontal and upward releases are possible, but not the downward release. In order to obtain the most conservative result the release direction with the most severe consequences should be selected.

In the case the hazardous material is flammable the high temperature of the hole edge is sufficient to ensure immediate ignition to the substance. Thus, atmospheric flammable liquid release due to is always followed by a pool fire scenario (Fig 4.19-a, Fig 4.19-b). Pressurized flammable gas releases caused by lightning produce a jet-fire scenario, instead (Figure 4.19-c).

In the case lightning strikes an EFRT containing flammable atmosphere a fire is likely to start at the rim-seal (Figure 4.19-a). In the case this fire is not extinguished in time the roof will sink in the stored liquid and a full surface tank fire will start (Necci et al., 2014b, Lees, 1996). The tank fire scenario does not produce high thermal heating to the respect of people placed at the ground level, and thus no direct serious consequences for humans are expected. However, the tank fire scenario has the potential to escalate more serious scenarios: to produce a boil-over scenario (Argyropoulos et al., 2012), to cause the tank collapse and the release of the burning total inventory in the bay area [REF] and/or to damage other tanks in the same storage facility beginning a domino chain accident with devastating consequences to the respect of the plant and of people (Reniers et al. 2013, 2005, Sengupta et al., 2011). Thus, full surface tank fire is

considered a major hazard scenario and its occurrence is handled as a severe emergency situation. Nevertheless, the quantification of the full surface tank fire escalation to more serious consequences is a complicated task, which represents an unknown at the actual state of knowledge. For this reason, the only risk associated to the thermal heating caused by the full surface tank fire is addressed in the followings, and not the contribution of all the possible derived scenarios.

Lightning affects the integrity of fixed roof atmospheric vessel (FRT) containing flammable material, since it represents a source of ignition. In the case lightning strikes a vessel, in which flammable atmosphere is present, a confined explosion will follow (Figure 4.19-b). The confined explosion may cause the tank failure and the release of the entire stored inventory. For this reason, a weak roof joint is applied to large atmospheric tanks, in order to provide a vent area that is supposed to fail to preserve the tank body integrity. However, a shockwave is generated and fragments of the tank roof are projected in the area. For smaller atmospheric tanks the weak joint may not be present, in this case the tank collapses due to the explosion energy, and the inventory is released to the basin and ignited immediately, causing a “catastrophic pool fire”: a pool fire that spread in the entire bund area.

Finally, in the case the stored substance is not flammable, but toxic, a dispersion is the only possible accidental scenario that follows the direct thermal damage due to a direct lightning strike.

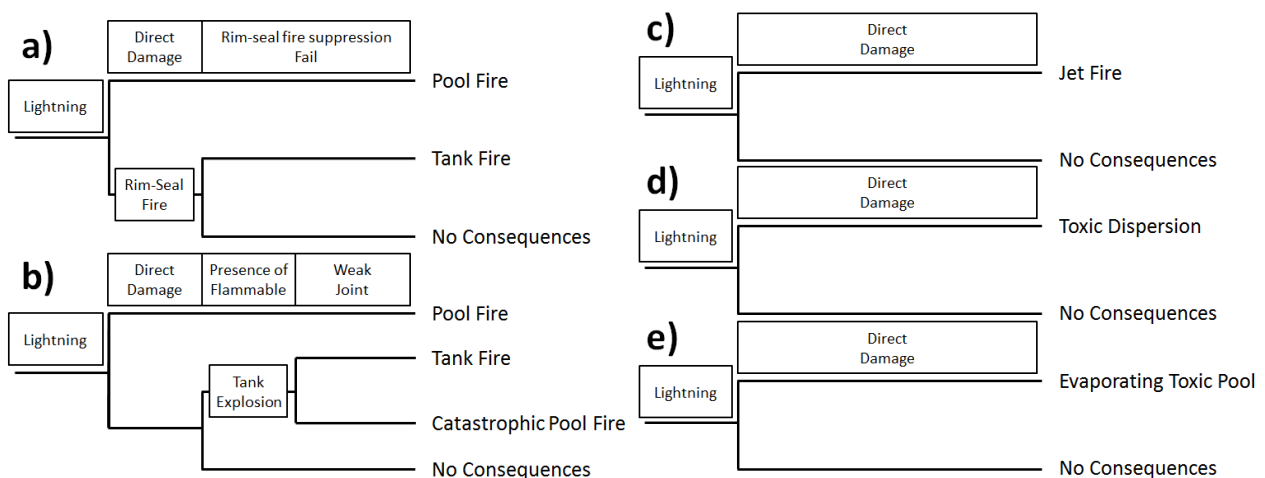


Figure 4.19: Lightning triggered event trees for different equipment typologies: a) EFRT filled with flammable liquid; b) FRT filled with flammable liquid; c) pressurized vessel filled with flammable gas (or liquefied vapour); d) pressurized vessel filled with toxic gas (or liquefied vapour); e) atmospheric vessel filled with toxic liquid. Positive gate response is upward. (Necci et al., 2014b)

4.6. Model for Lightning Damage

A Monte Carlo based procedure for assessing lightning damage due to local heating is presented in the following. The model, based on a simplified analysis of the physical damage mechanism due to metal melting, has been validated by using experimental data available in the literature. The application of the model allows the assessment of the conditional probability of damage given the lightning impact on process and storage vessels. The probability of damage depends mostly on the wall thickness and more generally on the geometry of the impacted vessel. The simplified version of the developed model is suitable for application in a QRA framework. In particular, it may be used to assess the overall frequency of loss of containment due to vessel perforation following lightning impact. Perspective work on the issue should allow the development of quantitative correlations for lightning-induced accidents in the chemical and process industry.

4.6.1 Effect of lightning strikes on process equipment

As described in section 4.5, lightning can cause indirect damage to process equipment due to the ignition of flammable vapours present near or inside specific process equipment items, such as floating roof tanks and other atmospheric tanks. In particular, rim-seal fire scenarios may be triggered by lightning in floating roof tanks, while confined explosions may follow the lightning-induced ignition of flammable atmospheres inside process or storage equipment, mainly in the case of storage tanks vented to the atmosphere. Flammable vapours may be ignited by lightning either at vent points or by electric arc at junction points where the metallic shell is not continuous, as in the case of flanges (Metwally et al., 2004).

However, a direct damage mechanism is also possible, due to the perforation of the equipment shell. The high energy of lightning flashes is able to melt or even to evaporate construction materials like steel, aluminium, copper or composite materials (Rupke et al., 2002). The volume of the molten metal depends on the lightning energy released at the attachment point with the equipment. The present study focused on this direct damage mechanism. As highlighted in several analyses of past accidents, the direct damage mechanism triggered a significant number of major accidents (Renni et al., 2010; Argyropoulos et al., 2012; EPA, 1997).

4.6.2 Arc erosion modeling

The electric arc formed by a lightning is a phenomenon having a high energy density. In the case of a lightning strike, the temperature of the strike point increases abruptly due to the high plasma temperature and by resistive heating. The temperature can reach very high values (even exceeding 15000°C) in a few milliseconds (CEI, 2013). The high temperature generated can melt (or even vaporize) part of the metal shell, causing a hole that may result in loss of containment usually leading to a major accident.

In order to model the damage induced by lightning strike, a model for lightning arc erosion is required. According to conventional theory on welding processes (Lancaster, 1986), the electric arc is defined as a discharge of electricity between electrodes. The arc is typically formed by three regions: the cathode region, the arc column region and the anode region. Each region is

characterized by a specific voltage drop, and the voltage drop at the cathode and at the anode should be of the order of the excitation potential of the electrode material (of the order of 10V). The flowing current can have any value above a minimum, which varies between 0.1A and 1A, depending on the electrode material.

Several theoretical models are available for the calculation of the erosion volume on metal surfaces at the attachment point of the arc channel (Lancaster, 1986; Argyropoulos et al., 2012; Di Bitonto et al., 1989; González and Noack, 2008). In spite of the very high temperature of the arc channel, the temperature at the arc spot is limited to values below or at most up to the boiling point of the electrode material (Lancaster, 1986; González and Noack, 2008). The heating at the attachment point is mainly produced by the charged particles (electrons and positive ions) which impinge on the metal surface and transfer their kinetic energy, gained because of their acceleration through the voltage drop region. The current density, the arc spot radius and the voltage drop at the electrode are thus the most important parameters to consider for the assessment of the heat transferred to the electrode. An important contribution to the overall heat transferred to the area around the arc spot is due to heat radiation from the arc channel (González and Noack, 2008).

González and Noack (2008) theoretically and experimentally described that positive strokes are characterized by the unsteady behaviour of the arc spot. The fast and short displacement of the arc spot over the sheet surface near the original attachment point spread the molten volume rather than making it deeper in the case of positive strokes. Negative long strokes are instead characterized by a stable behaviour. The resulting molten volume zone has shown to be deeper than wide, indicating a better transport in the axial direction.

Due to the variation and uncertainties related to the lightning current properties, it is extremely difficult to predict the duration and the intensity of the heating power of a lightning arc discharging through a solid structure. For the sake of simplicity, in Standard CEI EN 62305 (2013) the power associated to the electric arc (W) is evaluated as the product of the lightning current intensity, i , multiplied by the cathode or anode voltage drop, $u_{a,c}$. The typical value of $u_{a,c}$ is in the range of 10-20 V. The cathode or anode current drop is dependent on the current intensity amplitude and on the arc length, duration and polarity. A value between 13 and 17 V is suggested for this parameter in the literature (González and Noack, 2008).

The energy (E) released by the electric arc is the time integral of the power associate to the electric arc over the total duration of the strike. If the voltage drop is assumed constant, this becomes equal to the voltage drop multiplied by the electric charge (CEI, 2013):

$$E = \int W dt = \int u_{a,c} i dt = u_{a,c} \int i dt = u_{a,c} Q \quad (4.15)$$

where t is time and Q is the electric charge of the lightning. If heat dispersion to the surroundings is conservatively neglected, all the energy transferred to the solid material at the lightning attachment point (e.g. the vessel shell in the case of a process or storage equipment item) becomes available for heat-up, melting and vaporization.

The maximum volume of the molten metal may thus be calculated as follows (CEI, 2013):

$$V = \frac{u_{a,c}Q}{\gamma} \frac{1}{C_w(T_s - T_u) + c_s} \quad (4.16)$$

where V is the melted volume, γ is the material density, C_w is the material thermal capacity, T_s is the melting temperature, T_u is the ambient temperature and c_s is the latent heat of melting. In Eq.(2) all the heat transferred from the lightning, that can be calculated using Eq.(4.15), is conservatively assumed to contribute to the heat-up and melting of a portion of material. All other possible simultaneous phenomena (heat dispersion by conduction to other parts of the vessel wall, heat transfer by convection to the inner fluid, heat dispersion to the surroundings, further heat-up and evaporation of molten material) were neglected for the sake of simplicity, thus obtaining a conservative estimate for the molten volume. A hemispherical shape was assumed for the resulting pool of molten metal, as shown in Figure 4.20.

In order to calculate the extent and the shape of the molten region, the radius of the molten volume should first be calculated assuming that the shell is not perforated (see Figure 4.20-(a)) (Necci et al., 2013):

$$r_s = \sqrt[3]{\frac{3V}{2\pi}} \quad (4.17)$$

where V is the maximum molten volume calculated using Eq.(4.16). If the value of r_s exceeds the shell wall thickness, w , then the following equation should be used to calculate the values of r_s and D_h (see Figure 4.20-(b)) (Necci et al., 2013):

$$D_h = 2\sqrt{\frac{V}{\pi w} - \frac{2w^2}{3}} \quad (4.18)$$

Equation (4) was derived assuming that the shape of the molten volume is given by the intersection between the vessel wall (considered flat) and part of the hemisphere having radius r_s and the center in the attachment point of the lightning strike, as shown in Figure 4.20-(b).

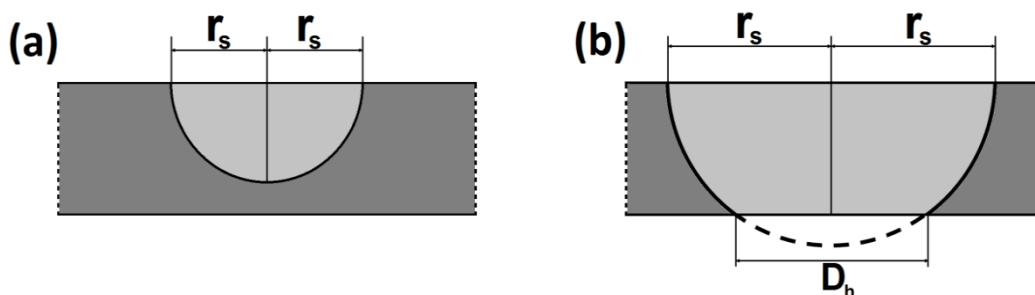


Figure 4.20: Geometry assumed for the pool of molten material: a) Vessel shell not perforated; b) Perforated vessel shell (r_s is the pool surface radius; D_h is the hole diameter) (Necci et al., 2013)

4.6.3 Validation of the model for molten volume calculation

The approach proposed in the previous section is a simplified and conservative method for the calculation of the molten volume and of the possible perforation diameter, D_h . This simplified approach is mostly adequate for thin metal skins, where longitudinal heat transfer by conduction is limited (CEI, 2013). Nevertheless, a specific validation was carried out, also considering the influence of the material and the lightning properties. In order to verify the validity of the model, the perforation diameter calculated using Eq.(4.18) was compared with the measured values of hole diameters obtained in experiments with known values of the electric charge (Q).

There are only few studies that report experimental data relating the electric charge to simulated lightning impact on metal plates. However, studies by González et al. (2006) and González and Noack (2008) report the results of experiments simulating lightning strikes on thin aluminium, steel and copper plates. Both the effect of the current pulse and of long duration current were investigated for positive and negative flashes, and the damage is reported both for the side of the arc attachment (larger hole diameter) and the opposite side of the plate (inner hole diameter). The effect of painting, wind and water on the metal surface was also investigated. Sueta et al. (2006) carried out experiments on the effect of simulated lightning strikes on metal layers with thermal insulation and LPS (lightning protection system) equipment. In several experiments the vaporization of the metal was observed. Porta et al. (2003) performed a study on the cutting (melting) speed of a plasma arc torch. The experimental data reported in these four studies provide results on a wide range of wall thicknesses, materials, and electric charge intensities, as shown in Table 4.11. Properties for carbon steel used for calculations are reported in standard CEI EN 62305 (2013).

Table 4.11: Experimental datasets available in the literature used to validate the model for the calculation of the molten metal volume(Neccì et al., 2013)

Dataset	Arc Polarity	Current	Plate thickness (mm)	Reference
Set 1	Positive	650 A continue; 19.2 kA Impulsive	0.55; 0.70	Sueta et al. 2006
Set 2	Positive and negative	200 A continue	2.00	González and Noack 2008
Set 3	Negative	10-60 A continue	0.60	Porta et al. 2004

Figure 4.21 shows a comparison between the experimental and calculated values of the holes formed in metal plates. Experimental data for perforation diameters, D_h , were obtained from the datasets described in table 4.11. The calculated values of the perforation diameter were obtained using Eqs.(4.15-4.18) and the reported value for the charge of simulated lightning strikes, Q . Material properties assumed for validation were those reported by standard EN 62305 (CEI, 2013), while a value of $u_{a,c}$ of 15V was assumed for the anode or cathode voltage drop (depending on the polarity of the lightning charge). As shown in the figure, sufficient agreement is present between model predictions and experimental data. Moreover, model errors are mostly on the safe side,

thus leading to a slight overestimation of the perforation diameter for the experiments performed with the largest plate thickness.

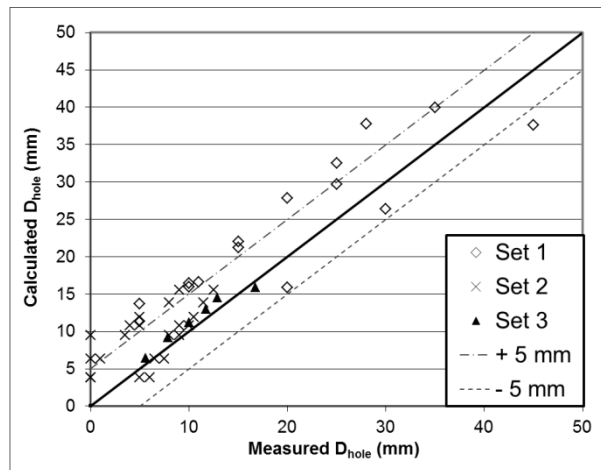


Figure 4.21: Comparison between experimental values of perforation diameters and values calculated using Eqs. (4.15-4.18). Upper and lower dashed lines represent model predictions ± 5 mm. Data set number refers to table 4.11. (Necci et al., 2013)

4.6.4 Calculation of equipment damage probability due to lightning strike

In order to assess the equipment damage probability due to lightning strike, the probability that a flash having a given charge strikes the equipment item of interest should be calculated.

The lightning ground flash density and the distribution of lightning charge for positive and negative strikes are available from historical data and often reported in standards or specific reports (Anderson and Eriksson, 1980). Cloud to ground event locations and estimates of the relevant current amplitudes are also provided by Lightning Location Systems (e.g., in Italy, SIRF (2013)). Several exposure models, i.e. models intended to describe the process of the lightning attachment with the structure, have been proposed in the literature. A recent review of the subject is provided by Cooray and Becerra (2010). In general, the attachment of lightning flashes to grounded structures depends not only on the prospective return stroke peak current but also on the geometry of the structure exposed. The classical electro-geometrical method, as well as the related rolling sphere method, assumes that there is a spherical region with a radius equal to the so-called striking distance and located around the tip of the stepped leader, and the first point of a grounded structure that enters into this spherical volume will be the point of attachment. The striking distance is a function of the prospective peak value of the return stroke current.

Approaches based on Monte Carlo methods are often adopted to estimate the frequency of flashes that hit a structure, on the basis of the selected model that represents the exposure of the structure to lightning events. For the evaluation of the so-called lightning performance of electric power distribution overhead lines, Borghetti et al. (2007; 2009) developed a procedure based on the use of Monte Carlo simulations and a computer code for the evaluation of the overvoltages along the line caused by lightning events that hit the ground in the vicinity of the line (Nucci and Rachidi, 2003). A Monte Carlo based approach was also proposed for the lightning risk assessment of storage tanks (Borghetti et al., 2010).

In the frame of the present study, the Monte Carlo method was applied together with the damage model described in section 2.2 for the calculation of the tank damage probability. A set of Cartesian coordinates \mathbf{x} and \mathbf{y} that indicate the lightning flash locations within an area and a same size set of first stroke peak current values I_p were generated randomly. Each triplet of values (x, y, I_p) allows determining if the capture condition is verified for each of the simulated lightning events. Once that capture occurs in a given simulation, a value of the electric charge Q correlated with the value of the peak current intensity I_p , is also randomly generated. The electric charge of a lightning is a statistical variable that follows a log-normal distribution with mean $\mu_{\ln Q}$ and standard deviation $\sigma_{\ln Q}$. The values of the parameters of the distribution are available in the CEI EN 62305 (2013) standard. In order to account for the statistical correlation between peak current I_p and electric charge Q , the mean value $\mu_{\ln Q}^*$ and the standard deviation $\sigma_{\ln Q}^*$ of the electric charge lognormal probability distribution related to a specific value of I_p are calculated as (Necci et al., 2013a):

$$\mu_{\ln Q}^* = \mu_{\ln Q} + \rho \frac{\sigma_{\ln Q}}{\sigma_{\ln I_p}} (\ln(I_p) - \mu_{\ln I_p}) \quad (4.19)$$

$$\sigma_{\ln Q}^* = \sigma_{\ln Q} \sqrt{1 - \rho^2} \quad (4.20)$$

where ρ is the correlation coefficient between the probability distribution of Q and the probability distribution of I_p , $\mu_{\ln Q}$ is the mean of $\ln Q$, $\mu_{\ln I_p}$ is the mean of $\ln I_p$, $\sigma_{\ln Q}$ is the standard deviation of $\ln Q$, and $\sigma_{\ln I_p}$ is the distribution of the standard deviation of the peak current.

When the molten pool radius, r_s , calculated by the randomly generated value of Q using Eq.4.17 is equal or higher the vessel shell thickness, w , perforation is assumed. Thus, the damage probability given the lightning capture can be calculated from the Monte-Carlo method as follows (Necci et al., 2013a):

$$P_{\text{damage}} = \frac{n_{\text{damaged}}}{n_{\text{captured}}} \quad (4.21)$$

where n_{damaged} is the number of events that causes a shell perforation and n_{captured} is the number of simulated events that hit the target equipment.

4.6.5 Simplified method for damage probability assessment

Although the developed Monte Carlo model allows for the assessment of the damage probability of an equipment item, its applicability in the practical framework of a quantitative risk assessment (QRA) is difficult, due to the significant calculation times required for the assessment of the damage probability for a high number of structures. Shortcut methods are commonly adopted in a QRA framework (Di Padova et al., 2011; Landucci et al., 2009; Tugnoli et al., 2012). Thus, a simplified method for the calculation of the lightning damage conditional probability was developed. The model allows the calculation of the damage probability of the vessel given that a lightning strike is captured by the equipment. As shown in the following, the use of the simplified model leads to a limited error, usually tolerable within a QRA.

For a given shell thickness, w , the minimum lightning electric charge, Q_{min} , required to form a hole may be calculated rearranging Eq.(4.16) as follows (CEI, 2013):

$$Q_{min} = \frac{V_{min} \gamma (C_w (T_s - T_u) + c_s)}{u_{a,c}} \quad (4.22)$$

where V_{min} , the minimum molten volume required for perforation, may be calculated using Eq.(4.17) (Necci et al., 2013a):

$$V_{min} = \frac{2}{3} \pi \cdot w^3 \quad (4.23)$$

The lightning damage conditional probability can thus be calculated as the probability that the electric charge of the captured lightning strikes is higher than Q_{min} obtained from Eq. (4.22).

The probability of having a lightning with a charge higher than Q_{min} can be calculated assuming that the captured flashes have a log-normal charge distribution:

$$P(Q_{min}) = 1 - \frac{1}{2} \operatorname{erfc} \left[-\frac{\ln Q_{min} - \ln \mu^*_{\ln Q}}{\sigma^*_{\ln Q} \sqrt{2}} \right] \quad (4.24)$$

For a single value of Q_{min} two values of probability should be calculated using Eq.(4.24): one for positive flashes and the other for negative flashes, by using the parameter values recommended by Anderson and Eriksson (1980).

The overall conditional damage probability is obtained as the average of the damage probability due to positive and negative flashes, weighted respectively by the expected ratio of positive or negative flashes with respect to the total number of simulated lightning events (Necci et al., 2013):

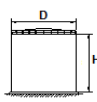
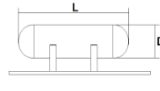
$$P_{damage} = P(Q_{min}) = \Psi_{pos} \cdot P(Q_{min})_{pos} + \Psi_{neg} \cdot P(Q_{min})_{neg} \quad (4.25)$$

where Ψ_{pos} is the fraction of positive flashes, whilst Ψ_{neg} is the fraction of negative flashes. According to the EN 62305 standard (CEI, 2013), a value of 0.1 may be assumed for Ψ_{pos} and a value of 0.9 for Ψ_{neg} .

In order to calculate the parameters of the distribution of the captured strikes, $\sigma^*_{\ln Q}$ and $\mu^*_{\ln Q}$, to be used in Eq.(4.24), a vessel database was built to obtain a representative range of possible vessel geometries. A total of 12 vertical cylindrical and 6 horizontal cylindrical tanks were considered. The database was obtained considering available data on tank items present in several industrial tank farms, data from widely used design standards (e.g. API Standard 650 (2003)), and available design standards from engineering companies. Geometrical data and further details on the vessels included in the vessel database are reported in (Landucci et al., 2012).

The average values of the charge distribution parameters of the events were calculated for the population of the vessel database: $\sigma^*_{\ln Q,av}$ and $\mu^*_{\ln Q,av}$. Table 4.12 reports the values obtained and the maximum and average deviations.

Table 4.12: Electric charge distribution parameters of captured lightning calculated for the tank database used in the study (D is the tank diameter, H is the height of vertical tanks, L is the length of horizontal vessels). (Necci et al., 2013a)

Tank type	Geometry	Value	$\mu_{lnQ,av}^*$ positive	$\sigma_{lnQ,av}^*$ positive	$\mu_{lnQ,av}^*$ negative	$\sigma_{lnQ,av}^*$ negative
 Vertical	$V = 38 \div 16300 \text{ m}^3$	Average	145.15	0.373	8.57	0.451
	$D = 3 \div 66 \text{ m}$	Max dev.	12.42	0.008	0.32	0.003
	$H = 5.4 \div 18 \text{ m}$	Mean dev.	6.14	0.004	0.16	0.001
 Horizontal	$V = 10 \div 25 \text{ m}^3$	Average	159.46	0.363	8.96	0.451
	$D = 1.6 \div 2.5 \text{ m}$	Max dev.	1.48	0.002	0.058	0.002
	$L = 4.5 \div 10.5 \text{ m}$	Mean dev.	0.96	0.001	0.029	0.0008

As the geometry of storage tanks, and in particular the height, does not vary significantly (usually being comprised between 1 and 20m, and around 10m for large atmospheric tanks), the average values of the charge distribution of captured lightning, $\sigma_{lnQ,av}^*$ and $\mu_{lnQ,av}^*$, can be used in Eq. (4.24).

Figure 4.22 reports a comparison of the conditional damage probabilities obtained by the Monte Carlo and the simplified model (Eqs. (4.22-4.25)). As shown in the figure, the simplified model reasonably reproduces the results of the Monte Carlo model.

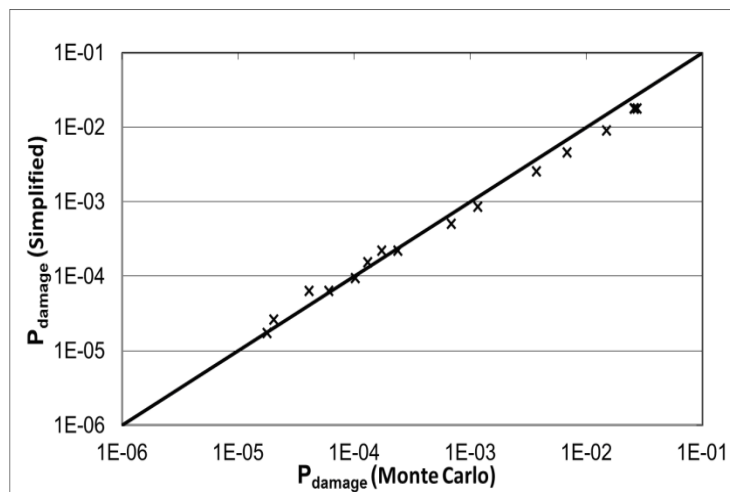


Figure 4.22: Parity plot for the results obtained by the Monte Carlo method and the simplified model for the vessel database considered. (Necci et al., 2013a)

4.6.6 Lightning damage probability calculation

The developed model allows the calculation of the damage probability as a function of a limited number of parameters. As evident from Eqs. (4.22-4.25), the shell thickness and some physical properties of the vessel material (density, melting temperature, latent heat of fusion, specific heat) are needed to apply the model. Figure 4.23-(a) shows the damage probability calculated as a function of wall thickness for four different construction alloys used in the chemical and process

industry. The physical properties used in the calculations were taken from current standards (CEI, 2013; IAEA, 2008; Geen and Perry, 2008) and are listed in Table 4.13.

Table 4.13: Thermal properties of different construction alloy (γ is the density, T_s is the melting temperature, C_s is the latent heat of fusion and C_w is the specific heat) (Necci et al., 2013a)

Parameter	Mild Steel	Stainless Steel	AISI 13XX	AISI 316
γ (kg/m ³)	7700	8000	7800	8000
T_s (°C)	1530	1500	1510	1430
C_s (J/kg)	272000	272000	270000	270000
C_w (J/kgK)	469	500	460	510

As shown in figure 4.23, the damage probabilities are comprised between 10^{-1} and 10^{-6} for wall thicknesses lower than 15mm. Damage probability values lower than 10^{-6} are obtained for thicknesses higher than 15mm, and fall below 10^{-7} for thicknesses higher than 20mm. Figure 4.23- (b), reporting the differences (%) in the results obtained for all materials with respect to those obtained for mild steel, shows that only very small differences in damage probability (lower than 7%) are obtained for the different construction alloys considered. Thus, in the following, for the sake of brevity only results obtained using the properties of material 1 (mild steel as defined by EN 62305 (CEI 2013)) will be reported.

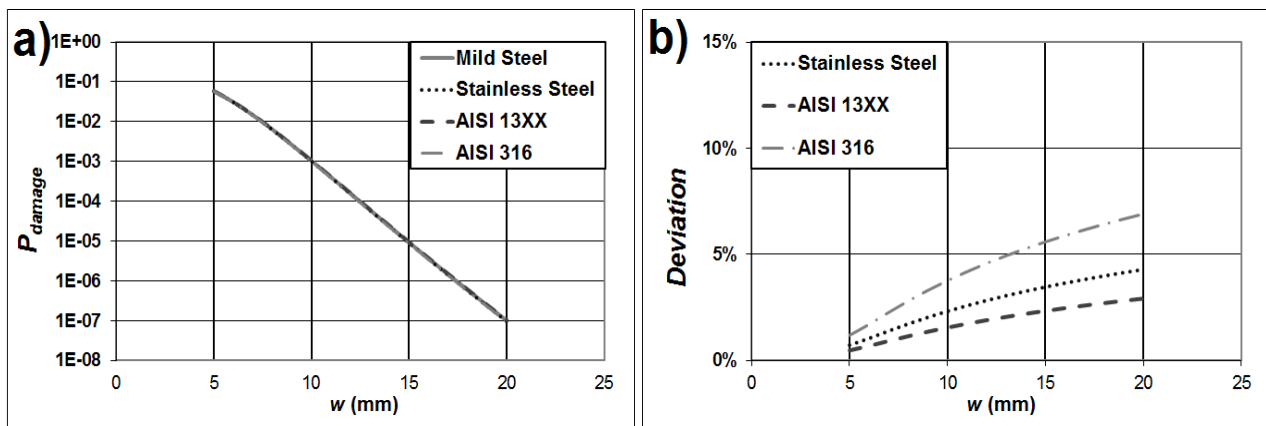


Figure 4.23: (a) Damage probability as a function of shell thickness (w) obtained for four different construction steel alloys; (b) % deviation of the results with respect to those obtained for the reference material selected (Material 1, Mild Steel as defined by CEI EN 62305). (Necci et al., 2013a)

As shown in Figure 4.23, an almost linear correlation is present between the logarithm of the damage probability and the shell thickness. This may be expressed as follows (Necci et al., 2013a):

$$\ln(P_{damage}) = 0.924 - 0.908 \cdot w \quad (4.26)$$

where w is the shell thickness in mm.

Figure 4.24-(a) shows the results obtained with Eq.(4.26) compared to those from the Monte Carlo model. As shown in the figure, Eq. (4.26) provides a reasonable approximation of Monte Carlo model.

Besides the probability that the vessel shell is perforated, also the hole size is relevant for understanding the potential consequences of a lightning impact in terms of possible hazardous-materials releases. Figure 4.24-(b) shows the average expected hole diameter due to lightning strike calculated as a function of vessel thickness considering the probability distribution of all captured strikes having a charge sufficient to cause vessel shell perforation.

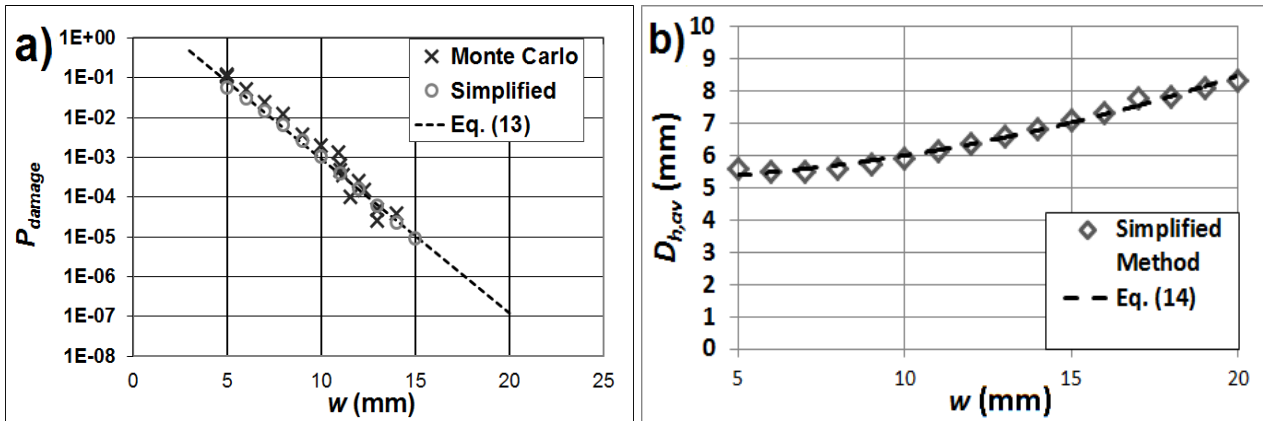


Figure 4.24: Damage probability (a) and average hole diameter (b) with respect to shell thickness (Necci et al., 2013a)

As shown in the figure, the average hole diameter is comprised between 5 and 8.5 mm for metal plates of up to 20 mm width. Also in this case, the average diameter can be calculated using an empirical correlation (Necci et al., 2013a):

$$D_{h,av} = 8.5 \cdot 10^{-3} w^2 - 6.6 \cdot 10^{-3} w + 5.23 \quad (4.27)$$

where D_h and w are expressed in mm. Figure 4.24-(b) shows that Eq. (4.27) provides a reasonable approximation of Monte Carlo model results.

In addition to the calculation of the overall damage probability, the developed model may also be easily applied for the calculation of the probability that a lightning causes a hole in the vessel wall having a diameter higher than a given limit value, D_l .

Equations (4.22-4.25) should be applied, using the following relation, derived from Eq.(4.18), for the calculation of the minimum volume, V_{min} , in Eq. (4.22) (Necci et al., 2013a):

$$V_{\text{min}} = \pi \cdot w \left(\frac{2w^2}{3} + \frac{D_l^2}{4} \right) \quad (4.28)$$

Figure 4.25 reports the cumulative probability $P(D_l)$ that a hole larger than a given limit diameter (D_l) is formed following lightning impact on a vessel wall having a given thickness. As shown in the

figure, even for atmospheric vessels having low thicknesses (5mm), the probability that the hole diameter is larger than 20mm is of the order 10^{-3} .

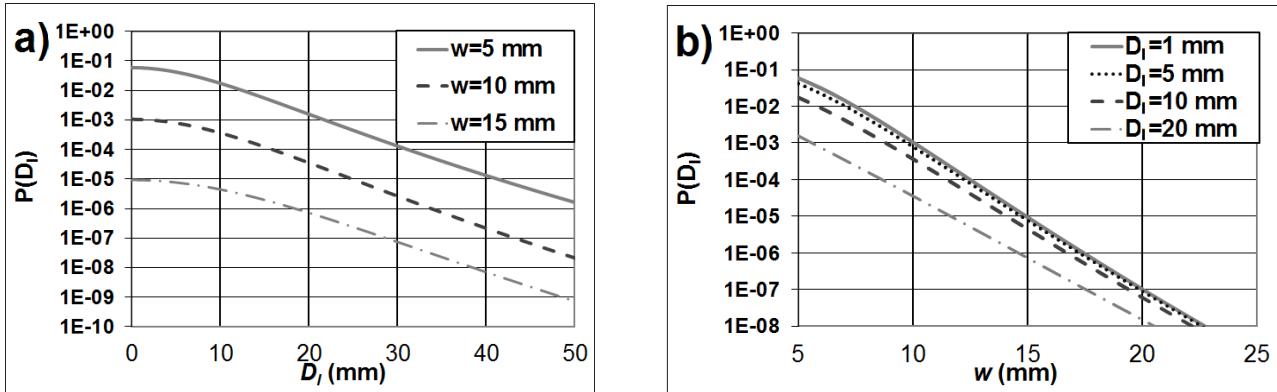


Figure 4.25: Probability that a lightning strike causes a hole of diameter higher than D_i obtained for different values of wall thickness. a) Probability as a function of the limit diameter, D_i , for fixed values of shell thickness, w ; b) probability as a function of the shell thickness, for fixed values of the limit diameter, D_i . (Necci et al., 2013a)

The model also allows assessing the probability that a lightning strike causes a hole having a diameter within a specific range. Table 4.14 reports the probability of different release categories as a function of shell thickness. The release probabilities were obtained integrating the probability of release for a given hole diameter range as follows (Necci et al., 2013a):

$$P(D_{l,range}) = \int_{D_{l,min}}^{D_{l,max}} P(D) dD \quad (4.29)$$

Table 4.14: Probabilities of different release categories following lightning impact. (Necci et al., 2013a)

Plate Thickness	Diameter Range				
	0-5 mm	5-10 mm	10-15 mm	15-20 mm	>20 mm
5 mm	1.96E-02	3.19E-02	1.50E-02	3.99E-03	1.04E-03
10 mm	1.87E-04	2.74E-04	1.19E-04	3.01E-05	7.06E-06
15 mm	2.59E-07	4.68E-07	2.85E-07	1.04E-07	3.52E-08

4.6.7 The contribution of positive flashes

The developed model takes into account both positive and negative lightning impacts. In the usual approach aimed at the assessment of damage to electrical equipment, positive flashes are usually not considered since they have a much lower frequency with respect to negative strikes. Thus it is interesting to understand the relevance of the contribution of positive strikes to equipment damage, since positive lightning strikes have a higher average value of electric charge compared to negative flashes (Anderson and Eriksson, 1980).

Figure 4.26 reports the contribution of damage due to positive lightning strikes to the overall damage probability (C_{pos}), calculated as follows (Necci et al., 2013a):

$$C_{pos} = \frac{P(Q_{min})_{pos}}{P_{damage}} \quad (4.30)$$

As shown in the figure, positive flashes provide the most important contribution to damage probability. When the wall thickness exceeds 7mm, the contribution of negative flashes to the overall damage probability is almost negligible, falling below 1%. These results suggest to allow neglecting the effect of multiple strokes, which is a phenomenon related to negative flashes only, and justifies the use of the molten metal model reported by standard EN 62305 (CEI, 2013).

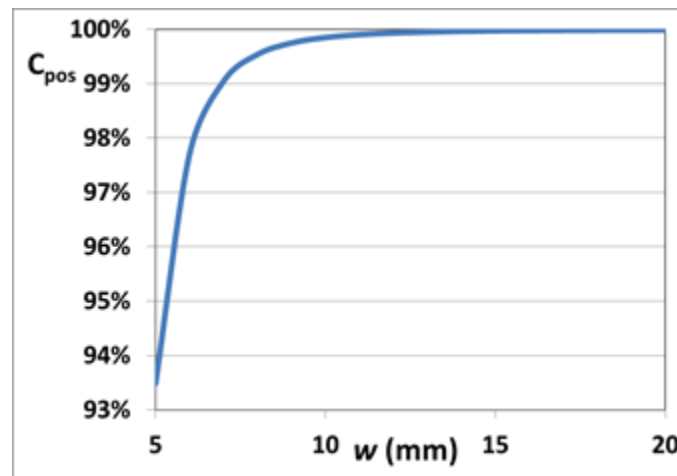


Figure 4.26: Contribution of positive flashes to overall damage probability. (Necci et al., 2013a)

4.6.8 Damage probabilities for a reference set of equipment items

In order to verify the applicability of the model in a realistic framework, the damage probability was calculated for a reference set of equipment items, identifying tank geometries widely used in industrial sites. Table 4.15 and 4.16 report the geometrical data used for a set of atmospheric and pressurized storage tanks, respectively.

In Figure 4.27 the probability that a lightning strike results in a hole with a diameter higher than 10mm is plotted (this hole size is of particular interest for the application to the consequence analysis (Uijt De Haag and Ale, 1999)). As shown in the figure, damage probabilities values higher than 10^{-2} are obtained for atmospheric tanks. Pressurized tanks have a damage probability that is at least an order of magnitude lower, that decreases with increasing design pressure due to the increasing shell thickness. These results are confirmed by past accident analysis, that evidence a much higher number of fires involving atmospheric tanks caused by lightning with respect to pressurized equipment (Rasmussen, 1995; Renni et al., 2010).

Table 4.15: Reference set of vertical cylindrical atmospheric storage tanks (*D*: tank diameter; *H*: tank height; *w*: shell thickness) (Necci et al., 2013a)

Tank n	Volume (m ³)	D (m)	H (m)	w (mm)
1a	38	3	5.4	5
2a	100	4.4	7	5
3a	250	7.7	7.5	5
4a	500	7.8	11	6
5a	750	10.5	9	7
6a	1000	15	6	9
7a	2500	54	5.4	11
8a	5200	25	11	11
9a	7634	30	10.8	12
10a	9975	42	7.2	12
11a	12367	54	5.4	13
12a	16303	66	5.4	13

Table 4.16: Reference set of horizontal cylindrical pressurized storage tanks. (*P_{des}*: Design pressure; *D*: tank diameter; *L*: vessel length; *w*: shell thickness). (Necci et al., 2013a)

Tank n	Volume (m ³)	<i>P_{des}</i> (bar)	D (m)	L (m)	W (mm)
1p	20	15	2	6	13
2p	25	15	2.3	7	15
3p	50	15	2.5	10.4	16
4p	50	15	2.7	10	17
5p	100	15	2.8	18	18
6p	250	15	3.8	24	24
7p	20	20	2	6	17
8p	25	20	2.2	6	19
9p	30	20	2.4	6.5	20
10p	50	20	2.7	10	23
11p	100	20	2.8	18	24
12p	250	20	3.8	24	32

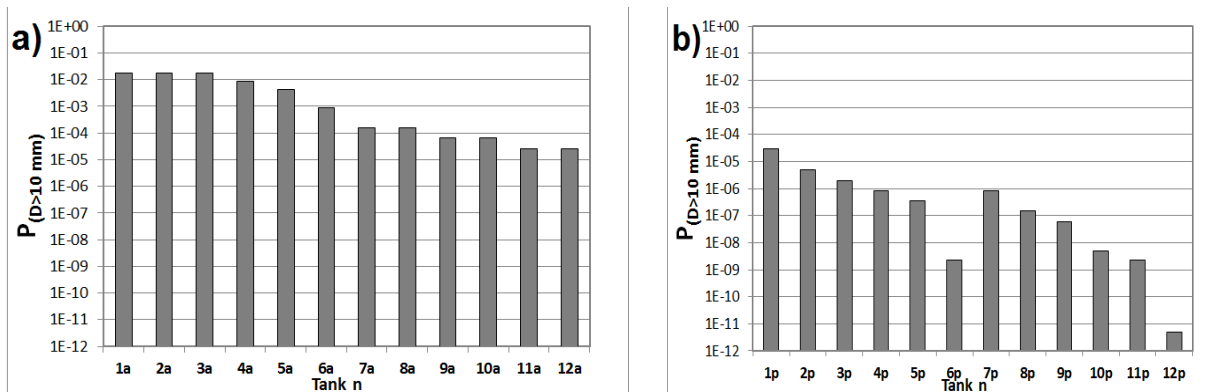


Figure 4.27: Probability of lightning damage causing a perforation having a diameter larger than 10mm for: (a) atmospheric storage tanks (Table 4.15); (b) pressurized storage tank (Table 4.16) (Necci et al., 2013a)

4.7 Assessment of accident frequency induced by lightning

Geometrical features and reference conventional safety barriers used in current industrial practice were defined for the tank categories of interest. The possible impact mode of lightning was then analysed, in order to develop reference accident chains applying event tree analysis (ETA) and to obtain reference event trees (ET) (see section 4.5). The reference ET were developed to include relevant protection barriers and were validated using detailed past accident records. The probability of failure on demand (PFD) of the safety barriers following lightning strike was calculated by fault tree analysis (FTA).

It should be remarked that the present analysis was carried out only considering the events following lightning impact. Thus possible protection by lightning rods or by other systems used to prevent lightning impact itself is not considered in the reference ETs provided.

4.7.1 Event tree analysis (ETA) and reference accident chains

An Event Tree Analysis (ETA) was carried out in order to determine the potential accident sequences following lightning impact and to evaluate the role of protection systems. The protection systems are intended as protective barriers which play their role when the lightning strikes on the storage tank. In the case the protective barrier is unavailable, the scenario evolves to the final accident. The unavailability of a protective barrier is presented as the probability of failure on demand (the lightning strike), PDF, of the system. In the case the system is not present the PFD value is set to 1. The reference event trees (ET) obtained are reported in Fig. 4.28. Fig. 4.28-a illustrates the reference ET obtained for EFR tanks (category “a”), while Fig. 4.28-b reports the ET obtained for CR and IFR tanks (category “b”). As shown in the figure, for both vessels categories two alternative possible final outcomes involving a fire are obtained: the pool fire associated to the ignition of spilled flammable liquid in the case of vessel direct damage, and the full surface fire (FSF) in the case of failure of safety barriers. The frequency of the fire scenarios may be obtained as follows (Necci et al., 2014b):

$$f_{PF} = f_c \times P_{DD} \quad (4.31)$$

$$f_{FSF} = f_c \times (1 - P_{DD}) \times \prod_{i=1}^{N_b} PDF_i \quad (4.32)$$

where f_c is the capture frequency of the target vessel, f_{PF} is the frequency of the pool fire associated to the ignition of the liquid released from the punctured tank, f_{FSF} is the frequency of the FSF scenario, P_{DD} is the probability of direct damage, PDF_i is the Probability of Failure on Demand of the i -th barrier, N_b is the total number of barriers.

For any cases, the probability of presence and ignition of flammable vapours is conservatively assumed equal to 1, at any point of the event tree, due to the effect of a direct lightning strike on the tank. Thus, event trees may be simplified, since the only final outcomes considered are fires.

For category “a” tanks, it is supposed that flammable vapours may be considered as always present at the rim-seal position. Thus, the probability of presence of a flammable mixture may conservatively be assumed as equal to 1. However, the automatic fire suppression system installed

on the tank is supposed to be able to prevent the escalation of the initial rim-seal fire to a full surface tank fire scenario.

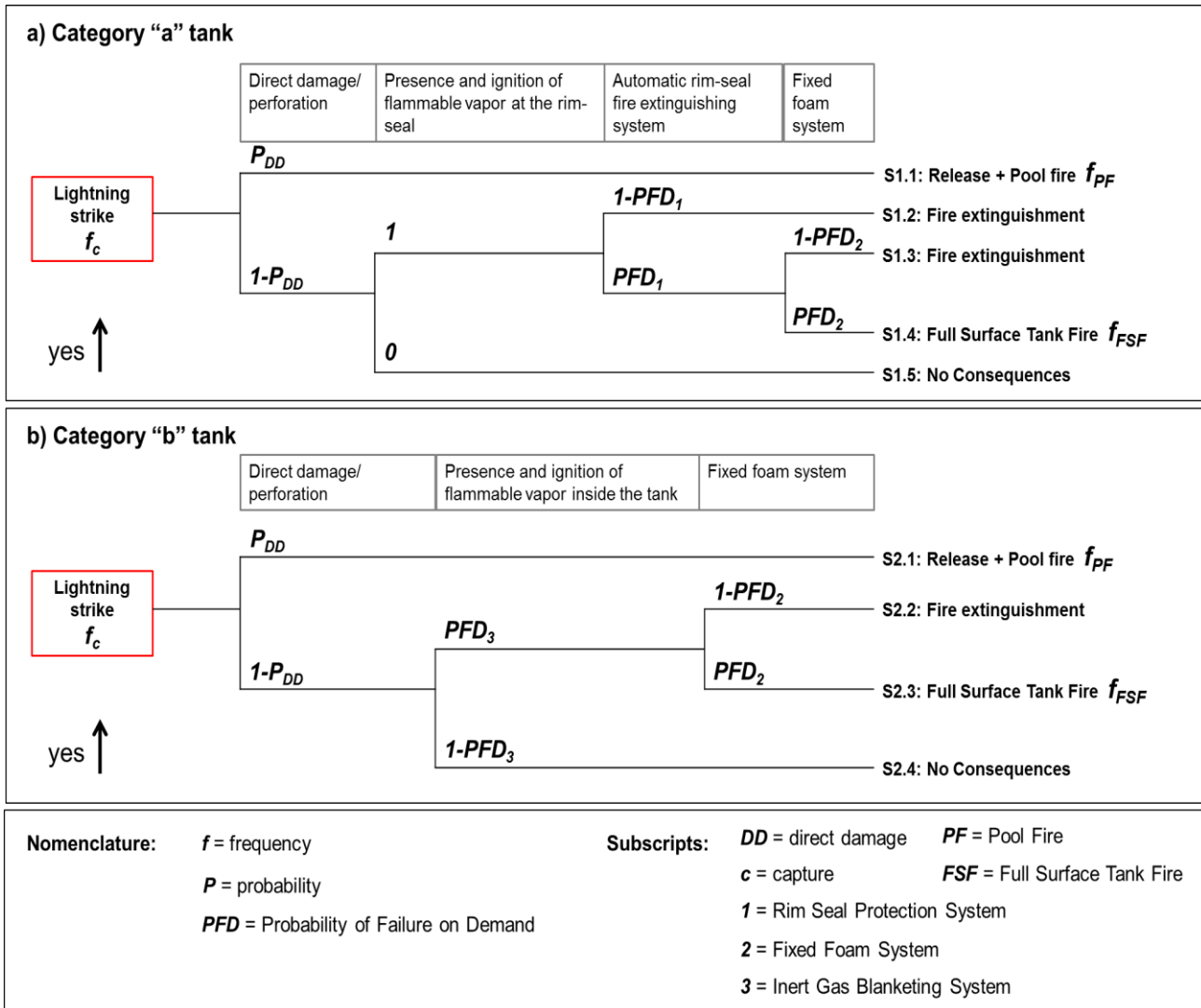


Figure 4.28: Event tree following lightning impact on atmospheric storage tanks containing flammable liquids: a) EFR tanks (category “a”); b) CR and IFR tanks (category “b”). At each gate: if the condition is verified, the upper branch event follows (Necci et al., 2014b)

4.7.2 Validation of ETA results

In order to assess the relevance of the event trees obtained, past accident data concerning major accidents triggered by lightning and involving atmospheric tanks storing hydrocarbons or generic flammable materials were retrieved and analyzed. The accident sequences reported in past accidents were then compared with the ETs reported in Fig. 4.28, in order to validate the event sequences assumed in the analysis.

Three different data sources were considered: the MHIDAS database (2001), The Accident Database (TAD) (2004) run by IChemE (Institution of Chemical Engineers, and a review on tank fire accidents occurred between 1951 and 2003 carried out within the framework of BRANDFORSK Project (Persson and Lönnermark, 2004).

Out of the over 1700 past accidents analysed, 1030 records concerning scenarios triggered by lightning were retrieved. Data records not reporting information on protection or mitigation systems were excluded from the analysis, reducing the dataset to 82 records. However, only 33 over these 82 records report sufficient details to allow a comparison with the ETs in Fig. 4.28. Table 4.17 reports four relevant samples of final dataset used for ET validation. Table 4.18 reports the list of the past events used for database validation and a detailed description of sample included in Table 4.17.

Table 4.17: Sample of past accident data used for the identified scenarios validation. (Necci et al., 2014b)

ID	Tank type	Protection system type	Success/ Failure	Validated event tree scenario (see Fig. 4.28)	Year and country
A1	Floating roof	Fixed foam system with foam pourers	Success	S1.2 <i>(rim-seal fire extinguishment)</i>	1972; Italy
A2	Floating roof	Rim-seal fire extinguishment system (generic) Fixed foam system (generic)	Failure Success	S1.3 <i>(rim-seal fire escalation to tank fire; & tank fire extinguishment)</i>	1979; USA
A3	Floating roof	Fixed foam system with foam pourers	Failure	S1.4 <i>(rim-seal fire escalation to tank fire; & tank fire burn out)</i>	1964; N.A.
A4	Internal Floating Roof	Inert Gas Blanketing system Fixed foam system with foam chambers	Failure Failure	S2.2 and S2.3	1987; USA

The role of inert gas blanketing systems availability in preventing the formation of flammable mixture inside “category b” fixed roof tanks found no direct confirmation in past accidents: although the scenario of roof blow off followed by tank fire in the case of ignition by lightning strike was confirmed by past accident data analysis (Persson and Lönnemark, 2004), none of the analysed records mentioned the presence or the failure of inert gas blanketing systems. However, the presence past accidents reporting a tank fire as the final outcome of lightning impact on “category b” tanks may be assumed as an indirect validation of the ET sequence.

All ET event sequences for “category a” external floating roof tanks assuming no direct damage were confirmed by case histories. Accident records where the unavailability of foam chambers made the full surface fire extinguishment impossible were considered appropriate for the validation of the ETs sequences deriving from failure and success of fixed foam systems both for “category a” and “category b” tanks (see accident A4 in Table 4.17).

Table 4.18: Past accident events used for ET validation. (Necci et al., 2014b)

ID	Date	Location	Tank category	Validated final scenario	Ref.
1	04/06/2003	Australia; Queensland	A	S1.4 Full surface fire	<i>MHIDAS</i>
2	02/08/2003	USA; Mississippi; Pascagoula	A	S1.2 Rim-seal fire extinguishment	<i>MHIDAS</i>
3	05/05/2001	Seria; United Arab Emirates	A	S1.2 Rim-seal fire extinguishment	<i>MHIDAS</i>
4	19/07/1996	Sarnia; Ontario; Canada	B	S2.3 Full surface fire	<i>MHIDAS</i>
5	14/06/1993	New Orleans; Louisiana; USA	A	S1.2 Rim-seal fire extinguishment	<i>MHIDAS</i>
6	04/04/1991	Pasadena; Texas; USA	A	S1.2 Rim-seal fire extinguishment	<i>MHIDAS</i>
7	21/06/1990	Karkateyev; CIS (ex URSS)	A	S1.4 Full surface fire	<i>MHIDAS</i>
8	22/03/1989	Sullom Voe; Shetland; UK	A	S1.2 Rim-seal fire extinguishment	<i>MHIDAS</i>
9	21/08/1975	Rozenburg; Zuid Holland; Netherlands	A	S1.3 Full surface fire extinguishment	<i>MHIDAS</i>
10	1999	-	A	S1.2 Rim-seal fire extinguishment	<i>TAD</i>
11	24/09/1977	USA	A	S1.3 Full surface fire extinguishment	<i>TAD</i>
12	December 1992	-	A	S1.2 Rim-seal fire extinguishment	<i>TAD</i>
13	August 1984	-	B	S2.3 Full surface fire	<i>TAD</i>
14	May 1978	USA	A	S1.2 Rim-seal fire extinguishment	<i>TAD</i>
A.1	27/07/1972	Italy	A	S1.2 Rim-seal fire extinguishment	<i>TAD</i>
A.3	20/09/1964	-	A	S1.4 Full surface fire	<i>TAD</i>
15	-	-	B	S2.3 Full surface fire	<i>TAD</i>

Table 4.18 continues: Past accident events used for ET validation. (Necci et al., 2014b)

ID	Date	Location	Tank category	Validated final scenario	Ref.
A.4	1987	Philadelphia, USA	B	S2.3 Full surface fire	<i>TAD</i>
16	24/09/1977	(Union Oil) Romeoville; Illinois; USA	B	S2.3 Full surface fire	Persson and Lönnermark, 2004
17	05/05/2002	(Trzebinia Refinery) Malopolska region, Poland	B	S2.3 Full surface fire	Persson and Lönnermark, 2004
21	1964	-	A	S1.4 Full surface fire	Persson and Lönnermark, 2004
A.2	1979	USA	A	S1.3 Full surface fire extinguishment	Persson and Lönnermark, 2004
22	07/12/1990	USA	A	S1.2 Rim-seal fire extinguishment	Persson and Lönnermark, 2004
23	1991	USA	A	S1.2 Rim-seal fire extinguishment	Persson and Lönnermark, 2004
24	25/12/1992	Castellon; Spain	A	S1.4 Full surface fire	Persson and Lönnermark, 2004
25	24/10/1995	Indonesia	B	S2.3 Full surface fire	<i>ARIA</i>
26	27/06/1994	Gernshein Hessen; Allemagne; France	B	S2.3 Full surface fire	<i>ARIA</i>
27	20/06/1987	France	A	S1.4 Full surface fire	<i>ARIA</i>
28	01/06/2006	Pasadena, Texas; USA	A	S1.2 Rim-seal fire extinguishment	<i>NRC</i>
29	7/06/2004	Bay St. Louis, Massachusetts; USA	B	S2.3 Full surface fire	<i>NRC</i>
30	8/09/2003	Friend; Oklahoma; USA	B	S2.3 Full surface fire	<i>NRC</i>
31	5/11/2001	Seminole, Texas; USA	A	S1.2 Rim-seal fire extinguishment	<i>NRC</i>
32	7/02/2001	Wilson; Oklahoma; USA	B	S2.3 Full surface fire	<i>NRC</i>
33	4/18/1981	Singapore	A	S1.4 Full surface fire	<i>TAD</i>

4.7.3 Quantification of event trees and frequency assessment

4.7.3.1 Lightning impact frequency assessment

A specific probabilistic assessment of the event trees in Fig. 4.28 was carried out, aiming at the calculation of conditional probability of the final outcomes given the lightning impact. The results obtained allow the assessment of the frequencies of the final outcomes if the capture frequency (frequency of lightning impact) is known.

The calculation of the capture frequency of storage tanks of known geometry requires specific models which have already been described in Section 4.4. It should be also recalled that the ETs in Fig. 4.28 only describe the events following lightning impact. Thus, the presence and the influence of specific lightning protection systems as lightning rods are not considered, since these should be accounted when assessing the capture frequency.

4.7.3.2 Probability of direct damage to the tank shell

As remarked in Section 4.6, a direct lightning strike may cause a direct damage of tank shell. At the attachment point between the electric arc and the storage tank, the melting of a portion of the shell may occur due to the large heat input as well as due to a concentration of resistive heating due to the high current densities. Perforation resulting in a loss of containment event (LOC) may thus occur.

The model of Necci et al. (2013a) allows the calculation of the fraction of lightning strikes that has the minimum energy required to perforate a steel course of given thickness. As fully described in section 4.6, Eq.4.33 may be used to calculate perforation probability (See section 4.6):

$$\ln(P_{d,j}) = 0.924 - 0.908 \cdot t_j \quad (4.33)$$

where $P_{d,j}$ is the perforation probability of the j -th steel course having a thickness t_j .

Two other factors should be considered to assess the overall conditional probability of damage, P_{DD} , needed to quantify the event trees in Fig.4.28. In order to cause a liquid spill, the perforation should occur on the side of the tank and not on the roof. Furthermore, very large storage tanks may feature decreasing values of board thickness at increasing height (Fig. 4.16). Thus, the overall conditional direct damage probability (P_{DD}) may be calculated as follows:

$$P_{DD} = \frac{\sum_i P_{d,i} \cdot S_i}{S_{tot}} \quad (4.34)$$

where $P_{d,i}$ is the perforation probability of the i -th course of the tank calculated by Eq.4.33 on the basis of its thickness, S_i is the exposed surface of the i -th course of the tank, and S_{tot} is the total exposed surface (including roof surface, but excluding tank bottom). In the application of Eq.4.34 only the courses below the maximum allowed liquid level should be considered.

4.7.3.3 Assessment of safety barriers

As shown in Fig. 4.28, the expected occurrence frequency of a full surface fire scenario also depends on the availability of the protection systems. As a matter of facts, the activation of the reference safety barriers identified in section 2.3 may prevent this final outcome. Therefore, in order to quantify all the branches of the ETs in Fig.4.28, the assessment of the PFD (probability of

failure on demand) of the identified reference protection systems was carried out. In order to address this issue, two possible procedures may be identified.

A case-specific detailed calculation is possible, deriving site-specific failure frequencies and calculating the actual PFD values for the case of interest.

As an alternative, generic values of PFD may be used. Table 4.19 reports generic values of PDF obtained in the present study for the reference safety barriers identified in section 2.3. Clearly enough, such values should be intended only as reference values for a preliminary assessment of the expected occurrence probabilities of the final events. The values in Table 4.19 were obtained from a Fault Tree Analysis (FTA) carried out for barrier availability, starting from generic literature reliability data (see Necci et al. 2014b for further details on the ET construction). The generic PFDs of automatically actuated rim-seal fire extinguishing systems and fixed foam systems featuring fixed discharge outlets and foam dam, identified as reference active protection systems, was assessed. Only fixed systems, with all components permanently installed, were considered. Both simple rim-seal fire extinguishing systems, with only automatic actuation upon fire detection, and systems, with either automatic and manual actuation, were analysed. The fixed foam systems considered have a foam distribution network that is connected to the fire water main network of the refinery, and by an actuation system that is integrated within the actuation logic of the fire-fighting system of the refinery. In a conservative approach, it is assumed that the failure of a single foam unit (in the case of automatically actuated systems) or of a single foam discharge device is sufficient to consider the entire rim-seal fire extinguishing system unavailable.

Since the requirements for inert gas blanketing systems are not detailed in specific standards (as a matter of fact only generic indications are provided by NFPA 69 (NFPA, 2008)), the features and architectures of these systems may vary considerably depending on tank types, tank sizes and global design considerations on the installation. Hence, instead of retrieving a reference scheme which could identify standard system architecture and allow the application of FTA, a risk-based approach was adopted in order to determine the required SIL (Safety Integrity Level) for the system by the adoption of a risk matrix approach, following the guidelines from IEC 61508 (IEC, 1998a; 1998b; Schüller et al., 1997). The SIL required was then assumed as a reference to estimate the maximum allowable PDF of the system. Further details on the procedures applied to carry out the analysis are provided in the paper by Necci et al. (2014b).

It has to be remarked that the FTA was carried out assuming that all the protection systems are not affected by the lightning. In other words, the lightning strike is not considered as a common cause failure for the system components. However, Common Cause Failure (CCF) which may affect more components (such as poor quality maintenance or external impact), not specifically involving the lightning event, was taken into account by the adoption of the beta factor method.

Table 4.19: Calculated Probability of Failure on Demand (PFD) for different fire protection systems. Necci et al. (2014b).

System ID	System Description	Calculated PFD value	Corresponding parameter in event tree (see Fig.4.28)	Type of analysis
A	Rim-seal fire extinguishing systems, only automatic actuation	2.38×10^{-2}	PFD_1	Fault tree analysis
B	Rim-seal fire extinguishing systems, both automatic and manual actuation	2.37×10^{-2}	PFD_1	Fault tree analysis
C	Fixed foam systems with fixed discharge outlets and foam dam	8.10×10^{-3}	PFD_2	Fault tree analysis
D	Inert gas blanketing systems	$10^{-3} - 10^{-2}$ (equivalent SIL 2)	PFD_3	Risk-based approach for SIL requirements determination

4.8 Consequence assessment of lightning-triggered scenarios

In order to characterize the different type of release, hazardous substances with different effects are considered. For atmospheric vessel a flammable and a toxic substance have been chosen; for pressurized vessel a flammable gas, a flammable pressurized liquefied vapor and a toxic pressurized liquefied vapor have been chosen. The following substances are considered in the study: Gasoline (approximated as n-heptane) and Crude Oil (approximated as n-octane) atmospheric releases; Propane and Chlorine for Pressurized vessels.

Due to their particular features lightning triggered scenarios have been separated from conventional scenarios used in quantitative risk assessment. In order to compare the risk obtained with and without the lightning triggered accident a brief description of the scenarios (following both conventional causes and lightning strikes impacting on the tank) considered in the following calculation is provided in this section.

4.8.1 Conventional scenarios

The conventional releases for QRA are collected from several sources (Uijt De Haag and Ale, 1999; Lees, 1996). Table 4.20 shows the considered release typologies and the suggested overall annual probabilities of occurrence. Conventional top events regards releases of hazardous material both from the vessel and from the connected pipeline. Only the top events due to mechanical failure or corrosion are considered and not those due to the operative conditions on a plant. This last type of analysis requires much more detailed data, which are specific of the system analyzed and therefore cannot be generalized. For this reason the only top events considered are listed in the following.

The vessel leakage is a continuous release of hazardous material due to a hole or a fracture in the vessel, characterized by a low release rate. The equivalent diameter considered for this release typology is 10 mm (Purple Book). It usually results in a small pool of hazardous material in the bund area for atmospheric storage tanks and in a jet release for pressurized tanks.

The release of the entire inventory in 10 minute is another standard loss of containment typology, characterized by a high release rate. It usually results in a large pool of hazardous material in the bund area for atmospheric storage tanks and in a jet release for pressurized tanks.

Instantaneous release, represent the immediate release of the entire inventory of the tank. It usually results in a large pool of hazardous material in the bund area for atmospheric storage tanks and in a BLEVE for pressurized tanks.

The leakage from a pipeline connected to the tank is a continuous release of hazardous material. Consequences are similar to those of the leakage from the vessel, but the release size is considered as a portion of the nominal diameter of the pipe.

The full bore rupture of a pipeline connected to the tank is a continuous release of hazardous material. It' consequences are similar to those of the leakage from the vessel, but the release size is considered as the entire nominal diameter of the pipe, resulting in a higher release rate.

Since the release frequencies and consequences depends on the pipe features, for both the full bore rupture and the pipeline leak, a total pipeline length of 10 m is considered.

The vessel major leakage, able to release the entire inventory of the tank in 10 min is a continuous release of hazardous material. Its consequences are similar to those of the leakage from the vessel, but the release rate is considered enough to empty the vessel content in less than 10 minutes, resulting in a much higher release rate. The vessel catastrophic rupture: is considered as an immediate release of the entire inventory of the tank.

The continuous releases are always considered to be positioned at 1 m from the ground level. The liquid release forms a pool on the ground, which can either ignite forming a pool fire or slowly evaporate, generating a cloud of hazardous substance in the atmosphere with toxic and/or flammable features. Pressurized storage tanks store gaseous (or liquefied vapors) hazardous material. Pressurized vessels are supposed to be supported on a concrete base ($h_c = 0.5\text{m}$) to evaluate the overall tank height and the release height. Continuous releases from pressurized vessels form gas jets (or two-phase vapor/liquid jets) that emit a high rate of hazardous substance in the atmosphere, generating a cloud with toxic and/or flammable features. The instantaneous release of the entire inventory is accompanied by the shockwave due to the rapid expansion of the pressurized stock.

For the calculation of consequences due to the ignition of a flammable vapor cloud for either the vapors evaporated from a liquid pool and the vapors generated after a jet dispersion, both flash fire and Vapor Cloud Explosion are considered. Data for conventional top event frequency, ignition probability and the Flash Fire/Explosion division considered in this work are taken from (Uijt De Haag and Ale, 1999). The values used to quantify the branches of the fault tree are resumed in table 4.20. Detail on event trees constructions for conventional scenarios used in QRA can be found in reference literature (Lees, 1996; Uijt De Haag and Ale, 1999).

Table 4.20: For every top event data for event trees assessment are provided: Frequency of the top event, Ignition probabilities, probability of Flash Fire / Vapor Cloud Explosion

Top Event	Typology	f	Substance	Immediate Ignition	Delayed ignition	Flash fire / Explosion
Leak from vessel	Atmospheric	10^{-4} y^{-1}	Liquid	0.065	0.9	0.3-0.7
Leak from vessel	Pressurized	10^{-5} y^{-1}	Gas or Two phase	0.2	0.9	0.3-0.7
Full bore Rupture	-	$2.5 \times 10^{-6} \text{ y}^{-1} \text{ m}^{-1}$	Liquid/Gas or Two phase*	0.065 / 0.5*	0.9	0.3-0.7
Leak from pipeline	-	$3.5 \times 10^{-6} \text{ y}^{-1} \text{ m}^{-1}$	Liquid/Gas or Two phase*	0.065 / 0.2*	0.9	0.3-0.7
Catastrophic rupture	Atmospheric	$5 \times 10^{-6} \text{ y}^{-1}$	Liquid	0.065	0.9	0.3-0.7
Catastrophic rupture	Pressurized	$5 \cdot 10^{-7} \text{ y}^{-1}$	Gas or Two phase	0.7	0.9	0.3-0.7
Release in 10 m	Atmospheric	$5 \cdot 10^{-6} \text{ y}^{-1}$	Liquid	0.065	0.9	0.3-0.7
Release in 10 m	Pressurized	$5 \cdot 10^{-7} \text{ y}^{-1}$	Gas or Two phase	0.5	0.9	0.3-0.7

4.8.2 Lightning triggered scenario modelling

Lightning-triggered scenarios have described in section 4.5 and the event tree response are described in Figure 4.19 and 4.28. Although, a description of the lightning triggered accidental scenarios modelling is provided in the following sections. In order to calculate lightning triggered accident frequencies, the lightning statistic properties are those provided by the directive (CEI, 2013). The annual flash density at ground is considered as a typical Italian value of 3 flashes/km²/y (SIRF, 2013).

Since lightning triggered accidents shows some atypical features a few indications should be given in order to give the reader the sensibility on how results are obtained. For the calculation of the pool fire surface, immediate ignition of the flammable material is considered. Thus, the pool diameter that causes an equilibrium between the release rate and the pool burning rate is considered. Full surface tank fire can be modeled as pool fire with a diameter equal to the diameter of the tank and placed at an elevation from the ground, which is equal to the tank height.

In order to model the confined explosion, the vapor space is assumed equal to the half volume of the tank. The concentration of the flammable vapor in mixture is assumed homogeneous in the vapor space and equal to the minimum value between to the equilibrium composition at the liquid interface, due to the liquid vapor pressure for a given storage temperature condition, and the upper explosive limit (UEL) of the substance. However, the portion of the explosion energy that is used to destroy the tank roof is usually very high, due to the roof (or tank) size and mass. For this reason the maximum value for this parameter is used, in the range proposed by (Gubinelli et al., 2009a; 2009b). Therefore, in some of the cases analyzed the overpressure is limited to very low values and short distances, thus the effect of the shockwave on humans has been neglected in the present study. Fragments projected can be the highest threat to nearby equipment, in particular the entire roof is likely to be thrown in a single piece, also at great distances. In the current methodology fragments impingement is not considered for the evaluation of human vulnerability, however it is worth to remark the importance of roof projection for future studies on domino effect triggered by lightning NaTech scenarios (see Chapter 3).

4.8.3 Meteorological Data

The meteorological aggregation should be chosen coherently with the site under investigation. Since no specific region is considered in this study, two conventional atmospheric conditions are selected, in order to shows exemplificative results, for the consequence calculation (F and D atmospheric stability according to Pasquill classification (Mannan, 2005):

- **Stability class F with a wind speed of 2 m/s**
- **Stability class D with a wind speed of 5 m/s**

The temperature is set at 20 ° C for all the calculations and the relative humidity is set to 70 % for all the conventional releases. Further considerations are needed for lightning triggered accidents. In order to perform a consequence analysis that is coherent with the lightning phenomenon, the typical atmospheric condition of a thunderstorm should be represented. The formation of a thunderstorm cloud happens in condition of high atmospheric instability and elevate air relative humidity. Moreover, thunderstorms are usually accompanied by strong winds and rain (Cooray

and Becarra, 2010). the following indications should be followed in order to have more realistic simulations:

- In order to represents strong wind and the atmospheric instability condition the use of stable and low wind conditions (e.g. wind velocity 2 m/s and stability class F) should be avoided. Thus, the wind direction probability should be chosen accordingly.
- In this document the “2F” stability class have been ignored while calculating the lightning-triggered scenario consequences; only class “5D” has been considered.
- A relative humidity equal to 100 % should be considered for all the lightning-triggered scenarios

The presence of rain, which contribute to mitigate the effect of the thermal radiation with the distance and may absorb the hazardous vapors, is not compatible with the most of models for consequence assessment. Thus, rain is conservatively not considered.

4.9 Application of QRA procedure: results

The accidents consequences are assessed by the use of conventional models for consequence assessment implemented in DNV's software Phast. The individual and societal risk was then calculated by the use of ARIPAR GIS: a software for Quantitative Area Risk Assessment (QARA) (Egidi et al.1995). Results are obtained with and without lightning triggered scenarios in order to evaluate the weight of those accidents. First, the methodology is applied to single equipment in order to analyze in detail the effect of lightning strikes on different equipment typologies. Finally, the methodology is applied to a realistic case study based on the map of the storage park area of an oil refinery.

4.9.1 "Conventional" risk assessment against risk contribution of "NaTech scenarios" for single equipment

The procedure for the introduction of lightning NaTech risk is applied to three single equipment: an external floating roof atmospheric tank (EFRT), a fixed roof atmospheric tank (FRT) and a pressurized tank (PT). For all the atmospheric tanks a square bund area which side is equal to the double of vessel diameter is considered. All the releases are considered as horizontal in the same direction as the wind. A uniformly distributed wind direction probability, is considered. Table 4.21 shows the features of the tank under analysis and the calculated frequencies for lightning triggered accidents for the three different vessel categories, considered as stand-alone equipment. Lightning impact frequency on the storage tank is calculated according the simplified method presented in Section 4.4.4, using a flash density at ground (n_g) of 3 flash/km²/y (typical Italian value (SIRF, 2013)); the shell perforation probability is calculated according the simplified method presented in Section 4.6; lightning-triggered scenario frequencies are finally calculated following the indications provided in Section 4.7.

Three different storage typologies are considered: external floating roof atmospheric tank (EFTR), cone roof atmospheric tank (CR) and pressurized tank (PT). Details on vessel geometries, as well as the calculated frequencies of the possible accident scenarios triggered by lightning strikes are reported in Table 4.21.

The EFRT is the biggest tank typology, thus is the one with the highest expected number of strikes per year; the highest PDD is instead for the CRT due to low vessel thickness. In order to evaluate the tank fire frequency foe EFRT, the tank is assumed to be protected by a fixed foam system only. A representative value for the probability of failure on demand of this system considered; a value of $7.03 \cdot 10^{-3}$ is assumed, according to Table 4.19.

Table 4.21: Features of tank analyzed. The expected number of lightning attracted per year, the probability of direct damage and the frequencies for the tank fire scenario and for the pool fire / jet fire scenario.

Type	Material	D (m)	H (m)	L (m)	V (m ³)	t _{min} (mm)	t _{max} (mm)	f _{cap} (y ⁻¹)	P _{DD}	f _{TF} (y ⁻¹)	f _{PF/JF} (y ⁻¹)
CR	Gasoline	21	12.6	-	4364	6	10.3	6.14×10^{-2}	4.82×10^{-3}	3.07×10^{-4}	2.96×10^{-4}
EFRT	Crude Oil	55	14.4	-	34200	8	20.5	9.42×10^{-2}	3.10×10^{-4}	6.62×10^{-4}	2.92×10^{-5}
PT	LPG	2.8	3.5	18	100	18	18	3.70×10^{-2}	2.01×10^{-7}	-	7.44×10^{-9}

In order to evaluate the tank fire frequency for the CRT, the tank is assumed to be protected by inert gas blanketing system only. A representative value for the probability of failure on demand of this system considered; a value of $5.0 \cdot 10^{-3}$ is assumed, according to Table 4.19. The direct damage result in a loss of containment with immediate ignition of the flammable material released. It results in a pool fire for the two atmospheric tanks and in a jet fire for the pressurized one.

Figure 4.29-a,4.29-b and 4.29-c represents the local specific individual risk, calculated with and without the scenarios caused by lightning strikes, reported against the distance from the vessel, obtained by the use of a GIS software tool, developed with the MATLAB software.

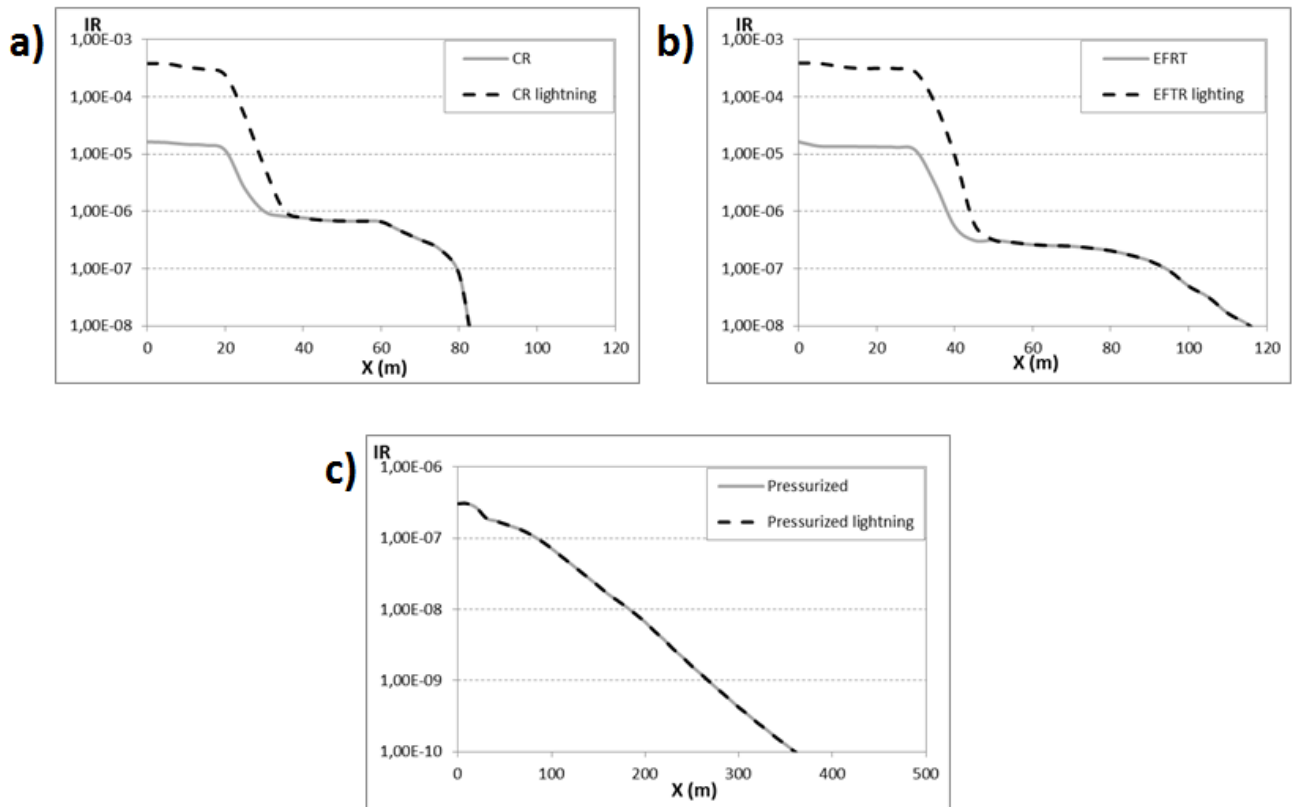


Figure 4.29: The value of individual risk against the distance from the tank center (X); the grey line is calculated for the conventional scenarios only, the dotted black line is calculated considering lightning triggered scenarios. a) cone roof tank (CFT); b) external floating roof tank (EFRT); c) pressurized tank

Figure 4.29-a and 4.29-b shows two distinct curves for the individual risk due to conventional scenarios only and for scenarios that include lightning triggered accidents. In particular at a short distance from the tank, the difference between the two curves is the highest, due to the increment of the number of accident scenarios with limited consequences (tank fires, fires in the bund), while the frequencies of those scenarios with major consequences (flash fire, VCE) remain unaffected.

4.9.2 “Conventional” risk assessment against risk contribution of “NaTech scenarios”: case study

A case study was analyzed with the aim of assessing the importance of the previously discussed extensions of QARA studies to NaTech scenarios triggered by lightning. A representation of the case study analyzed is reported in Figure 4.30. In the case-study, the NaTech quantitative risk assessment procedure (Figure 4.3) was applied to a storage section of an existing industrial site.

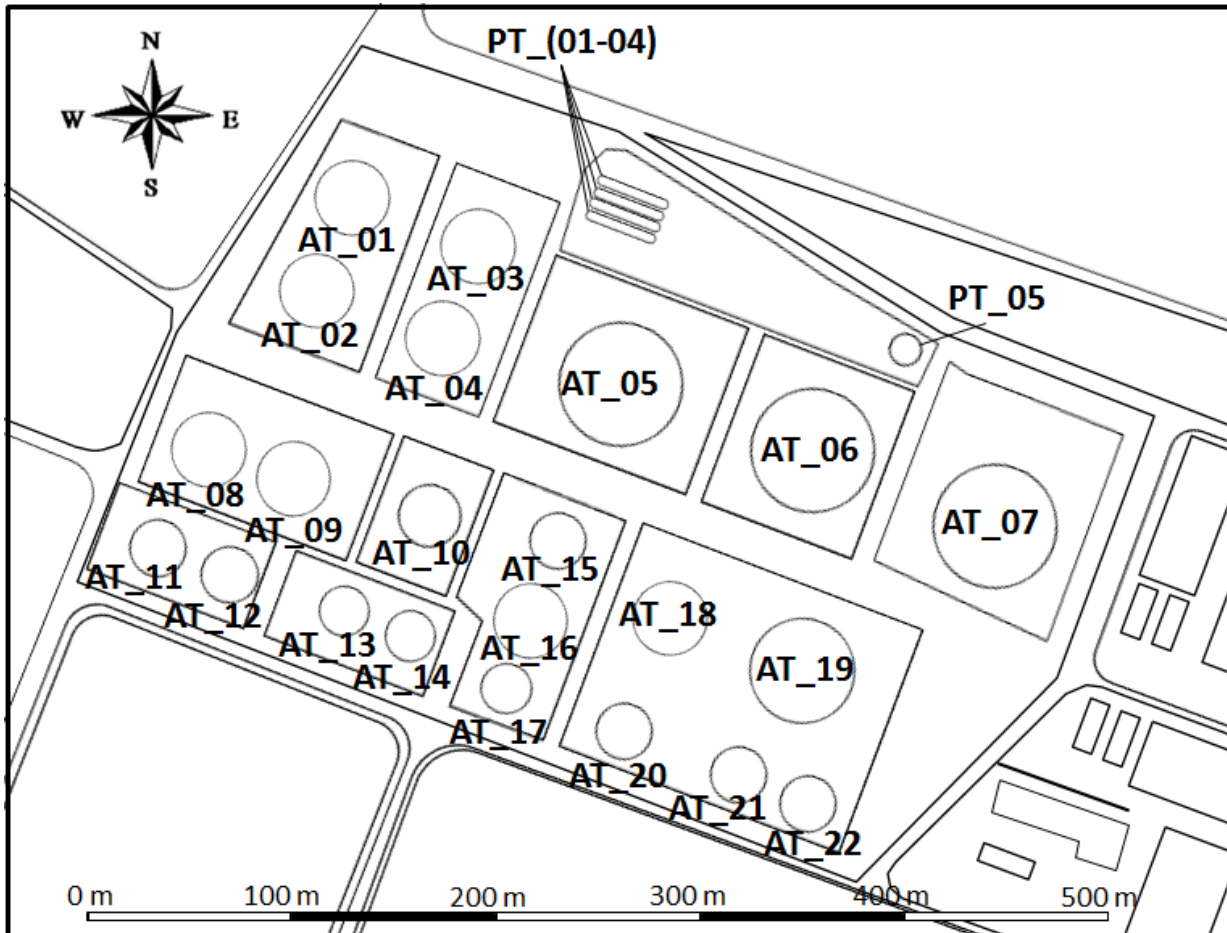


Figure 4.30: The footprint of the storage area of the industrial activity considered as a case study showing the vessels considered. Details regarding the equipment considered in the risk analysis are provided in Table 4.22

Table 4.22 shows the features of the vessels considered in the study and the inventory for the consequence calculation. Design features and relative position in the plant footprint are crucial variables for the assessment of lightning-triggered scenario frequencies. Thus expected attraction frequency assessment, direct damage probability assessment and the frequencies of Natech scenarios are reported in Table 4.23.

The calculated frequency of lightning impact on the tank in the layout considered are significantly lower than those calculated in the previous section for standalone equipment, due to the fact that several storage tanks are present in the same attraction area. Therefore, the resulting scenario frequency are significantly lower than those presented in Section 4.9.1.

Table 4.22: Features of the storage tanks reported in Figure 4.30: length (L), diameter (D), height (H), volume (V), height of the course (H_{course}), shell thickness at different heights (ts1 to ts6)

Tank ID	L (m)	D (m)	H (m)	V (m)	H_{course} (m)	ts1 (mm)	ts2 (mm)	ts3 (mm)	ts4 (mm)	ts5 (mm)	ts6 (mm)
TA_01	-	38	9	8160	1,8	9,9	8	8	8	12,5	-
TA_02	-	38	9	8160	1,8	9,9	8	8	8	12,5	-
TA_03	-	38	9	8160	1,8	9,9	8	8	8	12,5	-
TA_04	-	38	9	8160	1,8	9,9	8	8	8	12,5	-
TA_05	-	60	9,6	21700	2,4	16,27	11,96	8	8	-	-
TA_06	-	60	9,6	21700	2,4	16,27	11,96	8	8	-	-
TA_07	-	60	9,6	21700	2,4	16,27	11,96	8	8	-	-
TA_08	-	38	9	8160	1,8	9,9	8	8	8	12,5	-
TA_09	-	38	9	8160	1,8	9,9	8	8	8	12,5	-
TA_10	-	30	12	6780	2,4	10,4	8,2	6	6	6	-
TA_11	-	27	14,4	6590	2,4	11,3	9,3	7,4	6	6	6
TA_12	-	27	14,4	6590	2,4	11,3	9,3	7,4	6	6	6
TA_13	-	27	10,8	4940	1,8	11,3	9,3	7,4	6	6	6
TA_14	-	27	10,8	4940	1,8	11,3	9,3	7,4	6	6	6
TA_15	-	27	10,8	4940	1,8	11,3	9,3	7,4	6	6	6
TA_16	-	38	9	8160	1,8	9,9	8	8	8	12,5	-
TA_17	-	21	12	3320	2,4	7,3	6	6	6	6	-
TA_18	-	38	9	8160	1,8	9,9	8	8	8	12,5	-
TA_19	-	50	12	18840	2,4	17,3	13,96	10,15	8	8	-
TA_20	-	27	10,8	4940	1,8	11,3	9,3	7,4	6	6	6
TA_21	-	27	14,4	6590	2,4	11,3	9,3	7,4	6	6	6
TA_22	-	27	14,4	6590	2,4	11,3	9,3	7,4	6	6	6
PA_01	37	3,3	4,8	250	-	21	-	-	-	-	-
PA_02	37	3,3	4,8	250	-	21	-	-	-	-	-
PA_03	37	3,3	4,8	250	-	21	-	-	-	-	-
PA_04	37	3,3	4,8	250	-	21	-	-	-	-	-
PA_05	-	16	17,5	1700	-	24	-	-	-	-	-

Table 4.23: details regarding lightning-triggered scenarios for each equipment in the case study: the calculated capture frequency (f_{cap}), the probability of direct damage (P_{DD}), the frequency of the tank fire scenario (f_{TF}), the frequency of the pool fire or jet fire scenario ($f_{PF/JF}$), the tank category and the stored substance

Tank ID	$f_{cap} (y^{-1})$	P_{DD}	$f_{TF} (y^{-1})$	$f_{PF/JF}(y^{-1})$	Category	Substance
TA_01	2,74E-02	5,48E-04	1,37E-04	1,50E-05	CR	Gasoline
TA_02	1,79E-02	5,48E-04	8,94E-05	9,81E-06	CR	Gasoline
TA_03	1,56E-02	5,48E-04	7,81E-05	8,57E-06	CR	Gasoline
TA_04	1,13E-02	5,48E-04	5,65E-05	6,20E-06	CR	Gasoline
TA_05	2,72E-02	3,49E-04	2,20E-04	9,49E-06	EFRT	Crude OIL
TA_06	2,00E-02	3,49E-04	1,62E-04	6,98E-06	EFRT	Crude OIL
TA_07	4,53E-02	3,49E-04	3,67E-04	1,58E-05	EFRT	Crude OIL
TA_08	1,21E-02	5,48E-04	6,06E-05	6,66E-06	CR	Gasoline
TA_09	4,08E-03	5,48E-04	2,04E-05	2,24E-06	CR	Gasoline
TA_10	1,43E-02	4,21E-03	7,10E-05	6,01E-05	CR	Gasoline
TA_11	3,44E-02	4,11E-03	1,71E-04	1,41E-04	CR	Gasoline
TA_12	1,45E-02	4,11E-03	7,23E-05	5,96E-05	CR	Gasoline
TA_13	1,34E-02	3,71E-03	6,70E-05	4,99E-05	CR	Gasoline
TA_14	9,98E-03	3,71E-03	4,97E-05	3,71E-05	CR	Gasoline
TA_15	1,03E-02	3,71E-03	5,14E-05	3,83E-05	CR	Gasoline
TA_16	2,70E-03	5,48E-04	1,35E-05	1,48E-06	CR	Gasoline
TA_17	1,60E-02	6,50E-03	7,97E-05	1,04E-04	CR	Gasoline
TA_18	9,59E-03	5,48E-04	4,79E-05	5,26E-06	CR	Gasoline
TA_19	2,21E-02	3,71E-04	1,79E-04	8,21E-06	EFRT	Crude OIL
TA_20	1,34E-02	3,71E-03	6,70E-05	4,99E-05	CR	Gasoline
TA_21	1,69E-02	4,11E-03	8,39E-05	6,93E-05	CR	Gasoline
TA_22	2,80E-02	4,11E-03	1,40E-04	1,15E-04	CR	Gasoline
PA_01	2,22E-02	1,32E-08	-	2,92E-10	PT	LPG
PA_02	2,04E-03	1,32E-08	-	2,69E-11	PT	LPG
PA_03	1,22E-03	1,32E-08	-	1,61E-11	PT	LPG
PA_04	2,22E-03	1,32E-08	-	2,93E-11	PT	LPG
PA_05	3,53E-02	8,65E-10	-	3,05E-11	PT	LPG

A specifically developed software tool, implemented on the Matlab platform, was used to carry out the risk calculation and risk mapping for the case-study. The computer program applies the ARIPAR methodology (Egidi et al., 1995). By the application of conventional and lightning triggered scenarios to the possible accident sources, individual risk contours have been calculated. Figure 4.31 shows the local specific risk profile generated by the hazardous substances stored in the area. Figure 4.31-a shows the risk map for the lay-out of concern, obtained considering conventional scenarios only, while Figure 4.31-b shows the risk map obtained considering lightning triggered accidents together with conventional. Figure 4.31-b shows an increment of more than one order of magnitude of the risk value in the area in the close vicinity of the tanks to the respect of Figure 4.31-a, while the risk profiles at larger distance from the tanks are identical in both the panels.

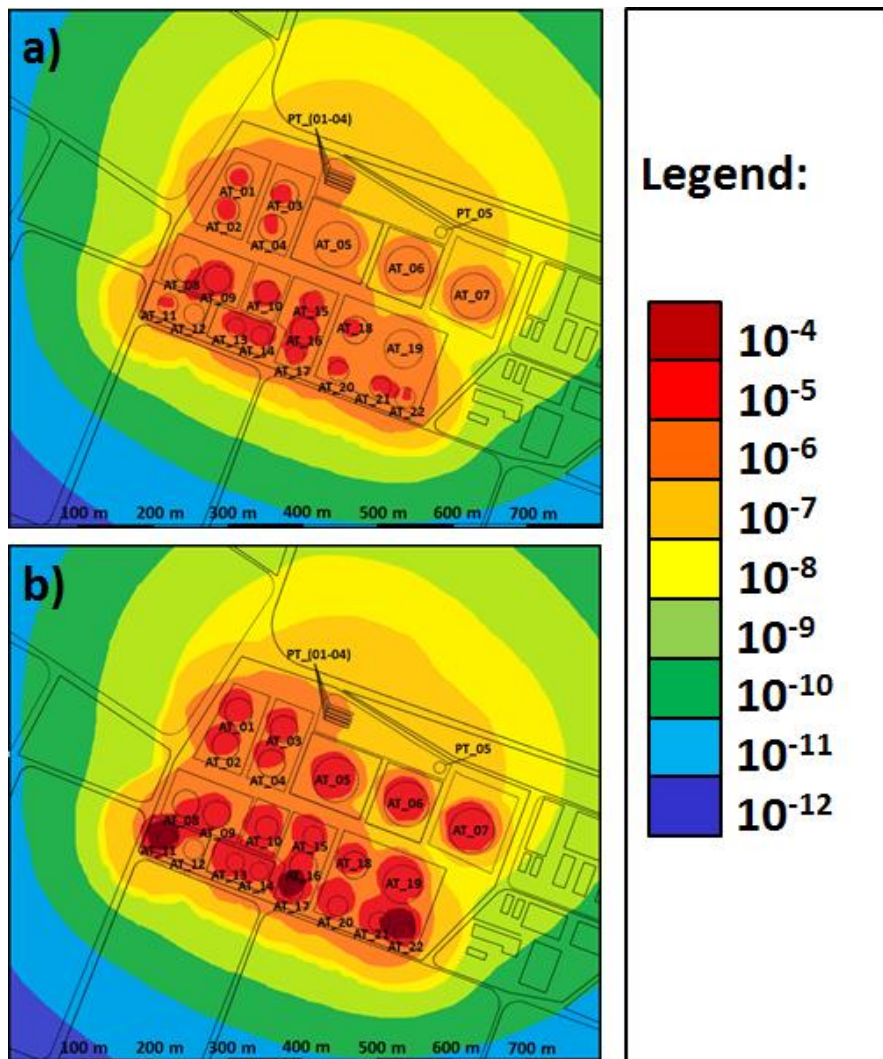


Figure 4.31: The risk profile of the storage area under investigation. The individual risk maps are calculated in panel a) using the conventional accident scenarios only and in panel b) using conventional accident scenarios together with lightning triggered scenarios

In order to better understand the entity of the risk associated to lightning strikes, the societal risk calculation has been carried out for the lay-out analyzed. A uniform population distribution of 100 persons per km² was selected to provide societal risk figures. Since this calculation has the only

purpose to show the effect of lightning triggered accidents, the same population density was applied both outside and inside of the plant, where only a few operators should be expected to be in place. Figure 4.32 shows the F-N risk curves for the three equipment considered, with (dotted black line) and without (grey line) the lightning-triggered accidents.

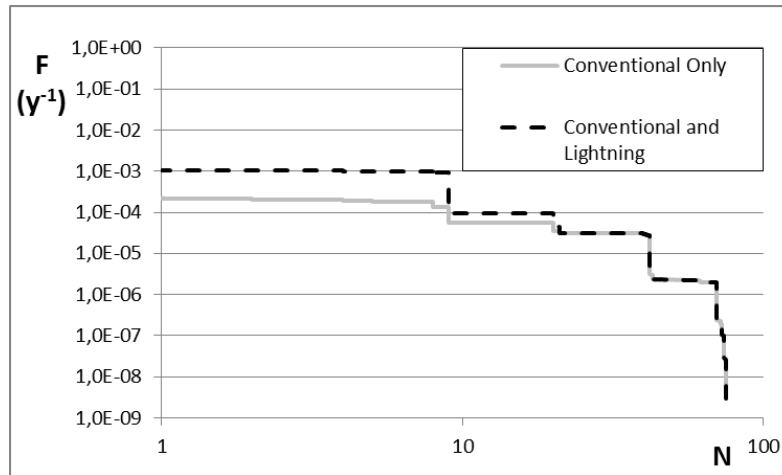


Figure 4.32: The societal risk expressed as F-N plot for the case study considered. Frequencies and casualties are calculate for conventional accident scenarios and for lightning triggered scenarios

As shown by the figure, the frequency of scenarios with a few casualties expected increases significantly with the introduction of lightning hazard, while the frequency of those scenarios with a high number of deaths, and therefore with a high impact on the community, are unaffected by the introduction of lightning-triggered scenarios.

Furthermore an index could be calculated to represent the impact of the industrial plant: the potential life loss (PLL) (Lees, 1996; Uijt De Haag and Ale, 1999). The value of PLL of the industrial plant in absence of lightning threat is 1.71, while introducing lightning- triggered scenarios the PLL rise to 9.39. The increase of this indicator is an interesting signal on the risk increment due to lightning strikes, despite the fact that only those accidents with limited consequences have been increased the PLL rises significantly. Again, in order to get the sense of these values, one should consider that an uniform population value was assumed.

4.9.3 Final considerations

Some general conclusions can be drawn based on the result obtained. The lightning triggered scenarios generally show a high frequency, which can be much higher than conventional scenarios, on the other hand, lightning scenarios consequences are characterized by fire and explosions with limited extension. Therefore, the risk profile of the industrial site, calculated considering lightning scenarios, is higher than the risk calculated using conventional methodologies for QRA, in the close vicinity of the storage tanks. Furthermore, since the consequence of Natech accidents due to lightning do not cross the tank perimeter, they are not supposed to increase the risk due to the industrial activity for nearby population. However, in the current analysis the possibility of accident escalation due to domino effect was not considered. Since the lightning triggered accidents occur with very high frequency and with the potential to

trigger an accident escalation process, they represent a frequent ignition for the escalation process. Moreover, the possibility of accident escalation within the tank itself was not considered: as a consequence of a tank fire the tank integrity could be lost and the entire inventory could be released, increasing the scenario severity. At the same time the tank fire scenario could lead to boil over, again increasing the accident severity. All those effects need to be considered in order to quantify the risk associated to Natech due to lightning strikes. Therefore, the development of tools to achieve these issues represent the future for the research of lightning triggered accidents.

4.10 Possible strategies for the lightning protection of storage tanks

Every year a large number of atmospheric storage tanks suffer a lightning related accident, usually a fire or an explosion. These events suggest that the atmospheric tanks should be protected with specific protective measures against lightning strikes, other than the safety barriers that prevents or mitigate the occurrence of fires, which have been already discussed in Section 4.5. For this reason oil industries worldwide decided to develop protective measures to protect tanks from the threat of lightning strikes. Recommended practice 545 from API (API, 2009) is the dedicated standard on lightning protection for storage tanks and substitute the previous indications provided by API 2003 standard (API, 2008). Two potential threats are identified for installation containing flammable substances: threat from a direct lightning strike, when the flash hits directly the storage tank and threat from indirect lightning strike, when the flash hit the ground (or another structure) in the vicinity of the tank. In either events, the lightning current (or a portion of it) flows through the tank, eventually causing sparking. There are two types of spark; thermal sparks, which are generated only in the case of direct lightning strike on the tank and voltage sparks, which form because discontinuities in the current paths may result in arcing across the gaps (API, 2009). Sparks and electric arcs may ignite the flammable atmosphere eventually present in the storage tank.

For this reason, the document lists several objectives to achieve, in order to protect the storage tank from the lightning threat. In particular, External Floating Roof Tanks (EFRT) should meet specific design requirement for the installation of shunts, seals and bypass conductors (API, 2009). These protective devices, together with specific indications about operational planning have the aim of avoiding ignition of flammable material, by minimizing spark generation probability, as a consequence of a lightning strike, and by preventing the formation of flammable-air mixture at the rim-seal.

The Indian “Oil Industry Safety Directorate (OISD)” provides its specific standard regarding the issue of lightning protection of storage tanks (OISD, 1999), on the basis of international standards (NFPA, 2004) of lightning protection of structures. It is similar in contents to the API RP 545, but it includes a section for the protection of the tank from the threat of direct lightning strikes by the use of dedicated air terminals (CEI, 2013). There is general agreement, among the different codes, about the fact that total protection from the lightning hazard in storage tank areas is just a hypothetical goal, due to the stochastic behaviour of lightning strikes. Thus, the design of lightning protection systems should be flanked by a dedicated risk analysis method (API, 2009).

4.10.1 Bonding

This is a specific requirement for External Floating Roof Tanks (EFRT). The gap between the roof and the tank shell is a major cause of lightning voltage spark. In order to mitigate this, standards on lightning protection recommends that a form of short circuit (direct connection) should be established between the roof and the shell so as to provide a flow path for the lightning current from the roof to the tank shell rather than through the air gaps.

In order to significantly reduce potential differences between the different parts of the tank, an electrical connection is provided among all the components. This measure create a “safe” path for the lightning current to the ground. An adequate bonding is achieved by the installation of shunts and bypass conductors between the storage tank body and the floating roof (API, 2009). Furthermore, any gauge or guide pole components or assemblies that penetrate the tank floating roof shall be electrically insulated from the tank floating roof.

Even if these measure are capable to completely protect the tank from the ignition threat due to indirect strike currents, the analysis of past accidents demonstrate that in case of direct lightning impact, bonding can slightly reduce the probability of ignition of flammable atmosphere, but does not ensure the prevention of incendiary sparks (Carpenter, 1996). Since there will always be sparking at the shunt-shell interface API recommended that the shunts should be installed submerged below the crude oil at a minimum depth of 0.3m in a region where flammable vapour does not exist such that even when sparks are generated the fire triangle will not be completed. Presently the submersible type of shunt is not available because the feasibility and effectiveness of such a design is not generally agreed on. This therefore challenges the effectiveness of shunts for current conduction. However, since the probability of indirect strikes is much higher than the probability of direct strike on the storage tank (as much as 1000 times larger (CEI, 2013)), bonding is considered a mandatory requirement for the design and installation of atmospheric storage tanks.

About grounding of the structure API RP 545 does not include specific requirement since the metal body of the storage tank provides adequate grounding itself. Furthermore, the eventual presence of sparking below the roof, where no flammables are present, should not be considered an hazardous situation.

4.10.2 External lightning protection system (ELPS)

The approach to solving the lightning induced fire issue is centred on eliminating voltage differential eliminating the chances of spark generation at the shunt-shell interface by ensuring that the lightning stroke does not terminate on the roof instead of a preferred conductive part.

An ideal protection for structures and services would be to enclose the object to be protected within an earthed and perfectly conducting continuous shield of adequate thickness, and by providing adequate bonding, at the entrance point into the shield, of the services connected to the structure. This would prevent the penetration of lightning current and related electromagnetic field into the object to be protected and prevent dangerous thermal and electro-dynamic effects of current, as well as dangerous sparking and over voltages for internal systems. In practice, it is often neither possible nor cost effective to go to such lengths to provide such optimum protection (CEI, 2013).

The OISD GRD 180 (1999) describes a methodology, based on the rolling sphere method, for the design of external lightning protection systems (ELPS) for storage tank parks. A lightning protection system (Conventional Air Terminal System) consists of the following three basic components:

a) Air terminal: capable of drawing the lightning discharge to it in preference to vulnerable parts of the protected structure.

b) Down conductor: provide a safe low-impedance path to the ground.

c) Earth connection: provides safe discharge of lightning current into the soil

Different air terminal provides different protection to the respect of direct strikes to the storage tank. The solutions proposed by OISD GDN 180 (OISD, 1999) are discussed in the following.

4.10.3 Lightning rods

The design of lightning rods (OISD, 1999) is performed by the use of the “rolling sphere method” (CEI, 2013), used to define the minimum number of rods per tank that shall be installed. Rods are designed to attract a stroke that would be directed to the tank roof and divert the resulting current via a preferred path (the down conductor) to earth. They are reasonably effective in performing these functions. However, air terminals can cause fires by attracting the strike, since the design assume to place the air terminal in close proximity to the flammables (top of tank body) and cause the ignition of the substance due to thermal sparking. Furthermore, the closer the stroke channel is to the flammables, the higher the related effects (bound charge and earth currents), and the greater the risk of a fire initiating arc. Thus, even if they are capable of reducing the dangerous effect of lightning strikes on storage tanks, i.e. neglecting the direct damage to the tank shell (Necci et al., 2013b), they also increase the chances of lightning hitting the tank and do not prevent the threat due to possible ignition of flammable vapours (Carpenter, 1996).

4.10.4 Lightning protection masts

Their mechanism is similar to the lightning rods. Air terminal are supported by tall masts, placed at some distance from the tank (at least 6 m in order to avoid side flashes (OISD, 1999) (Figure 4.33-a). Even though a single mast is capable to reduce significantly the frequency of lightning hitting smaller storage tanks (Necci et al., 2013b), for a significant protection of larger tanks a network composed by several mast surrounding the tank is suggested by the codes for lightning protection (OISD, 1999). The number of lightning masts that shall be applied is obtained by the use of the “rolling sphere method” (Table 4.24) based on a striking distance of 30 m.

Table 4.24: The use of lightning protection mast network: capture frequency calculation and reduction factor (Necci et al., 2014c)

<i>D (m)</i>	<i>Mast N</i>	<i>f_c (y⁻¹)</i>	<i>f_{cs} (y⁻¹)</i>	<i>LI</i>
up to 12	3	5.44E-02	2.59E-06	4.77E-05
13-21	4	6.08E-02	3.02E-06	4.97E-05
22-32	5	6.89E-02	1.38E-05	2.01E-04
33-38	6	7.37E-02	2.33E-05	3.17E-04
39-45	7	7.91E-02	3.72E-05	4.69E-04
46-51	8	8.42E-02	5.92E-05	7.03E-04
52-57	9	8.94E-02	1.03E-04	1.16E-03
58-63	10	9.46E-02	1.56E-04	1.64E-03
64-71	11	1.02E-01	2.52E-04	2.46E-03
72-79	12	1.10E-01	4.44E-04	4.04E-03

In Appendix 1 of OISD GDN 180 (1999) details on the use of the rolling sphere method for the design of ELPS are shown. In particular air terminal height, number and distance from the tank are reported. Lightning mast network should overcome the maximum tank height of 15 m; it should include one mast per every 24 m of the tank perimeter; masts should be placed at a minimum distance of 6 m from the tank. A reference tank height of 12 m has been considered in the following (OISD, 1999). Table 4.24 reports the indications provided by OISD GDN 180 for the installation of a lightning mast network around storage tank in a wide range of possible tank size. It also reports the f_c , the f_{cs} and the respective LI for each tank size, calculated for the largest diameter proposed in the range of applicability. Since this system is actually capable of attracting lightning away from the equipment, they are capable to reduce significantly the frequency of direct lightning strikes to the tank.

4.10.5 Overhead shield wire

A system of overhead earth wires placed at the top of dedicated supporting structures can be installed to protect a storage tank. The system is designed (OISD, 1999) according to rolling sphere concept based on a striking distance of 30 m (Figure 4.33-b). A single earth wire with a minimum clearance of about 8 m above the highest point of the tank can protect a tank of about 6 to 8 m diameter (OISD, 1999). For tank diameters between 8 to 30 m two parallel earth wires are used while for tank diameters between 30 to 80 m (Figure 4.33-b); three parallel wires are required to protect the tank. Again the lightning strike is attracted away from the storage tank with an expected reduction of the frequency of direct lightning strikes on the vessel.

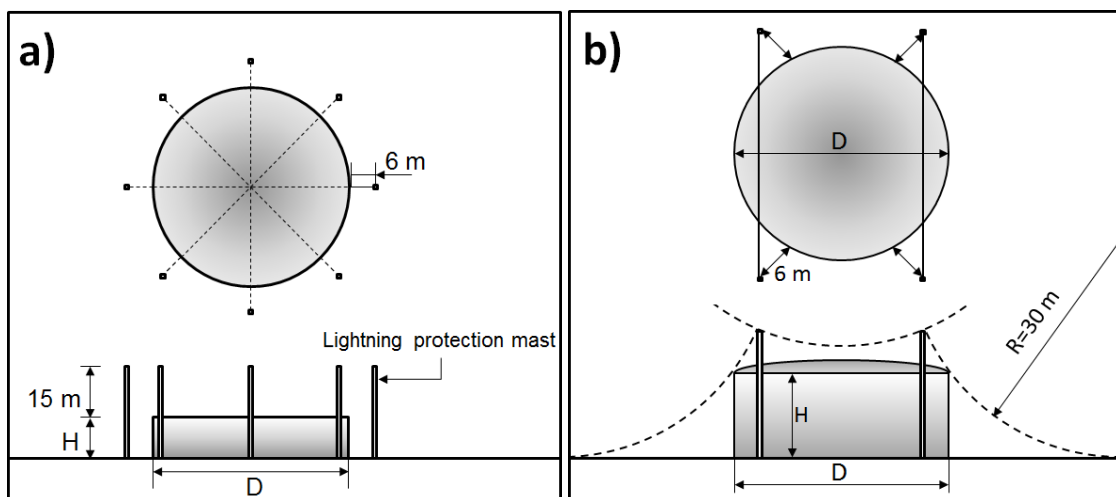


Figure 4.33: Air terminals for the ELPS: a) Lightning masts; b) overhead shield wire (Necci et al., 2014c)

Since the frequency of accidental scenarios triggered by lightning is directly proportional to the frequency of lightning strikes hitting the tank, the assessment of the reduction on the lightning attraction frequency result in an equivalent reduction of the frequency of the lightning-triggered accidental scenarios. In order to express the protection that can be achieved by the use of a protection system, a non-dimensional factor, the layout index (LI) defined in section 4.4.3 by

equation 4.6, can be used. This index represents the ratio between the lightning capture frequency of the unit in its specific layout and the capture frequency that the same unit would have in an unprotected open flat field. The complete methodology for the assessment of the lightning impact frequency and for the layout index calculation is provided in Section 4.4.

Table 4.25 reports the indications provided by OISD 180 for the installation of overhead shield wires network above a storage tank in three possible configuration, according to the tank size. It also reports the f_c , the f_{cs} and the LI for every tank size, calculated for the largest diameter proposed in the range of applicability.

Table 4.25: The use of overhead shield wire network: capture frequency calculation and reduction index (Necci et al., 2014c)

D (m)	Wire N	f_c (y^{-1})	f_{cs} (y^{-1})	LI
6-8	1	9.00E-06	5.19E-02	1.73E-04
9-30	2	5.00E-06	6.74E-02	7.42E-05
31-80	3	9.40E-05	1.11E-01	8.47E-04

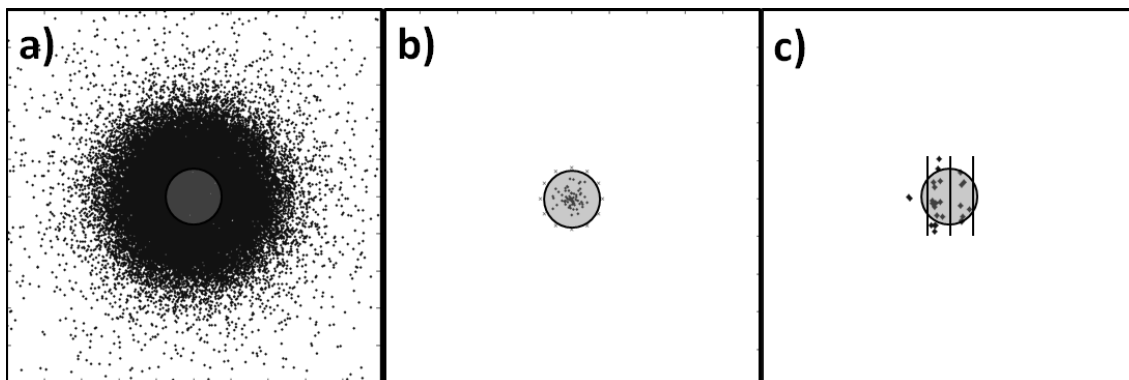


Figure 4.34: The use of Monte Carlo model to evaluate the protection provided by the ELPS. The location of attracted lightning on a map in three cases: a) the storage is tank unprotected; b) the storage tank is protected by lightning mast network; c) the storage tank is protected by overhead shield wires (Necci et al., 2014c)

Figure 4.34 shows a footprint of a simple lay-out in which the Monte Carlo method, described in section 4.4.3, has been applied. The figure is intended to provide a visual representation about the significant reduction on the number of lightning attracted by the tank, in the case of tank was protected. The point of formation of the descending step leader of those lightning strikes attracted by the storage tank are evidenced in dark gray, while the tank is light gray. The two different solutions are applied to protect the storage tank. Figure 4.34-a shows the attracted lightning for a huge tank of 79 m diameter in case the tank is unprotected; Figure 4.34-b the attracted lightning by the tank in the case it is protected by twelve masts (see Table 4.24); Figure 4.34-c shows the attracted lightning by the tank in the it is protected by three overhead shield wires (see Table 4.25). A number of 10^6 simulations were performed for each panel.

4.11 Conclusions

A methodology for the assessment of final outcomes following a lightning strike on storage tank containing hazardous liquids and gases was developed. In particular, accidents triggered by lightning strikes that took place in industrial installation have been analysed. The results discovered that most of accidents triggered by lightning strikes regarded storage sites containing flammable materials and in particular atmospheric storage tanks of petroleum industry. The reference scenarios and the mitigation barriers that may influence event sequences after lightning impact were identified. A methodology for the assessment of the so called Natech accidents due to lightning was presented. In order to apply the methodology several tools were developed. A dedicated methodology allowed the calculation of the expected frequency of lightning strikes on storage tanks, considering the lightning statistics collected at regional level, as well as design features of the industrial equipment units and the lay-out of the industrial site. A fragility model for direct damage to storage tank was developed, allowing to calculate a damage probability for vessel struck by lightning. The fragility model, based on a detailed analysis of possible thermal damage at the attachment point allowed the definition of a simplified correlation, suitable for the application to QRA studies. Reference event trees were obtained and validated using past accident data. The assessment of standard safety barriers applied in industrial practice allowed the quantification of event trees based on generic reference values for barrier probability of failure on demand. The application of the entire methodology to a case study confirmed on one hand that NaTech scenarios caused by lightning may have an important influence on the risk profile of a facility, and, on the other hand, evidenced the role of the safety barriers in preventing accident propagation.

Finally the possibility of risk reduction due to the application of lightning protection systems (LPS) was discussed. The risk reduction that can be achieved by the installation of lightning masts and shield wires was assessed in quantitative terms by the use of a dedicated lay-out index LI.

References

- American Institute of Chemical Engineers Center of Chemical Process Safety. AIChE-CCPS. Guidelines for Improving Plant Reliability Through Data Collection and Analysis. New York. 1998.
- American Petroleum Institute. API standard 650 - Welded steel tanks for oil storage. 8th ed. Washington D.C., USA. 2003.
- American Petroleum Institute. API RP 2003 - Protection Against Ignitions Arising Out of Static, Lightning, and Stray Currents. 7th ed. Washington D.C., USA. 2008.
- American Petroleum Institute. API RP 545 - Lightning Protection of Aboveground Storage Tanks for Flammable or Combustible Liquids. 1st Edition. Washington D.C. USA. 2009.
- American Petroleum Institute. API Publication 581- Risk-based Inspection. Base Resource Document. 2000.
- American Petroleum Institute. API Std 2000 - Venting Atmospheric and Low-pressure Storage Tanks. Washington D.C. USA. 1998.
- American Petroleum Institute. API-RP 2210 - Flame arresters for Vents of Tanks storing Petroleum Products. Washington D.C. USA. 2000.
- R.B. Anderson, A.J. Eriksson, Lightning parameters for engineering application, *Electra* 69 (1980), 65–102
- Antonioni G, Spadoni G, Cozzani V. A methodology for the quantitative risk assessment of major accidents triggered by seismic events. *J. Hazard. Mater.* 2007;147:48–59.
- Antonioni G, Bonvicini S, Spadoni G, Cozzani V. Development of a frame work for the risk assessment of Na-Tech accidental events. *Reliability Eng. & Syst. Saf.* 2009;94:1442–50.
- Argyropoulos CD, Christolis MN, Nivolianitou Z, Markatos NC. A hazards assessment methodology for large liquid hydrocarbon fuel tanks. *J. of Loss Prev. Process Ind.* 2012; 25:329-335
- Borghetti A, Nucci CA, Paolone M. An Improved Procedure for the Assessment of Overhead Line Indirect Lightning Performance and Its Comparison with the IEEE Std. 1410 Method. *IEEE Transactions On Power Delivery.* 2007; 22, 1, 684-692.
- Borghetti A, Cozzani V, Mazzetti C, Nucci CA, Paolone M, Renzi E. Monte Carlo based lightning risk assessment in oil plant tank farms. In *Proceedings of 30th International Conference on Lightning Protection, Cagliari: ICLP; 2010;1497:1-7.*
- Busini V, Marzo E, Callioni A, Rota R. Definition of a short-cut methodology for assessing earthquake-related Na-Tech risk. *J. Hazard. Mater.* 2011;192:329–39.
- Cadwallader LC. Idaho National Engineering Laboratory. Fire Protection System Operating Experience Review for Fusion Application. INEL-95/0396 1995.
- Carpenter, R.B. *Lightning Protection for Flammables Storage Facilities.* (1996) Lightning Eliminators, Consultants, Boulder, CO, USA (1996)
- Chang JI, Lin C. A study of storage tank accidents. *J. Loss Prev. Process Ind.* 2006; 19: 51–59.
- Cigré Working Group C4.407 Lightning parameters for engineering applications Cigré Technical Brochure, Paris (2013)
- Comitato Elettrotecnico Italiano CEI, EN 62305, Protection against lightning, Comitato Elettrotecnico Italiano, Milan (2013)
- V. Cooray, M. Becerra, Attachment of lightning flashes to grounded structures V. Cooray (Ed.), *Lightning protection*, IET, London (UK) (2010) Lightning Eliminators, Consultants Boulder, CO, USA
- Cozzani, V., M. Campedel, E. Renzi, and E. Krausmann. 2010. Industrial accidents triggered by flood events: analysis of past accidents. *Journal of Hazardous Materials* 175: 501–9.

- V. Cozzani, G. Antonioni, G. Landucci, A. Tugnoli, S. Bonvicini, G. Spadoni, Quantitative assessment of domino and NaTech scenarios in complex industrial areas, *J Loss Prev Process Ind*, 28 (2014), 10–22
- Council Directive 67/548/EEC of 27 June 1967 on the approximation of laws, regulations and administrative provisions relating to the classification, packaging and labelling of dangerous substances, *Off. J. Eur. Commun.* L196 (1967).
- Council Directive 96/82/EC of 9 December 1996 on the control of major-accident hazards involving dangerous substances, *Off. J. Eur. Commun.* (1997) L10.
- Cruz AM, Okada N. Consideration of natural hazards in the design and risk management of industrial facilities. *Nat. Hazards* 2008a;44:213–27.
- Cruz AM, Okada N. Methodology for preliminary assessment of Natech risk in urban areas. *Nat. Hazards* 2008b;46:199–220.
- Delvosalle C, Fievez C, Pipart A, Debray B. ARAMIS project: a comprehensive methodology for the identification of reference accident scenarios in process industries. *J. Hazard. Mater.* 2006; 130:200–219.
- Det Norske Veritas. Offshore Reliability Data OREDA. 3 edition. Høvik. Norway. 1997.
- Di Bitonto DD, Eubank PT, Patel MR, Barrufet MA. Theoretical models of the electrical discharge machining process. I. A simple cathode erosion model. *J. Appl. Phys.* 1989; 66:4095–4103.
- Di Padova A, Tugnoli A, Cozzani V, Barbaresi T, Tallone F, 2011, Identification of fireproofing zones in Oil&Gas facilities by a risk-based procedure, *Journal of Hazardous Materials* 2012; 191:83–93.
- Directive 1999/45/EC of the European Parliament and of the Council of 31 May 1999 concerning the approximation of the laws, regulations and administrative provisions of the Member States relating to the classification, packaging and labelling of dangerous preparations, *Off. J. Eur. Commun.* (1999) L200/1.
- Directive 96/82/EC, Council Directive 96/82/EC of 9 December 1996 on the Control of Major-Accident Hazards Involving Dangerous Substances. *Official Journal of the European Communities*, L 10/13, Brussels, 14.1.97.
- Directive 2012/18/EU, European Parliament and Council Directive 2012/18/EU of 4 July 2012 on Control of Major-Accident Hazards Involving Dangerous Substances, Amending and Subsequently Repealing Council Directive 96/82/EC. *Official Journal of the European Communities*, L 197/1, Brussels, 24.7.2012
- Egidi, D., Foraboschi, F. P., Spadoni, G., & Amendola, A. (1995). The ARIPAR project: analysis of the major accident risks connected with industrial and transportation activities in the Ravenna area. *Reliability Engineering & System Safety*, 49(1), 75–89.
- French Ministry of Ecology and Sustainable Development, Analyse, Recherche, et Information sur les Accidents (ARIA) , <http://www.aria.developpement-durable.gouv.fr/> (accessed 2006).
- González D, Noack F. Perforation of metal sheets due to lightning arcs. In: *Proceedings of 29th International Conference on Lightning Protection*, Uppsala: ICLP, 2008; p.84:1–14.
- González D, Noack F, Berger F, Rock M. Perforation of metal sheets due to lightning arcs. In: *Proceedings 28th International Conference on Lightning Protection*, Kanazawa: ICLP, 2006; p.1223–1228.
- Green DW, Perry RH (Eds.), *Perry's Chemical Engineers' Handbook*, 8th ed., New York: McGraw-Hill; 2008.
- Gubinelli, G., & Cozzani, V. (2009b). The assessment of missile hazard: evaluation of fragment number and drag factors. *Journal of Hazardous Materials*, 161, 439–449.
- IAEA, *Thermophysical Properties of Materials for Nuclear Engineering: A Tutorial and Collection of Data*. Vienna: International Atomic Energy Agency Vienna; 2008.
- International Electrotechnical Commission. IEC Std 61508—Functional safety of electrical/electronic/programmable electronic safety-related systems; 1998.

- International Electrotechnical Commission. IEC Std 61508 Annex D: Determination of safety integrity levels—a qualitative method: risk graph; 1998.
- Institution of Chemical Engineers (IChemE). The Accident Database (TAD), version 4.1. United Kingdom. 2004.
- International Electrotechnical Commission (IEC), IEC standard 62305-1 - Protection against lightning: General Principles. Technical Committee TC 81 of IEC. Geneva. 2003.
- Krausmann, E., V. Cozzani, E. Salzano, and E. Renni. 2011. Industrial accidents triggered by natural hazards: An emerging risk issue. *Natural Hazards and Earth System Sciences* 11: 921–9.
- Krausmann, E., A.M. Cruz, and B. Affeltranger. 2010. The impact of the 12 May 2008 Wenchuan earthquake on industrial facilities. *Journal of Loss Prevention Process Industries* 23: 242–8.
- Krausmann, E., E. Renni, M. Campedel, and V. Cozzani. 2011. Industrial accidents triggered by earthquakes, floods and lightning: Lessons learned from a database analysis. *Natural Hazards* 59: 285–300.
- Lancaster J.F. *The Physics of Welding*, Oxford: Pergamon Press; 1986.
- G. Landucci, G. Gubinelli, G. Antonioni, V. Cozzani, The assessment of the damage probability of storage tanks in domino events triggered by fire, *Accident Anal. Prev.* 41 (6) (2009) 1206–1215.
- Landucci G, Antonioni G, Tugnoli A, Cozzani V. Release of hazardous substances in flood events: Damage model for atmospheric storage tanks. *Reliability Eng. & Syst. Saf.* 2012; 106:200-216.
- Landucci, G., Necci, A., Antonioni, G., Tugnoli, A., Cozzani, V., Release of hazardous substances in flood events: Damage model for horizontal cylindrical vessels, *Reliability Engineering and System Safety* 132, (2014) 125-145
- Lanzano G, Salzano E, De Magistris FS, Fabbrocino G. Seismic vulnerability of natural gas pipelines. *Reliability Eng. & Syst. Saf.* 2013;117:73-80
- "LASTFIRE - Large Atmospheric Storage Tank Fires", Resource Protection International, 1997
- Lees FP. *Loss Prevention in the Process Industries*. 2nd ed. Butterworth-Heinemann. Oxford (UK). 1996.
- E.R. Love, Improvements on lightning stroke modeling and applications to the design of EHV and UHV transmission lines [M.Sc. dissertation]
- Mannan, S., 2005. *Lees' Loss Prevention in the Process Industries*, third ed. Elsevier, Oxford, UK.
- Metwally IA, Heidler F, Zieschank W. Measurement of the rear-face temperature of metals struck by lightning long-duration currents, *European Transactions on Electrical Power* 2003; 14:201–222.
- Milazzo MF, Ancione G, Basco A, Lister DG, Salzano E, Maschio G. Potential loading damage to industrial storage tanks due to volcanic ash fallout. *Nat. Hazards* 2013;66(2):939-953.
- National Fire Protection Association. NFPA 780 - Standard for the Installation of Lightning Protection Systems. 2004 Ed. Quincy USA. 2004.
- National Fire Protection Association. NFPA 69 - Standard on Explosion Prevention Systems. Quincy USA. 2008.
- Necci A, Antonioni G, Cozzani V, Krausmann E, Borghetti A, Nucci CA. A model for process equipment damage probability assessment due to lightning. *Reliability Eng. & Syst. Saf.* 2013; 115:91–99.
- Necci A, Antonioni G, Cozzani V, Borghetti A, Nucci CA. Reduction of NaTech risk due to lightning by the use of protection systems. *Chem. Eng. Transactions* 2013;31:763-768 DOI: 10.3303/CET1331128
- Necci, A., Antonioni, G., Cozzani, V., Krausmann, E., Borghetti, A., Nucci, C.A., Assessment of lightning impact frequency for process equipment, *Reliability Engineering and System Safety* 130, 2014, 95-105

- Necci, A., Argenti, F., Landucci, G., Cozzani, V., Document Accident scenarios triggered by lightning strike on atmospheric storage tanks, *Reliability Engineering and System Safety* 127, 2014b, 30-46
- Necci, A., Antonioni, G., Cozzani, V., Borghetti, A., Nucci, C.A., Quantification of risk reduction due to the installation of different lightning protection solutions for large atmospheric storage tanks, *Chemical Engineering Transactions* 36, 2014c, 481-486
- Nucci CA, Rachidi F. Interaction of electromagnetic fields with electrical networks generated by lightning. In: Cooray V. (ed.), *The Lightning Flash*, IEE Power and Energy series 34: 425-478. The Institution of Electrical Engineers. London. 2003.
- Oil Industry Safety Directorate. OISD - GDN-180- Lightning protection. OISD. New Delhi. 1999
- Oil Industry Safety Directorate. OISD STD 116 - Fire Protection Facilities for Petroleum Refineries and Oil/Gas Processing Plants. Committee for Fire Protection. New Delhi. 2007.
- Persson H, Lönnermark A. Tank Fires: review of fire incidents 1951-2003, SP REPORT 2004:14. Swedish National Testing and Research Institute. Sweden. 2004.
- Porta M, Indagine teorico-sperimentale sui metodi di taglio della carcassa di una lavatrice, Master Thesis in Management Engineering, University of Pisa, Pisa, Italy, 2003
- Rasmussen K. Natural events and accidents with hazardous materials. *J. Hazard. Mater.* 1995; 40:43-54.
- Renni E, Krausmann E, Cozzani V. Industrial accidents triggered by lightning. *J. Hazard. Mater.* 2010; 184:42-8
- Rupke E. *Lightning Direct Effects Handbook*, 1-031027-043-Design Guideline. Lightning Technologies Inc. Pittsfield, MA. 2002.
- Salzano E, Iervolino I, Fabbrocino G. Seismic risk of atmospheric storage tanks in the framework of quantitative risk analysis. *J. Loss Prev. Process Ind.* 2003;16:403-9.
- Salzano E, Garcia Agreda A, Di Carluccio A, Fabbrocino G. Risk assessment and early warning systems for industrial facilities in seismic zones. *Reliability Eng. & Syst. Saf.* 2009;94:1577-84.
- Salzano E, Basco A, Busini V, Cozzani V, Renni E, Rota R. Public awareness promoting new or emerging risks: Industrial accidents triggered by natural hazards (NaTech). *J. Risk Res.* 2013; 16 (3-4):469-485.
- Schüller JCH, Brinknam JL, Van Gestel PJ, Van Otterloo RW. *Methods for determining and processing probabilities (Red Book)*. Committee for the Prevention of Disasters. The Hague The Netherlands. 1997.
- Sengupta A, Gupta AK, Mishra IM. Engineering layout of fuel tanks in a tank farm. *J. Loss Prev. Process Ind.* 2011; 24: 568-574.
- SIRF 2013 lightning detection data, (http://www.fulmini.it/about_sirf/default.htm) ; 1996 - 2013 [last accessed 25.11.13].
- Sueta HE, Burani GF, Leite DM, Grimoni JA. Experimental verifications on the use of natural components of structures as part of a LPS. In: *Proceedings 28th International Conference on Lightning Protection*, Kanazawa: ICLP, Japan, 2006.
- Gubinelli, G., & Cozzani, V. (2009a). Assessment of missile hazard: reference fragmentation patterns of process equipment. *Journal of Hazardous Materials*, 163, 1008-1018.
- Uijt de Haag PAM, Ale BJM. *Guidelines for Quantitative Risk Assessment (Purple Book)*. Committee for the Prevention of Disasters. The Hague The Netherlands. 1999.
- United States National Response Center (NRC) Database, United States Coast Guard, <http://www.nrc.uscg.mil/nrchp.html> (accessed 2008).
- Univ. Colorado, Denver, CO, USA (1973) Health and Safety Executive. Major Hazard Incident Data Service (MHIDAS). United Kingdom. 2001.

- Young, S. (2002) 'Natural-technologic events: the frequency and severity of toxic releases during and after natural disasters with emphasis on wind and seismic events'. Paper presented at the UJNR (US–Japan Cooperative Program in Natural Resources) 34th joint meeting panel on wind and seismic effects, Gaithersburg, MD, 13–18 May.
- Young, S., L. Balluz and J. Malilay (2004) 'Natural and technologic hazardous material releases during and after natural disasters: a review'. *Science of the Total Environment*. 322(1–3). pp. 3–20.

Chapter 5:

Development of fragility models for risk assessment of Natech due to floods

5.1 Introduction

As showed in Section 3.3.4, in order to allow the QRA of NaTech events, a key point is the definition of equipment vulnerability models, that should allow the estimation of equipment damage probability on the basis of severity or intensity parameters of the flood event. A typical QRA study usually requires the assessment of a huge number of accidental scenarios. For this reason, risk analysts demand for simplified models and correlations able to yield a conservative estimation of equipment failure conditions, allowing the assessment of Natech scenario frequencies. Fragility curves and equipment vulnerability models have been specifically built for several industrial equipment items in the case of earthquake (Salzano et al., 2003; Fabbrocino et al., 2005; Iervolino et al., 2004), while simplified damage models for flood scenarios were available only for generic structures until a few years ago.

In a recent study, equipment vulnerability models were obtained for atmospheric vertical cylindrical storage tanks in the case of flood scenarios (Landucci et al., 2012). Specific fragility models for equipment vulnerability in the case of flood are thus not available for horizontal cylindrical storage tanks. Past accident data analysis (Cozzani et al., 2010) evidenced that these equipment items were often damaged in NaTech events triggered by floods. However, horizontal vessels are usually positioned on saddles or, more in general, are welded to supports anchored to the ground. For this reason flooding damage occurs by different mechanisms with respect to vertical cylindrical tanks, thus different damage models are required for this equipment typology. Actually, horizontal cylindrical vessels are mostly damaged due to displacement caused by water drag and/or to floating (Cozzani et al., 2010; Campedel, 2008), instead of instability, which on the contrary is the main damage mechanism for vertical atmospheric vessels (Landucci et al., 2012). For these reasons, one of the activities carried out within the present PhD project was the development of dedicated fragility models for horizontal storage tanks. In this chapter, the development of a model for the vulnerability assessment of horizontal cylindrical process and storage vessels involved in flood events is shown. In order to evaluate the resistance of the equipment items considered, a mechanical model was developed. The model, validated with respect to the available data obtained from past accident records, was applied to derive simplified vulnerability functions to calculate vessel failure probability in flood events. In order to explore the model features and potentialities. Finally, some case studies based on actual industrial lay-outs were analyzed.

5.2 Modelling the equipment damage due to flood events

The approach proposed to assess the vulnerability of equipment items involved in flood events is schematized in Fig. 5.1. The procedure follows the key steps of an analogous methodology developed for cylindrical vertical storage tank (Landucci et al., 2012) however considering the specific features of horizontal vessels.

As shown in Fig. 5.1, in the first step of model a simplified vessel and saddle geometry was represented. In step 2, on the basis of this schematization, a mechanical model was developed, able to assess the effects of floodwater impact on the vessel. In particular, two main damage modalities are possible in the case of horizontal vessels: damages caused by the displacement of vessels due to water drag and/or to floating, leading to the rupture of the connected pipelines and damage caused by a potential impact on the other equipment items or structures. Hence, on the basis of available data on past flooding events (New South Wales Government, 2005; Dutch Ministry of Infrastructure and Environment, 2005), the flood water impact was schematized considering a credible range of values for flood water depth and velocity (step 3). Reference data from past accidents caused by events were then used for model validation (step 4). In step 5, a vessel database was developed, obtained from actual data retrieved at industrial facilities and from current design standards. Either pressurized vessels (defined as vessels operating at pressures higher than 103.4 kPa (ASME, 1989) and atmospheric vessels were included in the database. A dataset of vessel failure conditions with respect to flood intensity parameters was obtained applying the mechanical model to the entire vessel database (step 5). In step 6, the simplified damage correlations, which relate the vessel geometry with the flood wave intensity parameters and used for the assessment of vessel failure probability, have been obtained by the dataset of failure conditions obtained in step 5 (step 7).

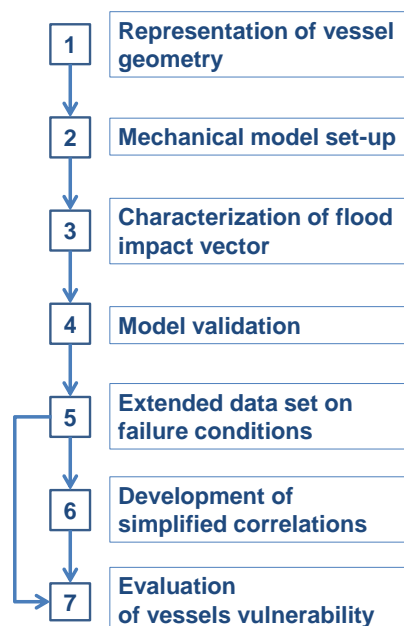


Figure 5.1: Schematization of the methodological approach adopted for the development of a vulnerability model for horizontal vessels involved in flood events. (Landucci et al., 2014)

Table 5.1: Vessel database considered in the present study: main features of tanks (see Fig. 5.2).

P_d = design pressure; ATM = operating at atmospheric pressure.

ID	P_d (MPa)	Capacity (m ³)	Dimensions (mm)		t	l_1	l_2	l_3	S_1	S_2
			D	L						
1	ATM	5	1600	3000	5	800	980	2200	140	1240
2	ATM	5	1300	3500	5	650	780	2850	140	900
3	ATM	5	1000	6100	5	500	680	5600	95	780
4	ATM	10	1600	4500	5	800	980	3700	140	1240
5	ATM	10	1200	7700	5	600	780	7100	140	900
6	ATM	15	1800	5500	5	900	1080	4600	140	1420
7	ATM	20	1500	9700	6	750	880	8950	140	1060
8	ATM	20	2000	6000	6	1000	1180	5000	140	1600
9	ATM	20	1900	7200	6	950	1080	6250	140	1420
10	ATM	25	1700	10500	6	850	980	9650	140	1240
11	ATM	25	2200	6000	6	1100	1280	4900	150	1780
12	ATM	25	2300	7000	6	1150	1280	5850	150	1780
13	ATM	30	2400	6500	6	1200	1380	5300	150	1960
14	ATM	30	1900	11100	6	950	1080	10150	140	1420
15	ATM	50	2100	13200	6	1050	1180	12150	140	1600
16	ATM	50	2800	8000	6	1400	1580	6600	150	2200
17	ATM	50	2700	10000	6	1350	1480	8650	150	2060
18	ATM	50	2500	10400	6	1250	1380	9150	150	1960
19	ATM	100	3200	12000	6	1600	1780	10400	150	2520
20	ATM	100	3200	13700	6	1600	1780	12100	150	2520
21	ATM	100	2800	18000	6	1400	1580	16600	150	2200
22	ATM	115	2750	20100	6	1375	1580	18725	150	2200
23	ATM	150	3200	19400	6	1600	1780	17800	150	2520
24	ATM	250	3800	24000	6	1900	1980	22100	150	2800
25	1.5	5	1600	3000	11	800	980	2200	140	1240
26	1.5	5	1300	3500	9	650	780	2850	140	900
27	1.5	5	1000	6100	7	500	680	5600	95	780
28	1.5	10	1600	4500	11	800	980	3700	140	1240
29	1.5	10	1200	7700	8	600	780	7100	140	900
30	1.5	15	1800	5500	12	900	1080	4600	140	1420
31	1.5	20	1500	9700	10	750	880	8950	140	1060
32	1.5	20	2000	6000	13	1000	1180	5000	140	1600
33	1.5	20	1900	7200	12	950	1080	6250	140	1420
34	1.5	25	1700	10500	11	850	980	9650	140	1240
35	1.5	25	2200	6000	14	1100	1280	4900	150	1780
36	1.5	25	2300	7000	15	1150	1280	5850	150	1780
37	1.5	30	2400	6500	16	1200	1380	5300	150	1960
38	1.5	30	1900	11100	12	950	1080	10150	140	1420
39	1.5	50	2100	13200	14	1050	1180	12150	140	1600
40	1.5	50	2800	8000	18	1400	1580	6600	150	2200
41	1.5	50	2700	10000	17	1350	1480	8650	150	2060
42	1.5	50	2500	10400	16	1250	1380	9150	150	1960
43	1.5	100	3200	12000	21	1600	1780	10400	150	2520
44	1.5	100	3200	13700	21	1600	1780	12100	150	2520
45	1.5	100	2800	18000	18	1400	1580	16600	150	2200
46	1.5	115	2750	20100	18	1375	1580	18725	150	2200
47	1.5	150	3200	19400	21	1600	1780	17800	150	2520
48	1.5	250	3800	24000	24	1900	1980	22100	150	2800
49	2	5	1600	3000	14	800	980	2200	140	1240
50	2	5	1300	3500	11	650	780	2850	140	900
51	2	5	1000	6100	9	500	680	5600	95	780
52	2	10	1600	4500	14	800	980	3700	140	1240
53	2	10	1200	7700	11	600	780	7100	140	900
54	2	15	1800	5500	16	900	1080	4600	140	1420
55	2	20	1500	9700	13	750	880	8950	140	1060
56	2	20	2000	6000	17	1000	1180	5000	140	1600
57	2	20	1900	7200	16	950	1080	6250	140	1420
58	2	25	1700	10500	15	850	980	9650	140	1240
59	2	25	2200	6000	19	1100	1280	4900	150	1780
60	2	25	2300	7000	20	1150	1280	5850	150	1780
61	2	30	2400	6500	21	1200	1380	5300	150	1960
62	2	30	1900	11100	16	950	1080	10150	140	1420
63	2	50	2100	13200	18	1050	1180	12150	140	1600
64	2	50	2800	8000	24	1400	1580	6600	150	2200
65	2	50	2700	10000	23	1350	1480	8650	150	2060
66	2	50	2500	10400	22	1250	1380	9150	150	1960
67	2	100	3200	12000	27	1600	1780	10400	150	2520
68	2	100	3200	13700	27	1600	1780	12100	150	2520
69	2	100	2800	18000	24	1400	1580	16600	150	2200
70	2	115	2750	20100	24	1375	1580	18725	150	2200
71	2	150	3200	19400	27	1600	1780	17800	150	2520
72	2	250	3800	24000	32	1900	1980	22100	150	2800
73	2.5	5	1600	3000	17	800	980	2200	140	1240
74	2.5	5	1300	3500	14	650	780	2850	140	900
75	2.5	5	1000	6100	11	500	680	5600	95	780
76	2.5	10	1600	4500	17	800	980	3700	140	1240
77	2.5	10	1200	7700	13	600	780	7100	140	900
78	2.5	15	1800	5500	19	900	1080	4600	140	1420
79	2.5	20	1500	9700	16	750	880	8950	140	1060
80	2.5	20	2000	6000	22	1000	1180	5000	140	1600
81	2.5	20	1900	7200	20	950	1080	6250	140	1420
82	2.5	25	1700	10500	18	850	980	9650	140	1240
83	2.5	25	2200	6000	24	1100	1280	4900	150	1780
84	2.5	25	2300	7000	25	1150	1280	5850	150	1780
85	2.5	30	2400	6500	26	1200	1380	5300	150	1960
86	2.5	30	1900	11100	20	950	1080	10150	140	1420
87	2.5	50	2100	13200	23	1050	1180	12150	140	1600
88	2.5	50	2800	8000	30	1400	1580	6600	150	2200
89	2.5	50	2700	10000	29	1350	1480	8650	150	2060
90	2.5	50	2500	10400	27	1250	1380	9150	150	1960
91	2.5	100	3200	12000	34	1600	1780	10400	150	2520
92	2.5	100	3200	13700	34	1600	1780	12100	150	2520
93	2.5	100	2800	18000	30	1400	1580	16600	150	2200
94	2.5	115	2750	20100	29	1375	1580	18725	150	2200
95	2.5	150	3200	19400	34	1600	1780	17800	150	2520
96	2.5	250	3800	24000	40	1900	1980	22100	150	2800

5.2.1 Representation of vessel geometry (step 1)

In the present study, storage tanks have been schematized using a simplified geometry consisting of a horizontal cylindrical body with spherical edges. The vessels were assumed as disposed on saddle-type supports, fixed to the ground by bolt connections. The references for the design and features of the tanks considered in the present study are the API Standard 620 (API, 2002) and the ASME Pressure Vessel Code (Sec. VIII of the ASME Boiler and Pressure Vessel Code (ASME, 1989)). Fig. 5.2a reports a schematic representation of the vessel geometry, while the relevant mechanical features considered are summarized in Table 1. As shown in Fig. 5.2a, one of the vessel saddles is assumed to be fixed to the ground with a bolt connection, while the other assumed to be only laid on the ground. This configuration is frequently adopted in the process industry in order to limit the stress due to steelwork thermal expansion (Sinnott, 1999). Fig. 5.2c shows in detail the schematization of the saddle base plate bolt connection to the ground assumed in the present analysis.

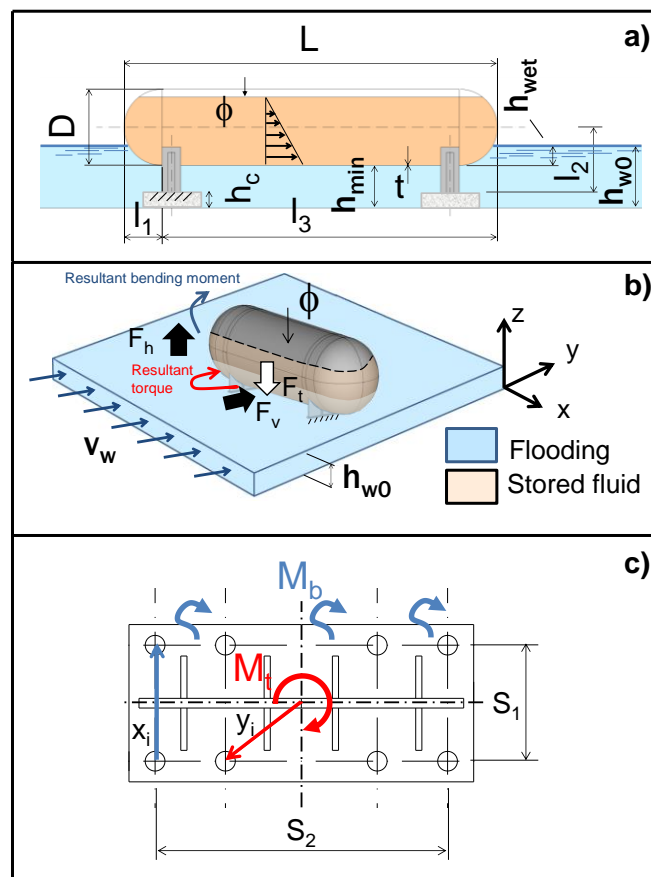


Figure 5.2: Schematization adopted to describe the impact of floodwater on horizontal vessels: a) definition of geometrical parameters and sketch of the vessel; b) force balance on the vessel and schematization of the wave impact; c) schematization of the base plate bolt connection to the ground.

5.2.2 Mechanical model set-up (step 2)

Flooding may cause damages to equipment or structures due to the pressure associated to both water speed (v_w) and water effective depth (h_w). In the case of atmospheric vertical cylindrical failures comes mainly as a consequence of buckling due to water external pressure due to flood events (Cozzani et al., 2010; Landucci et al., 2012; Campedel, 2005).

Horizontal cylindrical vessels are likely to experience different failure mechanisms in flood events: due to their smaller size and higher resistance they are more likely to be displaced than to experience bulking. The analysis of past accidents involving flooding in industrial facilities (Cozzani et al., 2010; Campedel, 2005) evidenced that failure caused by buckling was never experienced for horizontal vessels. Actually, horizontal cylindrical vessels, either atmospheric or pressurized, have a higher resistance to buckling if compared to vertical cylindrical storage tanks. Moreover, the analysis of past accidents evidenced that this category of vessels is more prone to undergo failures due to displacement in flood events. In particular, the rupture of the saddle framework and of its connection to the ground was experienced in several cases. The consequences of a displaced floating vessel are the rupture of the vessel pipe connections and, in some cases, in the impact of the displaced vessel with adjacent vessels or structures (U.S. Army Corps of Engineers, 1993; Grunfest et al., 1994).

Therefore, the mechanical model was developed focusing on the integrity of the saddle-type support, that is the element required to fail in the case of vessel displacement caused by flood water. In particular, the resistance of the saddle connection to the ground under load conditions caused by floodwater was investigated. Table 5.2 summarizes the procedure applied for the evaluation of the framework connection resistance to the flood water load.

Table 5.2a: Summary of input parameters implemented in the present. study DB: derived from the database provided in Table 1, CALC: parameter calculated on the basis of input data. (Landucci et al., 2014)

Operation	ID	Item	Description / Definition	Value	Units
1) Selection of input parameters: characterization of the equipment and storage system	1.1x	P_d	Design pressure of the vessel	0.01 ^a -2.5	MPa
	1.2x	D	Storage vessel external diameter	DB	m
	1.3x	L	Storage vessel length (end to end)	DB	m
	1.4x	t	Minimum thickness of the vessel wall	DB	m
	1.5x	l_1	Distance of the saddle from the vessel edge (Fig. 5.2a)	DB	m
	1.6x	l_3	Distance between the anchored saddle and the opposite vessel end (See Fig. 5.2a)	DB	m
	1.7x	ϕ	Operative filling level defined as the fraction of liquid volume respect to the total vessel inner volume	$\phi_{min} - \phi_{max}$	-
	1.8x	ϕ_{min}	Minimum operative filling level	0.01	-
	1.9x	ϕ_{max}	Maximum operative filling level	0.9	-
	1.10x	T_{st}	Storage temperature (ambient temperature)	300	K
	1.11x	P_{st}	Storage pressure. $P_{st} = 0.01$ barg for atmospheric tanks, $P_{st} =$ vapour pressure of stored liquid evaluated at T_{st} for pressurized vessels.	CALC	Pa
	1.12x	ρ_l	Density of stored liquid phase	500 - 1500	kg/m ³
	1.13x	ρ_v	Density of vapor phase in the top space of the vessel $\rho_v = (P_{st} M_w) / (Z R T_{st})$ where Z is the compressibility factor and M_w the vapor molecular weight (Liley et al., 1999)	CALC ^a	kg/m ³
	1.14x	ρ_s	Density of steel (vessel construction material)	7800	kg/m ³
	1.15x	ρ_{ref}	Density of the reference substance used for the definition of CFL correlations (see steps 5.3x and 5.4x)	1000	kg/m ³
	1.16x	V_{ext}	Vessel external volume (assuming spherical edges): $V_{ext} = \pi \frac{D^2}{4} (L - D) + \frac{D^3}{6}$	CALC	m ³
	1.17x	V_{int}	Vessel internal volume (assuming spherical edges): $V_{int} = \pi \frac{(D - 2t)^2}{4} (L - D) + \frac{(D - 2t)^3}{6}$	CALC	m ³
	1.18x	W_t	Vessel tare weight. If no data are available for the vessel under analysis this simplified evaluation can be used $W_t = \rho_s (V_{ext} - V_{int})$	Given or CALC	kg
2) Selection of input parameters: characterization of the equipment framework	2.1x	l_2	Saddle height parameter (Fig. 5.2a) which indicates the vessel axis height respect to the ground anchorage point	DB	m
	2.2x	S_1	Saddle width on the vessel axis (Fig. 5.2c)	DB	m
	2.3x	S_2	Transversal saddle width (Fig. 5.2c)	DB	m
	2.4x	h_c	Base parameter (Fig. 5.2a)	0.3 ^b	m
	2.5x	A_{res}	Resistance area of the bolt	157 ^c	mm ²
	2.6x	n_b	Number of bolts in the base plate connection	4-10	-
	2.7x	$f_{d,N}$	Normal design stress	560 ^c	MPa
	2.8x	$f_{d,S}$	Tangential design stress	396 ^c	MPa
	2.9x	$\sigma_{b,adm}$	Normal admissible stress	373 ^c	MPa
	2.10x	$\tau_{b,adm}$	Tangential admissible stress	264 ^c	MPa
3) Selection of input parameters: characterization of the flooding scenario	3.1x	h_{w0}	Actual depth of flood water over the ground level	0 - 4 ^d	m
	3.2x	h_w	Effective flooding depth given by $h_w = h_{w0} - h_c$	CALC	m
	3.3x	h_{min}	$h_{min} = l_2 - D/2$ minimum flooding height able to wet the vessel surface	CALC	m
	3.4x	h_{wet}	Wetting height, representing the height of the vessel wetted by flood	CALC	m
	3.5x	v_w	Velocity of flood water	0 - 3.5 ^d	m/s
	3.6x	ρ_w	Density of flood water	1100	kg/m ³
	3.7x	k_w	Flood hydrodynamic coefficient	1.8	-
	3.8x	t_r	Return period	10 - 500	y
	3.9x	f	Expected frequency of the flooding scenario	10 ⁻³ - 10 ⁻²	y ⁻¹
	3.10x	η	Geometrical parameter defined as follows: $\eta = \min [h_{min}; D]$	CALC	m
3.11x	ω	Vessel submerged fraction: $\omega = \min \left[\frac{L}{V_{ext}} \left(\frac{\pi}{8} D^2 + \frac{D^2}{4} \arcsin \left(\frac{2\eta - D}{D} \right) + \frac{2\eta - D}{2} \sqrt{2\eta D - \eta^2} \right); 1 \right]$	CALC	-	

- Saturation pressure data were derived from Liley et al., (1999).
- Assumed for the case study in Section 3.4
- Value selected for the present study. Other possible values may be inserted by the user according to Tables 3 and 4.
- Range assumed for the preparation of failure charts reported in Appendix (Figures A1-A4).

Table 5.2b: Summary of input parameters implemented in the present. DB: derived from the database provided in Table 5.1, CALC: parameter calculated on the basis of input data. (Landucci et al., 2014)

Operation	ID	Item	Description / Definition	Value	Units
4) Evaluation of vessel resistance with the mechanical model	4.1x	F_n	Buoyancy due to the flooding (Fig. 2b): $F_n = F_b - F_t = \omega V_{ext} \rho_w g - g(W_t + \phi V_{int} \rho_t + (1 - \phi) V_{int} \rho_v)$	CALC	N
	4.2x	$F_{n,b}$	Portion of the normal force on each bolt: $F_{n,b} = F_n / n_b$	CALC	N
	4.3x	M_b	Bending moment due to lift action (Fig. 2b): $M_b = \frac{1}{2} F_n l_3$	CALC	Nm
	4.4x	x_i	Distance from the "neutral axis" on which M_b is applied	-	m
	4.5x	$F_{x,i}$	Resultant normal force on each bolt due to the bending moment: $F_{x,i} = x_i \cdot M_b / \sum_{i=1}^{n_b} x_i^2$	CALC	N
	4.6x	$N_{tot,i}$	Overall normal force acting on each single bolt: $N_{tot,i} = F_{n,b} + F_{x,i}$	CALC	N
	4.7x	A_{ext}	External surface of the vessel wetted by the flooding (Fig. 2b): $A_{ext} = (L - 2l_1)\eta + \left(\frac{\pi}{8} D^2 + \frac{D^2}{4} \arcsin\left(\frac{2\eta - D}{D}\right) + \frac{2\eta - D}{2} \sqrt{2\eta D - \eta^2}\right)$	CALC	m ²
	4.8x	F_v	Drag force due to flooding (Fig. 2b): $F_v = \frac{1}{2} \rho_w k_w v_w^2 A_{ext}$	CALC	N
	4.9x	$F_{v,b}$	Portion of the drag force on each bolt: $F_{v,b} = F_v / n_b$	CALC	N
	4.10x	M_t	Torque due to drag force (Fig. 2b): $M_t = \frac{1}{2} F_v l_3$	CALC	Nm
	4.11x	y_i	Distance from the "neutral axis" on which M_t is applied	-	m
	4.12x	$F_{y,i}$	Resultant shear force on each bolt due to the torque action: $F_{y,i} = y_i \cdot M_t / \sum_{i=1}^{n_b} y_i^2$	CALC	N
	4.13x	$S_{tot,i}$	Overall shear force acting on each single bolt: $S_{tot,i} = F_{v,b} + F_{y,i}$	CALC	N
	4.14x	σ_i	Overall normal stress acting on the i-th bolt: $\sigma_i = N_{tot,i} / A_{res}$	CALC	MPa
	4.15x	τ_i	Overall shear stress acting on the i-th bolt: $\tau_i = S_{tot,i} / A_{res}$	CALC	MPa
	4.16x	FC1	Failure criterion FC1 for the i-th bolt: $\left(\frac{\sigma_i}{\sigma_{b,adm}}\right)^2 + \left(\frac{\tau_i}{\tau_{b,adm}}\right)^2 > 1$	-	-
	4.17x	FC2	Failure criterion FC2 for the i-th bolt: $\left(\frac{\sigma_i}{f_{d,N}}\right)^2 + \left(\frac{\tau_i}{f_{d,S}}\right)^2 > 1$	-	-
	4.18x	CFL	Critical filling level for a given storage system and assigned storage conditions. Repeat steps 4.1 to 4.18 in order to find the minimum ϕ which allows satisfying one of the two failure criteria (FC1 or FC2)	CALC	-
	4.19x	$v_{w,c}$	Critical velocity related to a specific vessel. Given an assigned flooding height h_w , repeat steps 4.8 to 4.18 in order to find the minimum v_w value which allows satisfying one of the two failure criteria (FC1 or FC2)	CALC	m/s
5) Evaluation of vessel resistance with correlations	5.1x	A	First CFL correlation coefficient evaluated for reference substance: $A = K_1 \cdot D^a$ where K_1, a are shown in Table 6	CALC	-
	5.2x	B	Second CFL correlation coefficient evaluated for reference substance: $B = K_2 (W_t + K_3)^b$ where K_2, K_3, b are shown in Table 6:	CALC	-
	5.3x	A'	Modified A coefficient considering a generic stored substance: $A' = (\rho_{ref} \cdot A) / (\rho_t - \rho_v)$	CALC	-
	5.4x	B'	Modified B coefficient considering a generic stored substance: $B' = (\rho_{ref} \cdot B - \rho_v) / (\rho_t - \rho_v)$	CALC	-
	5.5x	E	$v_{w,c}$ correlation factor: $E = K_4 \cdot L^c$ where K_4, c are shown in Table 6	CALC	-
	5.6x	F	$v_{w,c}$ correlation exponent: $F = K_5 \ln(L/D) + K_6$ where K_5, K_6 are shown in Table 6	CALC	-
	5.7x	CFL	Critical filling level evaluated with correlations: $CFL = A' \cdot h_w + B'$	CALC	-
	5.8x	$v_{w,c}$	Critical velocity evaluated with correlations: $v_{w,c} = E \cdot (h_w - h_{min})^F$	CALC	m/s
6) Evaluation of parameters implemented in QRA studies	6.1ax	Ψ	Vessel failure probability evaluation based on critical velocity (see Fig. 7): $\Psi = 1$ if $v_w \geq v_{w,c}$	CALC	-
	6.1bx	Ψ	If $v_w < v_{w,c}$, vessel failure probability evaluation based on CFL (step 4.19 or 5.7, see Fig. 7): $\Psi = (CFL - \phi_{min}) / (\phi_{max} - \phi_{min})$	CALC	-
	6.2x	f_{LOC}	Expected frequency of loss of containment (LOC) $f_{LOC} = \Psi \times f$	CALC	y ⁻¹

The schematic representation of the floodwater impact on a horizontal cylindrical vessel is reported in Fig. 5.2b. As shown in the figure, the vessel is subject to the hydrostatic lift force (F_h in Fig. 5.2b), which causes a vertical lift action, and, at the same time, to a horizontal drag force caused by the flood wave (F_v in Fig. 5.2b). Buoyancy (F_n in Fig. 5.2b) is the net force obtained considering the opposite actions of hydrostatic lift and of overall weight force (F_t in Fig. 5.2b), resulting from vessel weight and from the weight of the fluid inside the vessel:

$$F_n = F_h - F_t \quad (5.1)$$

Buoyancy may thus be expressed as a function of vessel geometry, weight and filling level:

$$F_n = \omega V_{ext} \rho_w g - g(W_t + \phi V_{int} \rho_l + (1 - \phi) V_{int} \rho_v) \quad (5.2)$$

where g is the gravity constant (9.81 m/s^2), W_t is the “tare weight” of the tank (i.e. the mass of the empty tank in kg), ρ_l is the liquid average density, ρ_v is the average density of the vapor in the top space of the vessel, ρ_w is the density of floodwater, V_{int} and V_{ext} are the inner and outer vessel volume respectively, and ϕ is the vessel volumetric filling level defined as the fraction of liquid volume respect to the total vessel inner volume V_{int} . If the value of vessel weight, W_t , is not available, this parameter may be estimated as follows, assuming the value of steel density ρ_s :

$$W_t = \rho_s (V_{ext} - V_{int}) \quad (5.3)$$

The parameter ω in Eq. 5.2 is the fraction of the vessel volume wetted by flooding. Geometrical relationships summarized in Table 2, which take into account the effective depth h_w of flood water, and the height of the saddles, l_2 , may be used for the evaluation of ω . Further details on the calculation of ω are provided in Section 5.2.3.

The drag force due to the floodwater wave kinetic energy (F_v) may be calculated as follows (Tilton, 1999; Gudmestad and Moe, 1996):

$$F_v = \frac{1}{2} \rho_w k_w v_w^2 A_{ext} \quad (5.4)$$

where k_w is the hydrodynamic coefficient (Tilton, 1999; Gudmestad and Moe, 1996) and A_{ext} is the projected area of the vessel external surface impacted by flooding in a plane normal to water flow. In order to obtain a conservative evaluation for the drag force, the water flow is assumed to impact on the side of the vessel featured by a higher external surface (see Fig. 5.2b). Table 5.2 summarizes the procedure for the evaluation of A_{ext} in Eq. 5.2, based on the vessel geometrical features and on water depth at vessel location, h_w .

Both the buoyancy, F_n , and the drag force, F_v acting on the vessel generate a stress on the vessel support (e.g., the saddle connected to the ground). Assuming that the vessel connection to the saddle is a dap-joint (i.e. a connection of infinite rigidity) the forces acting on the vessel directly affect the bolt connection between the saddle base plate and the ground, as shown in Fig. 5.2c. As usual in engineering practice, it is assumed that a total number n_b of bolts having the same features characterize the connection. The buoyancy F_n causes a normal stress on each of the n_b bolts of the connection (Sinnott, 1999; CEN, 1993):

$$F_{n,b} = F_n / n_b \quad (5.5)$$

where $F_{n,b}$ is the portion of normal force allocated to each bolt.

Beside the direct action of buoyancy on the connection, the contribution of the bending moment M_b must be taken into account. In fact, only one of the two vessel saddles is anchored

to the ground (see Figs. 5.2a and 5.2b), thus the buoyancy generates a bending moment on the support. The bending moment M_b may be expressed as follows:

$$M_b = \frac{1}{2} F_n l_3 \quad (5.6)$$

where l_3 is the distance between the anchored saddle and the vessel edge (see Fig. 5.2a). In the absence of more specific data, the position of the saddle can be conservatively assumed in correspondence of the end of the cylindrical part of the vessel, as shown in Fig. 5.2a (thus, $l_3 = L-l_1$). The action of the bending moment is distributed over the n_b bolts of the plate according to their distance from the “neutral axis” of the plate (x_i) as follows:

$$F_{x,i} = \frac{M_b}{\sum_{i=1}^{n_b} x_i^2} \cdot x_i \quad (5.7)$$

where x_i is the distance of the i -th bolt from the “neutral axis” of the plate (see Fig. 5.2c).

Finally, the overall action of buoyancy on the i -th bolt ($N_{tot,i}$) may be evaluated summing the contribution of the normal net force (Eq. 5.5) and of the bending moment (Eq. 5.7):

$$N_{tot,i} = F_{n,b} + F_{x,i} \quad (5.8)$$

It is worth to mention that buoyancy may also induce a bending moment opposite to M_b , thus acting on the bolts of the connection as a negative force (see the coordinate system in Fig. 5.2b) which results in an attenuation of the effective $F_{x,i}$ value. This effect was neglected in the model, thus obtaining conservative results.

A similar procedure allows evaluating the action on each bolt of the drag force, F_v , which affects the n_b bolts of the connection as follows (Sinnott, 1999; CEN, 1993):

$$F_{v,b} = F_v / n_b \quad (5.9)$$

where $F_{v,b}$ is the portion of shear force allocated to each bolt. Also in this case, the bolts undergo a supplementary force due to the torque caused by the vessel rotation induced by the drag force (see Fig. 5.2b). The torque (M_t) is schematized in Fig. 5.2c and may be evaluated as follows:

$$M_t = \frac{1}{2} F_v l_3 \quad (5.10)$$

It is worth to notice that Eq. 5.9 may lead to conservative results, since the friction associated to the slipping of the unanchored saddle may reduce the action of the net drag force on the bolts of the anchored saddle. The torque action of M_t is distributed over the i -th bolt according to its distance from the center of the plate (y_i) as follows:

$$F_{y,i} = \frac{M_t}{\sum_{i=1}^{n_b} y_i^2} \cdot y_i \quad (5.11)$$

where y_i is the distance of the i -th bolt from the base plate center (see Figure 5.2c).

Finally, the total shear force on the i -th bolt ($S_{tot,i}$) is evaluated summing the contribution of the shear force (Eq. 5.9) and of the torque (Eq. 5.11):

$$S_{tot,i} = F_{v,b} + F_{y,i} \quad (5.12)$$

The procedure reported in a reference technical standard for bolt connection integrity verification (Sinnott, 1999; CEN, 1993; RCSC, 2009) was adopted in the present study in order to

assess the failure conditions of the vessel anchorage caused by flooding. The procedure is based on the calculation of the total normal and shear forces acting on each bolt ($N_{tot,i}$ and $S_{tot,i}$ calculated by Eqs. 5.8 and 5.12) as a function of assumed flood intensity parameters (water velocity, v_w , and water effective depth, h_w) and of vessel geometry. The failure of the connection is assumed if at least one of the following criteria is verified for at least one of the n_b bolts of the base plate (see Fig. 5.2c):

$$\left(\frac{\sigma_i}{\sigma_{b,adm}}\right)^2 + \left(\frac{\tau_i}{\tau_{b,adm}}\right)^2 > 1 \quad (5.13a)$$

$$\left(\frac{\sigma_i}{f_{d,N}}\right)^2 + \left(\frac{\tau_i}{f_{d,S}}\right)^2 > 1 \quad (5.13b)$$

where: $\sigma_{b,adm}$ and $\tau_{b,adm}$ are respectively the normal and tangential admissible stress; $f_{d,N}$ and $f_{d,S}$ are respectively the normal and tangential design stress; σ_i is the average normal stress and τ_i is the average shear stress on the i -th bolt derived as follows from the loading conditions:

$$\sigma_i = N_{tot,i} / A_{res} \quad (5.14)$$

$$\tau_i = S_{tot,i} / A_{res} \quad (5.15)$$

in which A_{res} is the resistant area of each bolt. Conditions expressed by Eq. (5.13a) are derived from the application of the “maximum allowable stress” criterion (CEN, 1993; RCSC, 2009), while Eq. (5.13b) represents the “limit state” criterion (CEN, 1993; RCSC, 2009).

Table 5.3: Standard bolt connection materials classes (ASTM, 2004; ISO, 1984a; ISO, 1984b) evidencing the materials of interest (marked with “X”) (Sinnott et al., 1999). (see Table 5.2).

ID	Class type	Industrial application	$f_{d,N}$ (Mpa)	$f_{d,S}$ (Mpa)	$\sigma_{b,adm}$ (Mpa)	$\tau_{b,adm}$ (Mpa)
A	4.6		240	170	160	113
B*	5.6	X	300	212	200	141
C	6.6	X	360	255	240	170
D	8.8	X	560	396	373	264
E	10.9	X	700	493	467	330

* Selected for the development of mechanical model and correlations (see Table 2).

Table 5.4: Standard bolt dimensions range (ASTM, 2004; ISO, 1984a; ISO, 1984b) evidencing the dimensions of interest (marked with “X”) (Sinnott et al., 1999). See Table 5.2.

ID	Industrial application	Bolt Diameter (mm)	A_{res} (mm ²)	Typical diameter range (m) of supported tanks [33]
A		12	84	
B		14	115	
C	X	16	157	
D	X	18	192	
E*	X	20	245	<1.2
F	X	22	303	
G*	X	24	353	1.2 – 2.4
H*	X	27	459	>2.4
I		30	561	

* Selected for the development of mechanical model and correlations (see Table 5.2).

Clearly enough, the above conditions may be applied to any bolt connection provided that specific data are available. In the present study, a set of reference data were assumed to obtain representative failure conditions for the vessel geometries considered in the vessel database summarized in Table 5.1. The features assumed for the bolt connections considered are summarized in Tables 5.3 and 5.4, and were derived from technical standards (*ASTM, 2004; ISO, 1984a; ISO, 1984b; Kulak et al., 2001*).

5.2.3 Characterization of flood impact vector (step 3)

The elements needed for the characterization of the flood impact vector are the flooding frequency and the expected flood severity. The standard parameter for flood frequency evaluation is the return period (t_r) measured in years and given by hydrological studies (Ramachandra Rao and Hamed, 2000; Charlton, 2008; Bryant, 2005), usually available from local competent authorities (New South Wales Government, 2005; Rijkswaterstaat, 2005; Holmes, 2001; Dept. of Regional Development and Environment, 1991). The flooding frequency f can thus be estimated as follows:

$$f = 1/t_r \quad (5.16)$$

Since there are different types of flood events (e.g. floodplain inundations with high water level, flash floods with high water velocity, etc.), the possible modalities of flood impact (slow submersion, moderate speed wave, high speed wave) must be discriminated. As shown in Section 5.2.2, the flood severity can be quantified by two parameters: water effective depth (h_w) and water speed (v_w). The effective depth should take into account the possible effect of protection measures, such as concrete supports higher than the ground level to which the vessel saddles are fixed. Taking into account the schematization in Fig. 5.2a, if the height of the supports (h_c) is considered, the effective flood water height h_w may be calculated as follows:

$$h_w = h_{w0} - h_c \quad (5.17)$$

where h_{w0} is the actual depth of flood water. Clearly enough h_w is equal to h_{w0} if no protections are available.

On the basis of available data on past events, reasonable ranges for credible values of water height and water speed recorded in flood events were collected and are reported in Table 5.2. The higher values were derived analyzing the features of critical flooding events (Pistrika and Jonkaman, 2010; Bates et al., 2005; Ebersole et al., 2010), in order to obtain a worst case reference. Besides, a minimum value of flood height is also introduced (namely, h_{min}), that is defined as the minimum possible flooding height affecting vessels mounted on saddles. This parameter depends on the type of vessel and may be derived as follows (see Figure 5.2a):

$$h_{min} = l_2 - D/2 \quad (5.18)$$

Hence, h_{min} is the minimum flooding height needed to wet the surface of the horizontal vessel. Finally, in the evaluation of vessel damage due to flood impact, a further parameter is introduced in order to estimate the height of the vessel effectively wetted by flooding, namely the flooding wetting height:

$$h_{wet} = h_w - h_{min} \quad (5.19)$$

This latter parameter, representing the effective water depth, is particularly significant for the evaluation of vessels failure due flood impact, as explained in the following sections.

5.2.4 Model validation (step 4)

Past accident data analysis on NaTech scenarios involving flooding of process equipment are scarce and not detailed (Young et al., 2004; Cozzani et al., 2010; Landucci et al., 2012; Rasmussen, 1995; Krausmann et al., 2011). In the accident description, the flood parameters (water height and speed) needed to support model validation are usually not mentioned or only provided in qualitative terms (e.g.: “high depth flood”, “low speed flood”, “severe flood”, etc.). Nevertheless, a significant accident occurred in a park of propane tanks during the 1993 Mississippi River basin floods close to Des Peres River, Illinois. Fifty tanks, with nominal capacity of 30000 gallons (e.g., about 120 m³), supported by saddles, began to float under the action of the flood water (U.S. Army Corps of Engineers, 1993; Grunfest and Pollack, 1994). The water speed is not reported, but a water height h_w of 2.4m could be estimated (U.S. Army Corps of Engineers, 1993). Only small and localized flash fires occurred, with no catastrophic ruptures of vessels. A number of 12000 residents was forced to leave their homes for twelve days (U.S. Army Corps of Engineers, 1993; Grunfest and Pollack, 1994).

The available accident data were taken into account for a preliminary model validation. Input data used in the calculations are summarized in Table 5.2. The typical vessel geometry adopted for 30000 gallon tanks is included in the database reported in Table 5.1. However, since the design pressure of the flooded tanks is unknown, three tank geometries corresponding to tanks having the same diameter and length, but increasing thickness were considered: #46 with design pressure 1.5MPa; #70 with design pressure 2.0MPa; #94 with design pressure 2.5MPa (see Table 5.1 for further details). The procedure described in Section 5.2.2 and summarized in Table 5.2 was applied to assess possible vessel failure. The tanks were considered conservatively as containing propane up to their maximum filling level (thus assuming the minimum buoyancy according to Eq. 5.2) and assuming a water depth of 2.4m±0.25m (considering possible uncertainties in the actual reported floodwater height). The model evidenced that connection failure conditions for the three tank geometries assumed were verified independently of water velocity v_w . Thus, model results are in agreement with past accident evidence, pointing out the criticalities connected with high-depth flooding of storage vessels.

In order to extend model validation, generic threshold data on damage caused to equipment items by floods derived in previous studies (Landucci et al., 2012; New South Wales Government, 2005; Rijkswaterstaat, 2005) were considered. From available data, a flood wave with a velocity of 2m/s and a maximum height of 0.5m were considered as thresholds below which damages are not expected for generic structures. Fig. 5.3 shows the fraction of vessels contained in the database which fail under these reference flooding conditions. In order to consider reference conditions suitable for both atmospheric and pressurized equipment, water was assumed as the reference substance inside vessels and air was assumed in the top space of the vessels.

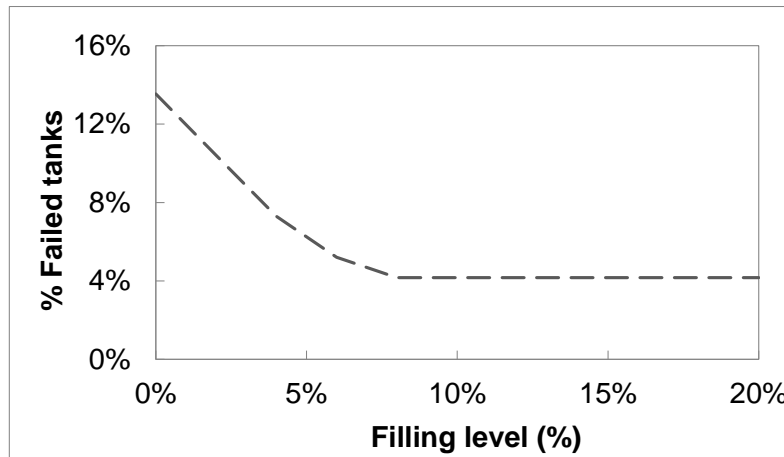


Figure 5.3: Results of the extended validation of the mechanical model: fraction of the tanks failed as a consequence of the reference flood ($h_w=0.5\text{m}$; $v_w=2\text{ m/s}$) as a function of vessel filling level. Stored fluid density considered for validation is that of water ($\rho_l=1000\text{ kg/m}^3$), and air is considered in the top space of the vessel ($\rho_v=1.2\text{ kg/m}^3$). The evaluation was carried out for all the vessels reported in the database (96 vessels, see Table 5.1).

As shown in the figure, most of the vessels do not fail even when empty (failure fraction for empty vessels is around 30%). When different filling levels are considered, the fraction of vessels which fails due to the flood impact decreases to 25%. Large tanks (i.e. having volumes higher than 100m^3) are not able to withstand the high water speed conditions even considering a 100% filling level, due to the high value of l_3 (12-15m), which dramatically increases the torque action on the support. However, it is worth mentioning that the model only considers the worst possible orientation of the vessel respect to the flood wave (e.g., the one which maximizes the A_{ext} in Eq. 5.4), thus obtaining the maximum value of drag force. Hence the results should be considered conservative, thus evidencing a sufficient agreement with the available literature data.

5.2.5 Dataset of failure conditions (step 5)

The vessel database reported in Table 5.1 was used to obtain a dataset of failure conditions considering the set of reference flooding conditions identified in step 3 (Section 5.2.3). A value of 1% of the reference lower bound, ϕ_{min} , was assumed as the minimum credible operational limit for the filling level. A range of filling levels between 1 and 90% was thus considered, as shown in Table 5.2. Table 5.5 reports the reference values assumed for the liquid and top space vapor density. Liquid density values are based on available data concerning substances released in past accidents (Cozzani et al., 2010). The density of the vapor was calculated assuming nitrogen blanketing in the top space of atmospheric vessels and the vapor at saturation pressure for liquefied pressurized storages. In both cases, equation (1.13x) in Table 5.2 was used for the estimation of vapor density.

Figs. A1 to A4 in the Appendix show the failure conditions obtained considering all the vessels in the database (see Table 5.1), different stored fluids and different operating conditions. Figs. A1 and A2 report the data obtained for atmospheric vessels, while Figs. A3 and A4 report the

data obtained for the pressurized vessels considered in the database. Fig. 5.4 reports some examples of failure plots derived from the failure tables reported in the Appendix. The failure plots synthetically represent the results obtained from the application of the model, and will be discussed in detail in Section 5.3.

Table 5.5: Reference substances, associated to the correspondent type of vessel, and flood conditions considered in the present analysis. PRES = pressurized vessel; ATM = atmospheric vessel

	Parameter ID	Reference parameters						
		Description	Liquid density ρ_l (kg/m ³)	Vapor density ρ_v (kg/m ³) ^a	Typical type of storage vessel	Flood water speed v_w (m/s)	Flood water actual height h_{w0} (m)	Expected occurrence frequency f (y ⁻¹)
Reference substances	S1	LPG	500	20.7	PRES	-	-	-
	S2	Ammonia	600	7.8	PRES	-	-	-
	S3	Gasoline or diesel fuel	750	1.2	ATM	-	-	-
	S4	Liquid aromatics or hydrocarbons	900	1.2	ATM	-	-	-
	S5	Water solutions with contaminant(s)	1100	1.2	ATM	-	-	-
	S6	Chlorine	1400	24.4	PRES	-	-	-
Reference flooding conditions	W1	High depth flooding condition	1100	-	-	0.5	2	2.0×10 ⁻³
	W2	High speed flooding conditions	1100	-	-	2	0.5	2.0×10 ⁻³
	W3	Intermediate severity flooding conditions	1100	-	-	1	1	5.0×10 ⁻³
	W4	Low severity flooding conditions	1100	-	-	0.5	0.5	3.3×10 ⁻²

^a See Table 5.2 for details on ρ_v evaluation

5.2.6 Simplified correlations for vessel damage (step 6)

The analysis of the dataset of failure conditions obtained in step 5 allowed the identification of the critical parameters leading to vessel failure. The plots reported in Fig. 5.4 highlight that the stored fluid has a strong impact on the failure region of the vessels. An increase in the filling level and/or a higher density of the stored fluid result in an increased resistance of the vessel to the action of buoyancy. Therefore, once the storage system is defined (i.e. defining the geometry of the vessel and the substance stored) the filling level ϕ is the only operating parameter which affects the vessel resistance to buoyancy caused by a given set of flooding conditions. The critical filling level (CFL) of a vessel may thus be defined as the minimum value of ϕ able to ensure the tank resistance to buoyancy caused by a flood wave having a given

intensity (Landuci et al., 2012). This parameter can be evaluated using the failure plots reported in Figure 5.4, based on the failure model described in Section 5.2.2.

Nevertheless, simplified correlations are also provided in the following to allow a simplified straightforward evaluation of vessel failure probability. The correlations are based on the analysis of the CFL behavior respect to the water effective height (h_w) assuming a reference value, ρ_{ref} , for the density of the stored substance. The effect of water speed is not taken into account to assess the CFL, since the CFL significantly affects only the resistance to buoyancy and has a limited influence on the resistance to the action of flood water drag force.

As shown by the examples reported in Fig. 5.5a, a linear empirical correlation may be used to relate the CFL to water height, given the vessel geometry and the stored fluid density:

$$CFL = A \cdot h_w + B \quad (5.20)$$

where the parameters A and B are only a function of the vessel geometry (hence, operating pressure and volume).

The data in Fig. 5.5a were obtained for the sample vessels considered for Fig. 5.4 assuming a reference fluid density (ρ_{ref}) of the stored fluid equal to 1000 kg/m³. Similar data were obtained for all the vessels in the database (see Table 5.1), and are not reported for the sake of brevity. The extended application of the mechanical model allowed the calculation of the values of the A and B parameters as a function of the geometrical features of the vessel. Figs. 5.5b and 5.5c show an example of the behavior of the A and B with respect to vessel diameter (D) and vessel tare weight (W_t).

The data reported in the figures were obtained for vessels having a specific design pressure (1.5 MPa). However, qualitatively similar results were obtained for the other types of vessels. It is worth mentioning that the CFL has a maximum value related to the operating capacity of the vessels (i.e. the maximum CFL value is equal to ϕ_{max}). Thus, the following empirical correlations were obtained for the A and B parameters with respect to vessel features:

$$A = K_1 \cdot D^a \quad (5.21)$$

$$B = K_2 (W_t + K_3)^b \quad (5.22)$$

The values calculated for the K_1 , K_2 , K_3 , a , and b parameters are reported in Table 5.6 for each category of vessel considered. Two sets of parameters were calculated:

- SET A: best fit parameters (dashed lines in Fig. 5.5);
- SET B: envelope parameters allowing a conservative estimation of CFL (solid lines in Fig. 5.5).

Clearly enough, the above set of parameters depends on the value assumed for the reference density of the stored fluid, ρ_{ref} . In order to take into account the actual density of the stored fluid, the following changes may be introduced in Eq. 5.20:

$$CFL = A' \cdot h_w + B' \quad (5.23)$$

The values of the A' and B' coefficients in Eq. 5.23 may be calculated from the A and B parameters obtained using the reference fluid density ρ_{ref} :

$$A' = \frac{\rho_{ref} \cdot A}{\rho_l - \rho_v} \quad (5.24)$$

$$B' = \frac{\rho_{ref} \cdot B - \rho_v}{\rho_l - \rho_v} \quad (5.25)$$

where ρ_l is the actual density of the stored fluid and ρ_v is the density of the vapor phase inside the vessel. The approach discussed above allows the calculation of a critical filling level below which the vessel may fail due to buoyancy. In order to account also for the action of the drag force, the simplified model needs to be extended. Flood waves with high water velocity, v_w , may lead to vessel failure due to drag force even in the case of limited water depth (see Section 5.2.4). Hence a critical water velocity, $v_{w,c}$, was defined as the v_w value able to damage a given vessel for an assigned value of wetting height (h_{wet} see Eq. 5.19). As a matter of fact, in case of a flood wave with a small h_{wet} value, thus unable to cause damages by buoyancy, $v_{w,c}$ represents the critical flood velocity value which causes the minimum drag force value required to damage the vessel.

Also in this case this parameter may be derived applying the mechanical model. Also in this case, simplified correlations based on h_{wet} (see Fig. 5.4) were obtained from failure plot analysis:

$$v_{w,c} = E \cdot h_{wet}^F \quad (5.26)$$

Figs. 5.5d and 5.5e show the behavior of E and F calculated for the sample vessels in Fig. 5.4. Similar trends were obtained for all the vessels in the database. Thus, also in this case it was possible to obtain empirical correlations for the E and F parameters with respect to vessel geometry:

$$E = K_4 \cdot L^c \quad (5.27)$$

$$F = K_5 \ln\left(\frac{L}{D}\right) + K_6 \quad (5.28)$$

where L is the vessel length and D is the vessel diameter. Again, for the c , K_4 , K_5 , and K_6 parameters a set of best fit (SET A, dashed lines in Fig. 5.5) and of envelope (SET B, solid line in Fig. 5.5) values were calculated and are reported in Table 5.6.

Table 5.6: Parameters for CFL and $v_{w,c}$ evaluation applying the simplified correlations (Eqs. 5.20-5.28). SET A: best fit parameters; SET B: envelope correlation parameters. P_d = design pressure (MPa); ATM = atmospheric pressure.

Correlation type	Vessel type	K_1	K_2	K_3	K_4	K_5	K_6	A	b	c
SET A	ATM	1.331	-2.163	-288.6	9.910	-0.037	-0.399	-0.990	-0.260	-0.718
	$P_d = 1.5$	1.287	-1.144	-499.2				-0.952	-0.112	
	$P_d = 2.0$	1.290	-1.305	-546.0				-0.966	-0.109	
	$P_d = 2.5$	1.256	-6.068	-234.0				-0.951	-0.263	
SET B	ATM	1.331	-1.882	-46.8	3.195	-0.037	-0.399	-0.990	-0.252	-0.341
	$P_d = 1.5$	1.347	-1.197	-475.8				-0.995	-0.129	
	$P_d = 2.0$	1.341	-1.365	-483.6				-0.976	-0.120	
	$P_d = 2.5$	1.355	-4.512	-234.0				-0.999	-0.239	

5.3. Results and discussion

5.3.1 Analysis of vessel failure conditions

The application of the mechanical model developed in the present study to the reference flooding conditions summarized in Table 5.2 and to all the vessels considered in the database (Table 5.1) allowed obtaining the failure charts reported in the Appendix (Figs. A1 and A2 for atmospheric vessels, Figs. A3 and A4 for pressurized vessels). The failure charts give an overview of reference conditions leading to vessel failure in flood events, considering a large set of vessels, several different flood conditions and assuming fixed filling level and fluid density, thus considering the same operating conditions for all the vessels. The failure charts may be used to carry out a direct and straightforward preliminary assessment of the credibility of vessel failure in different flooding conditions.

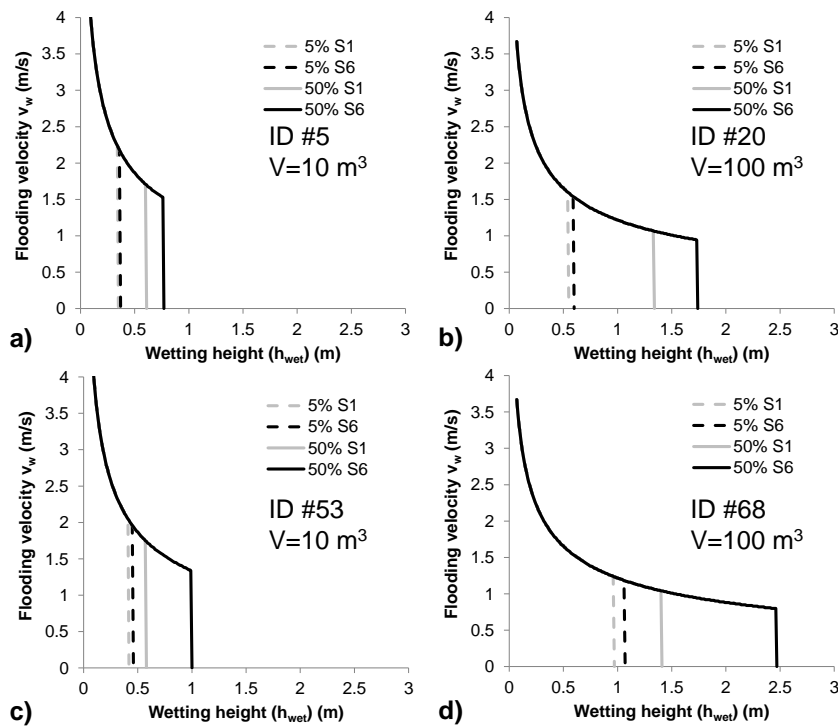


Figure 5.4: Example of failure plot for: (a) vessel #5; (b) vessel #20; (c) vessel #53; (d) vessel#68. Vessel data are provided in Table 5.1 at the correspondent ID number. Failure plots were obtained considering two different filling levels (5 and 50%) and two different reference substances (S1,S6, see Table 5.5).

More detailed data may be obtained by the use of failure plots, that require the application of the mechanical model to the actual data of the vessel of interest. Fig. 5.4 shows an example of the failure plots obtained for four representative vessels: two atmospheric tanks and two pressurized tanks. For each design pressure, two reference volumes were considered: 10 m^3 , representative of medium scale vessels, and 100 m^3 , representative of large scale storage. Table 5.1 reports the data of the vessels considered (see IDs #5, #20, #53 and #68).

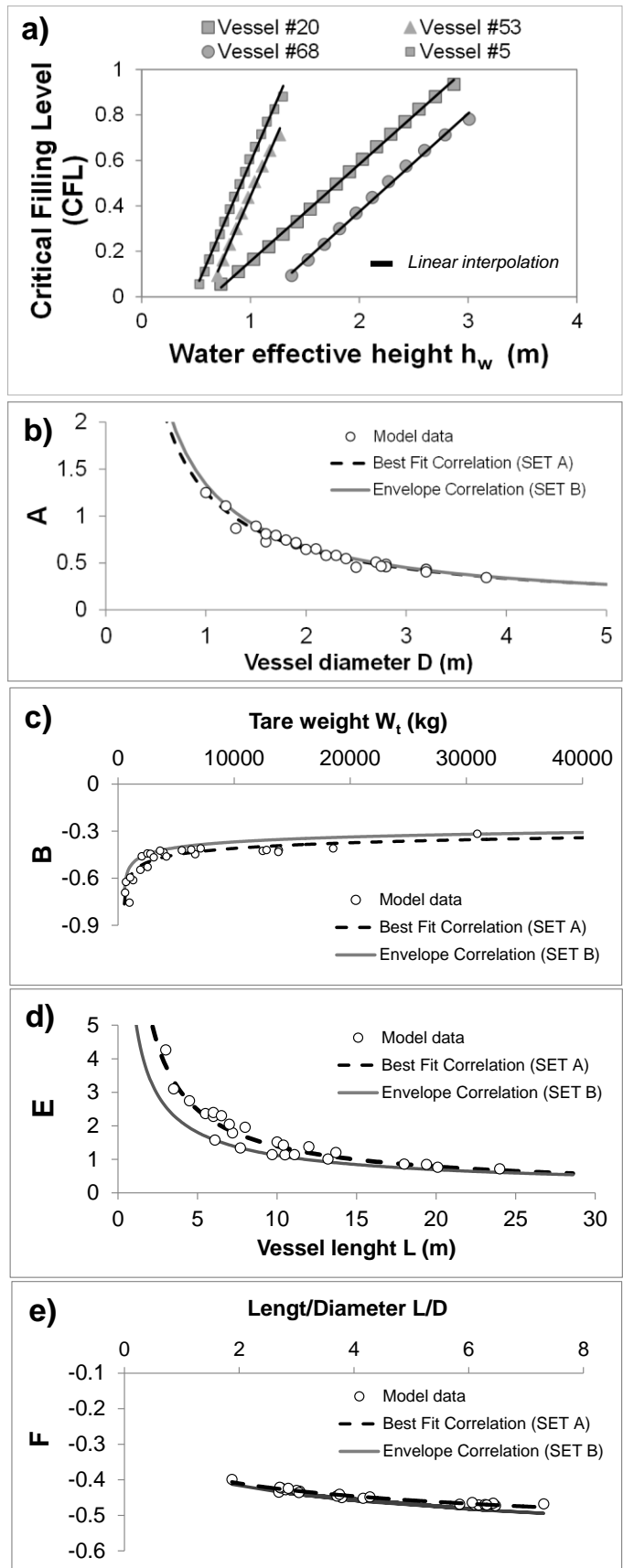


Figure 5.5: Plots of the coefficients developed for the simplified correlations derived from the extended data set of failure conditions: assessment of (a) critical filling level (CFL); (b) coefficient A in Eq. 5.21, (c) coefficient B in Eq. 5.22, (d) coefficient E in Eq. 5.27, and (e) coefficient F in Eq. 5.28.

The failure plots show the combinations of flooding parameters leading to vessel failure due to the failure of the support bolt connection. Two density values were assumed for the stored liquid (i.e. the lowest and the highest values considered credible in the present study, respectively associated to substances S1 and S6 in Table 5.5). The effect of two different filling levels (respectively 5 and 50%) was assessed. The plots in Figure 5.4 report the minimum value of water velocity, v_w , able to cause the failure of the connection at a given value of wetting height (h_{wet}). A peculiar behaviour of the curve is obtained, since when flood water height exceeds a critical value the connection is predicted to fail even in the case of low or negligible values of water speed. This corresponds to a critical value of buoyancy (F_n in Eq. 5.1), which, according the failure criterion assumed (Eq. 5.13a and 5.13b), leads to the rupture of the bolt connection even in the absence of drag force (F_v). Therefore, for a given vessel type and substance, the critical filling level (CFL, see Section 5.2.6) may be obtained from the failure plots in Fig. 5.4 as a function of flooding effective height (h_w). The results are reported in Fig. 5.5a.

The failure plots allow understanding the key parameters affecting the failure of the vessel related to the type of storage system. In fact, the failure zone of tanks with small inventory (Figures 5.4a and 5.4c) is more extended with respect to that of larger tanks (Figures 5.4b and 5.4d), thus indicating a higher vulnerability. This is due to the lower overall vessel weight (both considering inner fluid and vessel shell), which results in a lower resistance to the hydrostatic lift force. The significant change in the failure zone of a tank of given volume when its operative pressure, and thus its shell thickness as well as its overall weight, is increased (see the comparison of Figures 5.4a and 5.4b with Figs. 5.4c and 5.4d) confirms the higher vulnerability of smaller tanks to the respect of buoyancy forces. For the same reason, the increase of the filling level ϕ and of the stored fluid density have a significant effect on the vessel resistance. The effect of the increasing fluid density is more evident at higher values of ϕ (solid lines in Fig. 5.4), due to the growing importance of this parameter at higher filling levels.

5.3.2 Sensitivity and uncertainty analysis

The failure plots in Figure 5.4 were obtained assuming the values of several parameters (see Table 5.2) related to construction materials and bolt connection features on the basis of technical standards. However, some variability may exist in these key-parameters. Thus, a sensitivity analysis was undertaken to understand the influence of the geometry and mechanical properties of the connection on model results. Tables 5.3 and 5.4 respectively summarize the standard range of bolt material mechanical properties (i.e. the resistance class) and of geometrical parameters. Moreover, both tables report the typical values of the mentioned parameters commonly used for the anchorage of process and storage vessels.

The sensitivity analysis was carried out applying the mechanical model, considering all the possible combinations of bolts geometry and construction material class. Moreover, each combination was modelled considering different numbers of bolts (ranging from 4 to 10). For the sake of simplicity, as for the extended model validation (see Section 5.2.4) air was assumed in the top space of the vessels, water was assumed as the stored liquid and a fixed filling level (e.g., $\phi=10\%$) was considered.

Figure 5.6a shows the fraction of failed vessels in the database (Table 5.1) varying the bolt connection features imposing in the model the reference flooding condition used for model validation (see Section 5.2.4). Since this condition represents a threshold limit below which no failure is expected, as mentioned in Section 5.2.4, no change is expected in results, even if bolt connection parameters are changed.

Actually, the results show a significant variation (an increase of the fraction of failed vessels) only when low resistance connections are considered (e.g., bolt class lower than B and $A_{res} < 200 \text{ mm}^2$). However, such types of connections are usually not applied in industrial facilities for this type of anchorage (Sinnott, 1999; ISO, 1994a). In Figure 5.6a, the connection material type set for the present study is highlighted by the arrow. It clearly appears that the results obtained are the same of the case with higher resistance materials with failure fraction lower than 25% for any type of bolt with $A_{res} > 200 \text{ mm}^2$.

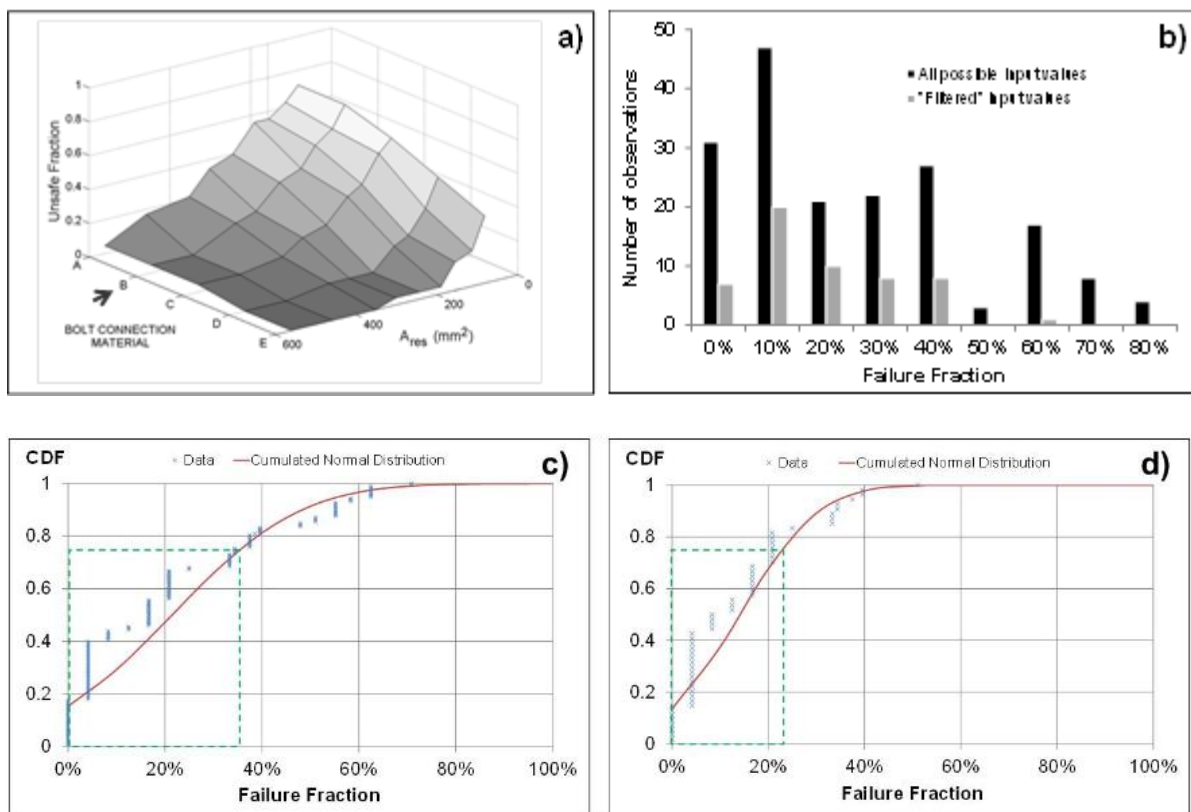


Figure 5.6: Results of the sensitivity and uncertainty analysis: a) fraction of the tanks failed as a consequence of the validation reference flood ($h_w = 0.5\text{m}$; $v_w = 2 \text{ m/s}$) considering different bolt connection materials (resistance class A to E) and bolt sizes (A_{res} in mm^2); b) distribution of failure fraction values obtained applying the model with different input types for all the vessels reported in the database (96 vessels, see Table 5.1); cumulated normal distribution of failure fraction values obtained applying the model with all possible input values (c) and limiting input data (d). Density assumed for the stored fluid is that of water ($\rho_l = 1000 \text{ kg/m}^3$), and air is considered in the top space of the vessel ($\rho_v = 1.2 \text{ kg/m}^3$). The dashed box in panels (c) and (d) represents the third quartile (Q3) of model predictions.

In order to evaluate model uncertainties, the statistical evaluation of model predictions was carried out determining the distribution of vessels failure fraction values considering the reference flooding conditions (see Section 5.2.4). At first, all the possible input values were

implemented in the model, thus the full range of bolt connection materials, bolts geometries and bolts number were used. Secondly, limited input values were implemented by only selecting the parameters commonly applied in industrial facilities according to Tables 5.3 and 5.4 (Sinnott, 1999). In this latter case, only 4, 8 and 10 bolts were considered for the base connection.

Fig. 5.6b shows the distribution of vessel failure fraction obtained applying the model with all possible combinations of input parameters and by “filtering” the input parameters according to Tables 5.3 and 5.4. Then, the results shown in Figure 5.6b were interpolated considering a normal distribution and obtaining the cumulative distribution functions (CDF) shown respectively in panels 5.6c and 5.6d for “full range” and “selected” input values. As shown in Figure 5.6c, if all possible input values are considered, values of failure fraction higher than 60% are obtained, since the weaker connections lead to the failure even in presence of the low severity flooding. However, if only the relevant connections types are considered, the failure fraction is lower than 50% even in the case of weaker connections. The third quartile (Q3) of the vessel failure distribution (highlighted by the dashed box in panels 5.6c and 5.6d) was taken into account in order to quantitatively evaluate the robustness of the model. Q3 of failure fractions is reduced from 36% to 22%, thus demonstrating the limited variability of model results considering relevant input parameters combinations.

It may be concluded that the only few critical parameters are determinant to assess the vessel resistance to a given flood scenario (identified by a given flooding height and velocity combination). In particular, given a vessel geometry, the key parameters to assess vessel resistance to flood impact are the fluid density and the vessel filling level. Clearly enough, these are the operating parameters of the storage system. These results are in accordance with the outcomes of a previous study concerning atmospheric vertical vessels (Landucci et al., 2012).

5.3.3 Assessment of vessel damage probability

The results discussed above evidence that two key parameters influence vessel failure in a given flooding scenario: the vessel filling level and the flood water velocity. Hence, in order to estimate the failure probability of a vessel due to flood impact (i.e. the vessel vulnerability to a flood), two threshold parameters may be used as a reference: the critical water velocity, $v_{w,c}$ (see Section 5.2.6), and the critical filling level, CFL (that may be calculated by Eq. (4.18) in Table 5.2b, see Section 5.2.6). The first represents a threshold condition for velocity over which the drag force generated by flood water is sufficient to cause the failure of the bolt connection for a given flooding height. Thus, connection rupture is predicted independently on vessel parameters other from vessel shape and volume (e.g. vessel design pressure, stored fluid density or filling level have a negligible influence, if any, on the drag force caused by flood water). The second threshold parameter identified, the CFL, represents the minimum value of the filling level, β , able to ensure the resistance of the bolted connection to buoyancy. Thus, a specific approach, schematized in Figure 5.7, was developed in order to assess vessel failure probability (ψ). The procedure for the assessment of ψ is outlined in the following, while the detailed steps needed to carry out the specific calculations required for the assessment of vessels damage probability are summarized in Table 5.2.

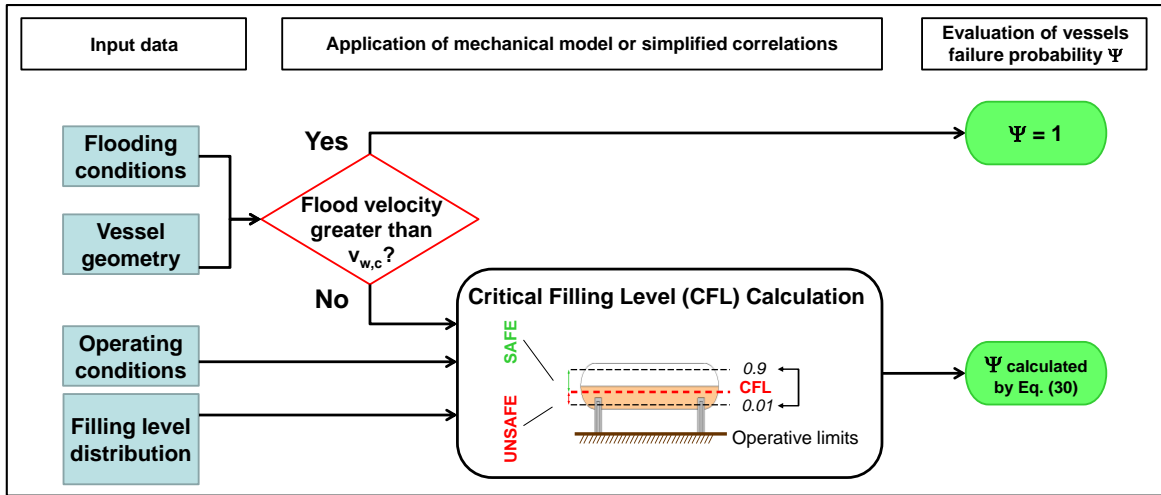


Figure 5.7: Algorithm for the determination of vessels failure probability as for given flooding scenario.

Given only the vessel geometry and the characteristic of the flooding, the critical water velocity, $v_{w,c}$, may be directly evaluated and compared with the actual velocity of floodwater, v_w , considered in the analysis. This may be done either with the detailed model or with the simplified correlations. If v_w is equal or greater than $v_{w,c}$ the upper-bound failure condition due torque action caused by the drag force is fulfilled. Thus a unit value of vessel failure probability may assumed:

$$\Psi = 1 \text{ if } v_w \geq v_{w,c} \quad (5.29)$$

If floodwater velocity is lower than the critical threshold for direct failure due to torque ($v_w < v_{w,c}$), also buoyancy should be taken into account. According to Figure 5.7, it is assumed that the CFL delimitates the “safe” operating conditions given the features of the storage system for a given flooding scenario. If the filling level is lower than the CFL, the tank is in the “unsafe” zone since the vessel support may not resist the flood water impact.

The filling level value may be determined on the basis of site specific historical data or by implementing statistical distributions which might be available for the site under analysis (as specified in Fig. 5.7). Thus, after having built a cumulative distribution function of filling level values (CDF_ϕ) one may define the failure probability Ψ as follows:

$$\Psi = CDF_\phi(CFL) \quad (5.30)$$

in which the CDF_ϕ (CFL) is the value of the cumulative distribution function evaluated for a filling level equal to the estimated CFL. In absence of any specific data for filling level distribution, a linear distribution of possible filling levels between ϕ_{min} (=1%) and ϕ_{max} (=90%) was used in this work for the calculation of Ψ . Under this assumption, the failure probability is derived by the ratio between the “unsafe” operative conditions with respect to all the possible operative conditions:

$$\Psi = \frac{CFL - \phi_{min}}{\phi_{max} - \phi_{min}} \quad (5.31)$$

This approach was followed in the evaluation of vertical atmospheric tanks vulnerability to flooding (Landucci et al., 2012). Either the complete model discussed in Section 5.2.2 or the simplified correlations may be applied to calculate the value of the CFL in Eq. 5.31.

In order to evaluate the performance of the simplified model, the results expressed in terms of damage probability, obtained by the rigorous mechanical model and by the simplified correlations have been compared (Figure 5.8).

Panels 5.8a and 5.8b report parity plots obtained for the comparison of the results obtained by the complete model and by the two sets of simplified correlations. The data displayed in the figure were obtained applying to all the vessels in the database (see Table 5.1) a matrix of reference flood conditions (see Table 5.5). Data were obtained assuming water as the stored fluid ($\rho_f=1000 \text{ kg/m}^3$) and air in the top space of the vessel ($\rho_v =1.2 \text{ kg/m}^3$). The vessels were considered anchored (thus $h_w=h_{w0}$).

Clearly enough, the simplified correlations allow a rapid and straightforward assessment of vessel failure probability. On one hand, as evident from Fig. 5.8a, the best fit correlations (SET A), provide results which are in good agreement with the detailed model even if some of the prediction are not on the safe side (i.e. failure probability is underestimated especially when values are near to 1). On the other hand, panel 5.8b shows that the use of the envelope correlations (SET B) allows for less accurate but always conservative predictions of vessel failure probability.

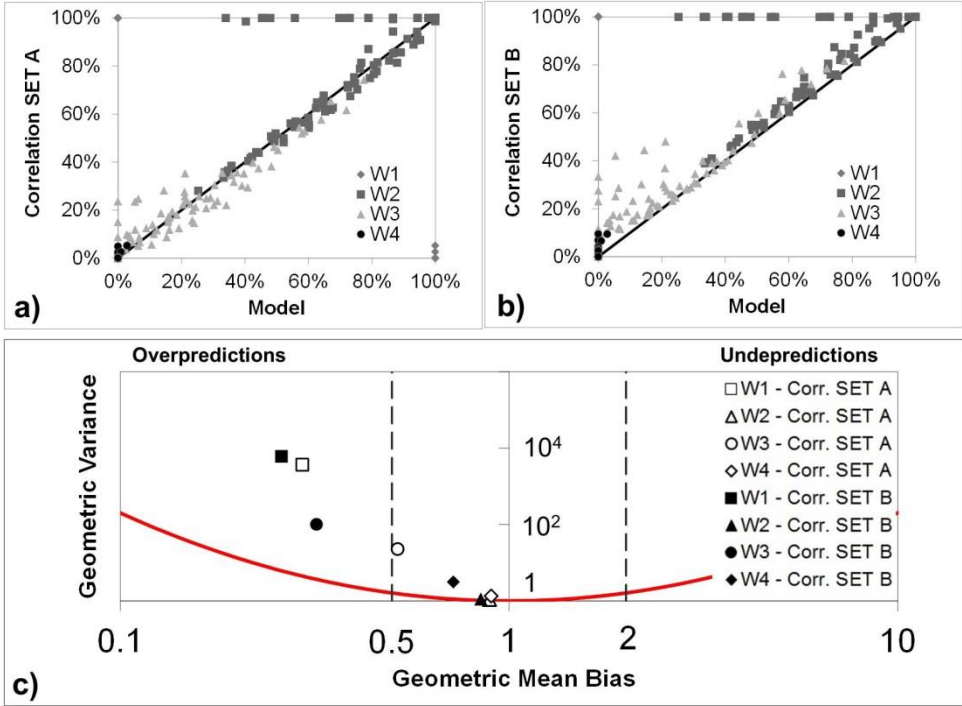


Figure 5.8: Comparison among the prediction of vessel vulnerability (%) carried out by the deterministic model and correlation SET A (a), SET B (b); geometric mean bias (MG) and geometric variance (VG) for correlations compared to deterministic model (c). Reference flooding conditions are reported in Table 5.5. Tank geometrical data are listed in Table 5.1. Density assumed for the stored fluid is that of water ($\rho_f=1000 \text{ kg/m}^3$), and air is considered in the top space of the vessel ($\rho_v =1.2 \text{ kg/m}^3$).

The method proposed by Hanna et al. (1993) was used to analyze the performance of correlations in predicting the failure probability and to compare them against the detailed model. The method is based on the calculation of the geometric mean bias (MG) and the geometric variance (VG) of the values of failure probability predicted by the detailed model (Ψ_{mod}) and by the simplified correlations (Ψ_{corr}):

$$MG = \exp \left[\overline{\ln(\Psi_{mod})} - \overline{\ln(\Psi_{corr})} \right] = \exp \left[\overline{\ln \left(\frac{\Psi_{mod}}{\Psi_{corr}} \right)} \right] \quad (5.32)$$

$$VG = \exp \left[\overline{(\ln(\Psi_{mod}) - \ln(\Psi_{corr}))^2} \right] = \exp \left[\overline{\left(\ln \left(\frac{\Psi_{mod}}{\Psi_{corr}} \right) \right)^2} \right] \quad (5.33)$$

The over-bars indicate that an average was performed over the data set. Good model performances are achieved when both MG and VG are close to unity. In order allow a systematic performance assessment, VG values may be plotted versus the corresponding MG values for each data set and may be compared to the following reference parabola:

$$\ln(VG) = (\ln(MG))^2 \quad (5.34)$$

As clearly appears from Eq. 5.32 and Eq. 5.33, Eq. 5.34 represents the relationship between VG and MG values in a correlation having only a mean bias with respect to the detailed model results (that is, a correlation for which the ratio of Ψ_{mod} / Ψ_{corr} is nearly constant), but showing no systematic deviations, hence with good statistic performance.

Panel 5.8c shows the chart with the results of Hanna et al. (1993) method. In the chart, for each flooding condition (e.g., W1 to W4) a point was obtained both for SET A and B correlations. The reference curve defined by Eq. 5.34 is also reported. As shown in Fig. 5.8c, for both correlation sets, the points fall above the reference curve, hence showing no systematic deviations. It is worth to mention that despite the high VG values, MG values are limited. In fact, all the points associated to correlation SET A are inside the range of MG between 0.5 and 2, thus demonstrating the good correlation performance (Hanna et al., 1993). Correlation SET B is, as expected, more conservative, but still with MG values close to 0.5.

5.4 Case study application

The methodology developed to assess vessel failure probability was applied to the analysis of an industrial lay-out in order to provide data on expected vessel failure probabilities, suitable for the use in a quantitative risk assessment (QRA) framework. Fig. 5.9 shows the storage area considered, in which several pressurized or atmospheric horizontal tanks are present in a flood-prone zone. Two different assumptions were considered for vessel supports: i) all vessels supports are fixed on the ground (thus the effective water height h_w corresponds to the actual flood height h_{w0}); ii) all vessel supports are fixed to a concrete base having a height above ground, h_c , equal to 0.3m (thus h_w is evaluated according to Eq. 5.17). Table 5.7 summarizes the features of the vessels analysed and the densities of the substances stored, while the reference flooding conditions used for model assessment and reported in Table 5.5 were applied to assess vessel resistance.

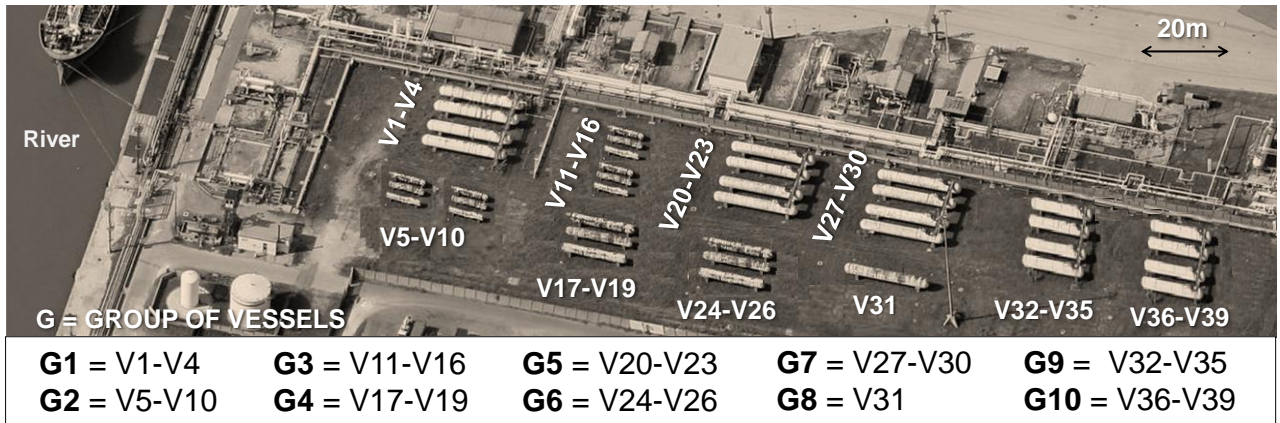


Figure 5.9: Layout of the facility analyzed in the case study. Tank data are reported in Table 5.7.

Table 5.7: Case study definition and results: features of the vessels considered and expected failure frequency (y^{-1}) due to each flooding condition defined in Table 5.5 considering the tanks anchored to the ground. MOD: frequency predicted by the deterministic model; SET A and SET B refer to data predicted by the correspondent set of simplified correlations; NF: No predicted failure. For stored substance features, see Table 5.5 at the correspondent ID.

		ID Vessel									
		V1-V4	V5-V10	V11-V16	V17-V19	V20-V23	V24-V26	V27-V30	V31	V32-V35	V36-V39
Capacity (m ³)		100	10	10	50	100	50	100	100	100	100
D (m)		2.8	1.2	1.2	2.1	2.8	2.1	2.8	2.8	3.2	3.2
L (m)		18	7.7	7.7	13.2	18	13.2	18	18	13.7	13.7
t (mm)		18	13	5	18	24	6	30	18	6	27
P _d (MPa)		1.5	2.5	ATM	2.0	2.0	ATM	2.5	1.5	ATM	2.0
Stored Substance ID		S2	S6	S5	S1	S1	S3	S1	S1	S4	S1
LOC frequency f_{loc} (y ⁻¹) W1	MOD	1.23×10 ⁻³	1.73×10 ⁻³	2.00×10 ⁻³	1.81×10 ⁻³	1.06×10 ⁻³	2.00×10 ⁻³	1.05×10 ⁻³	1.23×10 ⁻³	1.28×10 ⁻³	1.06×10 ⁻³
	SET A	1.72×10 ⁻³	2.00×10 ⁻³	2.00×10 ⁻³	1.68×10 ⁻³	1.10×10 ⁻³	2.00×10 ⁻³	1.10×10 ⁻³	1.72×10 ⁻³	8.72×10 ⁻⁴	1.10×10 ⁻³
	SET B	1.75×10 ⁻³	2.00×10 ⁻³	2.00×10 ⁻³	1.83×10 ⁻³	1.23×10 ⁻³	2.00×10 ⁻³	1.22×10 ⁻³	1.75×10 ⁻³	9.56×10 ⁻⁴	1.23×10 ⁻³
LOC frequency f_{loc} (y ⁻¹) W2	MOD	NF	NF	7.04×10 ⁻⁵	NF	NF	3.76×10 ⁻⁵	NF	NF	NF	NF
	SET A	1.02×10 ⁻⁴	NF	1.33×10 ⁻⁴	NF	NF	4.65×10 ⁻⁵	NF	1.02×10 ⁻⁴	NF	NF
	SET B	2.00×10 ⁻⁴	NF	1.90×10 ⁻⁴	NF	2.00×10 ⁻³	9.46×10 ⁻⁵	2.00×10 ⁻³	2.00×10 ⁻³	NF	NF
LOC frequency f_{loc} (y ⁻¹) W3	MOD	3.23×10 ⁻⁴	NF	2.43×10 ⁻³	8.66×10 ⁻⁴	5.51×10 ⁻⁵	1.86×10 ⁻³	NF	3.23×10 ⁻⁴	8.41×10 ⁻⁴	5.51×10 ⁻⁵
	SET A	1.60×10 ⁻³	8.57×10 ⁻⁴	2.54×10 ⁻³	6.70×10 ⁻⁴	8.13×10 ⁻⁵	1.91×10 ⁻³	1.07×10 ⁻⁴	1.60×10 ⁻³	NF	8.03×10 ⁻⁵
	SET B	1.67×10 ⁻³	1.84×10 ⁻³	2.69×10 ⁻³	9.24×10 ⁻⁴	3.11×10 ⁻⁴	2.03×10 ⁻³	3.17×10 ⁻⁴	1.67×10 ⁻³	1.07×10 ⁻⁵	3.11×10 ⁻⁴
LOC frequency f_{loc} (y ⁻¹) W4	MOD	NF	NF	1.16×10 ⁻³	NF	NF	6.21×10 ⁻⁴	NF	NF	NF	NF
	SET A	1.68×10 ⁻³	NF	2.20×10 ⁻³	NF	NF	7.67×10 ⁻⁴	NF	1.68×10 ⁻³	NF	NF
	SET B	2.10×10 ⁻³	NF	3.13×10 ⁻³	NF	NF	1.56×10 ⁻³	NF	2.10×10 ⁻³	NF	NF

In Figure 5.10 results of the application of the model to the case study are reported. Panels 5.10a, 5.10b, 5.10c and 5.10d show the vulnerability values obtained for the tanks following the developed methodology and applying the envelope correlations (SET B) for vessels fixed on the ground, while panels 10e to 10h show the results obtained considering the presence of the concrete support. As shown in the figure, high failure probability values are obtained for the first three reference flooding conditions considered (W1 to W3), while the low-severity flooding W4 does not affect most of the vessels. In the case of high-speed flooding, vessel failure is mostly due to the excessive drag force (W2 conditions). Buoyancy is responsible of vessel failure for high-depth floods (W1 and W3 conditions). Low volume vessels, due to the reduced sizes, are more resistant to flood action, since the momentums acting on the bolted connections are lower. Actually, vessels V5 to V10 are those showing the higher resistance to flood action. Moreover, such vessels also have a lower inventory that may be release in the case of failure.

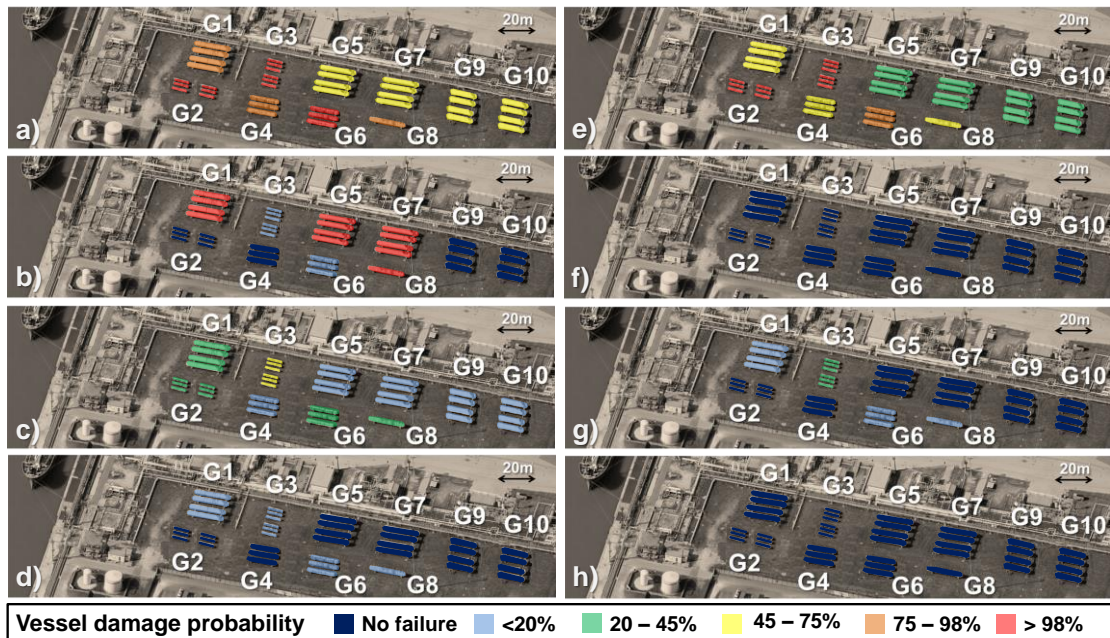


Figure 5.10: Example of case study results: vessel failure probability (%) given the flooding conditions reported in Table 5.5. Panels (a) and (e): flooding W1; panels (b) and (f): flooding W2; panels (c) and (g): flooding W3; panels (d) and (h): flooding W4. Panels (a) to (d): vessels anchored to the ground. Panels (e) to (h): vessels on a concrete base ($h_c = 0.3$ m). G = group of vessels defined in Fig. 5.9.

As shown in Figure 5.10, a greater height of the supports (h_c) may be effective in protecting the vessels only if the actual water depth h_{w0} (see Section 5.2.3) is lower than the overall vessel height. If the expected frequency, f (years⁻¹), of a flood event having a given intensity ($v_w; h_w$) is known, the frequency of loss of containment (LOC) associated to the damage induced by flooding may be calculated as follows:

$$f_{LOC} = \Psi \times f \quad (5.35)$$

The value of f may be derived from site specific data available from local authorities, or may be evaluated with specific models present in the literature (New South Wales Government , 2005; Riskwaterstraat, 2005; Holmes, 2001; Dept. of Regional Development and Environment , 1991). Table 5.5 reports the values of f used in the case study, that were based on the actual values obtained for an Italian site (Italian Ministry of the Interior, 1994). Table 5.7 and Table 5.8 show the LOC frequencies, f_{LOC} , calculated for each tank on the basis of the vulnerability assessment carried out applying both sets of simplified correlation and the deterministic model developed. The data were obtained both for the case of vessels anchored to the ground and for vessels having a concrete support. As evident from the tables, the simplified approach yields conservative values for f_{LOC} , in good agreement with those predicted by the complete model, with maximum discrepancies that in general are lower than a factor 2.

Table 5.8: Expected failure frequency (y^{-1}) due to each flooding condition defined in Table 5.5 implementing the concrete base ($h_c = 0.3$ m). MOD: frequency predicted by the deterministic model; SET A and SET B refer to data predicted by the correspondent set of simplified correlations; NF: No predicted failure. For vessels features refer to Table 5.7 at the correspondent ID.

ID Vessel	LOC frequency f_{LOC} (y^{-1}) W1			LOC frequency f_{LOC} (y^{-1}) W2			LOC frequency f_{LOC} (y^{-1}) W3			LOC frequency f_{LOC} (y^{-1}) W4		
	MOD	SET A	SET B	MOD	SET A	SET B	MOD	SET A	SET B	MOD	SET A	SET B
V1-V4	8.98×10^{-4}	1.40×10^{-3}	1.42×10^{-3}	NF	NF	NF	NF	7.94×10^{-4}	8.58×10^{-4}	NF	NF	NF
V5-V10	1.66×10^{-3}	2.00×10^{-3}	2.00×10^{-3}	NF	NF	NF	NF	NF	NF	NF	NF	NF
V11-V16	2.00×10^{-3}	2.00×10^{-3}	2.00×10^{-3}	NF	NF	NF	1.08×10^{-3}	1.22×10^{-3}	1.36×10^{-3}	NF	NF	NF
V17-V19	1.37×10^{-3}	1.26×10^{-3}	1.39×10^{-3}	NF	NF	NF	NF	NF	NF	NF	NF	NF
V20-V23	7.48×10^{-4}	7.83×10^{-4}	8.96×10^{-4}	NF	NF	NF	NF	NF	NF	NF	NF	NF
V24-V26	1.74×10^{-3}	1.77×10^{-3}	1.82×10^{-3}	NF	NF	NF	8.01×10^{-4}	8.34×10^{-4}	9.54×10^{-4}	NF	NF	NF
V-27- V30	7.26×10^{-4}	7.85×10^{-4}	8.89×10^{-4}	NF	NF	NF	NF	NF	NF	NF	NF	NF
V31	8.98×10^{-4}	1.40×10^{-3}	1.42×10^{-3}	NF	NF	NF	NF	7.94×10^{-4}	8.58×10^{-4}	NF	NF	NF
V32-V35	9.99×10^{-4}	5.85×10^{-4}	6.70×10^{-4}	NF	NF	NF	1.31×10^{-4}	NF	NF	NF	NF	NF
V36-V39	7.48×10^{-4}	7.83×10^{-4}	8.96×10^{-4}	NF	NF	NF	NF	NF	NF	NF	NF	NF

Calculated LOC frequency values for the reference flood scenarios considered range between 1×10^{-5} and $3 \times 10^{-3} y^{-1}$. A comparison was carried out with the frequencies of LOC events due to internal failures available in the technical literature. In particular, according to the “Purple Book” (Uijit de Haag and Ale, 1999), data for pressurized vessels range between $5 \times 10^{-7} y^{-1}$ (catastrophic and 10 minute release of entire inventory) and $1 \times 10^{-5} y^{-1}$ (release from a 10 mm equivalent diameter). In the case of atmospheric storage tanks with single containment, the conventional expected LOC frequencies are quite higher: $5 \times 10^{-6} y^{-1}$ (catastrophic and 10 minute release of entire inventory) and $1 \times 10^{-4} y^{-1}$ (release from a 10 mm equivalent diameter). These figures are more than one order of magnitude lower than the site-specific flood-induced LOC events calculated in the case-study. This confirms that in flood-prone zones, NaTech scenarios triggered by floods may significantly contribute to the risk of an industrial facility. Nevertheless, an increase in the height of the anchorage was evidenced as a possible protection barrier.

5.5 Conclusions

A model was developed to calculate the failure probability of horizontal cylindrical vessels as a function of flood severity. The modelling approach was validated against available literature data and allowed the identification of the more critical parameters affecting the vessel resistance to the flood. Several simplified correlations were derived for the straightforward estimation of vessel resistance. The application of the developed model and of the simplified correlations to a case-study confirmed that NaTech scenarios caused by floods may have an important influence on the risk due to major accidents caused by the release of hazardous substances. The importance of an appropriate design of the vessel support and basements was evidenced, highlighting the potential importance of mitigation barriers in the prevention of NaTech scenarios triggered by floods. However, while selecting appropriate basements one should take into account both parameters related to the credible flooding scenarios and the resistance of the vessel.

References

- American Petroleum Institute (API). Design and Construction of Large, Welded, Low-Pressure Storage Tanks - API standard 620. 10th ed. Washington, D.C.: American Petroleum Institute; 2002.
- American Society of Mechanical Engineers (ASME) Boiler and Pressure Vessel Committee. Boiler and Pressure Vessel code, Section VIII, Div. 1. New York: American Society of Mechanical Engineers; 1989.
- American Society for Testing Material (ASTM). ASTM standard F 568M-2004 Standard specification for carbon and alloy steel externally threaded metric fasteners. West Conshohocken, Pa: ASTM; 2004.
- Antonioni G, Bonvicini S, Spadoni G, Cozzani V. Development of a frame work for the risk assessment of Na-Tech accidental events. *Reliab Eng Syst Saf* 2009;94:1442–50.
- Antonioni G, Spadoni G, Cozzani V. A methodology for the quantitative risk assessment of major accidents triggered by seismic events. *J Hazard Mater* 2007;147:48–59.
- Bates PD, Dawson RJ, Hall JW, Horritt MS, Nicholls RJ, Wicks J et al. Simplified two-dimensional numerical modelling of coastal flooding and example applications. *Coastal Eng* 2005;52:793–810.
- Boyce MP. Transport and storage of fluids, Section 10. In: Perry's Chemical Engineers' Handbook. 7th ed. New York: McGraw-Hill; 1999.
- Bryant E. Natural Hazards. New York: Cambridge University Press; 2005.
- Campedel M. Analysis of major industrial accidents triggered by natural events reported in the principal available chemical accident databases. Report EUR 23391 EN. Ispra (I): Commission of the European Communities; 2008.
- Charlton R. Fundamentals of fluvial geomorphology. Abingdon, Oxon: Routledge; 2008.
- Cozzani V, Campedel M, Renni E, Krausmann E. Industrial accidents triggered by flood events: Analysis of past accidents. *J Hazard Mater* 2010;175:501–9.
- Department of Regional Development and Environment Executive Secretariat for Economic and Social Affairs Organization of American States. Primer on Natural Hazard Management in Integrated Regional Development Planning. Washington, D.C.: Dept. of Regional Development and Environment, Executive Secretariat for Economic and Social Affairs, Organization of American States; 1991.
- European Committee for Standardization (CEN). European Standard EN 1993-1-8:2005. Eurocode 3: Design of steel structures. Part 1-8: Design of joints. ICS 91.010.30. Brussels: CEN; 1993.
- G. Fabbrocino, I. Iervolino, F. Orlando, E. Salzano, Quantitative risk analysis of oil storage facilities in seismic areas, *J. Hazard. Mater.* 123 (2005) 61–69.
- Grunfest E, Pollack D. Warnings, mitigation, and litigation: Lessons for research from the 1993 flood. *Update Water Resources* 1994;95:40-5.
- Gudmestad OT, Moe G. Hydrodynamic coefficients for calculation of hydrodynamic loads on offshore truss structures. *Marine Struct* 1996;9:745-58.
- Hanna SR, Strimaitis DG, Chang JC. Hazard response Modeling uncertainty (A quantitative method). Report ESL-TR-01-28. Sigma Research Corporation: Westford, MA, USA, 1993.
- Holmes RR Jr. Field methods for hydrologic and environmental studies. In: Holmes RR Jr., Terrio PJ, Harris MA, Mills PC editors, Introduction to field methods for hydrologic and environmental studies, Open-File Report 01-50, Urbana: US Department of Interior U.S. Geological Survey; 2001, p. 1-75. Available at http://il.water.usgs.gov/pubs/ofr01-50_chapter1.pdf

- I. Iervolino, G. Fabbrocino, G. Manfredi, Fragility of standard industrial structures by a response surface based method, *J. Earth. Eng.* 8 (2004) 1.
- International Organization for Standardization (ISO). ISO 7411:84 Hexagon bolts for high-strength structural bolting with large width across flats (thread lengths according to ISO 888) -- Product grade C -- Property classes 8.8 and 10.9. Geneva: ISO; 1984a.
- International Organization for Standardization (ISO). ISO 7413:1984 Hexagon nuts for structural bolting, style 1, hot-dip galvanized (oversize tapped) -- Product grades A and B -- Property classes 5, 6 and 8. Geneva: ISO; 1984b.
- Italian Ministry of the Interior. Decreto Ministeriale 14/02/1997, Direttive tecniche per l'individuazione e la perimetrazione, da parte delle Regioni, delle aree a rischio idrogeologico. Rome: Italian Ministry of the Interior; 1994.
- Krausmann E, Renni E, Campedel M, Cozzani V. Industrial accidents triggered by earthquakes, floods and lightning: lessons learned from a database analysis. *Nat Hazards* 2011;59:285–300.
- Kulak GL, Fisher JW, Struik JHA. Guide to design criteria for bolted and riveted joints. 2nd ed. Chicago: American Institute of Steel Construction, Inc; 2001.
- Landucci G, Antonioni G, Tugnoli A, Cozzani V. Release of hazardous substances in flood events: Damage model for atmospheric storage tanks. *Reliab Eng Syst Saf* 2012;106:200-16.
- Landucci G, Necci A, Antonioni G, Tugnoli A, Cozzani V. Release of hazardous substances in flood events: Damage model for horizontal cylindrical vessels. *Reliab Eng Syst Saf* 2014;132:125-145.
- Liley PE, Thomson GH, Friend DG, Daubert TE, Buck E. Physical and chemical data. In: Perry's Chemical Engineers' Handbook. 7th ed. New York: McGraw-Hill; 1999.
- Necci A, Antonioni G, Cozzani V, Krausmann E, Borghetti A, Nucci CA. A model for process equipment damage probability assessment due to lightning. *Reliab Eng Syst Saf* 2013;115:91–9.
- New South Wales Government. Floodplain Development Manual: the management of flood liable land, Appendix L "Hydraulic and Hazard Categorization". Sydney: Dept. of Infrastructure, Planning and Natural Resources; 2005.
- Pistrika AK, Jonkman SN. Damage to residential buildings due to flooding of New Orleans after hurricane Katrina. *Nat Hazards* 2010;54:413–34.
- Ramachandra Rao A, Hamed KH. Flood frequency analysis. London: CRC Press; 2000.
- Rasmussen K. Natural events and accidents with hazardous materials. *J Hazard Mater* 1995; 40:43–54.
- Research Council on Structural Connections (RCSC). Specification for structural joints using high-strength bolts. Chicago: RCSC; 2009.
- Rijkswaterstaat. Flood risks and safety in the Netherlands (Floris), Report DWW-2006-014. Delft: Rijkswaterstaat, Dutch Ministry of Infrastructure and Environment; 2005.
- Salzano E, Iervolino I, Fabbrocino G. Seismic risk of atmospheric storage tanks in the framework of quantitative risk analysis. *J Loss Prev Process Ind* 2003;16:403–9.
- Sinnott RK. Coulson & Richardson's Chemical Engineering, Vol. 6, 3rd ed. Chemical Engineering Design. Oxford: Butterworth-Heinemann; 1999.
- Tilton JN. Fluid and particle dynamics, Section 6. In: Perry's Chemical Engineers' Handbook. 7th ed. New York: McGraw-Hill; 1999.
- Uijt de Haag PAM, Ale BJM. Guidelines for quantitative risk assessment (Purple Book). The Hague: Committee for the Prevention of Disasters; 1999.
- U.S. Army Corps of Engineers. The great flood of 1993 post-flood report: Upper Mississippi River and lower Missouri River basins. St. Louis: U.S. Army Corps of Engineers; 1993.

Young S, Balluz L, Malilay J. Natural and technologic hazardous material releases during and after natural disasters: a review. *Science of the Total Environment* 2004;322:3–20.

Chapter 6:

Probability assessment of multilevel domino scenarios

6.1 Introduction

In the risk analysis of accident scenarios, cascading events in industrial sites are raising a growing concern. The so called domino effect has become a main safety issue that needs to be managed in order to avoid major accidents that affected the chemical and process industry (Reniers and Cozzani, 2013). Difficulties arise when trying to assess risk due to domino events, often related to the lack of specific tools and methodologies.

In the last 20 years a lot of work has been performed on the research in the field of domino accidents, and novel tools and procedures are now available. Nevertheless, knowledge gaps concerning domino effect assessment are still relevant. In particular one of the main issue is related to the assessment of accident propagation, due to tendency of domino accidents to grow in complexity as the size of the plant grows in size.

By the use of Markovian analysis this paper aims at the statistical description the possible multilevel domino propagation of domino scenarios associated with an industrial activity. The probability and frequency calculation for those domino scenarios provide the required input parameter for the quantitative risk assessment of industrial accidents due to domino events.

The main element that identifies scenarios where a “domino effect” takes place is the “propagation” effect. It is universally recognized that in a “domino” accident the propagation (in space and/or in time) of an initiator accident should take place to start one or more than one secondary accidents. Thus, two further elements of a domino scenario may be identified in relation to the “propagation” element: the presence of a “primary scenario” and of one or more than one “secondary scenarios”. The result is a set of contemporary accidents that takes the name of “domino scenario” (Reniers and Cozzani, 2013b).

To study the propagation of domino accidents means to analyze the mechanisms by which equipment are damaged by the accidental scenarios and generate new accidents themselves. Nevertheless, while dealing with domino scenarios one should take into account an important fact: the propagation is relevant only if it results in an “escalation” of the consequence of primary event (Cozzani et al., 2005). Four elements may thus be considered to characterize a domino event (Reniers and Cozzani, 2013b):

- (i) A primary accidental scenario, which triggers the domino effect.
- (ii) A propagation effect following the primary event, due to the effect of escalation vectors caused by the primary event on secondary targets.
- (iii) One or more secondary scenarios, involving the same or different plant units, causing the propagation of the primary event to other equipment.
- (iv) An escalation of the consequences of the primary event, due to the effect of the secondary scenarios.

The escalation is caused by the damage of at least one equipment item, due to the physical effects (e.g. fires, blast waves, fragments) of the primary event (Landucci et al., 2009a; Landucci et al., 2009b; Leslie and Birk, 1991; Birk and Cunningham, 1994; Birk, 1995; 1996; Cozzani et al., 2004). The damage to process equipment usually result in secondary accidents. Moreover, the secondary accident scenarios have chances to generate further accidents, which may eventually be the cause of further propagation of the event and augmenting the overall consequences of the domino scenario (Reniers et al., 2013b).

Figure 1 shows alternative propagation patterns that may be assumed in the analysis of domino scenarios (Reniers et al., 2013 CHAPTER IN DOMINO BOOK). A “simple” propagation may be assumed, defining a “one-to-one” correspondence, that is, a single primary scenario triggering a single secondary scenario (Delvosalle et al., 2002). Alternatively, second-, third- and more in general multilevel propagation may be assumed, defining a so-called multilevel “domino chain”: a first accident scenario triggers a second accident scenario, the second accident scenario triggers a third accident scenario, and so on.

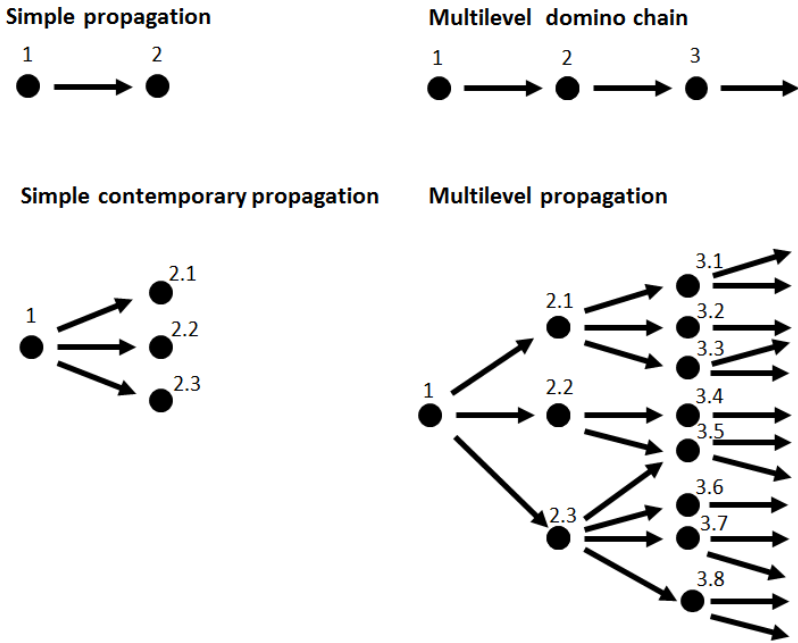


Figure 6.1. Different escalation patterns used for the description of the domino propagation mechanism

The paper by Cozzani et al. (2005) remarks that more than one secondary scenario may take place simultaneously, given a single primary event. Secondary scenarios may also trigger more than one secondary scenario, defining a complex net of sequential and parallel propagation possibilities. This mechanism takes the name of “multilevel propagation” (Reniers et al., 2013). This mechanism may be extremely complex to analyze even if the number of equipment units, which are mutually capable to trigger domino effect one to the other, is limited. It is easy to imagine that, as the number of units increases, the complexity rises exponentially. In the

original framework proposed by Cozzani et al. (2005; 2006), only domino scenarios deriving directly from the primary events are considered. Thus, only first level escalation is considered and scenarios deriving from the further escalation of secondary events (the so called multilevel-escalation (Cozzani et al., 2013a)) is not considered. However, higher level domino events may be accounted as well by the extension of the proposed methodology (Cozzani et al., 2014; Antonioni et al., 2009). Nevertheless, the application of the procedure for simultaneous domino event to domino scenarios that may have multilevel propagation, has a very high computational demand as the system grows in complexity and the computing times may become prohibitively high.

In order to assess the probability of the accident scenarios generated in a such complicated mechanism, a dedicated mathematical methodology is required. The study by Abdolhamidzadeh et al. (2010) presents a methodology for the calculation of domino accident frequencies based on Monte Carlo simulations, in order to avoid the complexity given by the complication of the combinatorial analysis. Bayesian networks may be also applied in order to assess the probabilities of a event in a complex environment and have been applied to the frequency assessment of domino accidents as well (Khakzad et al. (2013)).

The aim of the present work is to develop a methodology to evaluate the probability of every accident scenario produced at the end of the entire accident chain that constitute the escalation process. Knowing the probabilities for each domino scenario to occur allows the calculation of domino scenario frequencies in order to obtain input data for the QRA procedure. In this chapter an advanced methodology tool for the calculation of domino accident frequencies is presented. The transition of the system from each domino scenarios to any possible higher level domino scenario is considered allowing the drawing of the possible propagation pattern. Using the Markovian analysis the probabilities of transition between each scenario to the others may be obtained. Transition probabilities allows to represent the evolution of the system with time, therefore the probabilities of the all the final states of the system, which represent all the possible domino scenarios, can also be assessed. Finally, the frequencies of all the possible secondary accidents can also be calculated.

6.2 Multilevel domino assessment using Markov analysis

6.2.1. Methodology Overview

The current study is aimed at the development of a dedicated methodology for the assessment of the domino scenario frequency caused by complex accident chains, in which secondary accidents are cause of further accident escalation themselves. As shown in chapter 2, it is possible to associate a single escalation vector and a single vulnerability vector to each scenario. In the reference literature, domino accident frequencies are calculated as follows:

$$f_{de} = f_{pe}P_d = f_{pe}P(E|PE) \tag{6.1}$$

where f_{de} the domino event frequency, f_{pe} is the primary event frequency and $P(E|PE)$ is the conditional probability of escalation (E) given the primary event (PE) (Cozzani et al., 2005), which depends on the target vulnerability, P_d . If calculating the conditioned probability of escalation to the respect of a primary scenario, characterized by a single accident, is already a complicated task that requires the tools of frequentistic probability and combinatory logic, it becomes even more complex when the secondary scenarios can also generate complex events. Furthermore, even calculating the vulnerability of secondary targets to the respect of complex scenarios is not an easy task, since many sources for equipment damage are present in the area at the same time.

For these reasons a novel methodology, able to deal with the dynamics of the accident propagation process is proposed in the present document. A schematic description of the methodology is provided in Table 6.1.

Table 6.1: Detailed description of the three steps of the methodology

1 Modelling the consequences	1.1 Identification of all the primary accident and of a single secondary accident for every equipment unit 1.2 Consequence assessment of all the primary scenarios and of for every equipment that stores hazardous substances in the plant 1.3 Selection of a primary accident
2 Hazard identification	2.1 Identification of possible target units 2.2 Calculation of the ensemble of the possible configuration the domino system can assume: the set of accidental scenario 2.3 Identification of the possible paths for the transitions between the states of the domino system by the DAG construction
3 Frequency calculation	3.1 Estimation of the damage probability for each target unit to the respect of every domino scenarios 3.2 Calculation of transition probabilities between the possible states of the domino system 3.3 Probability calculation for every domino scenario at the end of the escalation process 3.3 Calculation domino scenario frequencies

The first step of the methodology is to assess the consequences for every accident of all the equipment units that stores hazardous substances in the industrial facility. A set of accidental scenarios is identified for every equipment; one, or more, scenarios may be the starting point

of a domino event. Furthermore, one of the scenarios is selected to be the secondary accident, for each unit, depending on the substance stored and on the equipment typology. Each scenario able to cause domino effect (i.e. fire and explosion scenarios) is called “primary scenario”; each primary scenario must be analyzed in order to assess the probability of domino scenarios to occur. One at once, all the primary scenarios are selected. Each scenario represents specific accident consequences, calculated for a given accident typology, weather stability class, wind speed and direction.

The second step is to identify the hazards associated to the escalation process, in particular to identify all the possible scenarios, intended as a combination of simultaneous accidents. The identification of all the possible equipment involved in the escalation process is, thus, a crucial task, which is achieved by the application of consequences of the primary scenario to the map containing the industrial layout, thus selection of the secondary units by a threshold-based criteria. Furthermore, all the possible paths for the accident escalation process must be identified. The ensemble composed by: the primary scenario, all the secondary accidents and the possible escalation paths represent the “domino system”, which is going to be analyzed in order to calculate domino accident frequency. Each combination of the domino system elements represent one of the possible states that can be taken by the system at a given time after the escalation has started. Each combination, which describe a system state, represents also a possible domino scenario. The “domino system” can be schematized by the construction of a “Directed Acyclic Graphs” (DAG), in which all the states that can be eventually taken by the system are drawn, as well as conditional dependencies between the states are reported.

The third step is the probability and frequency calculation for all the domino scenarios which have been identified. A new combinatorial methodology is developed for the probability assessment of these scenarios, based on the Markovian analysis and on the calculation of probability of transition between different states of the domino system. This method allows to consider multiple sequential and parallel steps for the propagation/escalation process and to evaluate the probabilities of domino scenarios due to “multilevel propagation”. In this step, the vulnerability of target units are calculated to the respect of each possible scenarios. Then, the transition probabilities from one state to another are also calculated, allowing the calculation of the probabilities of each domino scenarios. Finally, by the application of the primary event frequency to the probability of all the possible scenarios, also the expected frequencies of domino scenarios are calculated.

6.2.2. Preliminary considerations regarding domino scenarios

In conventional QRA several procedures are may be applied for the assessment of the frequency of an accidental scenario. The most popular technique is the use of dedicated event trees (REF Purple), in which the calculation of accident scenario frequencies represents the final step. When dealing with domino effect one should consider each scenario as a potential initiator event for a devastating escalation process, which generates secondary accidents, usually with more serious consequences than the initiator accident. The secondary scenarios, which are caused by a specific initiator accident, called “primary accident” , may have the

potential to damage or to destroy other structure or equipment containing hazardous material. As a secondary target get damaged, a secondary accident immediately follows. Moreover, secondary accidents may eventually generate other accidents themselves. Thus, every “primary scenario” which has escalating potential should not be analyzed as a single scenario, but as an entire “set of accidental scenarios” (Figure 6.2). When assessing QRA procedure with the intent to analyze domino accidents this consideration should be applied to every accident which is able to damage neighbor equipment, i.e. every fire and explosion scenarios.

It is worth to remark that the probability to experience secondary accidents, for the most of causes (e.g. pool fires, jet fires, VCE), is strongly influenced by the wind speed and direction. In order to analyze the damage to humans and the possibility for further domino escalation, for “domino scenario” it is considered the combinations of the consequences of the primary scenario and of each secondary scenario, which represent a characteristic accident combination. Furthermore, a scenario can be modelled only, if the three variables that govern the meteorological condition (the stability class, the wind speed and the wind direction) are known.

Nevertheless, other data are required to apply the procedure defined in Table 6.1: information regarding the lay-out of the site examined, in particular, the position on the lay-out of the potential primary events (consequences and frequency of the primary events must be well known) and of all the potential targets for the escalation (again consequence of secondary accidents should be known). Likely, all these data are already provided when addressing a conventional QRA, thus the additional work for data collection is limited.

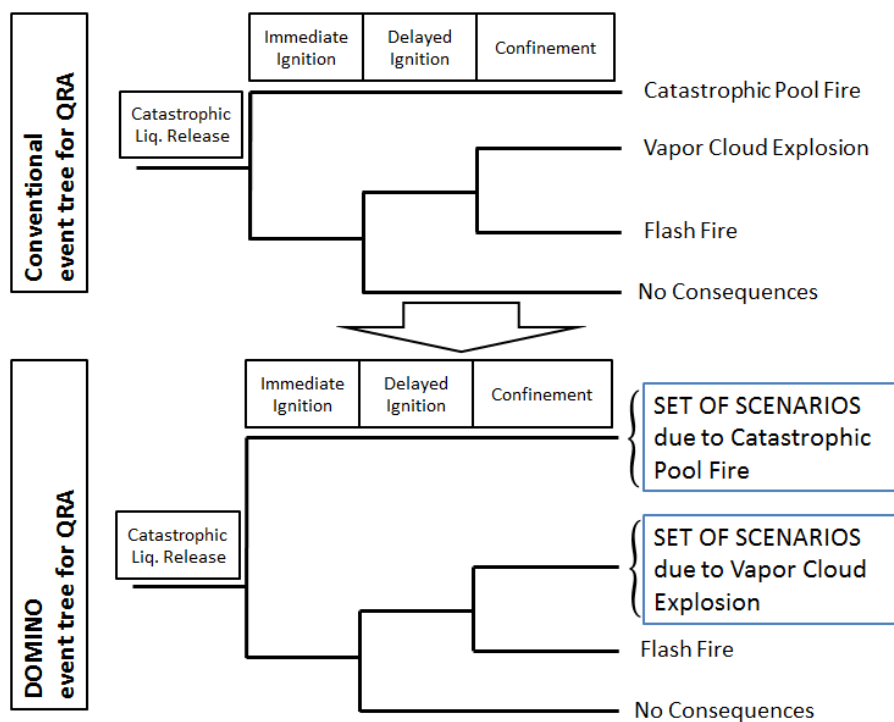


Figure 6.2. The example of catastrophic liquid release has been considered in order to show the difference between the approach for conventional QRA and QRA of domino scenarios

6.2.3. Secondary accident typology selection

In this study a single typology of damage modality, and thus of “secondary accident”, is considered per typology of target equipment, independent from the escalation vector that triggered the secondary accident. In order to identify the secondary accident typology the following data are required: the pressure condition of the vessel; the aggregation state of the stored substance (Liquid, Gas, Liquefied Vapour) and the hazardous properties of the substance (Flammable and/or toxic). Moreover, often physical effect related to an accidents may have differenced effects for humans and for other target equipment. A list of damage modalities, secondary scenarios, escalation vectors and physical lethal consequences for all the possible secondary target typologies is reported in table 6.2.

Table 6.2: Secondary accident selection criteria

Secondary Target	Stored substance hazardous properties	Damage modality	Secondary scenarios	Associated escalation vector	Associated physical lethal effect
Atmospheric	Flammable Liquid	Cat. Rupture + immediate ignition	Pool Fire	Thermal radiation	Thermal radiation
	Toxic Liquid	Cat. Rupture	Pool Evaporation + Toxic Dispersion	None	Toxic Dose
	Toxic + Flammable Liquid	Cat. Rupture + immediate ignition	Pool Fire	Thermal radiation	Thermal radiation (Toxic Dose?)
Pressurized	Flammable Gas	Cat. Rupture + immediate ignition	EXPLOSION mech	Overpressure + Fragment	Overpressure
	Toxic Gas	Cat. Rupture	EXPLOSION mech + Toxic Dispersion	Overpressure + Fragment	Overpressure + Toxic Dose
	Toxic + Flammable Gas	Cat. Rupture + immediate ignition	EXPLOSION mech + Toxic Dispersion	Overpressure + Fragment	Overpressure + Toxic Dose
	Flammable Liq. vapour	Cat. Rupture + immediate ignition	BLEVE + FIREBALL	Overpressure + Fragment + Heat Load	Overpressure + Heat Load
	Toxic Liq. Vapour	Cat. Rupture	BLEVE + Toxic Dispersion	Overpressure + Fragment	Overpressure + Toxic Dose
	Toxic + Flammable Liq. vapour	Cat. Rupture + immediate ignition	BLEVE + FIREBALL	Overpressure + Fragment + Heat Load	Overpressure + Heat Load

6.2.4. Identification of targets for the escalation process and domino system definition

The definition of the accident escalation process target equipment and, thus, the typology of secondary accidents triggered, is a critical issue, because the set composed by the primary accident and by all the possible secondary accident represents the closed system in which the entire escalation process proceeds, the “domino system”. Furthermore, the secondary accidents generated may trigger the escalation to other equipment themselves. Thus, the quantitative assessment of domino events requires the identification, the frequency evaluation and the consequence assessment of all the credible domino scenarios, considering all the possible combinations of secondary scenarios that may be originated by each primary scenario. The identification of targets and of the respective secondary accidents triggered by a primary scenario scenario is a also a main issue. The set composed by the primary scenario and by all the possible secondary scenarios represents the “domino system” in which the entire escalation process proceed.

Table 6.3 Modality and escalation criteria for the most common accidents divided by typology

Scenario	Escalation vector	Modality	Escalation criteria	
			Atmospheric Vessel	Pressurized Vessel
Flash fire	Heat radiation	Fire impingement	Unlikely	Unlikely
Fireball	Heat radiation	Flame engulfment	$I > 100 \text{ kW/m}^2$	Unlikely
		Stationary radiation	$I > 100 \text{ kW/m}^2$	Unlikely
Jet-fire	Heat radiation	Fire impingement	Always possible	Always possible
		Stationary radiation	$I > 10 \text{ kW/m}^2$	$I > 40 \text{ kW/m}^2$
Pool fire	Heat radiation	Flame engulfment	Always possible	Always possible
		Stationary radiation	$I > 10 \text{ kW/m}^2$	$I > 40 \text{ kW/m}^2$
VCE	Overpressure	$MEM F \geq 6;$ $M_f \geq 0.35$	$P > 22 \text{ kPa}$	$P > 16 \text{ kPa}$
Confined explosion	Overpressure	Blast wave interaction	$P > 22 \text{ kPa}$	$P > 16 \text{ kPa}$
Mechanical explosion	Overpressure	Blast wave interaction	$P > 22 \text{ kPa}$	$P > 16 \text{ kPa}$
		Fragment projection	Fragment impact	Fragment impact
BLEVE	Overpressure	Blast wave interaction	$P > 22 \text{ kPa}$	$P > 16 \text{ kPa}$
		Fragment	Fragment impact	Fragment impact
Point-source explosion	Overpressure	Blast wave interaction	$P > 22 \text{ kPa}$	$P > 16 \text{ kPa}$

The identification of the credible domino scenarios should be based on escalation criteria addressing the possible damage of equipment due to the physical effects of the primary and secondary scenarios. The physical effects resulting from an accidental scenarios are applied on the map containing possible targets, allowing the assessment of the value of the harmful effect at the target position. The use of threshold values, which are compared with the values of the physical effect actually applied at the location of the process units containing hazardous materials allows the identification of potential domino targets. The use of threshold-based criteria is a common practice for the preliminary analysis of domino risk (Ref Cozzani and Salzano., 2006). An extended discussion on the procedures for the identification of the possible

contemporary domino scenarios due to a primary event, by the use of threshold values, is reported elsewhere (Cozzani et al., 2005). Table 6.3 summarizes the suggested threshold values obtained in the previous study and adopted herein to identify the credible escalation targets. Literature models from the “Yellow Book” (Van Den Bosh & Weterings, 2005) were used in the present approach for the calculation of the physical effects arising from the final outcomes of primary events.

However, in the case of multilevel propagation a further step must be made. Once the secondary targets are identified the secondary scenarios must also be identified and, their consequences can be applied on a map. This allows the calculation of possible tertiary targets and tertiary scenarios are also identified. The procedure continues until either all the remaining equipment units suffer an amount of damage which is below the threshold, or all the units in the area have been considered already.

Figure 6.3 reports an example of the application of threshold criteria for the identification of possible targets for the propagation process. A simplified layout composed by 5 units is considered. In this example P is the primary source, while A, B and C are possible escalation targets and, thus, secondary sources, D is another item which is not involved in the escalation process. The system analyzed is composed by: the primary accident, and the accidents of equipment A, B and C. The same threshold values, applied for determining the escalation criteria at the primary accident, apply also to secondary accidents.

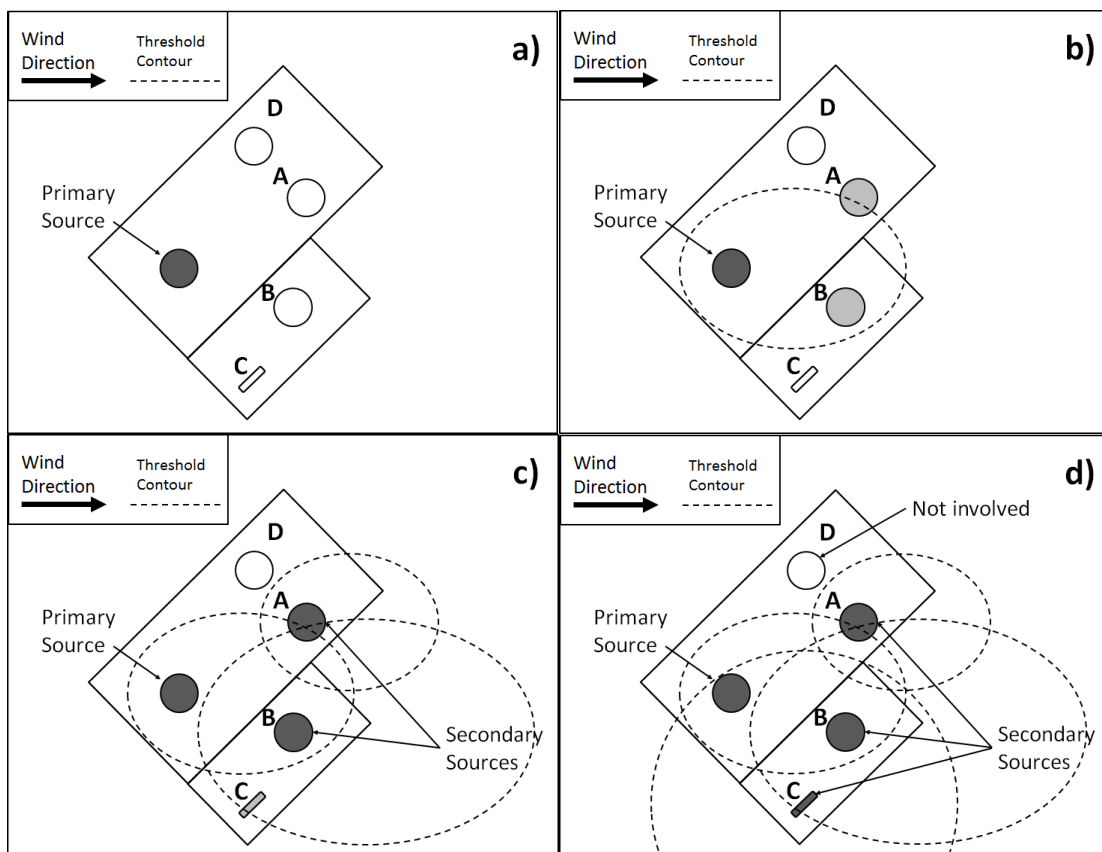


Figure 6.3: Example of the threshold criteria application to assess possible secondary target and sources for domino accidents; a) The primary source; b) Threshold contour for the primary accident that contains the potential secondary targets; c) threshold contours of secondary sources containing potential tertiary targets; d) threshold contours of all sources, with no further targets

On the contrary of other methods, Cozzani et al.,(2005; 2006) consider target for accident escalation only those units affected by the consequences of the primary scenario, in the example shown in the figure also the targets of secondary scenarios (i.e. the item C) are considered.

6.2.5 The accidental scenario set

Cozzani et al. (2005; 2006) presented a methodology that allows the calculation of individual and societal risk caused by domino accidents contribution in the risk profile of an industrial plant, that analyses the entire “set of possible domino scenarios” triggered by the primary event. The domino scenario set is composed by all the possible combinations of the primary and all the secondary scenarios. In the reference literature, the probability of accident escalation have been calculated by the use of dedicated vulnerability models (Cozzani and Salzano 2004a; 2004b; Landucci et al. 2009; Gubinelli and Cozzani, 2009a; 2009b).

In multilevel propagation, the probabilities of accident escalation to one scenario or to the other are mutually conditioned and all the possible combinations of the credible and relevant secondary events should be considered in the analysis. Each combination of secondary scenarios represent one possible domino scenario. Therefore, the probability of all the secondary scenario combinations must be calculated in order to assess the risk related to escalation scenarios, for a given primary event.

If first level escalation only is considered (Reniers and Cozzani, 2013b), the event combinations may be reasonably considered as independent from a probabilistic point of view. However, when multilevel propagation is considered, the probabilities of the scenarios are the one conditioned to the happening or non-happening of the other scenarios.

Table 6.4: The set of all the possible accidental scenarios due to escalation to three equipment, other than the initial scenario. Each scenario is represented by a vector of Boolean variables: 0 represents the safe condition; 1 represents the failed condition. P indicates the equipment where the primary scenario occurs, which is obviously considered damaged, A, B, C represent the three possible targets.

STATE	P	A	B	C
S01	1	0	0	0
S02	1	1	0	0
S03	1	0	1	0
S04	1	0	0	1
S05	1	1	1	0
S06	1	1	0	1
S07	1	0	1	1
S08	1	1	1	1

Given the number of target vulnerable equipment n_t , the possible scenario combinations are determined by the possibility that every equipment is either “healthy” or “failed”. In the condition “healthy”, no harm is assumed to the unit, while in the condition “failed” the unit is considered significantly damaged, furthermore an accident is considered to take place. The

typology of accident should be selected according to the indications provided in table 2. Each combination can be expressed as a vector of Boolean variables that represent the conditions healthy (0) and failed (1). These combinations represents the ensemble of the possible domino scenarios for the risk analysis. Furthermore, each combination can be considered as a possible state that can be assumed by the domino system at a given time after the start of the propagation process.

Combinations of n_t binary items (healthy, failed) can be calculated, for a total of 2^{n_t} admissible combinations, including the combination in which no domino effect occurs, which is also representative of the initial state of the domino system in which domino effect have not happened yet.

As an example it is considered a primary accident which expose other three equipment ($n_t=3$), containing hazardous substances, to a physical effect with potential destructive effects. The possible domino scenarios are $2^3=8$, represented as all the possible combinations of three binary objects: A,B, C and the primary event, P, (see Figure 6.2) are reported in Table 6.4, organized in growing order for the number of accidents that compose the scenarios.

6.2.6 System and “states” description: the construction of the Directed Acyclic Graph (DAG)

In order to evaluate the probability of escalation from one domino scenario to another, every “scenario” represents one possible “state” that can be assumed by the domino system at a given time after the primary accident have happened. With the time progression, “states” have a possibility to further evolve at a domino scenario with a higher number of secondary scenarios. In fact, in the propagation mechanism it is possible to catch causal dependencies between domino scenarios. Domino scenarios characterized by a high number of secondary accidents, can be caused either directly by the primary scenario or by domino scenarios with a lower number of accidents.

One method to help understand the evolution of the system, which is dependent by the reciprocal relationship between the probabilities of each domino scenario to occur, is to use graphical representation in order to view the causal effects between the different variables. A Directed Acyclic Graph (DAG) is a graphical tool for reasoning under uncertainty in which the nodes represent variables and are connected by means of oriented arcs. In the directed acyclic graph (DAG) approach, an arrow connecting two variables, or nodes, indicates causation; variables with no direct causal association are left unconnected. In the case of domino events, arcs, which describe a causation relation, represent a probability of transition from one state of the domino system (or domino scenario), to another. Each node represents the probability of a given domino scenario, or state of the system at a given time. Assuming that several equipment may be effected at the same time, arrows draw the trajectories for the transitions from the one state toward all the possible admissible states with a higher number of secondary scenarios.

In order to draw the DAG, the domino scenarios must be grouped on the basis of the number of contemporary secondary scenarios. The assumption of non-repairable system components is applied, therefore every arc, originated in one node, can be directed either to other nodes with a larger number of accidents (accident propagation) or back to the same node (no further propagation).

In Figure 6.4 the example of DAG due to a system composed by a primary source and 3 target secondary equipment: A,B,C, is reported (the same of Table 6.4 and figure 6.3). Eight domino scenarios, thus the system can take eight possible state at a given time, represented in the figure as nodes. Each node is characterized by a color, thus the arcs that start in one node have the same color in order highlight the state transition which are possible or not possible, given a node.

The present methodology is developed to assess the probability of domino scenarios intended as the “end states” of the escalation process. For the calculation of the probability of a generic “end state” one should considers all the possible path that may lead to the final accidental scenario. However, the methodology remains exclusively combinatory. Thus, the dynamic investigation regarding the number of steps or the time necessary for the accident escalation, from the primary accident to the end state, are not concern of this work.

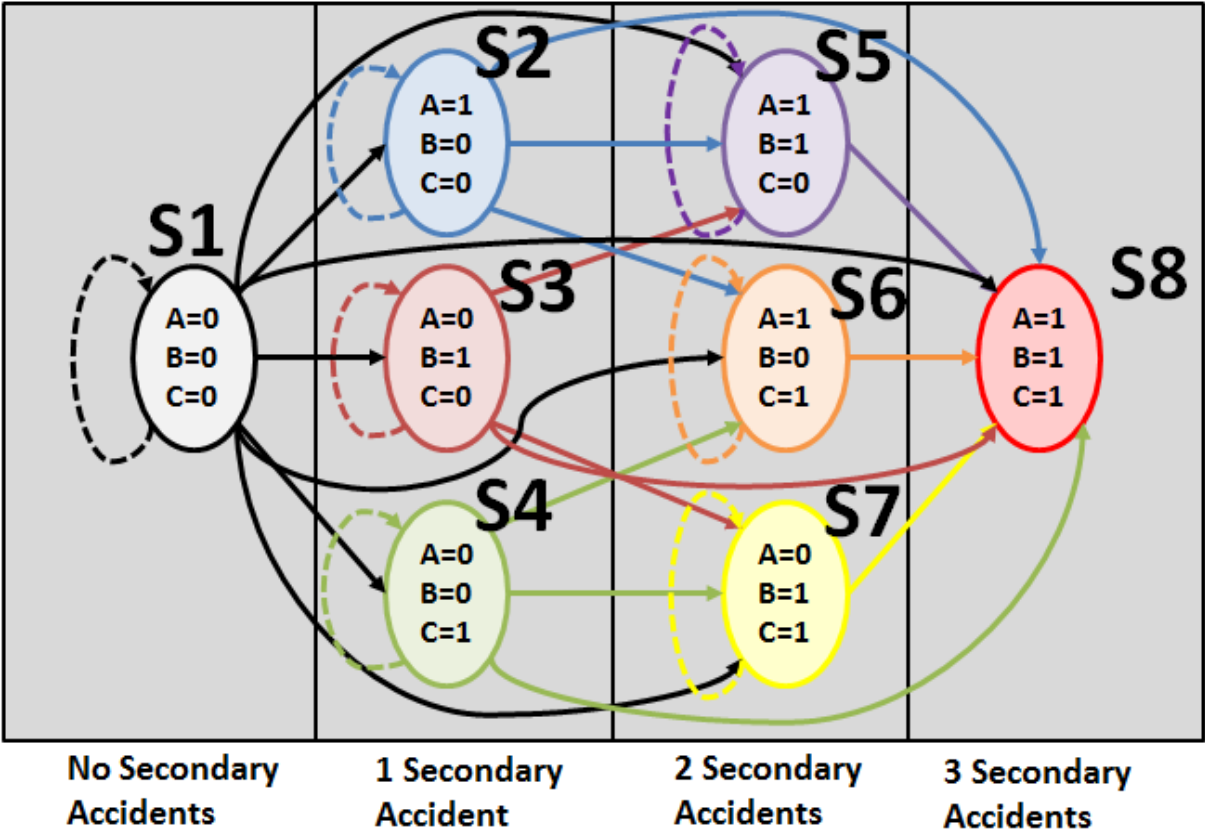


Figure 6.4: The DAG that represents the accident propagation to three possible secondary targets: A, B, C. Each node is Arrows represent all the possible transitions for the evolution of the system, the nodes represent the 8 states, S1-S8, the system may take.

6.2.7 Probability of accident escalation: transition between states

In the DAG, the arcs denote dependencies or causal relationships between the linked nodes. Since the domino system evolves with time the arcs represents the transition of the system from one state to another. Each transition is characterized by a finite probability of happening. In case of multilevel propagation, the accident escalation process can be simplified as a

sequence of transitions between the possible states that system can assume. In order to assess the probability of a given scenario, intended as a specific combination of secondary accidents, the probability of transition from one scenario to one of the others, characterized by a higher level of escalation, must be assessed.

In order to describe the system evolution, it is worth to define a methodology for the straightforward calculation of transition probability between the possible states of the systems. As a first step, Markovian analysis for the calculation of the transition probabilities and for the calculation of “end state” probability is applied. Since the probability of one state is independent of the rest of the states in the system given its immediate lower-level neighbors, the “local Markov property” is unequivocally valid for every node of the process. Furthermore, the value of the Initial state of the system, represented by the combination in which only the primary scenario is active, is known. It is also known that every state is conditioned only by the other states with a lower number of failed components and that the states with the same number of failed components are mutually exclusive.

Under those conditions, it is assumed that the transition probability from one generic “parent state”, at any position in the accident escalation chain (including the primary scenario), to a generic “son state” is function of the probability of the “parent state” only and not of the story that produced the “parent state”. In other words, the global Markov property is considered valid for all the states of the system under investigation and a transition matrix can be built. The edge is that all the transition probabilities are dependent only by the node where the transition start, if the global Markov property can be applied. This simplification allows to consider the possible states of the system as an ensemble of all accident combinations only. All the domino scenarios characterized by the same accident combination are merged into one, neglecting the differences due to the different paths that produces a specific domino scenario. This assumption is reasonably valid in the case the transition probabilities are constant until the transitions end. This condition is obtained when the physical effects, responsible of the escalation vectors, are also constant during the entire escalation process. Thus, the Markov property applies to domino scenarios composed by steady fires scenarios, but it does not apply to domino scenarios composed by explosion scenarios. This is because the effects of the explosion scenarios do not last in time, so they should be accounted for one transition only and do not apply to any further transitions. Therefore, the path that produced one scenario does influence the transition probabilities and the global Markov property cannot be applied. However, in the following the procedure will show how to deal with instantaneous scenarios, while maintaining the formalism which depends on the global Markov property.

6.2.7.1 Equipment vulnerability due to several secondary scenarios

The problem of multiple scenario sources has been addressed in the past for the assessment of human vulnerability. A vulnerability map of each domino event is calculated as a combination of the vulnerability maps of the primary and of the secondary scenarios that compose the domino scenario. Several possible strategies are suitable for the combination of the vulnerabilities, that are actually probability values (See section 6.2.4.3). However, the results of a previous study (Cozzani et al., 2005) suggested to calculate the domino vulnerability as the

sum of the death probabilities due to all the single scenarios which take place in the domino event, with an upper limit of 1. In the present study the same advice is applied for addressing equipment vulnerability due to multiple sources.

Once all the equipment, and thus the related accidents, that compose the system are identified, for each accident, being either a primary or secondary accident, it is possible to build a vector of vulnerabilities that reports the vulnerability of each target to the respect of a given source, being either a primary or secondary scenario. Each position of this vector ($P_{d,i}$), reports a value of target equipment vulnerability for each target, expressed as probability values. These damage probabilities are obtained, by the application of dedicated vulnerability expressions, which relate the target equipment vulnerability to gravity of the suffered destructive physical effect of the scenario (Cozzani et al., 2004; Landucci et al., 2009).

Each domino scenario is given by the combination of the effects of the primary scenario with the effect of one, or more secondary scenarios. For every domino scenario, a vulnerability map to the respect of people is built, as well as a “domino scenario vulnerability vector” that reports the values of target equipment vulnerability for each target, calculated as follows:

$$P_{d,i}^S = \min[(P_{d,i}^P + \sum_{j=1}^{nt} \delta(j, J_S^k) P_{d,i,j}, 1)] \quad (6.2)$$

where $P_{d,i}^S$ represents the vulnerability of i -th target to the respect of the overall effects due to the combined accidents in domino scenario S , $P_{d,i}^P$ represents the vulnerability of the i -th target to the respect of the effects of the primary accident P , $P_{d,i,j}$ represents the vulnerability of the i -th target to the respect of the effects of the j -th secondary scenario, J_S^k is a vector whose elements are the indexes of the combination of k secondary events that compose the domino scenario S , and the function $\delta(i, J_S^k)$ is defined as follows:

$$\delta(j, J_S^k) = \begin{cases} 1 & j \in J_S^k \\ 0 & j \notin J_S^k \end{cases} \quad (6.3)$$

Furthermore, in the case of secondary scenarios being targeting their own unit ($i=j$), $P_{d,i,j}$ is considered 1, since the unit has failed already. Therefore, the vulnerability of a generic equipment to high level domino scenarios are, generally, higher than the vulnerability to the primary scenario only, due to the additive contribution of all the secondary sources to the equipment damage. Thus, the transition probability between states is typically higher between high level states of the system, than those states at the beginning of the escalation process.

High level domino scenarios are composed by several accidents, which may significantly differ one to the other to the respect of the typology of dangerous physical effect and on gravity. Moreover, some secondary scenarios may happen simultaneously, while others may happen in sequence. In order to combine equipment vulnerabilities of several scenarios for a given domino scenario, two main accident typologies are thus identified to the respect of accident escalation assessment:

-“continuous escalation accidents” (CEA), which generate physic effects that last until the end of the escalation process and that contribute to the transition probability from the actual state of the system to all the subsequent states of the domino propagation process

- “instantaneous escalation accidents” (IEA), which generate physic effects that last for a very short time and that contribute to the transition probability from the actual state of the system to the first subsequent domino scenarios of the domino propagation process only.

The main difference is that those domino scenarios entirely composed by “continuous escalation accidents” follow the Markov property, while those constituted by at least one “instantaneous escalation accident” don’t.

In order to combine equipment vulnerability from a domino scenario composed by multiple continuous sources, the vulnerability vectors of each single scenario are added, according to equation (6.2). In this vector the probability of damage of all the survived equipment is reported to the respect of the additive effect of all the accidents of the current domino scenario. However the probabilities of the “instantaneous escalation accident” present in the domino scenarios must be considered with particular caution for the calculation of the vulnerability vector of the scenario, since their contribution last for the duration of one escalation step only. This property implies that only that the contribution to equipment vulnerability that comes from an **IEA** is not valid if the domino scenario representative of one state was produced by another state where that component was already failed. Moreover, if the primary event was an IEA, its contribution to the overall vulnerability of second, or higher, level scenarios should not be considered, with the exception of those transitions from the initial state to the others.

For a given state, **S**, in which the *m*-th is an **IEA** , the $P_{d,i,m}$ for the *m*-th scenario must be multiplied by a reductive factor, φ_m^S , given by the following expression:

$$\varphi_m^S = \frac{\sum_{L=1}^{nL} (J_m^{nL} \cdot B_L) \cdot P_L \cdot P_{L-S}}{\sum_{L=1}^{nL} P_L \cdot P_{L-S}} = \frac{\sum_{L=1}^{nL} (J_m^{nL} \cdot B_L) \cdot P_L \cdot P_{L-S}}{P_S} \quad (6.4)$$

Where nL is the number of parent states, B_L is the Boolean vector that identifies the *L*-th state, P_L is the probability of the *L*-th parent state, P_{L-S} is the transition probability between the *L*-th state and state *S*, P_S is the overall probability of state *S* to occur, due to all the possible parental states, J_m^{nL} is a Boolean vector with nL elements, whose elements are all zeros, except the one in position *m*, which is 1. In other words φ_m^S represents the ratio between: 1-the probability that the state *S* derives from other scenarios in which the event m^{th} was not happened yet, so it can be accounted for a further transition, and 2-the probability of state *S* to occur.

Figure 5 shows an example of the application this method by the use of graphs. State **p** and state **q** are both capable to generate state **r**; all three represent a combination of three Boolean variables: A, B, C. C is assumed to be IEA. In state **q**, C is positive, meaning it has already happened, while in scenario **p**, C is negative. In this example, the contribution of the event C to the overall vulnerability vector of state **r**, must take into account the happening of state **p** and not of state **q**.

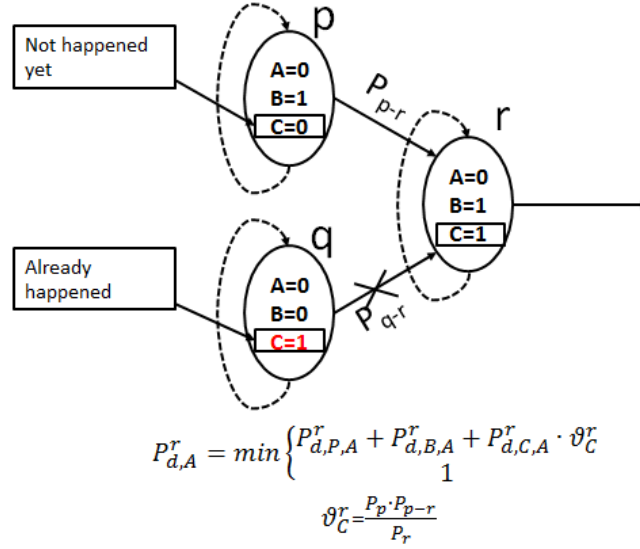


Figure 6.5: Example of the application of the methodology for the calculation of transition the vulnerability of element A to the respect of state r. In this picture C is IEA, and has happened in state q, but not in state p.

6.2.7.2 Transition probability calculation

After vulnerability vectors have been calculated for each domino scenario, transition probabilities between states can be assessed. A new vector: the transition vector, which has the same length as the number of domino scenarios N_s , is created for every scenario. In this vector the transition probabilities from one parent state to a son state (or to itself, meaning non further escalation) are reported. These probabilities are actually conditional probabilities, in the sense that they are conditioned to the happening of the referred parent state.

In order to calculate transition probabilities from one j^{th} parent state to i^{th} son state, the respective Boolean vectors, B_j and B_i , which are used to identify the scenarios and the states, must be compared element by element. The response this comparison is a new variable, $R_{j,i}$. The value of the response are reported in Table 6.5. Finally the transition probability can be calculated as the joint probability of all the n_t conditions addressed by the response, using the following equation:

$$P_{j-i}|P_j = \prod_k^{n_t} R_{j,i}(k) \quad (6.5)$$

Where $P_{j-i}|P_j$ is the transition probability from the j -th parent state to the i -th son state. An important outcome of this comparison tells us which transition are possible, since even one response of zero means that the transition cannot be made.

Table 6.5: The possible responses of the comparison of the k -th elements (k) of the Boolean vectors B_j and B_i

$B_j(k)$	$B_i(k)$	$R_{j,i}(k)$	Description
1	0	0	Impossible transition
1	1	1	Already damaged, no influence
0	1	$P_{d,k}^j$	Probability of damage
0	0	$(1 - P_{d,k}^j)$	Probability of non-damage

6.2.8 Application of the Bayes theorem: Conditional transition probabilities calculation and domino frequency assessment

The transition probabilities from one state to another are conditioned by the happening of the parent state where the transition starts. What is actually required for the calculation of the final scenario probabilities (or end state probabilities) for the domino scenario set is to calculate the transition probabilities, conditioned to the happening of the primary event.

One possible approach is to start from the first state of the domino system (the state in which all the target are safe and the only active scenario is the primary scenario) and to proceed to other states, following a growing order number of secondary scenarios. This rule forces to calculate the transition probabilities for all the “parent” states of the system, before to calculate the conditioned transition probabilities for the “son” states. A very simple calculation of conditioned transition probabilities it therefore performed, since all the variables needed to assess the transition probabilities are known. In order to calculate the probability of a generic transition $P_{j-i}|P_1$, conditioned to the initial scenario P_1 , by the use of $P_{j-i}|P_j$, the Bayes theorem can be applied:

$$P_{j-i}|P_1 = P_{j-i}|P_j \cdot P_j \quad (6.6)$$

Where P_j is the total probability for the system to assume the j -th state, independently by the path. Thus, it is calculated as the sum of all the contribution of all the conditional transition probabilities, conditioned to the happening of the initiator scenario, which target the j -th scenario.

$$P_j = (\sum_{k=1}^{j-1} P_{k-j}|P_1) \quad (6.7)$$

As a matter of fact without a primary accident no domino propagation occurs, therefore P_1 is considered 1. The procedure considers the number of failed secondary targets for each scenario and then continues in ascending order. No further criteria are needed for the selection among scenarios with the same number of failed components. This order is necessary because the local Markov property is valid, thus the parent state probability must be known before to assess the probability of derivate states. This order is also needed to assess φ_m^S , which can be calculated only if the story that produced the referred state it is known.

Once the new values of transition probability are calculated, new conditioned transition vectors can be generated. For each j -th state of the system the most important value for the transition vector is $P_{j-j}|P_1$. This value contains the joint probability that the j -th scenario has happened, conditioned to the primary scenario, and that this scenario has not propagated further.

In other words it represents the probability of the j -th scenario at the end of the escalation process: the conditional probability of the j -th domino scenario.

Once the end state probabilities are known, by the use of Eq. (6.1) the domino scenario frequency can also be calculated:

$$f_{ds,j} = f_{pe} \cdot P_{j-j}|P_1 \quad (6.8)$$

where $f_{de,j}$ the frequency of the j -th domino scenario, f_{pe} is the primary event frequency and $P_{j-j}|P_1$ is the end state probability, given the initiator event (state 1).

6.3 Results

6.3.1 Application to simplified case study

In order to apply the methodology a simple layout made of 4 items: a vessel where the primary accident occurs (P) and three potential targets (A, B and C) has been chosen. The layout selected was shown in Figure 6.3. Details for the definition of equipment typologies and for the selection of primary and secondary scenarios are reported in Table 6.6. The domino system is identified according to the threshold based approach proposed in section 6.2.4.

Table 6.6: Details of the units reported in the simplified case study. Scenario typology and damage probabilities of primary and secondary scenarios. (Cozzani et al., 2006)

	Typology	Substance	Primary	Secondary
P	Atmospheric	Gasoline	Pool Fire - CEA	-
A	Atmospheric	Gasoline	-	Pool Fire – CEA
B	Atmospheric	Gasoline	-	Pool Fire – CEA
C	Pressurized	LPG	-	BLEVE/Fireball - IEA

In order to identify the propagation probabilities, and thus to identify the transition vector there is the need to set damage probabilities. Three example values: low (0.01), medium (0.1) and high (0.6) are used for the damage probabilities. Negligible probability (10^{-7}) is assumed for those equipment outside the damage threshold contours drawn in Figure 6.3. Table 6.7 reports the damage probabilities for those equipment units in the case study.

Table 6.7: Vulnerability vectors for the units in the case study

Tank ID	Target A	Target B	Target C
P	0.01	0.1	10^{-7}
A	1	10^{-7}	10^{-7}
B	0.01	1	0.1
C	10^{-7}	0.6	1

The domino accident scenario set is, thus, identified on the basis of all possible combination of secondary accident scenario, each one can be identified as a Boolean vector. The scenario set has been already reported in Table 6.4. The transition probabilities from each scenario to the others, conditioned to the happening of the primary scenario, have been calculated following the instructions provided in section 6.2.7 and 6.2.8. The results, expressed as transition probabilities, collected in transition vectors, are reported in Table 6.8; the probability values lower than 10^{-6} are not considered, therefore a value of 0.00 is reported instead.

Table 6.8: The conditioned transition vectors containing the transition probabilities and the probability of domino scenarios

ID	S01	S02	S03	S04	S05	S06	S07	S08
Vector S01	8.91×10^{-1}	9.00×10^{-3}	9.90×10^{-2}	0.00	1.00×10^{-3}	0.00	0.00	0.00
Vector S02	0.00	8.10×10^{-3}	0.00	0.00	9.00×10^{-4}	0.00	0.00	0.00
Vector S03	0.00	0.00	0.00	0.00	8.91×10^{-2}	0.00	0.00	9.90×10^{-3}
Vector S04	0.00	0.00	0.00	0.00	0.00	0.00	0.00	0.00
Vector S05	0.00	0.00	0.00	0.00	8.19×10^{-2}	0.00	0.00	9.10×10^{-3}
Vector S06	0.00	0.00	0.00	0.00	0.00	0.00	0.00	0.00
Vector S07	0.00	0.00	0.00	0.00	0.00	0.00	0.00	0.00
Vector S08	0.00	0.00	0.00	0.00	0.00	0.00	0.00	1.90×10^{-2}
Domino Scenarios Probability vector	8.91×10^{-1}	8.10×10^{-3}	0.00	0.00	8.19×10^{-2}	0.00	0.00	1.90×10^{-2}

Vector S01 reports the results of the domino propagation due to primary scenario only and the transition probability values of this vector are the same of those obtained by the methodology proposed by Cozzani et al. (2005) for simple contemporary propagation. The overall probability of any domino scenario (the sum of all domino scenario probability) is the same considering both simple and multilevel propagation (about 11 %) and therefore the probability of “no domino”, represented by S01 is the same in both the cases (89%). The main difference of the two approaches is the repartition of the probability of domino event to occur among the possible domino scenarios. In this simple case study the probability of domino with two or more failed objects is very low (0.1 %) if a domino propagation of the first level is considered, while the probability of domino scenarios with a single secondary scenario account for the remaining probability of domino scenarios. On the contrary, if a multilevel domino propagation logic is assumed, domino scenarios with two or more secondary scenarios account for about the 10% of the domino scenario probability, with a surprising 1.9% for the scenario representative of the failure of all four the units composing the system.

6.3.2 Comparison with previous models

In the study performed by Cozzani et al. (2006) the propagation probabilities, as well as the domino scenario probabilities have been calculated for simple realistic case studies. In the following the probability of domino scenarios have been assessed. A comparison of the results obtained by the mean of the model presented by Cozzani et al. (2005; 2006), which consider simple contemporary propagation and by the mean of the model presented in this paper is performed. The layout of concern is described in Figure 6.6 (Cozzani et al., 2006), while Table 6.9 reports the features of the equipment reported. The initiator event is a pool fire scenario in the vessel “AT_2F”. In Table 6.9 the secondary accidents are described and the damage probabilities for every target of the primary scenario and for every target of each secondary scenario are also reported (Cozzani et al., 2006). Damage probabilities of equipment due to fires and explosions are calculated by the mean of existing vulnerability models (Cozzani et al., 2004; Landucci et al., 2009a).

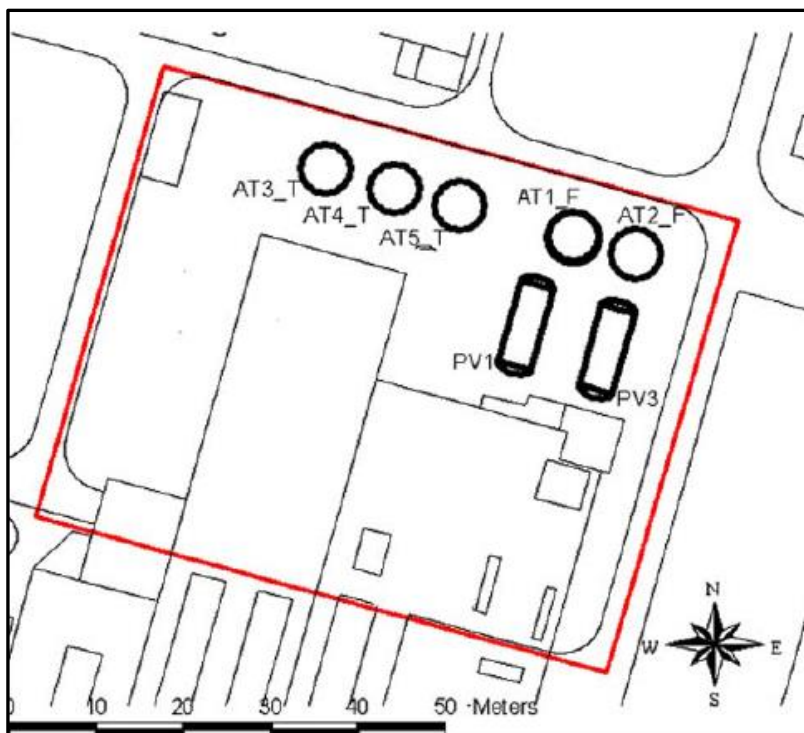


Figure 6.6 The layout of concern described by Cozzani et al. (2006)

Table 6.9 Details of the units reported in the case study. Typology and damage probabilities of primary and secondary scenarios. (Cozzani et al., 2006)

	Typology	Substance	Primary	Secondary	Pd AT_1F	Pd PV1	Pd PV3	Pd AT_3T	Pd AT_4T
AT_2F	Atmospheric	Methanol	Pool Fire - CEA	-	0.227	0.060 6	0.564	0.0708	0.382
AT_1F	Atmospheric	Methanol	-	Pool Fire - CEA	1	0.564	0.060 6	0.0071	0.0708
PV1	Pressurized	LPG	-	BLEVE Fireball - IEA	1	1	0.9	0.95	0.95
PV3	Pressurized	LPG	-	BLEVE Fireball - IEA	1	0.9	1	0.95	0.95
AT_3T	Atmospheric	Hydrofluoric acid	-	Toxic Dispersion - CEA	0	0	0	1	0
AT_4T	Atmospheric	Hydrofluoric acid	-	Toxic Dispersion - CEA	0	0	0	0	1

Results of the calculation of domino scenarios, obtained using either simple and multilevel propagation logic, are reported in table 6.10. In this case the set of accident scenarios is composed by 32 possible domino scenarios. In the case of simple contemporary propagation, the most of accidents show valuable probabilities, which ranges between 10^{-4} and $3 \cdot 10^{-1}$. In the case of simple propagation, 4 out of 32 accident, show high probabilities (higher than 0.1). In the case multilevel domino propagation is considered, the accidents in PV1 and PV2 have very high probability to generate higher-level domino accidents, since the Pd of targets due to secondary scenarios are very high (higher than 0.9).

Table 6.10: Domino scenario probabilities calculated using both simple contemporary propagation and multilevel propagation criteria. The domino scenario with a dramatic difference between the values calculated by the multilevel propagation to the respect of the values obtained considering simple propagation are evidenced with (*)

Scenario	AT_1F	PV3	PV1	AT_3_T	AT_4_T	Scenario Probability Multilevel Propagation	Scenario Probability Simple Contemporary Propagation
S01	0	0	0	0	0	1.82X10 ⁻⁰¹	1.82X10 ⁻⁰¹
S02	1	0	0	0	0	3.80X10 ⁻⁰³	5.34X10 ⁻⁰²
S03	0	1	0	0	0	0.00 (*)	2.35X10 ⁻⁰¹ (*)
S04	0	0	1	0	0	0.00	1.17X10 ⁻⁰²
S05	0	0	0	1	0	2.71X10 ⁻⁰³	1.39X10 ⁻⁰²
S06	0	0	0	0	1	3.31X10 ⁻⁰² (*)	1.12X10 ⁻⁰¹ (*)
S07	1	1	0	0	0	0.00	6.91X10 ⁻⁰²
S08	1	0	1	0	0	0.00	3.44X10 ⁻⁰³
S09	0	1	1	0	0	0.00	1.52X10 ⁻⁰²
S10	1	0	0	1	0	4.00X10 ⁻⁰⁴	4.07X10 ⁻⁰³
S11	0	1	0	1	0	0.00	1.79X10 ⁻⁰²
S12	0	0	1	1	0	0.00	8.94X10 ⁻⁰⁴
S13	1	0	0	0	1	5.96X10 ⁻⁰³	3.30X10 ⁻⁰²
S14	0	1	0	0	1	0.00 (*)	1.45X10 ⁻⁰¹ (*)
S15	0	0	1	0	1	0.00	7.25X10 ⁻⁰³
S16	0	0	0	1	1	4.04X10 ⁻⁰³	8.56X10 ⁻⁰³
S17	1	1	1	0	0	0.00	4.46X10 ⁻⁰³
S18	1	1	0	1	0	0.00	5.26X10 ⁻⁰³
S19	1	0	1	1	0	0.00	2.62X10 ⁻⁰⁴
S20	0	1	1	1	0	0.00	1.16X10 ⁻⁰³
S21	1	1	0	0	1	0.00	4.27X10 ⁻⁰²
S22	1	0	1	0	1	0.00	2.13X10 ⁻⁰³
S23	0	1	1	0	1	0.00	9.38X10 ⁻⁰³
S24	1	0	0	1	1	8.50X10 ⁻⁰⁴	2.51X10 ⁻⁰³
S25	0	1	0	1	1	0.00	1.11X10 ⁻⁰²
S26	0	0	1	1	1	0.00	5.52X10 ⁻⁰⁴
S27	1	1	1	1	0	0.00	3.39X10 ⁻⁰⁴
S28	1	1	1	0	1	0.00	2.75X10 ⁻⁰³
S29	1	1	0	1	1	0.00	3.25X10 ⁻⁰³
S30	1	0	1	1	1	0.00	1.62X10 ⁻⁰⁴
S31	0	1	1	1	1	0.00	7.15X10 ⁻⁰⁴
S32	1	1	1	1	1	7.67X10 ⁻⁰¹ (*)	2.10X10 ⁻⁰⁴ (*)

Therefore, once a secondary accident is started, it is very likely to have further escalation. In the case of multilevel propagation the only two scenarios with high probability are: the scenario of total destruction of the site, S32 (0.767), and the scenario in which no domino effect occurs, S01 (0.182). In other words, once the domino propagation has started, the most probable scenario, is the one representative of the damage of all the units in the site, S32, which results in six contemporary scenarios: the primary scenario and all five the secondary scenarios. The other interesting fact is that, excluding S01 in which no domino occurs, S32 is the only domino scenario with damage probability higher than 10⁻¹.

The results showed that by the use of the proposed model, domino scenarios with a higher level are considered more frequently than they were considered by the use of previous models

which followed a simple propagation logic. The expected difference in terms of risk calculation is that the overall frequency of domino scenarios is exactly the same in either the case of simple and multilevel propagation, but what it changes is the risk. In fact, considering multilevel propagation allows to consider domino scenarios with a higher number of contemporary secondary scenarios, which inevitably result in more serious consequences and on an increment of the scenario magnitude.

6.4 Conclusions

Due to the need to analyze a multilevel domino escalation process, a novel tool has been proposed for the assessment of domino scenario frequencies. The presented methodology is based on the Markovian analysis for the assessment of the transition probabilities between possible domino scenarios. Possible combinations of secondary scenarios are identified and transition probabilities between the possible states taken by the domino system are assessed. The probabilities, and frequencies of domino scenarios are calculated by the use of the Bayes theorem. The application of the methodology to case studies and to previous work based on simple logic for the propagation of domino accidents, allowed the assessment of a set of realistic domino scenarios, and of their probabilities. The results obtained by the use of this novel methodology are compared with those obtained by the previous models based on a single propagation level. The result is that the overall domino probability of any of the possible domino scenarios is exactly the same, but the probabilities are distributed in a different manner. Results obtained using a multilevel propagation logic are characterized by a higher probability of those domino scenarios with a higher number of secondary scenarios, the ones with the most serious overall consequences. Therefore, multilevel propagation logic allows the consideration of domino scenarios with higher magnitude.

The availability of this new tool enables the calculation of complex accidental scenario probabilities and frequencies. The simplicity of this methodology allows the automation of the procedure, and its inclusion on those software used for QRA, allowing the quantitative risk assessment associated to these domino scenarios and the calculation of individual and societal risk indicators.

References:

- Abdolhamidzadeh B, Abbasi T, Rashtchian D, Abbasi SA. A new method for assessing domino effect in chemical process industry. *Journal of Hazardous Materials*, 2010; 182:416–426.
- Antonioni, G., Spadoni, G., & Cozzani, V. (2009). Application of domino effect quantitative risk assessment to an extended industrial area. *Journal of Loss Prevention in the Process Industries*, 22(5), 614-624.
- D.F. Bagster, R.M. Pitblado, *Proc. Safety Environ. Protect.* 69 (1991) 196.
- A.M. Birk, M.H. Cunningham The boiling liquid expanding vapor explosion *J. Loss Prev. Process Ind.*, 7 (1994), pp. 474–480
- A.M. Birk, Scale effects with fire exposure of pressure-liquefied gas tanks *J. Loss Prev. Process Ind.*, 8 (1995), pp. 275–290
- A.M. Birk Hazards from propane BLEVEs: an update and proposals for emergency responders *J. Loss Prev. Process Ind.*, 9 (1996), pp. 173–181
- CCPS, *Guidelines for Evaluating the Characteristics of Vapor Cloud Explosions, Flash Fires and BLEVEs*, AIChE, New York, 1994
- CCPS *Guidelines for Consequence Analysis of Chemical Releases*, Center for Chemical Process Safety American Institute of Chemical Engineers, New York (1999)
- V. Cozzani, E. Salzano, The quantitative assessment of domino effects caused by overpressure. Part I: probit models, *J. Hazard. Mater.* A107 (2004a) 67–80.
- V. Cozzani, E. Salzano, The quantitative assessment of domino effects caused by overpressure Part II: case studies, *J. Hazard. Mater.* A107 (2004b) 81–94.
- Cozzani, V., Gubinelli, G., Antonioni, G., Spadoni, G., & Zanelli, S. (2005). The assessment of risk caused by domino effect in quantitative area risk analysis. *Journal of Hazardous Materials*, 127(1e3), 14-30.
- Cozzani, V., Antonioni, G., & Spadoni, G. (2006). Quantitative assessment of domino scenarios by a GIS-based software tool. *Journal of Loss Prevention in the Process Industries*, 19(5), 463-477.
- Cozzani, V., Tugnoli, A., & Salzano, E. (2009). The development of an inherent safety approach to the prevention of domino accidents. *Accident Analysis & Prevention*, 41(6), 1216-1227.
- Cozzani V., Antonioni G., Khakzad N., Khan F., Taveau J., Reniers G., *Quantitative Assessment of Risk Caused by Domino Accidents, Domino Effects in the Process Industries, Modeling, Prevention and Managing*, Elsevier, Amsterdam, The Netherlands, (2013a)
- Cozzani V., Tugnoli A., Bonvicini S., Salzano E., *Threshold-Based Approach, Domino Effects in the Process industries, Modeling, Prevention and Managing*, Elsevier, Amsterdam, The Netherlands, (2013b)
- Cozzani V, Antonioni G, Landucci G, Tugnoli A, Bonvicini S, Spadoni G, Quantitative assessment of domino and NaTech scenarios in complex industrial areas *.Journal of Loss Prevention in the Process Industries* 28 (2014) 10-22
- Delvosalle C., *Domino effects phenomena: definition, overview and classification*, in: *Direction Chemical Risks* (Ed.), European Seminar on Domino Effects, Federal Ministry of Employment, Brussels, 1996, pp. 5–15.
- Di Padova A, Tugnoli A, Cozzani V, Barbaresi T, Tallone F. Identification of fireproofing zones in oil & gas facilities by a risk-based procedure. *Journal of Hazardous Materials* 2011; 191:83–93.
- Egidi, D., Foraboschi, F. P., Spadoni, G., & Amendola, A. (1995). The ARIPAR project: analysis of the major accident risks connected with industrial and transportation activities in the Ravenna area. *Reliability Engineering & System Safety*, 49(1), 75-89.

- Gubinelli, G., Zanelli, S., & Cozzani, V. (2004). A simplified model for the assessment of the impact probability of fragments. *Journal of Hazardous Materials*, 116, 175e187.
- Gubinelli, G., & Cozzani, V. (2009a). Assessment of missile hazard: reference fragmentation patterns of process equipment. *Journal of Hazardous Materials*, 163, 1008-1018.
- Gubinelli, G., & Cozzani, V. (2009b). The assessment of missile hazard: evaluation of fragment number and drag factors. *Journal of Hazardous Materials*, 161, 439-449.
- Khakzad N, Faisal Khan F.I., Amyotte P, Valerio Cozzani V *Risk Analysis* Volume 33, Issue 2, pages 292–306, 2013
- F.I. Khan, S.A. Abbasi Models for domino effect analysis in the chemical process industries *Process Saf. Prog.*, 17 (1998a), pp. 107–123
- F.I. Khan, S.A. Abbasi DOMIFFECT: a new user friendly software for domino effect analysis *Environ. Model. Softw.*, 13 (1998b), 163–177
- F.I. Khan, S.A. Abbasi, Studies on the probabilities and likely impacts of chains of accident (domino effect) in a fertiliser industry, *Process Saf. Prog.*, 19 (2000a), 40–56
- F.I. Khan, B. Natarajan, S.A. Abbasi, Avoid the domino effect via proper risk assessment, *Chem. Eng. Prog.*, 96 (2000b), 63–76
- G. Landucci, G. Gubinelli, G. Antonioni, V. Cozzani, The assessment of the damage probability of storage tanks in domino events triggered by fire, *Accident Anal. Prev.* 41 (6) (2009) 1206–1215.
- I.R.M. Leslie, A.M. Birk, State of the art review of pressure liquefied gas container failure modes and associated projectile hazards, *J. Hazard. Mater.*, 28 (1991), 329–365
- Mannan, S., 2005. *Lees' Loss Prevention in the Process Industries*, third ed. Elsevier, Oxford, UK.
- Reniers, G., Dullaert, W., Ale, B., Soudan, K., Developing an external domino accident prevention framework: *Hazwim Journal of Loss Prevention in the Process Industries* 18 (2005a), 127–138
- Reniers, G., Dullaert, W., Soudan, K., & Ale, B. The use of current risk analysis tools evaluated towards preventing external domino accidents. *Journal of Loss Prevention in the Process Industries*, Volume 18, 3, (2005b), 119-126
- G.L.L. Reniers, W. Dullaert, A. Audenaert, B.J.M. Ale, K. Soudan. Managing domino effect-related security of industrial areas. *Journal of Loss Prevention in the Process Industries*, 21, 3, (2008) 336-343
- G. Reniers, W. Dullaert, K. Soudan, Domino effects within a chemical cluster: a game-theoretical modeling approach by using Nash-equilibrium, *J. Hazard. Mater.* 167 (1/3) (2009) 289–293.
- G. Reniers An external domino effects investment approach to improve cross-plant safety within chemical clusters, *Journal of Hazardous Materials* 177 (2010) 167–174
- G. Reniers, V. Cozzani, *Domino Effects in the Process Industries, Modeling, Prevention and Managing*, Elsevier, Amsterdam, The Netherlands, (2013a)
- G. Reniers, V. Cozzani, *Features of Escalation Scenarios, Domino Effects in the Process Industries, Modeling, Prevention and Managing*, Elsevier, Amsterdam, The Netherlands, (2013b)
- Tugnoli A, Cozzani V, Di Padova A, Barbaresi T, Tallone F, Mitigation of fire damage and escalation by fireproofing: A risk-based strategy, *Reliability Engineering and System Safety* 105 (2012) 25–35
- Uijt de Haag, P. A. M., & Ale, B. J. M. (1999). *Guidelines for quantitative risk assessment (Purple book)*. The Hague (NL): Committee for the Prevention of Disasters.

Chapter 7:

Final Conclusions

Cascading events are capable to generate accidental scenarios with serious consequences for the population that lives in the vicinity of process plants. The issues related to cascading event were analyzed and discussed in detail in this thesis. Both the topics of NaTech and domino events have been developed during this research activity.

The state of the art of technical, scientific and managerial knowledge concerning such accident scenarios, caused by domino events was described. The analysis of scientific publications concerning domino effect was carried out addressing four main issues: past accident analysis, vulnerability models, risk assessment and safety management of domino scenarios. A number of open points still remain, in order to improve the effectiveness of existing tools aimed at the assessment and prevention of risk due to domino. This is the case of risk assessment tools addressing escalation effects to the respect of those complex multi-level scenarios, which requires major improvement in order to be fully applicable.

A short review of the past works regarding NaTech accidents has been carried out. Attention was focused on several research addressing NaTech data collection from past accident studies, as well as the improvements of risk analysis methodologies to the respect of NaTech accident has been discussed. However, the availability of partial or fragmented data regarding this kind of accidents increases the difficulty of this research. A critical task Land use planning has been found to be an important factor in the mitigation of natural disasters and economic losses from disasters in regions subject to natural hazards. Another possible strategy to improve safety of the industrial installation is by providing useful design indications, which account for a safer layout disposal and recommendation on equipment construction in NaTech prone zones. Furthermore, by the tool of preliminary hazard analysis the critical units can be identified. The level of preparation to respond to NaTech is also an important indication for the safety of an industrial area. However, a huge work is still needed to increase the understanding of this particular risk, in order to prevent and to mitigate the impact of such scenarios. The aim of the current research work was to investigate more in detail the NaTech hazard, providing novel tools to assist operators in the assessment of NaTech risk.

Within this framework, a methodology for the assessment risk due to lightning strikes on process installation was developed. Past accident analysis showed that atmospheric storage tanks are the equipment typology most frequently damaged by the impact of lightning. Reference scenarios have been identified, with the respects of possible safety barriers installed on the tanks. In order to evaluate the risk due to accidents triggered by lightning strikes, several technical tools were developed. A dedicated methodology allowed the calculation of the expected frequency of lightning strikes on storage tanks. A fragility model that assess the possibility of direct structural damage was developed, allowing to calculate a damage probability for vessel struck by lightning. Reference event trees were obtained and validated using past accident data. Reliability analysis carried out on safety barriers applied in industrial

practice allowed the quantification of event trees. The application of the entire QRA methodology to a case study confirmed on one hand that NaTech scenarios caused by lightning may have an important influence on the risk profile of a facility, and, on the other hand, evidenced the role of the safety barriers in preventing accident propagation.

Due to the fact that dedicated fragility models for the assessment of equipment damage probability in case of flood was lacking, a model able to calculate the failure probability of horizontal cylindrical vessels as a function of flood severity was developed. Due to the necessity to analyse a huge number of scenarios, simplified correlations were derived for the quick estimation of vessel resistance. The importance of an appropriate design of the vessel support and basements was evidenced, highlighting the potential importance of mitigation barriers in the prevention of NaTech scenarios triggered by floods.

As evidenced by the state of the art on domino events, a recognized unique methodology for the assessment of multilevel domino events is lacking. A novel tools has been proposed for the assessment of domino scenario frequencies. The presented methodology is based on the Markovian analysis for the assessment of the transition probabilities between possible domino scenarios, allowing the assessment of multilevel propagation. Possible combination of secondary scenarios are identified. The probabilities, and frequencies of domino scenarios are calculated. The results obtained by the use of this novel methodology are compared with those obtained by the previous models based on a single propagation level. Results obtained using a multilevel propagation logic are characterized by a higher probability of those domino scenarios with a higher number of secondary scenarios: the ones with the most serious overall consequences. Therefore, multilevel propagation logic allows the consideration of domino scenarios with higher magnitude.

On the one hand, the relevant research work carried out in the past years provided a framework to approach the assessment of cascading events, being either domino or Natech event. On the other hand, the relevant work carried out still needs to be consolidated and completed. The tools and methods provided within this very study had the aim to assist the progress toward a consolidated and universal methodology for the assessment and prevention of cascading events, contributing to enhance safety and sustainability in the chemical and process

Appendix

This Appendix presents the results obtained for simplified regular lay-outs as that in Figure 10. Three further cases were considered: 6 tanks in a 2 rows - 3 columns matrix; 9 tanks in a 3 rows - 3 columns matrix; 20 tanks in a 4 rows - 5 columns matrix. As for Figure 10, identical tank geometries were considered for all tanks in the lay-outs (Tank ID 9 in Table 4).

The results are reported in Tables A1, A2 and A3. A comparison of the three tables with data in Table 6 shows that the values of LI for the three different types of positions (Angle, Edge, Centre) are identical in these lay-out configurations, due to symmetry. Thus, the results suggest that LI is mainly influenced by the distance and type of position (Angle, Edge, Centre), and not by the number of the tanks in the lay-out. However, it should be noted that these results apply only to storage tank parks in which tank sizes are similar.

Table A1: Values of LI for a simple lay-out of 6 atmospheric tanks in a 2 rows - 3 columns matrix.

Number	Position	Distance, d			
		10m	20m	30m	50m
1	Angle	0.41	0.46	0.50	0.60
2	Edge	0.18	0.24	0.30	0.42
3	Angle	0.41	0.46	0.50	0.60
4	Angle	0.41	0.46	0.50	0.60
5	Edge	0.18	0.24	0.30	0.42
6	Angle	0.41	0.46	0.50	0.60

Table A2: Values of LI for a simple lay-out of 9 atmospheric tanks in a 3 rows - 3 columns matrix.

Number	Position	Distance, d			
		10m	20m	30m	50m
1	Angle	0.41	0.46	0.50	0.60
2	Edge	0.18	0.24	0.30	0.42
3	Angle	0.41	0.46	0.50	0.60
4	Edge	0.18	0.24	0.30	0.42
5	Centre	0.07	0.12	0.17	0.29
6	Edge	0.18	0.24	0.30	0.42
7	Angle	0.41	0.46	0.50	0.60
8	Edge	0.18	0.24	0.30	0.42
9	Angle	0.41	0.46	0.50	0.60

Table A3: Values of LI for a simple lay-out of 20 atmospheric tanks in a 4 rows - 5 columns matrix.

Number	Position	Distance, <i>d</i>			
		10m	20m	30m	50m
1	Angle	0.41	0.46	0.50	0.60
2	Edge	0.18	0.24	0.30	0.42
3	Edge	0.18	0.24	0.30	0.42
4	Edge	0.18	0.24	0.30	0.42
5	Angle	0.41	0.46	0.50	0.60
6	Edge	0.18	0.24	0.30	0.42
7	Centre	0.073	0.12	0.17	0.29
8	Centre	0.073	0.12	0.17	0.29
9	Centre	0.073	0.12	0.17	0.29
10	Edge	0.18	0.24	0.30	0.42
11	Edge	0.18	0.24	0.30	0.42
12	Centre	0.073	0.12	0.17	0.29
13	Centre	0.073	0.12	0.17	0.29
14	Centre	0.073	0.12	0.17	0.29
15	Edge	0.18	0.24	0.30	0.42
16	Angle	0.41	0.46	0.50	0.60
17	Edge	0.18	0.24	0.30	0.42
18	Edge	0.18	0.24	0.30	0.42
19	Edge	0.18	0.24	0.30	0.42
20	Angle	0.41	0.46	0.50	0.60

In the following, the results of the application of the failure model are reported. The results are summarized in charts that allow a quick overview of the vessels response to pre-determined flood conditions (some examples are reported in Figs A1, A2, A3, A4). For each vessel, identified by the vessel ID in Table 1, the failure to a given flood condition (identified by the imposed flood velocity v_w in m/s and effective depth h_w in m) is highlighted by a red color. On the contrary, if the model does not predict a failure, the box is white.

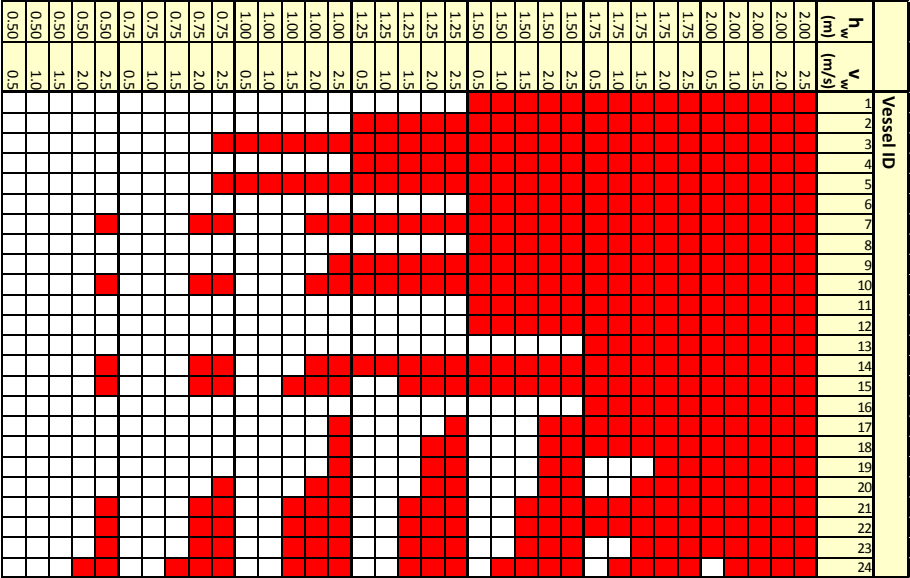


Figure A1: Failure chart for the vessels considered in the present study assuming 50% filling level and stored liquid density of 1100 kg/m^3 (water solution containing toxic contaminant).

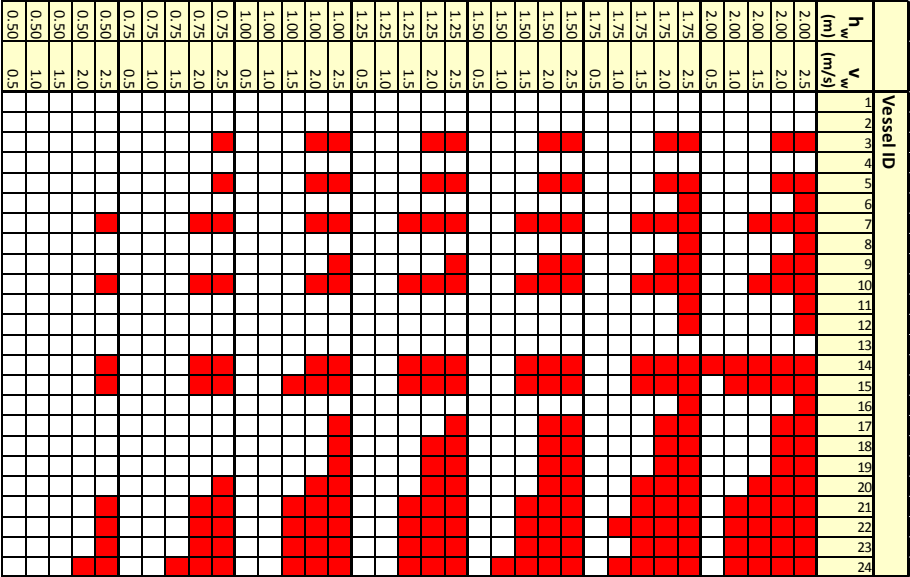


Figure A2: Failure chart for the atmospheric vessels considered in the present study assuming 90% filling level and stored liquid density of 1100 kg/m^3 (water solution containing toxic contaminant).

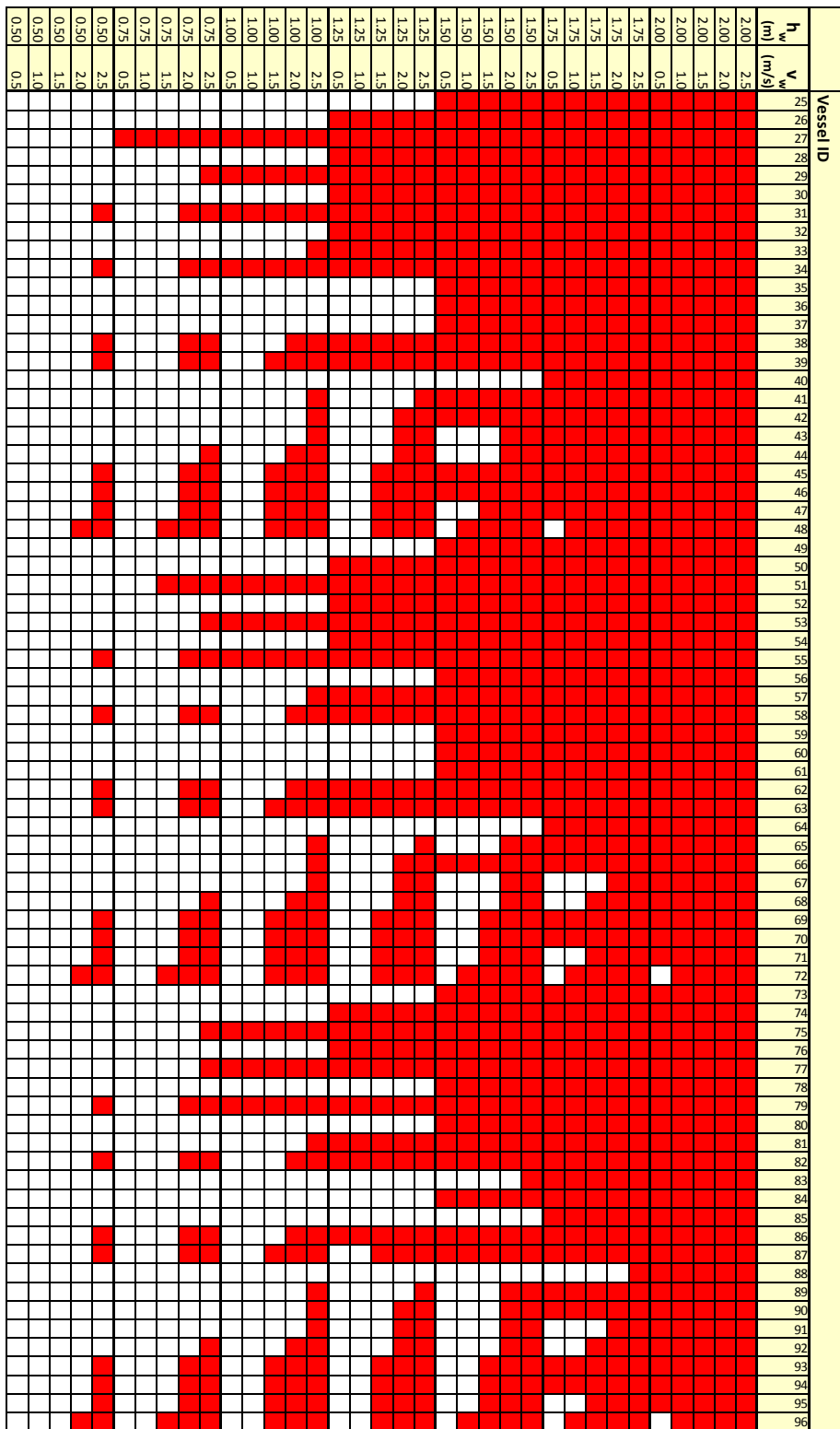


Figure A3: Failure chart for the pressurized vessels considered in the present study assuming 50% filling level and stored liquid density of 600 kg/m³ (ammonia).

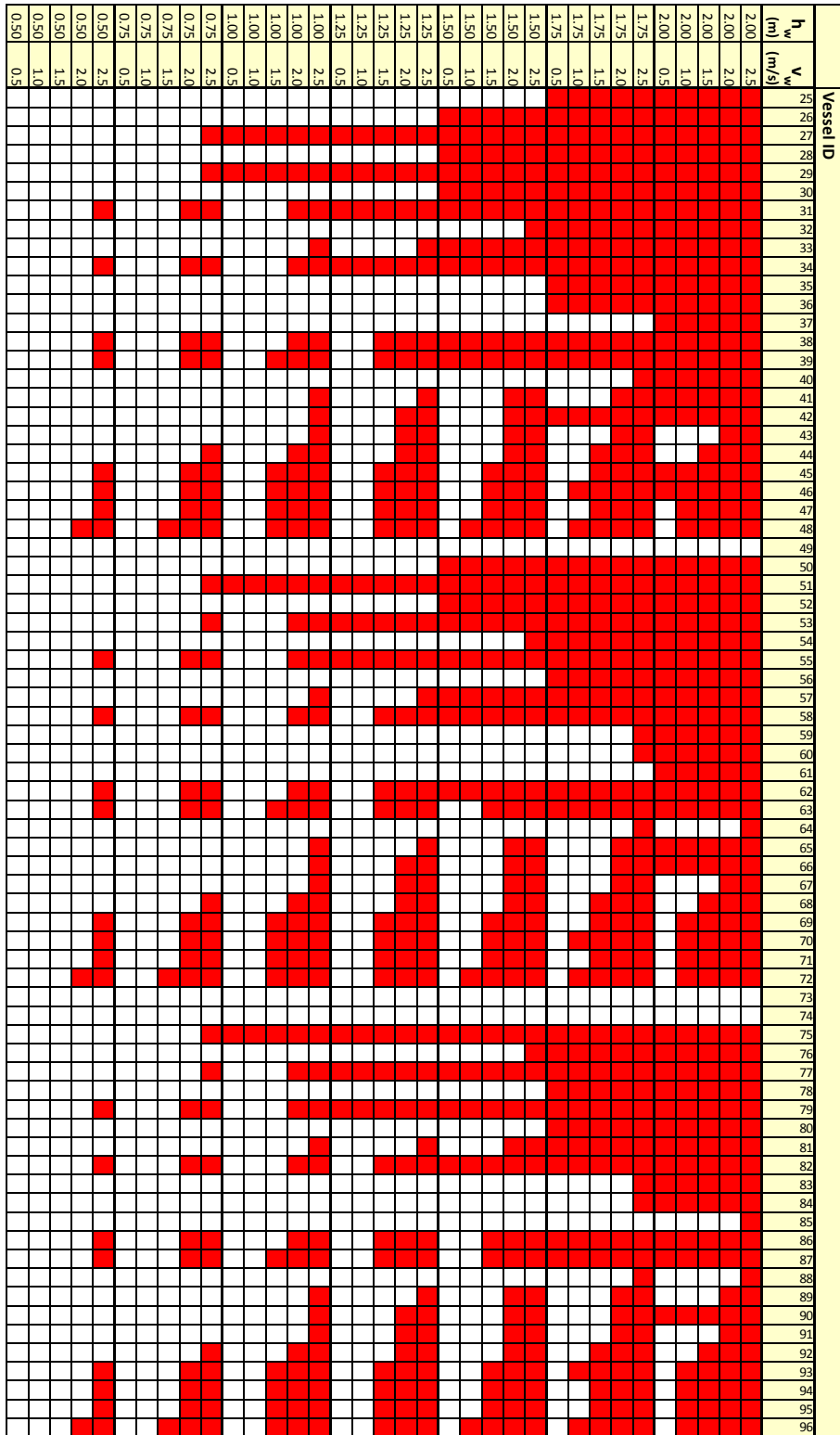


Figure A4: Failure chart for the pressurized vessels considered in the present study assuming 90% filling level and stored liquid density

Acknowledgements

First, I would like to thank the primary and continuous sustain from my mother, Gianna, a woman with unfailing endurance. To her I owe everything; she really taught me to read and to write.

Thanks to my sister Alice and her ability to make me tolerate the toughest issues.

I would like to acknowledge the fundamental support of my supervisor, professor Valerio Cozzani, whose leadership was for me the compass that pointed the direction during these three years. The working experience made with him is the most important of all the lessons I learned. Thank you very much.

I would like to thank Giacomo Antoioni for his aid. He is a friend to me other than a colleague.

Many thanks to all the colleagues of the research team, either PhD students and researchers, with whom I shared every single day of those years.

Finally, I would like to thank professor Khan and the whole staff of Memorial University of Newfoundland for the warm welcome they provided me during my stay in Canada

Ringraziamenti

In primo luogo mi piacerebbe ringraziare il sostegno costante e imprescindibile di mia madre, Gianna: donna dalla sconfinata pazienza, alla quale devo in sostanza tutto e che mi ha insegnato a leggere e scrivere.

Ringrazio mia sorella Alice e la sua capacità di farmi sopportare con facilità gli impegni più stressanti.

Ringrazio il mio tutor, il Professor Valerio Cozzani, la cui guida è stata la bussola che mi ha impedito di perdermi in questi tre anni di studio. L'esperienza di lavoro diretto in cui mi ha coinvolto è stata di fatto la lezione più importante che chiunque mi abbia mai impartito, e per questo lo ringrazio di cuore.

Ringrazio Giacomo Antonioni, nel quale ho trovato una figura amica, oltre che un collega.

Ringrazio inoltre tutti i ragazzi del gruppo di ricerca, assegnisti e dottorandi, con i quali ho condiviso giorno dopo giorno l'esperienza di questi anni.

Infine vorrei ringraziare il professor Khan e la Memorial University of Newfoundland per la cordiale ospitalità durante i mesi passati in Canada.